ORIENTED FIBRE ARRAYS AND SHAPE CONTROL IN CERTAIN NUCLEI, CELLS AND TISSUES

Sally Anne Mathews

A Thesis Submitted for the Degree of PhD
at the
University of St Andrews

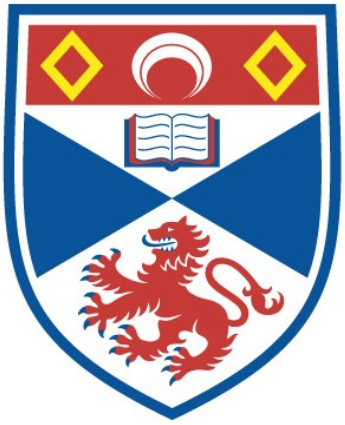

1983

ABSTRACT

New aspects of shape control and fibre deployment are reported for three situations: certain insect ovarian follicles, certain insect wings, and an unusual nucleus, the ciliate micronucleus.

The shaping of insect follicles includes the spatio-temporal integration of intracellular and extracellular fibre arrays in the cockroach follicle. The situation is more complex than previously supposed. Similar events occur in Rhodnius prolixus follicles. It is argued, largely on the basis of my survey, that all insect follicles are involved in the control of egg shape.

Evidence is also presented for follicular re-organisation and involvement as a contractile tissue during egg discharge. This possibility has never been considered before. It involves a previously undetected post-vitellogenic phase of cytoskeletal co-ordination.

Epidermal cells exhibit a striking sequence of very marked changes in shape during wing morphogenesis in the dipteran insect Calliphora erythrocephala. This includes two epithelial cell contraction-elongation cycles that are spatio-temporally co-ordinated and apparently help to define the shape of a growing wing.

It has been shown for Paramecium that an unusual type of spindle microtubule differentiation is involved in micronuclear mitosis. This microtubule differentiation occurs with remarkable spatial and temporal precision at specific locations within the spindle at specific stages in micronuclear elongation.

ORIENTED FIBRE ARRAYS AND SHAPE CONTROL IN CERTAIN NUCLEI, CELLS AND TISSUES

by

Sally Anne Mathews

Department of Zoology

University of St. Andrews

A thesis submitted for the degree of Doctor of Philosophy.

April, 1981

DECLARATION

I hereby declare that this thesis is my own composition, and that the experimental work was performed by me alone, except for the fixation of P. tetraurelia (which were donated by Mr. D. Roche and Dr. J. Beisson) and Figure 139 which was donated by Dr. J.B. Tucker.

None of the material in this thesis has been submitted for any other degree.

Dated 18 April, 1981

Candidacy of Mrs. Sally A. Mathews for the Degree of Doctor of Philosophy at the University of St. Andrews.

I certify that the conditions of the Resolution and Regulations (as they apply to Ph.D. candidates and as set out in St. Andrews University Calendar) have been fulfilled.

14th May, 1981.

DR. J.B. TUCKER,

Supervisor

UNIVERSITY CAREER

I entered the University of Natal, Pietermaritzburg in February 1973, and graduated with a second class B.Sc. in Zoology and Entomology in November 1975.

In October 1976 I started post-graduate research in the Zoology Department of the University of St. Andrews on oriented fibre arrays and shape control in certain insect cells and tissues. The University Senate agreed in January 1980 to change my degree course from a M.Sc. to a Ph.D. Oriented fibre arrays and shape control in certain ciliate nuclei was then included in my research.

ABSTRACT

New aspects of shape control and fibre deployment are reported for three situations: certain insect ovarian follicles, certain insect wings, and an unusual nucleus, the ciliate micronucleus.

The shaping of insect follicles includes the spatio-temporal integration of intracellular and extracellular fibre arrays in the cockroach follicle. The situation is more complex than previously supposed. Similar events occur in Rhodnius prolixus follicles. It is argued, largely on the basis of my survey, that all insect follicles are involved in the control of egg shape.

Evidence is also presented for follicular re-organisation and involvement as a contractile tissue during egg discharge. This possibility has never been considered before. It involves a previously undetected post-vitellogenic phase of cytoskeletal co-ordination.

Epidermal cells exhibit a striking sequence of very marked changes in shape during wing morphogenesis in the dipteran insect Calliphora erythrocephala. This includes two epithelial cell contraction-elongation cycles that are spatio-temporally co-ordinated and apparently help to define the shape of a growing wing.

It has been shown for Paramecium that an unusual type of spindle microtubule differentiation is involved in micronuclear mitosis. This microtubule differentiation occurs with remarkable spatial and temporal precision at specific locations within the spindle at specific stages in micronuclear elongation.

SUMMARY

New aspects of shape control and fibre deployment are reported for three situations: certain insect ovarian follicles, certain insect wings, and an unusual nucleus, the ciliate micronucleus.

The shaping of insect follicles includes the spatio-temporal integration of intracellular and extracellular fibre arrays in the cockroach follicle. The situation is more complex than previously supposed. For example, microtubules and microfilaments positioned close to the outer surfaces of cockroach follicle cells are oriented circumferentially at right angles to the longitudinal (polar) axes of the follicles during anisometric expansion of the epithelium. Similar events occur in Rhodnius prolixus follicles. Cytoskeletal and extracellular fibres are spatio-temporally integrated during anisometric follicle growth. It is argued, largely on the basis of my survey, that all insect follicles are involved in the control of egg shape.

Evidence is also presented for follicular re-organisation and involvement as a contractile tissue during egg discharge. This possibility has not been considered before. A previously undetected post-vitellogenic phase of cytoskeletal co-ordination takes place in follicle cells which appears to be concerned with the discharge of mature oocytes from ovarioles.

Epidermal cells exhibit a striking sequence of very marked changes in shape during wing morphogenesis in the dipteran insect, Calliphora erythrocephala. This includes two epithelial contraction-elongation cycles that are spatio-temporally co-ordinated and apparently help to define the shape of a growing wing. Assembly and disassembly of microtubule and microfilament arrays in epithelial cells is involved during

these changes. Intercellular spatial co-ordination of cytoskeletal orientation, growth and breakdown at different localities in the epithelium appear to be effected *via* the association of microtubules and microfilaments with cell junctions, cell interdigitations and filopodial cell interconnections.

It has been shown for *Paramecium* that an unusual type of spindle microtubule differentiation is involved in micronuclear mitosis. This microtubule differentiation occurs with remarkable spatial and temporal co-ordination at specific locations within spindles at specific stages in micronuclear elongation.

CONTENTS

PAGE

CHAPTER 4

INTRODUCTION

This dissertation deals with certain aspects of shape control in animals at several levels of organisation: at the organelle level, at the cellular level, and at the tissue level. Three main systems have been investigated: the ovarioles of two insect species (Periplaneta americana and Rhodnius prolixus), the developing wing of another insect (Calliphora erythrocephala), and the dividing micronuclei of two species of the ciliate Paramecium (P. primaurelia and P. tetraurelia). In all these investigations attention has mainly been directed at the impact of aligned fibre arrays during shape control.

1 SPATIAL INVOLVEMENT OF CELLS DURING TISSUE SHAPING

There are several ways in which cells could, at least in theory, be spatially involved during tissue shaping. A high level of cell division in a particular tissue locality results in a local increase in size. Oriented cell divisions can help to promote elongation in certain directions. Localised cell death sometimes participates during definition of tissue shape; this occurs, for example, during vertebrate limb morphogenesis. Patterns of dying cells contribute to the ultimate shape of certain wings and legs. The pattern of necrosis is stage-specific and characteristic of each appendage (Saunders, 1966). If cells change their positions within a tissue by migrating to another tissue region, the shape of the tissue may change as a consequence. A good example of this has been provided by studies of the migratory behaviour of certain vertebrate neural crest cells. Neural crest cells exhibit directed migration to specific organ sites. Sensory and sympathetic ganglia flanking the spinal column, and supportive cells of nerves such as Schwann cells and glia cells are among a large group of tissues derived from neural crest cell migration. A fifth way in which

cells can influence tissue shaping is by themselves changing in shape. If cell shape changes were integrated over considerable areas, flattening or elongation of cells could bring about a change in tissue shape. This appears to be important and widespread during embryogenesis.

This dissertation is largely concerned with the impact of cell shape changes on the control of tissue shaping. A brief survey of situations where cell shape changes have been shown to be important during tissue growth is provided below.

(a) Gastrulation

'Gastrulation rearranges all organ-forming areas of the blastula into three sheets, each with different inside-outside relationships and recognition properties' (Grant, 1978). Gastrulation usually involves the combination of two basic types of movement ie. epiboly and emboly. Although gastrulation may differ amongst animal groups, it usually seems to be initiated by cell shape changes. In the protochordate Amphioxus, for example, gastrulation is initiated by the large ventral cells that become columnar and then wedge-shaped as their inner surfaces become wider. As this occurs, the ventral surface flattens. Subsequently ventral cells become more wedge-shaped. The vegetal pole buckles in as a result until the blastocoele cavity has been obliterated (Conklin, 1932).

During echinoderm gastrulation, cell shape changes are very evident. Ventral cells of the blastula change shape from elongate wedges to cylinders. This causes the ventral region of the blastula to thicken into a plate which bulges into the blastocoele. Cells of the ventral plate undergo further shape changes. They produce fine filopodia which extend as far as the inner wall of the animal half

of the blastocyst, exert tension, and pull the ventral plate further into the blastocoele (Gustafson & Wolpert, 1967).

The first visible sign of amphibian gastrulation is a sinking in of a few cells at the site previously occupied by the grey crescent. This is effected by a change in shape of these cells from cuboidal to elongate-bottle-shaped (they become wider at their inner surfaces than at their outer ones). Adjacent cells attached to bottle cells by tight junctions seem to be drawn in over the dorsal lip of the blastopore by the elongating bottle cells (Baker, 1965).

During chick gastrulation, the primitive streak is the counterpart of the amphibian blastopore lip because endoderm and mesoderm invaginate at this point. Epiblast cells in the middle of the primitive streak become flask-shaped as they elongate into the blastocoele to form the primitive groove. These elongating cells produce filopodia that help to pull adjacent cells into the groove (Trelstad, Hay & Revel, 1967).

(b) Neurulation

During neurulation, a two-dimensional sheet of cells becomes transformed into a tube. The most significant factor in this process seems to be the degree of cell elongation in different regions of the neural plate. Cells at the lateral margins change in shape from low columnar to tall columnar giving rise to lateral folds. The folds move towards one another as cells in the middle area of the neural plate become wedge-shaped. The apical ends of the cells become narrow while basal ends remain wide. This causes the plate to roll up. Eventually the folds fuse and separate from the overlying ectoderm to produce a neural tube (Schroeder, 1970; Burnside, 1971; Karfunkel, 1974; Messier, 1978).

(c) Salivary gland morphogenesis

A salivary gland starts as a small epithelial bud and grows into a branching system of grape-like clusters of tubules which make up a salivary gland. Branching is initiated by the continuous appearance of clefts in expanding epithelial lobules. This repetitive branching morphogenesis also occurs in certain other endodermally derived organs such as the pancreas, thyroid and lung. It seems that the distal cells of lobules become wedge-shaped. Apical ends of cells are narrower than basal ends. As a result, clefts are produced (Wessels & Evans, 1968; Spooner & Wessels, 1972; Spooner, 1975; Bernstein & Wollman, 1976).

(d) Neuron outgrowth

This is an extreme example of cell shape change that mediates a change in tissue shape. Nerve morphogenesis consists very largely of the elongation of nerve cell processes - namely, the axons (Yamada, Spooner & Wessels, 1971; Rakic, 1972).

(e) Myogenesis

The development of muscle involves a change in the shapes of its cells from roughly spherical to highly elongate and spindle shaped. Correllated with this, the muscle tissue becomes elongate (Fischman, 1967; Warren, 1974).

(f) Vertebrate placode morphogenesis

Lens development involves the initial formation of a flattened lens placode which is accomplished by elongation of ectodermal cells towards the adjacent optic cup. This evaginates inside the optic cup and pinches off. In the ear and nasal placodes, cells

change shape in a similar way, orient towards the inducing tissue, and then round up into vesicles (Byers & Porter, 1964; Pearce & Zwaan, 1970).

(g) Heteropeza follicle development

Elongation of follicle cells in a direction parallel to the polar axis of a developing follicle appears to initiate a change in follicle shape in the gall midge, Heteropeza pygmaea. The initially spherical follicles become progressively more elongate with respect to their polar axes (Tucker & Meats, 1976).

(h) Drosophila wing morphogenesis

Waddington (1941) has shown that there is a sequence of shape changes in epidermal cells of metamorphosing Drosophila wing imaginal discs. These may play an important part in control of wing shape.

This dissertation is mainly concerned with investigating the ways in which cell shape changes are mediated and how these changes are related to tissue shape changes. It is generally agreed that cytoskeletons play an important role in the control of cell shaping.

2. CYTOSKELETONS

Animal cell shaping is largely determined by the spatial layout and activities of various types of cytoskeletal arrays (Wessels et al., 1971; Goldman, Pollard & Rosenbaum, 1976; Burgess & Schroeder, 1979). There are three main types of cytoskeletal fibres.

(a) Microtubules

Microtubules occur in all types of eukaryotic cells (Dustin, 1978; Roberts & Hyams, 1979). These tubular structures are usually about

24 nm in diameter, but microtubules with diameters of as little as 14 nm, or as great as 40 nm have occasionally been reported. Microtubule walls are usually made up of a circular palisade of 13 aligned protofilaments. Protofilaments are chains of a dimeric protein called tubulin. Most microtubules include other proteins called microtubule associated proteins. Some of these are attached to the outer surfaces of the protofilaments (see Raff, 1979).

Microtubules are stiff, rigid structures. Some of them are rather labile. Both *in vivo* and *in vitro* they can rapidly assemble or disassemble. Disassembly can be promoted experimentally by low temperatures, high pressure and treatment with anti-mitotic drugs such as colchine and vinblastine sulphate.

Microtubules are spatially associated with several types of cell motility. For example, they are associated with the beating of cilia and flagella, and with anaphase chromosome movement. Microtubules are also involved during the elongation of cells, or parts of cells, and during maintenance of cell shape. In addition, microtubules appear to facilitate certain types of intracellular transport by active propulsion of materials alongside oriented microtubules. This seems to occur, for example, during the movement of ribosomes in telotrophic ovarioles (McGregor & Stebbings, 1970). This action is thought to be facilitated by contractile microtubule-associated proteins.

(b) Microfilaments

Microfilaments also occur in all types of eukaryotic cells (Wessels *et al.*, 1971; Pollard & Weihing, 1974). They are about

6 nm in diameter. Microfilaments are composed of actin molecules. Other proteins such as myosin, tropomyosin and α actinin are often associated with microfilaments. They are thought to generate movement, and effect cell shape changes, by a sliding system similar to that which operates in skeletal muscle. Contractile forces set up tension between and within cells. The direction of locomotion and/or cell shape change depends on the alignment of microfilaments in some cases (Spooner, 1975; Dunn & Heath, 1976). The drug cytochalasin B interferes with a number of microfilament-mediated cellular activities and induces depolymerisation of microfilaments or alteration of microfilament arrangement (Schroeder, 1970; Cloney, 1972; Spooner, 1975).

(c) Intermediate filaments

Intermediate filaments are also referred to as neurofilaments and tonofilaments in certain situations. They occur in a wide range of metazoan tissue cell types but have yet to be demonstrated convincingly in plant cells. These filaments are composed of a variable number of protein species (neurofilaments have four, for example) that are twisted into a 'rope' with a diameter of about 10 nm.

Intermediate filaments are much more stable than microtubules and microfilaments. Their depolymerisation is not induced so readily. So far, unlike the case for microtubules and microfilaments, there are no indications for their direct involvement in contractile interactions. They simply seem to act as stress-resisting fibres which help to maintain cell shape, and tissue shape (when they are anchored to attachment desmosomes) (Hoffman

& Lasek, 1975; Cooke, 1976; Hull & Staehelin, 1979; Edwards & Dysart, 1980). They have not been detected in any of the cells dealt with in this dissertation.

3. CYTOSKELETAL INVOLVEMENT DURING CELL SHAPING

Elongation of cells or parts of cells often appears to involve microtubules and microfilaments.

Microtubules are usually aligned parallel to the longitudinal axes of cell extensions or parallel to the direction of cell elongation. The ways in which microtubules direct and effect the elongation of cells and cell processes is not fully resolved. Suggestions include rapid polarised polymerization of microtubules, intertubule sliding, and directional microtubule-mediated cytoplasmic transport (see Tucker, 1979). Several examples of microtubule-mediated cell elongation occur during some of the morphogenetic events discussed in section 1 above. Microtubules appear to be involved in cell elongation during Heteropeza follicle elongation (Tucker & Meats, 1976), placode development (Byers & Porter, 1964), myoblast elongation (Warren, 1974), axon outgrowth (Rakic, 1972), and the production of wedge-, flask-, and bottle-shaped cells during gastrulation and neurulation (Baker, 1965; Schroeder, 1970).

Microfilaments are believed to generate changes in the shapes of cells or parts of cells by virtue of their contractile activities. Cell cleavage provides a striking example of such involvement. Microfilaments form a 'contractile ring' which actively constricts and draws the cleavage furrow inwards (Schroeder, 1976). Microfilaments also appear to be responsible for cleft formation during salivary gland morphogenesis (Spooner, 1975). Microfilaments apparently help to

produce wedge-, flask-, and bottle-shaped cells during gastrulation and neurulation. Contraction of a microfilamentous 'ring' narrows one end of each cell by a 'purse-string' action (Baker, 1965; Schroeder, 1970; Burnside, 1971). Furthermore it has been proposed that movement of migratory cells during gastrulation and neurulation is accomplished by contraction of filopodia and that this is due to sliding interactions between microfilaments (Trelstad, Hay & Revel, 1967; Tilney & Gibbins, 1969; Spooner, 1975).

4 CYTOSKELETAL CO-ORDINATION IN METAZOAN TISSUES

Co-ordinated changes in the shapes of cell neighbours can produce movement or elongation of an epithelial population as a whole. This leads to changes in tissue shape. For example, co-ordinated elongation in a restricted group of cells in a continuous epithelium produces a flattened placode or 'plate'. This occurs during the development of lens placodes and neural plates. Co-ordinated constriction at one end of cells in a discrete subpopulation of an epithelium can cause bending or folding of the epithelial sheet. This occurs during neural tube and lens vesicle development. Co-ordinated contraction of filopodia in neighbouring epithelial cells can help to bring about migration of the epithelium as a whole (as in epiboly during gastrulation). In these situations, intracellularly aligned cytoskeletons which effect individual cell shape changes are also spatially co-ordinated on an intercellular basis. During some changes in tissue shape, the cytoskeletal fibres in cell neighbours are aligned with each other (see Tucker, 1981).

Spatially co-ordinated cell shape changes also appear to be influenced by variations in cell-cell adhesion. Cell surface regions

often form specialised adhesion regions such as septate junctions and attachment desmosomes which enable groups of cells to function together as structural units. Microtubules and microfilaments are often positioned on either side of desmosomes. They probably transmit tensional forces between cells via desmosomes thereby providing intercellular co-ordinating networks which help to control tissue shaping (Weihing, 1979).

Other types of surface interactions between adjacent cells may also contribute to intercellular cytoskeletal co-ordination. Specific glycoprotein receptors at cell surfaces may interact with those of neighbouring cells and also bind to cytoskeletal arrays and re-orient/re-organise them. This could assist intercellular cytoskeletal alignment and co-ordination of cell movement. Such activity may be especially pronounced in regions where adjacent cells interdigitate (Edelman, 1977; Tucker, 1981).

5. EXTRACELLULAR MATRICES AND TISSUE SHAPING

Multicellularity in animal tissues is matrix-dependent. Most animal cells secrete mucopolysaccharide matrices that accumulate between cells and help to hold them together. In most epithelia, extracellular matrices are secreted as a layer over the basal surface of the cell sheet where they form a basement lamina. Basement laminae are sometimes fairly stiff and bulky. Their mechanical integrity must have some effect on the shapes of adjacent cells. Extracellular matrices often include aligned fibres which are embedded in a less obviously structured matrix (for example, collagen fibres). There is evidence that the presence of both collagen and certain mucopolysaccharides is required for branching morphogenesis during salivary gland, lung and pancreas development. It has been

suggested that differential patterns of collagen deposition might control various branching arrangements in these tissues (Wessels & Cohen, 1968; Bernfield et al., 1973).

Extracellular materials such as collagen and mucopolysaccharides provide adhesive substrates. It has been suggested that collagen may mark routes of cell migration in most vertebrate embryos (Hay, 1973).

An interesting situation occurs during the growth of goldfish and squirrel fish scales (Byers, Fujiwara & Porter, 1980). Microtubules in adjacent scleroblasts are aligned. Collagen fibres are secreted by the scleroblasts and are oriented in the same direction as the microtubules. It has been suggested that the microtubules orient collagen fibrillogenesis in this instance. Here is a situation where intracellularly co-ordinated cytoskeletal elements seem to orient fibres in the extracellular matrix and the two types of fibres may act in concert to effect intercellular co-ordination for tissue shape control.

6. SELECTION OF MATERIAL FOR SHAPE CONTROL ANALYSIS

Particular situations have been selected for analysis. The reasons for these selections are outlined below.

Studies of oogenesis in a cockroach, Periplaneta americana (Tucker & Meats, 1976), and a gall midge, Heteropaeza pygmaeae (Tucker & Meats, 1976; Went, 1978), indicate that the spatial organisation of follicle cell microtubules with respect to embryonic axes in oocytes is correlated with the shape of these follicles and oocytes. The oocytes studied by these investigators (Tucker & Meats, 1976; Went, 1978) develop in ovarioles of panoistic and polytrophic types.

I have made an attempt here to gain an overall picture of the role of oriented fibre arrays in insect ovarioles generally. Follicle shaping in a panoistic ovariole as well as in a representative of the third type, a telotrophic ovariole, have been examined. Although other investigators have studied the growth of these types of follicles, (for example, Schlottman & Bonhag, 1956; Anderson, 1964; Anderson & Telfer, 1969; Heubner & Anderson, 1970; Ullmann, 1973; Heubner, Tobe & Davey, 1975; Dunlap-Pianka, 1979; Kelly & Telfer, 1979), very little attention has been concentrated on fine structural aspects of shape control. The present study reveals that the situation is more complex than previously supposed and that in P. americana (panoistic type ovariole) and R. prolixus (telotrophic type ovariole) follicle shape is correlated with well-oriented intracellular and extracellular fibre arrays.

During ovulation, oocytes are ejected from ovarioles and from their follicles. Some suggestions about how this may be achieved have been proposed by other investigators (Singh, 1958; Bonhag & Arnold, 1961; Raven, 1961; King & Aggarwal, 1965; Chapman, 1972). Detailed studies of follicles and corpora lutea in P. americana and R. prolixus described here indicate that cell shape changes and cytoskeletal elements are also important during ovulation. These possibilities were not considered by previous investigators.

The developing wing of a holometabolous dipteran insect (Calliphora erythrocephala) was selected for analysis of shape control because Waddington's (1941) studies of Drosophila wing morphogenesis indicate that dramatic cell shape changes are involved during dipteran wing development. Furthermore, several studies (for example, Wehman, 1969; White & Gregory, 1972; Fristrom & Fristrom, 1975; Edwards,

Milner & Chen, 1978) indicate that oriented fibre arrays are present during the initial and final stages of insect wing growth. However, little else has been done to investigate cytoskeletal involvement during wing growth nor has the whole process of wing shape modelling been investigated at the cellular level. The insect wing is especially suitable for such analysis since its principal components, the epidermal cells, are arranged in a single layer throughout the entire growth process. My examinations leave little doubt that the spatial and temporal organisation of cytoskeletal elements within these epidermal cells are intercellularly co-ordinated with striking precision during the growth and shaping of insect wings.

Ciliate micronuclei undergo remarkable elongation during division. This elongation is associated with highly oriented microtubule assembly and elongation within a membrane-bound 'sac' (Tucker, 1967; Jurand & Selman, 1969; Davidson & LaFountain, 1976). The micronuclear envelope remains intact throughout the elongation procedure. Hence the situation is similar to microtubule-associated cell elongation in some respects. Microtubule bundles form intranuclear 'separation spindles' which cause micronuclei to elongate up to ten times their interfission lengths in certain ciliates. Micronuclear division in Paramecium has been investigated because it multiplies rapidly in culture and micronuclear elongation is particularly pronounced in the two species that have been examined.

The information obtained from these studies on the ovarian follicles, corpora lutea and wings of certain insects, and on a ciliate micronucleus reveal some previously undetected ways in which cytoskeletal and extracellular fibres are associated with shape control in these particular situations.

MATERIALS AND METHODS

1 CULTURE PROCEDURES

(a) Periplaneta americana (Dictyoptera)

Female P. americana adults were supplied by Mr. J. Stevenson (Gatty Marine Laboratory, St. Andrews, Scotland). They were maintained in a ventilated glass cage at high humidity and constant illumination, and fed on bran and water.

(b) Rhodnius prolixus (Hemiptera; Reduviidae)

Female R. prolixus in their 4th and 5th larval instars, were obtained from Dr. B.O.C. Gardiner, A.R.C. Invertebrate Physiology Unit, Department of Zoology, Cambridge University, Cambridge, England. They were maintained in an incubator set at 28°C at high humidity (Uribe, 1925; Buxton, 1930). The animals were reared in glass jars covered with gauze. The base of each jar was lined with Whatman No. 1 filter paper. The animals were fed on the blood of New Zealand white rabbits. For this purpose the ears of the rabbits were shaved. The larvae were fed, and moulted to adults. Thereafter the adults were fed every 10 days for 15-30 minutes. Standard feeders were made of a perspex tube with a flanged base and screw-on lid as described by Gardiner and Maddrell, 1972.

(c) Calliphora erythrocephala (Diptera)

C. erythrocephala were obtained in their last larval instar from T. Gerrard and Company, Gerrard House, East Preston, Sussex, U.K. They were kept in ventilated plastic boxes filled with sawdust in a cooled incubator set at 20°C and about 70% relative humidity. The animals

required no feeding and pupated within one or two days of arrival.

(d) Paramecium (Ciliata)

P. primaurelia were obtained from Miss C. McTavish, Department of Zoology, St. Andrews University. P. tetraurelia were obtained from Dr. J. Beisson, Centre de Génétique Moleculaire, Gif-sur-Yvette, France. Organisms were inoculated into a Scotch grass culture medium containing Klebsiella aerogenes (McTavish, personal communication). Cultures were maintained under sterile conditions and sub-cultured every week. They were kept in a cooled incubator set at 25°C in 250 ml flasks.

2 LIGHT MICROSCOPY

Female cockroaches were decapitated and immediately immersed in a physiological saline (Yamasaki & Narahaski, 1959) at room temperature. Whole ovarioles were excised under a Zeiss binocular dissecting microscope using spring scissors and fine forceps. They were pipetted directly onto a slide and covered with a coverslip supported by drops of silicone grease so as not to distort the shape of oocytes and their follicles. Rhodnius prolixus ovarioles were dissected in the same manner except that a different physiological saline was used (King et al, 1956).
Follicles were examined using a Zeiss Universal Microscope fitted with bright field and Nomarski differential interference-contrast optics. Measurements were taken using an eyepiece graticule calibrated against a micrometer slide. Photographs were taken with a Zeiss attachment camera (using a microflash attachment) loaded with Kodak Panatomic-X film.

Calliphora pupae were immersed in a physiological saline (King et al, 1956) at room temperature. Wing imaginal discs or developing wings were excised immediately using spring scissors and fine forceps.

In the case of organisms which had undergone apolysis, the shed pupal cuticle over developing wings was removed. The discs were pipetted into depression slides and covered with a coverslip. Developing wings were examined, photographed and measured using the procedures outlined above. Thick sections (about 1 μm) of Araldite-embedded material (see transmission electron microscopy material preparation) stained with methylene blue (see staining procedures) were photographed using bright field optics and the microflash attachment. The illumination was adjusted to suitable values using neutral density filters. Feulgen stained whole mounts were similarly photographed.

3 STAINING PROCEDURES

(a) Feulgen

Wing imaginal discs and wings at subsequent stages of development were fixed in a 3:1 mixture of absolute alcohol : glacial acetic acid, hydrolysed at 60°C, transferred to Schiffs reagent and washed in SO_2/H_2O and then dehydrated before mounting in euparol on slides. They were then examined using bright field microscopy.

(b) Methylene blue

Araldite-embedded fixed material was sectioned with an LKB ultramicrotome at a thickness of 0.5 - 1.0 μm using glass knives. These 'thick' sections were stained with 1% methylene blue dissolved in a 1:1 mixture of 1% borax : 70% ethanol and examined using bright field microscopy. Material prepared and stained by this method provides a more accurate representation of cell boundaries than paraffin wax-embedded material since the material is relatively free of artifacts eg. pulling apart of cells and tissues, shape distortion and shrinkage.

(c) Dippell's stain

A temporary stain for Paramecium using acetocarmine, acetic acid, HCl and fast green was used according to the method described by Dippell, (1955) in order to follow nuclear changes during cell division.

4. ELECTRON MICROSCOPY

(a) Transmission electron microscopy

The procedure followed for fixation for transmission electron microscopy was the same for all the organisms studied apart from a small variation in the case of fixation of Paramecium which will be discussed below. Ovarioles and imaginal discs were dissected in physiological saline as described for light microscopy. Imaginal discs and developing wings were dissected from pupae at regulated times and were immediately pipetted into phosphate-buffered glutaraldehyde (pH 7.5) and post-fixed in osmium according to the method described by Tucker (1967). Apolysed cuticle was removed to facilitate penetration of fixatives. Whole ovaries were excised from adult P. americana and R. prolixus females and then placed immediately into the glutaraldehyde solution where they were immediately separated by means of spring scissors into unit ovarioles or left intact. Paramecia were pipetted directly from the culture medium into the glutaraldehyde fixative using finely drawn pipettes. Organisms were selected when cleavage furrows were first apparent in organisms examined using a dissecting microscope. Organisms destined for cold treatment were similarly selected but were immediately pipetted into covered embryological watch glasses containing culture medium which had been cooled to $0^{o}C$ in an insulated polystyrene 'Igloo' containing ice chips for one hour. The organisms were shock cold treated in this manner for 30 minutes. Cold treatment was carried out in an attempt to induce the disassembly of certain microtubules (see Chapter 5).

Treatment for periods longer than 30 minutes results in the death of organisms. After cold treatment, the organisms were pipetted directly into the glutaraldehyde fixative. After post-fixation in osmium tetroxide Paramecia were embedded in small discs of 2% agar and then dehydrated as usual.

Ovarioles, imaginal discs, developing wings and Paramecia were embedded in araldite. Thin sections (50 - 60 nm) were cut with glass knives using an LKB ultramicrotome. The thin sections were collected onto formvar or celloidon carbon-coated hexagonal grids and stained for 90 minutes (or 2 hours in the case of the ovarioles) in uranyl acetate, (a saturated solution in 50% ethanol) followed by 2 minutes in lead citrate solution (Reynolds, 1963). The sections were then examined with a Philips 301 transmission electron microscope at 60 kV. Photographs were taken on Ilford type EM-4 film or on glass plates.

(b) Transmission electron microscope calibration

The lattice spacing of crystalline catalase was used to calibrate the magnification settings of the transmission electron microscope in order to obtain accurate assessments of Paramecium spindle microtubule diameters. The method used was one adapted from Wrigley (1968) by Mr Ian Roberts (Scottish Horticultural Research Institute, Invergowrie, Dundee, Scotland). Catalase suspension was fixed in 1% glutaraldehyde at pH 6.5 for 15 - 20 minutes, washed in phosphate buffer, and stained in 2% ammonium molybdate (pH 7.0). The fixed crystals (Fig. 160) were photographed at X 29,000 magnification. Immediately afterwards, stained sections of micronuclear microtubules in Paramecium at all the stages studied were photographed at the same magnification and at the same magnification as that used for the crystals. The magnification of

prints prepared from negatives of crystals was calculated using the following equation:

$$\text{Magnification} = \frac{\text{spacing of N lattice planes on print in } \mathring{A}}{N \times \text{catalase lattice spacing in } \mathring{A} \ (86) \times \text{print enlargement factor}}$$

(c) Scanning electron microscopy

Developing wings were excised as described previously and immediately pipetted into phosphate-buffered glutaraldehyde followed by post-fixation in osmium tetroxide. They were dehydrated in an acetone series and then critical-point freeze dried. The material was then mounted on stubs, sputter coated with gold and examined with a Cambridge Stereoscan S 600. Photographs were taken using an Exacta attachment camera.

CHAPTER 1

CONTROL OF FOLLICLE SHAPING IN THE PANOISTIC OVARIOLES OF PERIPLANETA AMERICANA

INTRODUCTION

When anisometric growth of oocytes and their follicles commences, a sub-surface array of circumferentially oriented microtubules is present in all the follicular epithelial cells along the sides of elongating oocytes in P. americana (Tucker & Meats, 1976). These investigators only examined an initial growth stage. This chapter deals in detail with all the subsequent features of growth and shaping that follow during the production of a mature oocyte, especially in terms of follicular organisation. The examination reveals that shape control is more complex than previously realised. It involves a sequence of modifications in follicular architecture, exploitation of bundles of microfilaments and extracellular fibres, as well as microtubules.

RESULTS

1 FOLLICLE GROWTH

An individual ovariole contains follicles in a single linear array at progressive stages of growth and maturation. Five ovariole regions have been distinguished by previous investigators (Bonhag, 1959; Anderson, 1964) but in this study five growth phases for oocytes and their follicles have become apparent (Fig. 1). Measurement of the diameters and lengths of follicles 1 - 5 in a large sample of ovarioles reveals changes in the relationship with their occupation of ovariole regions 4 and 5 (Fig. 3). For example, oocytes exhibit growth phase 3 followed by phase 4 in region 4, and do not switch to phase 5 until situated in region 5 (Fig. 3).

Thus growth and shaping is more accurately described by using a follicle numbering system in conjunction with the growth phase system (Fig. 3) rather than using the existing ovariole region system.

2 OVARIOLE SHEATHS AND OOCYTES

An individual ovariole consists of a chain of oocytes. Each oocyte is surrounded by follicle cells, and each ovariole is covered by an ovariole sheath. There are no indications that either the oocytes or the ovariole sheaths play a major role in oocyte or follicle shaping because no marked or well-oriented cytoskeletal arrays were detected in oocytes or in sheath cells unlike the situation in follicle cells (see below).

(a) Ovariole sheaths

An external ovariole sheath in P. americana is a cellular sheath covering each ovariole separately (from the germarium to region 5) but is separated from the ovariole by haemolymph. A light microscopical study of ovariole sheaths has been detailed (Bonhag & Arnold, 1961) but as yet the ultrastructure of sheaths has not been described.

An ovariole sheath is an open 'network' of cells composed of anastomosing aggregates of sheath cells of variable shapes connected by cellular strands. Tracheal branches and tracheoles ramify amongst the sheath cells (Fig. 4). The groups of cells, cellular strands, tracheae and tracheoles are all surrounded by an extracellular lamina which varies in thickness from 90 nm - 420 nm (Fig. 5). The cells comprising each sheath contain microtubules, whorls of endoplasmic reticulum, glycogen, lipid droplets, many mitochondria and often bacteria. The orientation of the microtubules within sheath cells is variable (Fig. 6). They probably serve a supportive function. Ovariole sheaths are devoid of muscle cells unlike the ovariole sheaths of some other insects.

(b) Oocytes

A few microtubules have been detected in the ooplasm during growth phase 3, but their orientation is variable. During growth phase 4 and 5, the ooplasm accumulates numerous yolk spheres and protein and no microtubules were found.

3 FOLLICLE CELLS

Each oocyte in regions 3 - 5 is completely surrounded by a follicular epithelium. This epithelium is represented by a single layer of follicle cells along the sides of oocytes. Near the poles of oocytes, the epithelium forms transverse partitions across the ovariole called plugs (Davey, 1965), that separate adjacent oocytes. Each plug is several cell layers deep.

(a) Shapes and dimensions of follicle cells

At the start of growth phase 3, follicle cells are cuboidal in shape with lengths of about 10 μm. At the end of this growth phase and during growth phase 4, the follicle cells have become much more elongate and narrow (length about 20 μm; width about 5 μm). At the start of growth phase 5 the cells become more or less squamous in shape (apico-basal lengths about 20 μm; widths about 30 μm) and vitellogenic channels run between adjacent cells (Anderson, 1964).

(b) Ultrastructure of follicle cells

During growth phase 3 follicle cells contain large numbers of microtubules and microfilaments. These are situated alongside each other just beneath and close to the outer surfaces of follicle cells (those most distant from the oocyte) at the level of the apical desmosomes (Fig. 7). The microfilaments (about 6 nm in diameter) and some of the microtubules are grouped in bundles of varying sizes. Some

microtubules occur 'singly'; they are associated with microfilaments and are situated up to about 0.5 μm from the nearest adjacent microtubule. The longitudinal axes of the microfilamentatous bundles and nearly all the microtubules run circumferentially at right angles to the longitudinal (polar) axes of elongating follicles and their oocytes, and parallel to the outer surfaces of the follicle cells. Some of the tubules and filaments are associated with apical desmosomes (Fig. 8). Others run at right angles to the plane of the outer surfaces of follicle cells alongside the lateral follicle cell membranes (Fig. 9). Microtubules are also found extending along the interiors of interdigitations between adjacent follicle cells. Tubules occur at other levels in follicle cells at a variety of orientations. Such microtubules are sparsely distributed and nowhere do they form a well-oriented and concentrated array like that at the outer surfaces of these cells.

A very similar situation exists in follicle cells during growth phase 4 except that the microtubules and especially the microfilaments are more closely packed together (Figs. 10 & 11). The attachment of the circumferentially oriented filaments to desmosomes (Fig. 12) and to the lateral membranes of adjacent follicle cells provides an interconnected network of filaments throughout the follicular epithelium (Fig. 13).

During growth phase 5, the apical microfilamentous bundles have become reduced in diameter to about 60 nm. The apically situated microtubules and desmosomes are absent. Thin microfilamentous bundles and microtubules (usually occurring 'singly') follow the shapes of the developing vitellogenic channels along the lateral follicle cell membranes (Fig. 14). The structure of these channels has not previously been described ultrastructurally. Channels develop during stage 5 at points

where three cells meet (Fig. 14). Follicle cells also become detached from the tunica propria at such points (Fig. 17). Later on during growth phase 5 the extent of surface detachment from the tunica increases (Fig. 15). Furthermore, at follicle cell bases, the microvilli are withdrawn thus creating a space between the oolemma and the follicular epithelium. Channels are filled with flocculent material (Fig. 16).

(c) Epithelial plug cells

Microtubules and bundles of microfilaments are found at the apices of plug follicle cells directly beneath the tunica propria. The tubules and filaments appear to be intimately associated with lateral follicle cell membranes and run parallel to the outer surfaces of these follicle cells and at right angles to the oocytes' polar axes (Fig. 22).

In addition rather larger bundles of microtubules run alongside the lateral membranes of the cells. They run parallel to the longitudinal axes of the follicle cells, and meet their lateral membranes at various points along the lengths of these membranes (Fig. 23). Large numbers of microtubules run radially within the follicle cells (Fig. 24) i.e. parallel to the longitudinal axes of individual follicle cells and radially with respect to the longitudinal axis of an ovariole. These tubules also meet the lateral membranes at various points (Fig. 25).

4 THE TUNICA PROPRIA

The tunica propria is a basement membrane secreted by the outer surface of the follicular epithelium. It has been described as a structureless membrane covering the ovariole (Bonhag & Arnold, 1961),

but little else is known about it. Longitudinal and transverse sections show that during growth phase 3, the tunica propria has a layered or laminated composition (Fig. 18). At the start of growth phase 3, the tunica is approximately 0.8 μm thick but by the end of growth phase 3 it has increased in thickness to approximately 2.5 μm (Fig. 19).

Longitudinal, transverse and tangential sections of follicles in growth phase 4 reveal fibrous elements about 12 - 14 nm in diameter embedded within the amorphous material of the tunica propria (Fig. 20). Towards the end of growth phase 4, the fibres have become condensed into a layer about 2 μm thick on the side of the tunica nearest the follicular epithelium. The fibres are mainly oriented circumferentially in directions at right angles to the polar axes of oocytes and parallel to the outer surface of the follicular epithelium. Some fibres are grouped into bundles up to 30 nm in diameter (Fig. 20).

During growth phase 5, the tunica propria becomes further differentiated but reduced in thickness to about 0.75 μm (Fig. 17). The thickness of the fibrous layer becomes reduced from about 2.5 μm to about 0.5 μm. The largest fibres are up to 36 nm in diameter, and have a cross-banded appearance (Fig. 21) (periodicity of about 15 nm). Smaller fibres of about 12 - 14 nm in diameter are found amongst the larger fibres.

An additional layer within the tunica propria that is not included during earlier growth phases, is present during growth phase 5. This granular layer is about 0.25 μm thick and extends over the fibrous layer on the side of the tunica furthest away from the follicular epithelium. Sections at a variety of orientations reveal

that the granules really are spherical in shape and that the circular profiles shown in Figure 21 do not represent cross-sections of fibres. The granules are about 25 - 30 nm in diameter with a centre-to-centre spacing of about 50 - 70 nm and are separated by low density material.

DISCUSSION

1 TENSION TRANSMISSION AND FOLLICLE GROWTH

The results presented above show that oocytes and follicles grow anisometrically as they pass posteriorly down the ovariole. It is possible that oocytes and follicles elongate purely as a result of forces generated and directed from within oocytes by cytoskeletal elements which have not yet been detected. However, most elongating animal cells contain well-oriented microtubule arrays (Byers & Porter, 1964; Tilney & Gibbins, 1969; Burnside, 1973; Warren, 1974; Tucker, 1979). Alternatively, shape could be controlled or influenced by elements outside the oocyte.

The oocyte is contained within three structures; the ovariole sheath, the tunica propria and the follicular epithelium. The structure of the ovariole sheath is such that it probably does not influence follicle and oocyte shape changes. In contrast, the tunica propria and follicular epithelium appear to play major roles in follicle and oocyte shaping. Circumferentially oriented arrays of cytoskeletal elements and extracellular fibres are formed in the follicle cells and tunica propria, respectively, during anisometric growth.

The shape changes during the anisometric growth of elongating

follicles have been described here in terms of five growth phases. Histological and ultrastructural examinations of follicles indicate that changes in follicle cytoarchitecture and in the composition of the tunica propria are correlated with transitions between the 'anisometric' growth phases (3 - 5).

During growth phase 3 a system of circumferentially arranged microtubules and microfilaments in association with desmosomes is situated at the outer surface of follicle cells. This arrangement is such that the microtubules, microfilaments and desmosomes could provide a cytoskeletal mechanical continuum between and within follicle cells. This might be capable of transmitting tension circumferentially throughout the follicular epithelium thereby restricting growth of the follicle perpendicular to the polar axis of the oocyte. If this is the case, follicles would therefore become more elongate in a direction which parallels the polar axis of the oocyte.

Examinations of a wide range of cell types indicate that microtubules are rigid cytoskeletal elements (Tucker, 1968; Ockleford & Tucker, 1973) which are capable of transmitting tension and compressive forces along their lengths (Ockleford, 1974; Tucker, 1974). These properties are exploited in many instances in which oriented microtubule arrays are involved in defining and maintaining the shapes of individual cells and cell processes (Tilney, 1968; Burnside, 1971; Poodry & Schneiderman, 1971) by imparting stiffness to certain cell regions. Ultrastructural and experimental analyses of Heteropeza pygmaea follicles have provided evidence that desmosomes and circumferentially oriented microtubules within the

follicular epithelium of these gall midges form part of a mechanism defining the elongate shape of follicles and oocytes (Tucker & Meats, 1976; Went, 1978). In P. americana an additional cytoskeletal contribution in the form of interlinked bundles of circumferentially oriented microfilaments in association with the microtubules and desmosomes is present. The microfilaments may be responsible for active production of tensile forces in the circumferentially oriented intercellular cytoskeletal complex. Possibly microfilaments act similarly in Heteropeza but were not detected.

During growth phase 4, the volume of the follicles increases markedly (from about 1 mm^3 to about 6.5 mm^3). In order to accommodate this size increase and yet maintain and create further elongation of the follicle, there is a change in the composition of the tunica propria, and a change in follicle cell shape.

Follicle cell shape changes from cuboidal to columnar during the transition from growth phase 3 to growth phase 4. The columnar shape is somewhat surprising since the volume of the oocyte increases considerably; one would expect the follicle cell shape to become flattened or, if cell division is occurring, to remain cuboidal. Bonhag (1959) reports that in Region 4 (during growth phase 3) cell division is continuous; spindle axes are always oriented in the plane of the epithelium. However, at the posterior end of Region 4 (as growth phase 4 begins) mitotic spindles lie perpendicular to this plane and nuclear divisions are not followed by cytokinesis. Bi- and multinucleate cells are produced. Since cell volume remains fairly constant during the change from cuboidal to columnar, these nuclear divisions could be responsible for columnar shaping of the follicle cells because the additional nuclei have to be accommodated one above the other relative to the oocyte surface.

The tunica propria is juxtaposed against the outer surface of the follicular epithelium which secretes it (Bonhag & Arnold, 1961). Circumferentially oriented fibrous elements in the matrix of the tunica propria are first detectable as the oocyte enters growth phase 4. This is in contrast to the uniformly laminated non-fibrous tunica propria of growth phase 3. The tunica also becomes reduced in thickness as this occurs. This is perhaps because of stretching due to the increase in volume of the enclosed follicle and oocyte. The composition of insect connective tissues has been reviewed by Ashurst, (1968) and Smith, (1968). Many indications of the presence of fibrils within insect basement laminae have been reported. Chemical and autoradiographic studies of insect basement laminae suggest that the filamentous component of the basement lamina is collagen (Fawcett, 1966). Fibril diameters vary in different insect species (Smith & Treherne, 1963). Fibres with the greatest diameters (30 - 40 nm) are usually cross banded (Ashurst, 1968); smaller fibres (diameters from 6 - 20 nm) are usually non-banded (Ashurst & Chapman, 1961; Beaulation, 1968; Locke & Huie, 1972). Secretion of small fibres usually precedes that of larger fibres in basement laminae that finally include both small and large fibres (Ashurst & Costin, 1974). This is the situation found in the tunica propria of P. americana. The occurrence of fibres and their structural resemblance to the fibres observed in other insect species strongly supports the hypothesis that collagen is present in the tunica propria of P. americana although additional evidence is necessary to substantiate this assumption. Biochemical, X-ray and autoradiographic researches are limited mainly by the difficulty of isolating collagen from the tunica propria. Whether collagenous or elastic in nature, the 'scaffolding' arrangement of such fibres would have obvious mechanical

importance to the gross form of the tunica. The fibres only appear during growth phase 4 when the follicle is about 900 µm in length and 360 µm in diameter. This implies a correlation between size and the presence of fibres. De Biasi and Pilotto (1976) found a correlation between body weight and structure of neural lamellae in various dipterans. Bundles of collagenous fibres only appear in species of larger size. This would support the idea of a structural or mechanical role for the tunica propria fibres.

During growth phase 5 anisometric growth continues until the follicle attains the shape of a prolate spheroid. Oocyte volume increases dramatically (from 6.5 mm^3 – 19.5 mm^3). Mitotic divisions of follicle cells cease and follicle cells change in shape from columnar to squamous. Vitellogenic channels that pass between adjacent follicle cells become established. Concommitantly, follicle cells lose the organised circumferential sub-surface arrangement of microtubules, microfilaments and desmosomes which is so marked during growth phases 3 and 4. If the interlinked microtubules, microfilaments and desmosomes are involved in tension transmission between follicle cells, their loss would cause the follicle cells to flatten and assume the characteristic squamous shape of follicle cells during growth phase 5. The loss of apical desmosomes may also aid in the development of vitellogenic channels.

Although the circumferential sub-surface arrangement of microtubules, microfilaments and desmosomes is lost, circumferential tunica propria fibres are present by this time and also an additional layer has developed in the tunica, although the latter has decreased in thickness. With the onset of vitellogenesis, oocyte volume increases and this presumably stretches the tunica propria and may create considerable

tension in the latter. The fact that the tunica contracts appreciably after ovulation strongly indicates that this is so. The tension in the tunica propria might be resisted by the granular as well as the fibrous layer. The granular layer might be more pliable than the fibrous layer and help to prevent disruption of the fibrous layer as oocyte volume increases. A granular layer has not previously been reported for the tunica propria of any other insect. Dense granules (diameter 50 nm) have been found amongst fibres in the basement lamina of the developing chick neuro-epithelium (Cohen & Hay, 1971). These 'interstitial granules' are thought to be precursors of the fibrillar components of the matrix. Although similar in size and appearance to those of the tunica propria in P. americana, the latter granules only appear after the production of fibres in the tunica.

2 THE 'FOLLICLE-TUNICA' SEQUENCE DURING ANISOMETRIC OOCYTE GROWTH (FIG. 26)

During growth phase 3, circumferential resistance to follicle growth is apparently provided by a cytoskeletal system of microtubules, microfilaments and desmosomes. During growth phase 4, the addition of circumferential fibrous elements to the tunica propria could also contribute circumferential resistance to follicle growth as oocyte volume increases, and compensate for the loss of the intracellular system during growth phase 5. The vitellogenic channels would probably impair the effectiveness of a microtubule-microfilament system at this stage so that circumferential resistance to follicle growth is seemingly provided by the tunica propria alone. The addition of an outer granular layer to the tunica at this time may be mechanically significant in this context.

CHAPTER 2

CONTROL OF FOLLICLE SHAPING IN THE TELOTROPHIC OVARIOLES OF RHODNIUS PROLIXUS

INTRODUCTION

A circumferential tension transmitting cytoskeletal system is apparently operating in some, and perhaps all, panoistic and polytrophic ovarioles during oogenesis (see Chapter 1). It was therefore necessary to examine an example of the third group of ovariole-types, the telotrophic ovarioles, to ascertain whether they also operate a similar system. This chapter deals with fibre arrays that seem to influence follicle shape during the production of mature oocytes in Rhodnius prolixus. It reveals that although shape control is different from that in P. americana in some respects, an intercellularly coupled system of cytoskeletal fibres is also present.

RESULTS

1 OVARIOLE ORGANISATION

Since the telotrophic ovariole has no germarium once the adult condition is reached, no new oocytes are produced. Shortly after the last nymphal moult, the ovarioles of adults have their full complement of oocytes located at the base of the tropharium. Thus, complete developmental sequences are never present within one organism at any one time. Measurements of the diameters and lengths of all follicles in a large sample of ovarioles removed from adult females reveal changes in the relationship of these two parameters that correlate with pre-vitellogenic and vitellogenic growth (Figs. 27 & 28).

2 FOLLICLE FINE STRUCTURAL ORGANISATION

A detailed cytological study has been conducted for R. prolixus ovarioles by Heubner and Anderson, (1972 a, b and c). The account which follows deals mainly with structures that are apparently concerned with follicle shaping. Most of these structures were not examined in detail by Heubner and Anderson.

(a) The tunica propria

During early previtellogenic growth, the tunica propria is about 320 nm thick. By late previtellogenesis the tunica is reduced in thickness to about 255 nm, and during vitellogenesis is further reduced to 95 nm (Figs. 29, 30 & 31). Throughout growth of the tunica propria, its composition remains fairly constant. Fibrous elements ramify between the amorphous material of the tunica. The fibres are concentrated into a layer up to 128 nm thick on the side of the tunica nearest the follicular epithelium. Fibres are often grouped into bundles that are 25 - 30 nm in diameter. The fibres are mainly oriented circumferentially in directions at right angles to the polar axes of oocytes and parallel to the outer surface of the follicular epithelium (Figs. 32 & 33).

(b) The follicle cells

During previtellogenic growth, bundles of microfilments that are about 300 nm in diameter are apparent at the apex of each cell directly beneath follicle cell outer surfaces (Fig. 29). Bundles are oriented circumferentially at right angles to oocytes' polar axes and parallel to the outer surfaces of follicle cells. Microtubules with the same orientation occasionally interdigitate between the microfilament bundles (Fig. 32). Microtubules also run parallel to the long axes of cells (Fig. 34). These may help to maintain the columnar shape of follicle cells (Heubner & Anderson, 1970; 1972 a).

The outer surfaces and apical lateral membranes of follicle cells are highly irregular in shape. Filopodial cell extensions that are about 190 nm in diameter project from follicle cells. Microfilament bundles extend along the interiors of these extensions (Fig. 35).

At the bases of follicle cells, the plasma membranes of adjacent cells are connected by desmosome complexes. These include septate desmosomes, gap junctions and desmosomes of the zonula adhaerens variety (Fig. 36). At the level of these basal zonula adhaerentes, and closely associated with these desmosomes, microfilament bundles (about 300 nm thick) extend across each cell (Fig. 37). Nearly all of the bundles are circumferentially arranged. The microfilaments run parallel to the outer surfaces of follicle cells and at right angles to the polar axes of oocytes. The same arrangement of desmosomes and microfilament bundles occurs throughout previtellogenesis although during late previtellogenesis (when follicles are about 600 µm long) the follicle cell/oocyte boundary becomes 'peaked' (Fig. 38). The 'peaks' occur at the point where adjacent follicle cells meet each other. In these instances, the microfilament bundles extend from 'peak' to 'peak'. Basal microfilament bundles are only found in elongating follicles. Very early previtellogenic follicles are spherical. Their follicle cells do not have basally positioned microfilament bundles.

Vitellogenic oocytes (about 1100 µm - 2000 µm in length) are distinguished by the presence of channels between follicle cells (Fig. 39). These channels are extracellular spaces that are widest (about 3 - 5 µm) at the extreme outer and inner surfaces of the epithelium (Figs. 40 & 41). Channels only form between follicle cells along the sides of oocytes while those cells which form the cap or apical region of a follicle are longer and closely apposed to one another. Thin bundles of microfilaments

(about 120 - 130 nm thick) follow the margins of the developing vitellogenic channels along cell membranes at the sides of follicle cells (Figs. 42 & 43).

Along the sides of follicles, cells retain their association with each other, despite the presence of channels, via cell surface projections. Bundles of microfilaments extend along the interiors of these projections. Projections from the outer surfaces of follicle cells approach the tunica propria as is the case during earlier stages of oogenesis (Fig. 44) while those from the inner surfaces of follicle cells approach the oolemma (Fig. 45).

The large apical and basal microfilament bundles observed in follicle cells of previtellogenic oocytes are absent during vitellogenesis.

DISCUSSION

The results presented above show that oocytes and their follicles grow anisometrically as they pass posteriorly down the ovariole. Furthermore, there are changes in the cytoskeletal organisation of follicle cells during the transition from previtellogenic to vitellogenic growth of oocytes (Fig. 46). This may be an indication that the follicle cells are closely involved in follicle shaping. There are no indications that the oocytes and the ovariole sheaths play a major role in follicle shaping. For example, the oocyte contains no well oriented cytoskeletal arrays. The two ovariole sheaths are contractile (Heubner & Anderson, 1972 a). However, each sheath is a reticular network of cells separated from one another and from the follicles by haemolymph. Any tension transmitted from myoepithelial cells to follicles via the haemolymph could provide 'corset-like' support to follicles but it is doubtful whether they play a major role in follicle shaping.

Instead, follicular resistance to circumferential expansion may be

largely responsible for defining the elongate form of R. prolixus oocytes. Most oocyte elongation occurs during the period preceding vitellogenesis (de Wilde & Loof, 1974). During previtellogenesis, a system of circumferentially oriented microfilaments and specialised junctions is situated at both the outer and the inner surfaces of follicle cells. The arrangement of microfilaments is such that they may be responsible for the active production of tensile forces between and within follicle cells. There is evidence that cytoplasmic contractile proteins may function as a cytoskeletal system in the cytoplasmic matrix (Pollard, 1976). Microfilaments found in Drosophila melanogaster follicle cells have been found to bind to heavy meromyosin (Wellings, J.V., Personal Communication). This reveals that the microfilaments are actin filaments and therefore probably act in conjunction with myosin to produce a contractile effect. It is highly likely that the microfilaments observed in R. prolixus follicle cells are similarly composed although further experimentation is necessary to substantiate this. The 'peaked' arrangement of follicle cell bases of late previtellogenic follicles may be an indication of tension production. The circumferential tension could be distributed throughout the follicular epithelium (the cytoplasmic projections may play a supporting role in this respect) thereby restricting circumferential expansion of the follicle. If this is so, follicles would become more elongate in directions which parallel the polar axis of the oocyte.

The results show that the growth of follicles during vitellogenesis is virtually isometric. The vitellogenic channels would obviously impair the effectiveness of the previtellogenic microfilament/junction system, so during vitellogenesis, circumferential resistance to follicle growth is apparently provided by the tunica propria alone. This would account for the less marked resistance to circumferential growth observed

during vitellogenesis as compared with previtellogenesis. It is not known to what extent organised, oriented extracellular structures, such as the fibrous tunica propria, are responsible for the form and integrity of the cellular systems they clearly support. However, it is generally supposed that extracellular fibres confer rigidity in maintaining shape permitting the range of cell action to extend in space far beyond that of a single cell.

Circumferential systems have been found in all follicles that have been selected with a view to examining examples of each of the three ovariole types as shown in Table 1. Therefore, presumably most insect follicles have such a system. It is interesting that a circumferential system of both microtubules and microfilaments appear to be utilized during P. americana follicle elongation, whereas a circumferential system consisting predominantly of microfilaments (circumferential microtubules are rarely encountered) is apparently utilized during R. prolixus follicle elongation. Microtubules do occur in telotrophic ovarioles where they act in other developmental capacities. For example, microtubules apparently facilitate ribosomal flow in nutritive tubes of R. prolixus (McGregor & Stebbings, 1970; Stebbings & Bennett, 1975).

All this fine structural evidence for follicular control of oocyte shaping and elongation in P. americana and R. prolixus is circumstantial. However, experimental support has been provided by Went, (1978) for Heteropeza pygmaea. Oocytes grow isometrically and fail to elongate when they develop in vitro after treatments which prevent the enclosure of oocytes by a follicular epithelium.

TABLE 1 CIRCUMFERENTIAL FIBRE ARRAYS OF INSECT EGGS

OVARIOLE TYPE	INSECT STUDIED	CIRCUMFERENTIAL SYSTEM COMPONENTS	REFERENCE
Panoistic	*Periplaneta americana*	i Microtubules ii Microfilaments iii Extracellular Fibres	Chapter 1
Telotrophic	*Rhodnius prolixus*	i Microfilaments ii Extracellular Fibres	Chapter 2
Polytrophic	*Heteropeza pygmaea* (Paedogenic)	i Microtubules	Tucker & Meats, (1976) Went (1978)
Polytrophic	*Drosophila melanogaster*	i Microfilaments	Wellings, J.V. (Personal Communication)

CHAPTER 3

THE MECHANISM OF OVIPOSITION AND CORPUS LUTEUM FORMATION IN THE PANOISTIC OVARIOLES OF P. AMERICANA AND THE TELOTROPHIC OVARIOLES OF R. PROLIXUS

INTRODUCTION

The passage of the oocyte from the ovariole into the oviduct is one of the main ovulatory events in insects. It involves the escape of an oocyte from the follicular epithelium and the breakdown of the epithelial plug at the entrance to the oviducal pedicel. Virtually nothing is known about the means by which these events are effected (Davey, 1965). Various theories have been proposed to account for the posteroid movement of oocytes in the ovariole and their subsequent release. These theories include 'crowding' (Raven, 1961), muscular peristalsis of myoepithelial cells of the ovariole sheaths (King & Aggarwal, 1965; Chapman, 1972), and elastic action on the part of the tunica propria (Singh, 1958; Bonhag & Arnold, 1961; Chapman, 1972). However, it seems likely from my studies that no one of the factors described above is entirely responsible and that, in addition, cytoskeletal elements and extracellular fibres may also be involved. It seems that follicle cell cytoskeletons may be concerned with propulsion of oocytes into oviducts (after helping to define oocyte shaping in certain insects) and that they adopt new configurations to accomplish this task as they enter a post vitellogenic phase of mechanochemical activity.

RESULTS

1 POST-VITELLOGENESIS

Little is known about what brings about the cessation of vitellogenesis and the onset of chorion deposition (Heubner & Anderson, 1972a). However,

changes in the follicular epithelium occur in close temporal association with these events, which contrast with those observed during vitellogenesis.

(a) Rhodnius prolixus

When oocytes attain lengths of about 1.9 mm they enter a post-vitellogenic phase. Vitellogenic channels become occluded and the follicle cells become low columnar in shape (25 - 30 μm in length). The ovariole sheath lies very close to these post-vitellogenic follicles. It is separated from it by a gap of about 0.25 μm (Fig. 47). Evidence for two distinct layers of sheath cells such as those referred to by Heubner & Anderson, (1972 a) are not clearly apparent in electron micrographs (Fig. 47). As in vitellogenic oocytes, follicle cells are connected to adjacent follicle cells by means of cell interdigitations. Microfilaments extend along the interiors of such interdigitations. Unlike the situation in follicle cells of vitellogenic oocytes, discrete bundles of circumferentially oriented microfilaments occur at intervals beneath the outer surfaces of follicle cells. Lateral membranes of follicle cells are very convoluted in shape (Fig. 48).

(b) Periplaneta americana

At the time of vitelline membrane formation follicles are about 4 mm in length. As during stage 5, follicle cells are squamous in shape. However, vitelline channels are much reduced in size. Many microtubules are situated directly beneath the outer surfaces of follicle cells contrary to the situation during stage 5. The microtubules are circumferentially oriented parallel to the outer surfaces of follicle cells, and at right angles to the oocytes' polar axes (Fig. 49). Furthermore, groups of microfilaments occur at intervals directly beneath follicle cell outer surfaces.

Once chorion formation has begun, fixatives and resins do not penetrate into the oocyte. Because of this, thin sectioning is not feasible and hence chorionated follicles just prior to ovulation were not studied.

2 CORPUS LUTEUM FORMATION

After the release of a terminal oocyte, the remaining follicle (i.e. the follicular epithelium and tunica propria) is situated at the base of the ovariole where it forms a corpus luteum. In spite of a considerable reduction in volume of the space previously occupied by the oocyte, no crumpling of the follicular epithelium takes place. Neither is the epithelium separated from the tunica propria. However, the tunica is highly folded. This is an indication of the contraction of the follicle and is a situation peculiar to post-ovulation tunica propria. In P. americana both an outer granular and an inner fibrous layer are present as in stage 5 (Fig. 50). In R. prolixus too, the inner fibrous layer is present as in follicles prior to ovulation (Fig. 51). However, there is evidence that some degeneration of the tunica propria layers occurs in 'old' corpora lutea where the folds of the tunica propria become more conspicuous because of secondary folding (Fig. 52 & 53).

Many of the cells of the corpus luteum undergo pyknotic degeneration and exhibit large nuclei in various stages of autolysis. The degeneration appears to begin at the centre of the corpus luteum and then proceeds outwards towards the tunica. The signs of degeneration are clearly apparent too, in the cytoplasm (Fig. 55).

More importantly, microtubules are very conspicuous in cells not yet showing signs of degeneration. Large numbers of microtubules run

parallel to the long axis of each cell in both P. americana and R. prolixus (Figs. 56 & 57). Longitudinal and transverse sections indicate that the microtubule orientation is radial with respect to the longitudinal axis of the corpus luteum. In P. americana, in addition to the radially oriented microtubules there are circumferentially oriented microtubules. These occur directly beneath and parallel to the outer surfaces of follicle cells, and at right angles to the longitudinal axis of the ovariole (Fig. 58). Although circumferentially oriented microtubules occur prior to ovulation in P. americana, radially arranged microtubules are peculiar to post-ovulation follicle cells. Radially arranged microtubules in R. prolixus are also unlike the situation prior to ovulation.

As in the follicle cells of P. americana and R. prolixus prior to ovulation, cells of the corpus luteum contain bundles of microfilaments directly beneath their outer surfaces (Figs. 58 & 59).

A diagrammatic representation of the situation prior to, and after, ovulation in P. americana and in R. prolixus is shown in Figure 60.

DISCUSSION

A continuous and rhythmic reproductive cycle has been observed in P. americana (Bell, 1969; Maa & Bell, 1977). This cycle is thought to be controlled in part by an endogenous 'clock-like' mechanism within ovarian follicles (Maa & Bell, 1977). In R. prolixus, ovulation is not synchronous for different ovarioles within the same individual (Heubner & Anderson, 1972 b). Ovulation must therefore be controlled by a mechanism within each ovariole. The mechanism is very probably an active process since ovulation only occurs once the oocyte is fully mature, i.e. when the chorion is completed. The follicle does not increase in size

during chorionation since the chorion develops within the 'space' between oocyte and follicular epithelium. The volume occupied by the oocyte during this stage is constant. Something must be driving the oocyte down into the oviduct, and it seems that the follicle is involved.

The tunica propria of the corpus luteum becomes highly folded. It has been suggested (Singh, 1958) that ovulation in Locusta migratoria is followed by 'progressive contraction of the tunica propria through the formation of secondary folds'. However, there is no known case of actively contractile extracellular fibres. The presence of cytoskeletal elements within cells previously practically devoid of these elements and during a time when oocyte growth has ceased is significant. There is a strong case for proposing that the follicular epithelium becomes actively contractile as it enters a new phase of cytoskeletal co-ordination. The radial orientation of microtubules (in follicle cells of corpora lutea) may be responsible for the elongated shape of follicle cells in corpora lutea compared with follicle cells prior to ovulation. The latter are squamous (P. americana) or low columnar (R. prolixus) in shape and contain no microtubules parallel to their long axes. Microtubules are spatio-temporally associated with cell elongation in a wide range of cell types (Renaud & Swift, 1964; Tilney & Porter, 1967). Any necessary increase in lateral membranes is already present; follicle cell boundaries are highly convulated prior to ovulation. This change in cell shape throughout the follicular epithelium in a direction at right angles to the fairly rigid chorionated oocytes' polar axes, together with aid from a tunica propria, which is perhaps elastic and under tension prior to oocyte discharge, might create the necessary force required to discharge an oocyte. Assistance may be provided by the circumferentially oriented microfilaments at the apices of follicle cells.

In R. prolixus, the ovariole sheaths contain myoepithelial cells. Since the ovariole sheaths lie very close to mature follicles, they may also assist in the process of ovulation. The ovariole sheath of P. americana contains no myoepithelial cells or any other contractile elements and therefore probably exerts no direct force on follicles but rather offers a corset-like support to the ovariole.

The possibility remains that oocytes are released purely as a result of the breakdown of the epithelial plug which separates follicles from the pedicel perhaps by muscular contraction or peristalsis of the pedicel and/or oviduct. However, how would these elements 'know' when oocytes are mature? It seems more likely that the epithelial plug is actively 'broken through' by the combined forces exerted on the rigid chorionated egg by the tunica propria, cytoskeletal elements within the follicular epithelium, and in some cases a muscular ovariole sheath. Thereafter crowding (Raven, 1961) and the elastic nature of the tunica propria (Singh, 1958; Bonhag & Arnold, 1961; Guthrie & Tindall, 1968; Chapman, 1972) may effect the posteriad movement of follicles down the ovariole.

The versatile nature of the follicular epithelium is once more apparent. It seems that the follicular epithelium prior to ovulation contains cytoskeletal arrays which appear to be spatially and temporally co-ordinated for shape control during the production of mature oocytes, but that once oocytes are fully mature, the follicular epithelium enters a new phase of cytoskeletal co-ordination concerned with the discharge of the mature oocytes.

CHAPTER 4

SPATIO-TEMPORALLY CO-ORDINATED EPIDERMAL CELL SHAPING DURING WING DEVELOPMENT IN CALLIPHORA ERYTHROCEPHALA

INTRODUCTION

Waddington's (1941) examination of wing development in Drosophila melanogaster indicates that epidermal cells undertake a remarkable sequence of shape changes as the compact highly folded imaginal wing disc expands during pupation to form a flattened blade-like adult wing. The sequence is apparently more complex than any other reported for an epidermis during embryogenesis. The initially very elongate cells shorten, then re-elongate by producing fine basal extensions. These subsequently shorten, and finally cell bodies flatten, but yet again produce basal extensions. Such material therefore provides an excellent opportunity to examine the ways in which the shaping of individual cells is related to overall changes in epidermal shape and surface area, and the ways in which changes in cytoskeletal organisation and cell contact are spatially and functionally co-ordinated with cell and tissue shaping. Waddington's account was based on light microscopical examination of sections of paraffin wax embedded material. It did not provide the information required to tackle all the issues raised above. This chapter provides such information for wing development in Calliphora erythrocephala. The information has been obtained by a detailed examination of the morphometrics, histology, and ultrastructure of the wing epidermis as an imaginal disc is converted into an adult wing.

Studies on the development of Calliphora wing discs are not extensive (Lewerenz, 1961; Agrell, 1966, 1968; Sprey, 1970; 1971; Sprey & Oldenhave, 1974; Vijverberg, 1974 a, b). These authors have con-

centrated mainly on light microscopical investigations of larval discs or very early stages in evagination. No ultrastructural studies of developing Calliphora wings have been published.

RESULTS

1 THE MAIN STAGES OF WING EPIDERMAL SHAPING, EXPANSION AND GROWTH

The development of the wing of C. erythrocephala at 20°C (from the start of puparium formation to emergence of the adult) occurs in about 14 days. The duration of the morphogenic events reported below is approximate since the time course of development varies from one disc to another and between individual organisms. The criteria used to distinguish puparium formation were: cessation of locomotory movements, eversion of the anterior spiracles, and shortening of a larva as it adopts a barrel-like shape characteristic of the puparium. Puparium formation was designated as time 0 hours. As development proceeds, there is a well defined temporal sequence of distinct stages (Table 2).

At the start of puparium formation (0 hours) the wing disc has a proximo-distal length of approximately 1.5 mm, and is folded in a characteristic way (Fig. 61). Three main parts can be distinguished (Fig. 62). This study has been confined to the distal part of the wing disc which forms the wing blade. It is approximately 0.5 mm long.

For the first 20 hours after the initiation of puparium formation, a progressive outgrowth of the wing imaginal disc occurs within the constraints of the peripodial membrane. The process is known as evagination or eversion. The term is somewhat confusing since there is no actual evagination. The process merely involves shape modifications of an existing epidermal 'sac' (Fig. 64).

At about 4 hours, a concave region known as the wing pouch can be

TABLE 2 TABLE OF THE DEVELOPMENT OF THE WING OF C. ERYTHROCEPHALA FROM THE START OF PUPARIUM FORMATION TO ECLOSION

STAGE	HOURS AFTER THE START OF PUPARIUM FORMATION	MORPHOGENETIC EVENTS
1	1 - 20	Development, extension, and dorso-ventral flattening of wing pouch. Formation of an epidermally bilayered wing blade.
2	21 - 22	Loss of peripodial membrane. Secretion of pupal cuticle begins.
3	24 - 36	Further expansion and flattening of wing blade. Formation of prepupal veins.
4	36 - 40	Wing blade swells.
5	48 - 50	Apolysis.
	90 - 96	Re-flattening of wing blade and re-formation of a compact epidermal bi-layer. Formation of pupal veins. Adult cuticle secretion begins.
6	96 - 120	Differentiation and formation of adult cuticular structures.
7	120 - 264	Expansion and folding of wing blade within pupal cuticle
8	264 - 336	Pigmentation of cuticular structures. Adult cuticle deposition completed.
9	336	Eclosion.

seen (Fig. 65). This pouch extends distally and protrudes further into the peripodial cavity (Fig. 66). It abutts on the peripodial membrane (Fig. 67). Concommitantly, the epidermal layers on opposite sides (putative dorsal and ventral layers of the wing) of the wing pouch become more closely situated, and finally make contact to form an epidermal 'bilayer', in which the basal portions of epidermal cells are juxtaposed (see later) (Fig. 67). The bilayer forms progressively, starting at the most distal region of the disc which becomes the wing tip (Figs. 62 & 63).

From about 16 - 20 hours, the elongating wing disc begins to bend. The wing appears to twist on its axis so that when it escapes from the peripodial membrane, the wing now lies in a cephalocaudal direction with respect to the larval body (Fig. 68).

Stage 2 marks the point in time at which the peripodial membrane is no longer detectable. (It apparently ruptures and breaks down. See later). The wing is a thickened blade-like structure 1.3 mm in length which is oval in transverse section (Figs. 69 & 70). The lacunae of the presumptive prepupal veins can be distinguished (Fig. 70) and secretion of the pupal cuticle begins.

Stage 3 occurs from about 24 - 36 hours. The wing rudiment becomes transformed very rapidly into a thin flattened blade-like structure about 2 mm long (Fig. 71). The wing continues to flatten, more slowly than at first, and during this stage eventually reaches a length of about 2.6 mm. During stages 1 - 3, wing length increases from about 0.5 mm to about 2.6 mm, whereas the width only increases from about 0.7 mm to about 1 mm. The prominent features of this stage are expansion and flattening. The wing is thin enough for whole mounts to be fairly transparent so that the prepupal veins are clearly apparent (Fig. 71).

At about 36 hours, the pupal head is everted. This marks the beginning of the pupal period (Robertson, 1936). At this time, the wing blade increases in thickness. The whole blade swells markedly (Fig. 72). It has the appearance of a hollow bag lined by epidermal cells (see later). The prepupal veins are no longer apparent. Dissection of the wings at this stage proves difficult as the wings and the rest of the organism are covered with a sticky substance. This may be an end product of larval tissue breakdown or is perhaps related to pupal cuticle secretion.

Apolysis occurs between 48 and 50 hours. The detached pupal cuticle remains throughout further pupal development and encloses the developing wing blade.

From about 50 - 96 hours after puparium formation, during stage 5, the wing blade again flattens into a thin blade-like structure and lies freely within the pupal cuticle (Fig. 73). The flattened blade is approximately the same size, in terms of length and width as the swollen wing blade of stage 4. The dorsal and ventral epidermal layers become closely juxtaposed again, and the pupal veins become apparent (Fig. 74). During this bi-layer formation the outline of the wing undergoes certain subtle changes which bring it into the adult shape. Deposition of the adult cuticle begins.

About 3 days (72 hours) after the onset of puparium formation, specialised wing cuticular structures are apparent.

From 4 - 10 days (stage 7) the surface area of the wing again increases, eg. wing length increases from 4 mm to the final adult length of 9 mm. Since the pupal cuticle imposes size restrictions on the developing wing, the wing blade becomes folded in a characteristic manner within the pupal cuticle (Fig. 75). The characteristic feature of

stage 7 is expansion. The ultimate size of the adult wing is reached during this stage.

From 11 - 14 days (stage 8) pigmentation of cuticular structures and the final deposition of adult cuticle occurs.

Eclosion occurs about 14 days after the onset of puparium formation (stage 9). The wing unfolds and becomes sclerotised (Fig. 76).

2 STAGE 1: THE PSEUDOSTRATIFIED EPIDERMIS

The terminology used in the following account is shown in Figure 77. The portion of the wing imaginal disc which will become the adult wing is almost entirely composed of epidermal cells (apart from haemocytes present within the haemocoel). The epidermal cells which comprise the peripodial membrane are organised into a single layer of mainly squamous cells. In contrast, epidermal cells of the disc proper are organised into a pseudostratified layer about 110 μm thick (Fig. 78). Individual cells are spindle shaped. The portion of cell at the level of the nucleus is the widest region (about 10 μm in width) along the length of each cell. Each cell spans the entire thickness of the epidermal layer. The nuclei of these cells are arranged at different levels within the pseudostratified layer, but most nuclei were observed in the basal halves of cells. Those nuclei situated near the apical surface of the epithelium were dividing (Fig. 79). All mitoses were confined to this level. Above and below the nucleus in each cell are long cell extensions. One process extends inwards from the nucleus to the basement lamina. (The basement lamina is 4 - 6 nm thick and has an amorphous appearance (Fig. 84)). The other process extends outwards from the nucleus to the outer surface of the wing disc. The extensions contain microtubules which are oriented parallel to the long axis of the

cell (Fig. 81). Epidermal cells are closely packed with no intercellular spaces. Septate desmosomes join adjacent cells. At cell apices adjacent cells interdigitate and are joined by zonulae adhaerentes (Fig. 82). Filopodial extensions project from cell bases.

The epidermal cells are highly vacuolated (Fig. 78). These vacuoles are concentrated mainly at cell apices and bases. At cell apices 'blebs' of cytoplasm often occur (Figs. 78 & 82).

3 CELL DEVELOPMENT DURING DORSO-VENTRAL POUCH FLATTENING AND EXTENSION

Table 2 and Figures 62 & 63 show progressive stages in the development of the wing imaginal disc during stage 1. The wing pouch elongates distally. Peripodal membrane cells are squamous in shape (width 260 µm; length 40 µm) in the region of wing pouch extension. Cell proliferation occurs throughout stage 1 (Figs. 79 & 83). Cells undergoing mitosis are 'rounded-up' and are always found at the apex of the epithelium. Spindle axes are predominantly oriented parallel to the proximo-distal disc axis in the plane of the epidermis (Fig. 83).

As continued extension of the wing pouch occurs, the most distal cells of the disc meet at cell bases (Fig. 67). Filopodial extensions project from cell bases. Filopodial interdigitation occurs between adjacent cells in the same epidermal layer as well as between dorsal and ventral cells (Fig. 80). The basement lamina is no longer recognisable as a complete entity in this region. Instead, isolated patches of electron lucent material occur amongst the interdigitating filopodia . These patches may represent the remains of the basement lamina. Adjacent to, and proximal to, the region where interdigitation occurs, the basement lamina is intact. The bases of cells in these regions also possess filopodia, but these extend into the matrix of the basement lamina (Fig. 84).

All filopodia contain filamentous material which runs along their lengths.

Haemocytes within the imaginal disc lacuna often become 'trapped' between the two (dorsal and ventral) epidermal layers as they approach each other (Fig. 85). By the end of stage 1, the epidermal layers have made contact along the entire length of the imaginal disc distal region (now the wing blade), except in certain regions which are the putative prepupal veins.

4 STAGE 2

The wing blade dorsal and ventral surfaces are represented by two basally connected pseudostratified epidermal layers (Fig. 70). The spindle-like shape of individual cells and the stacked nature of their nuclei is retained from stage 1. The cells are closely packed in regions apical to nuclei, but basal to nuclei, large intercellular spaces are apparent between adjacent cells (Fig. 86).

Many microtubules run parallel to the long axis of each cell (Fig. 87). Others run parallel to the apical surfaces of cells (most of these lie around apical borders of the cells). Zonula adhaerens junctions connect adjacent cells (Fig. 88). Microfilaments are also found in close association with the zonulae adhaerentes. Like the zonulae adhaerentes, the microfilament bundles appear to run right around the perimeters of the apical region of each cell (Fig. 89). They form microfilamentous 'rings'.

The dorsal and ventral epidermal layers are connected by interdigitating filopodia which protrude from epidermal cell bases (Fig. 90). Microtubules often run along the lengths of filopodia (Fig. 91). Electron dense plaques often occur at points where the surface membranes of the largest filopodia from dorsal and ventral layers come into contact (Figs. 90+ 92).

In two regions, lucanae separate the dorsal and ventral epidermal layers. The lacunae, which are the putative prepupal veins, are situated near wing margins. These lacunae contain haemocytes (Figs. 70 & 94). The nuclei within cells dorsal and ventral to the lucanae are concentrated in the basal halves of the cells. The cell extensions apical to nuclei are therefore longer than those basal to them (Fig. 93). The apical cell extensions are narrower at the outer surface than those in intervein regions. Filopodia at cell bases interdigitate with those of adjacent cells. Some basal cell extensions extend around vein lacunae (Fig. 94).

Epidermal cells at wing margins are wider at their outer surfaces than those in intervein regions, and more closely packed at their bases (Fig. 95). Large bundles of microfilaments (about 12 nm in diameter) in association with zonulae adhaerentes are found at cell apices. Cell apices of adjacent cells are highly interdigitated, and are joined by septate desmosomes (something not seen in the other epidermal cells) (Fig. 96).

5 STAGE 3: WING BLADE EXPANSION AND FLATTENING

As noted above, the characteristic features of this stage are dorso-ventral wing flattening and wing surface area increase. Concommitantly, there is a change in the arrangement of the epidermal cells as well as a change in the shape of individual cells. The cells no longer have a pseudostratified arrangement. Instead, epidermal cells and their nuclei are arranged at the same level in a single layer (Fig. 97). Epidermal thickness is reduced from about 230 µm (stage 2) to about 70 µm during stage 3. Individual cells are columnar in shape

(width about 6 μm; length about 35 μm). The outer surfaces of early stage 3 wings (about 24 hours after puparium formation) are smooth and flat. Later on in wing development the outer surfaces of epidermal cells are highly convex (except at wing margins where they remain flat), (Figs. 98 & 99) and the cuticle is ridged. The long axes of most of the undulations or ridges run parallel to the proximo-distal wing axis (Fig. 100). Microtubules are abundant within the apical portions of the epidermal cells (Fig. 101). Apical microtubules within cells with highly convex outer surfaces are regularly arranged. Sections cut through one such wing at both longitudinal and transverse orientations show that in most cells, the apical microtubules run parallel to the plane of the epidermis and at right angles to the proximo-distal wing axis.

The shapes of epidermal cells dorsal and ventral to the prepupal veins are different from those in intervein regions. The former cells have basal cell extensions which extend around vein lacunae and terminate in filopodia which interdigitate with filopodia from cells in the other epidermal layer (dorsal or ventral) (Fig. 102). These filopodia contain microtubules which run along their lengths (Fig. 103). The flattened bases of dorsal and ventral epidermal layers in intervein regions are connected by desmosomal plaques (Fig. 104).

Nuclei occupy central positions in all the epidermal cells. Nuclei have changed in shape from spheroidal to spherical and appear to be larger in size than nuclei at earlier stages (Figs. 105 & 106). Feulgen staining indicates that no wing cell division is taking place during this stage.

6 STAGE 4: WING BLADE SWELLING

During wing blade swelling, the cell bodies of the dorsal and ventral epidermal layers become separated by up to 200 µm (Fig. 107). Cell bodies initially remain closely juxtaposed against the overlying pupal cuticle. Nuclei are arranged in a single layer. Below each cell body a long cytoplasmic extension, up to 90 µm long, projects into the wing interior (Fig. 108). Adjacent extensions lie parallel to one another and are connected by thin filopodia (up to 8 µm long and 0.5 µm in diameter). Filopodia mainly run at right angles to the cell extensions. It is difficult to follow individual cell extensions along their entire lengths since they are so thin. This makes it difficult to ascertain whether cell extensions from the dorsal and ventral epidermal layers meet midway across the wing blade, perhaps on a basement lamina, or whether they traverse the entire distance between the cell bodies of the two layers. There are indications that cell extensions of dorsal and ventral layers traverse the entire thickness of the wing blade in regions of maximum swelling (Figs. 107 & 110) but that cell extensions of dorsal and ventral layers are connected midway across the wing blade at wing margins (Fig. 109). Some are connected to haemocytes or run around them (Fig. 110). Although tracheae, nerves and haemocytes are present within the wing blade, no distinct venation is apparent.

Directly after apolysis mitotic figures are apparent within the wing epidermis.

7 STAGE 5: RE-FLATTENING OF THE WING BLADE

Epidermal cells in intervein regions are columnar in shape (Figs. 111a & b). Their nuclei are arranged in parallel rows (Fig. 112). Adjacent cells are anchored at their apices by means of maculae adhaerentes desmosomes (Fig. 113). The bases of cells in the dorsal

and ventral epidermal layers are connected by zonulae adhaerentes junctions (Fig. 114). Between adjacent cell bases, 'pockets' of haemolymph and haemocytes are often present (Figs. 115 & 116). These may represent regions where haemolymph has not been displaced during flattening of the wing blade. This probably accounts for the characteristic 'spongy' appearance of the stage 5 wing blade (Fig. 112).

Epidermal cells that are immediately dorsal and ventral to the pupal veins are columnar in shape and narrower than those in intervein regions (Fig. 117) (about 5 μm wide). Many microtubules run parallel to the long axis of these cells. Filopodial extensions connect adjacent cell bases and zonulae adhaerentes junctions anchor cell apices. Microtubules run along the lengths of the filopodia (Fig. 118).

The cells of the wing margin where bristles occur are arranged in a pseudostratified epidermal layer, unlike the cells of the remainder of the epidermis which are arranged in a single layer (Fig. 119). This is probably due to the inclusion of additional cells associated with bristle development.

8 CUTICULAR DIFFERENTIATION

The mitoses which occur immediately prior to re-flattening of the bilayer are probably associated with cuticular differentiation. In *C. erythrocephala* cuticular differentiation includes the production of a double row of trichomes along the posterior wing margin, several types of bristles along the anterior (costal) margin and rows of trichomes over the remainder of the wing blade (Sprey & Oldenhave, 1974) (Fig. 76). The development of bristles and hairs in *C. erythrocephala* has not been previously studied at the ultrastructural level.

(a) Trichomes

The surface of the wing blade is covered by evenly spaced trichomes which usually have a centre-to-centre spacing of about 12 μm (Fig. 120). Since cells dorsal and ventral to veins are narrower than intervein cells, adjacent trichomes are packed closer together over veins than they are in intervein regions (Fig. 121).

Each trichome is an outgrowth from a single epidermal cell (Fig. 122). During their early development, large bundles of microfilamentous material are seen at trichome bases and margins. Microtubules are found in association with the microfilament bundles. Both microtubules and microfilaments are oriented longitudinally with respect to trichome outgrowth (Fig. 122).

(b) Bristles

The DNA content of the bristle shaft (trichogen) cell nuclei is increased above the normal diploid amount (Peters, 1965) and this is reflected in the increased nuclear diameter (12.0 μm), as compared with the other epidermal cell nuclei (6.0 μm) (Fig. 123). Early in bristle development, longitudinally oriented microtubules and microfilaments are found in the regions just apical to the nuclei of bristle shaft cells. Subsequently, bundles of microfilaments extend into the bristle shaft. The microfilaments are grouped into bundles of characteristic shape and size (Fig. 124). The bundles are spaced at intervals of 400 nm. Inside the shaft, microtubules and microfilaments predominate whereas other organelles are sparse. Later, during cuticle secretion, longitudinal cuticular ridges are formed by certain bristles (Fig. 125). Not all bristles form cuticular ridges. The ridged bristles are concentrated along the proximal portion of the anterior wing margin (Sprey & Oldenhave, 1974) (Fig. 126).

9 STAGE 7: CELL BODY SEPARATION AND THE FINAL FLATTENING AND EXPANSION OF THE WING BLADE

The wing blade lies folded in a characteristic manner within the pupal cuticle (Fig. 75). Epidermal cell bodies are squamous in shape (Fig. 127) (lengths about 5 μm; widths about 10 μm) unlike the columnar cells characteristic of stages 5 and 6.

Adjacent cells are held together by means of apically situated zonulae adhaerens junctions and laterally situated septate desmosomes (Fig. 128). Cell bodies of the dorsal and ventral epidermal layers are separated by a distance of about 20 μm. The basal extremities of the epidermal cells from both dorsal and ventral layers are extended into a complicated series of thin cytoplasmic processes which run across the internal portion of the wing blade which is filled with haemolymph (Fig. 127). The cells contain numerous bundles of microtubules about 24 nm in diameter which extend along the interiors of the cytoplasmic extensions (Fig. 129). At the basal borders of the cells, cells from dorsal and ventral layers are connected by means of a three-layered intercellular cementing material (Fig. 130).

The cells of proximal and distal wing margins are arranged as a pseudostratified epidermis (Figs. 131 & 132) unlike the cells of the rest of the wing which are arranged in a single layer. This is correlated with the inclusion of additional cells associated with cuticular differentiation at the wing margins. Adjacent cells at wing margins are connected by numerous interdigitations and filopodia.

Cells dorsal and ventral to veins also have a different cyto-architecture. These cells are narrower than those in intervein regions

THE CELL SHAPE AND CONTACT RITUAL

A schematic representation.

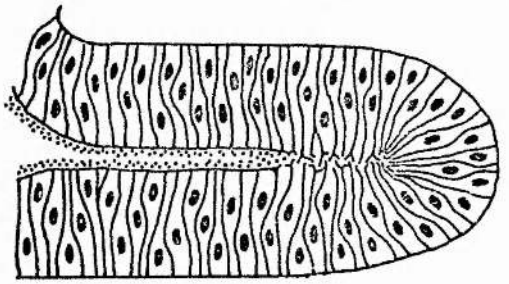

STAGE 1

Bilayer formation ('zipping-up')
Pseudostratification

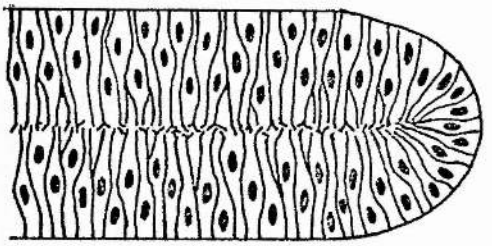

STAGE 2

The last pseudostratified stage

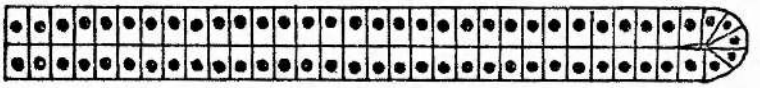

STAGE 3

1st flattening and expansion phase

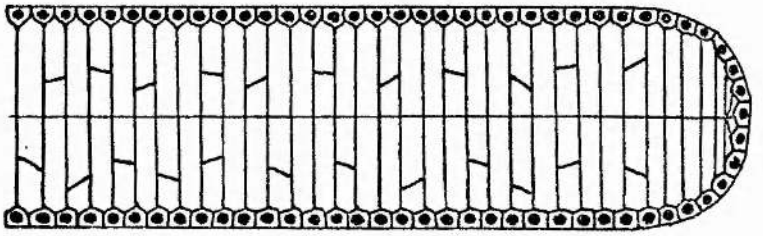

STAGE 4

Blade swelling

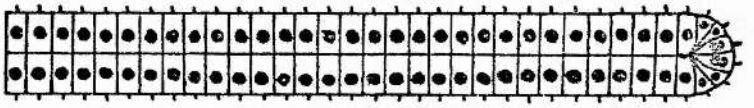

STAGE 5 / 6

2nd flattening phase

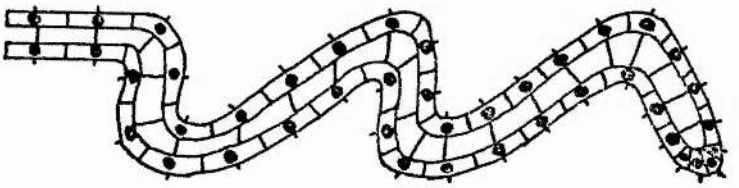

STAGE 7

3rd flattening phase and 2nd expansion phase

(about 8 μm wide and 16 μm long). Adjacent cells are attached at their bases by means of interdigitating filopodia (Fig. 133), and at their apices by cell interdigitations and septate desmosomes.

In intervein cells, microtubules run parallel to outer cell surfaces in a direction which is parallel to the proximo-distal wing axis (Fig. 134). This is a reversal of the orientation of the apically situated microtubules observed in epithelial cells during stage 3.

DISCUSSION

THE CELL SHAPE AND CONTACT RITUAL - AN OVERVIEW

This analysis of wing growth and shaping reveals the extraordinary and complex sequence of changes that individual epidermal cells undertake as the wing pouch of an imaginal disc is modelled into a mature wing blade. For example, cell bodies are apparently drawn together by the interaction of filopodia that extend from cells of the putative dorsal and ventral surfaces to create a bilayer. The long spindle-shaped cells then shorten, but subsequently re-elongate separating opposing cell bodies, only to shorten again later. Following this, cell bodies of opposite layers again separate and subsequently flatten to adopt a squamous shape. Construction and re-modelling of cytoskeletal arrays, specific deployments of desmosomes, filopodia and certain other cell junctions and cell extensions are spatio-temporally correlated with this sequence. The dipteran wing epidermis ritual is more complex and sophisticated than any previously described for tissue development. It highlights the importance of spatio-temporal control of cytoskeletal arrays for shape specification at both cell and tissue levels.

1 BILAYER FORMATION

The first step in the metamorphosis of wing discs is 'evagination'.

This involves a change in the shape of a rounded form, the wing pouch, to an elongate and flattened form, the wing blade. These changes also include the formation of a flattened epidermal bilayer. Ultrastructural observations suggest that the bilayer may be created by means of filopodial extensions from the bases of epidermal cells which intertwine. The fact that the filopodia contain microfilamentous material is significant. Microfilaments might push out surface extensions from epithelial cell bases to produce filopodia as well as promoting filopodial shortening. Microfilaments are involved in force generation during some types of cell extension and may also be involved in the elongation of some types of cells (Yamada, et al., 1971; Bunge, 1973; Clarke & Spudich, 1977; Tucker, 1979). The process of creating a bilayer appears to be akin to 'fastening a zipper'. Perhaps microfilament bundles within entwined filopodia contract to draw epidermal cell bases together. The fact that certain substances which bind to cell surfaces (for example, Concanavalin A) inhibit Drosophila imaginal disc 'evagination' (Mandaron, 1974; Fekete et al., 1975), is consistent with this suggestion because these substances alter microfilament deployment and cell surface adhesion properties.

Other insect epidermal cells develop contractile cell extensions or 'feet' which are similar in appearance to the filopodia observed in C. erythrocephala wings (Locke & Huie, 1981 a, b; Tucker, 1981). Filopodia also occur in many other embryonic situations where their contraction appears to assist shape changes, for example, during neurulation and gastrulation (see Baker & Schroeder, 1967; Trelstad, Hay & Revel, 1967; Tilney & Gibbins, 1969; Revel & Brown, 1976).

During the process of bilayer formation, the basement lamina

becomes fragmented. There is a possibility that haemocytes are concerned with the fragmentation of the basement lamina. Haemocytes become 'trapped' between the epidermal layers during bilayer formation. The ultrastructure of the haemocytes is similar to that of the F-cell type haemocyte which is concerned with phagocytosis in C. erythrocephala (Crossley, 1964). Phagocytosed basement lamina material has been observed within haemocytes of C. erythrocephala leg discs at a similar stage in development (Van Ruiten & Sprey, 1973).

2 PSEUDOSTRATIFICATION AND INTERKINETIC NUCLEAR MIGRATION

During bilayer formation, the developing imaginal wing disc epidermal cells divide mitotically and exhibit interkinetic nuclear migration which results in the accumulation of mitotic figures at the epidermal surface. This also results in the production of a pseudo-stratified epidermis which is an important preliminary to a phase of epidermal flattening and expansion. Many other embryonic epithelia exhibit interkinetic nuclear migration (I.N.M.) (Sauer, 1936; Sauer & Walker, 1959; Fujita, 1960; Langman, Guerrant & Freeman, 1966; Karfunkel, 1974; Messier, 1978; Nagele & Lee, 1979). Developing leg discs also exhibit this phenomenon (Sprey, 1970; Van Ruiten & Sprey, 1973; Madhaven & Schneiderman, 1977). The process is thought to involve severing of the basal contact with the basement membrane, loss of microtubules in the cell extensions, relaxation of apical micro-filaments and the migration of nuclei to an apical position (Langman, Guerrant & Freeman, 1966; Nagele & Lee, 1979). A similar process may be operating in the wing disc because the nuclei of mitotic cells are in an apical position, basal cell extensions appear to be lost, cytoplasmic bridges are always apical, and in some regions portions of the cytoplasm appear to have been forced past the cell apex and bulge

outwards forming a bleb-like structure. The latter feature has been observed in another tissue exhibiting I.N.M. (Nagele & Lee, 1979). These authors suggest that a higher cytoplasmic viscosity together with nuclear movement during I.N.M. may cause the 'blebs' of cytoplasm at cell apices in developing chick neuroepithelium. The 'blebs' are probably not artefacts. Wings at growth stages 1 and 3 were fixed together. 'Blebbing' is only apparent at stage 1 when I.N.M. seems to be occurring but not at stage 3 when there is no evidence for I.N.M.

3 CHANGES IN CELL SHAPE AND CYTOSKELETAL ORGANISATION DURING INITIAL WING BLADE FLATTENING

The expansion and flattening of the wing blade observed during stage 3 involves changes in epidermal cell shaping. The arrangement of cells into a pseudostratified epithelium during stages 1 and 2 ensures the initial packing of large numbers of cells beneath a relatively small wing-surface area. These cells and their nuclei all become situated at one level so that the surface area of the wing increases. As this takes place the cells shorten. The long spindle shape of cells changes to a shorter columnar shape with no marked change in cell volume so that the epidermis decreases in thickness as its surface area increases (i.e. it flattens out).

The cellular mechanisms most likely to be involved in these processes are intercellular interactions involving surface properties of cells, especially differential adhesiveness (Steinberg, 1970) and forces generated by intracellular organelles especially microtubules and microfilaments (Byers & Porter, 1964; Cloney, 1966; Gibbins, Tilney & Porter, 1969; Beinbrech, 1970; Wrenn & Wessels, 1970; Spooner & Wessels, 1972; Messier, 1978; Tucker, 1979). In the wing blade, the specialised apical

attachment devices of adjacent cells, the zonulae adhaerentes, could ensure the adhesion of all cells in the epidermis and facilitate spatio-mechanical integration of shape changes in individual cells, or groups of cells, while the shape of the epidermis changes.

Microtubules within epithelial cell extensions may serve to maintain the cellular anisometry of the spindle-shaped cells observed during stages 1 and 2. Cytoplasmic microtubules are often involved in maintenance of cellular anisometry (Byers & Porter, 1964; Tilney, 1968; Behnke, 1971; Tucker, 1979). In addition to their role in maintenance of cellular anisometry, the microtubules within cell extensions could also be responsible for the apical positions of nuclei during stage 2. Nuclei are more apically positioned within the epithelium during stage 2 than during stage 1 where they are usually more basally positioned. Microtubules have previously been implicated in nuclear migration (Holmes & Choppin, 1968; Zwaan, Bryant & Pearce, 1969; Northcote, 1971; Messier, 1978; Nagele & Lee, 1979). Nuclear migration within spindle-shaped cells to broaden the apical region of each cell, and increase the wing blade surface area may perhaps be prevented during stage 2 by the microfilament 'rings' which encircle and constrict the apical surface of each cell (as occurs during neurulation (Messier, 1978)). Fragmentation of these microfilaments might relax the apical constriction and perhaps enable nuclear migration to proceed until all nuclei are arranged into one layer. If the microtubules were to fragment thereafter, assuming that they are responsible for the maintenance of cellular anisometry, the cytoplasm of cell extensions would retract into cell bodies, causing a reduction in cell length ie. cell flattening. The bilayer would be preserved since cells of both layers interdigitate at their bases, or are connected by desmosomes. As in

Drosophila (Waddington, 1941), cell flattening and wing expansion are fairly rapid events. This is consistent with an overall breakdown of microtubules in the epidermal cells. There are many microtubules oriented along the long axes of cells during stage 2 when cells are elongated, and none in the long axes of cells during stage 3 when cells have flattened.

The situation is further complicated by the fact that by the end of stage 3, wing length has increased (since stage 2) by a factor of 2 while the width has increased by a factor of 1.5 i.e. expansion is somewhat anisometric. During cell flattening, microtubules become oriented parallel to the plane of the epidermis and at right angles to the proximo-distal wing axis. It is possible that these microtubules, by the nature of their orientation, may restrict an increase in cell width but allow unrestricted cell elongation in a direction parallel to the long axis of the wing. The majority of cells are slightly longer in this direction (Fig. 100). The cuticle ridges which are subsequently deposited run parallel to the long axis of the wing. These ridges probably serve to re-inforce and maintain the elongate cell shape.

4 CHANGES IN WING SHAPE DURING WING BLADE SWELLING

Pronounced swelling occurs during stage 4. Wing blade swelling has been observed during a similar phase of development in other insects (Schlüter, 1933; Hundertmark, 1936; Waddington, 1941). The swelling process appears to go much further in Drosophila and Calliphora than it does in Tenebrio or Habrobracon. It has been suggested that hydrostatic pressure is responsible for wing blade swelling (Robertson, 1936; Bodenstein, 1950; Waddington, 1941; Mandaron, 1971). At the beginning of stage 4, the head of the organism is everted. The eversion is achieved by muscular action which creates hydrostatic pressure within

the haemolymph. Since insects have an open blood system, it is possible that this hydrostatic pressure could be transmitted throughout the haemocoele including that within the wing blades. The pressure created may force the epidermal layers apart. It is significant that in Calliphora the legs also become swollen at this time (personal observation).

Although wing blade swelling is somewhat surprising at this stage in wing development, since a flattened blade-like structure similar in shape to the adult wing is created prior to swelling, it does have certain advantages. Swelling stretches the pupal cuticle. Apolysis occurs when swelling is most pronounced. When re-flattening takes place during stage 5, a space is created between pupal cuticle and wing blade. This space may be of value when further flattening and surface area increase occur during stage 7 because it can accommodate the blade-folds which form during the final phase of expansion in wing area. Furthermore, the separation of dorsal and ventral epidermal layers would facilitate tracheolar migration so that the pupal veins can be formed. These are quite distinct in number and position from those of the prepupal veins. The process would be more difficult if dorsal and ventral epidermal layers had a compact arrangement like that during stage 3.

5 SECOND PHASE OF WING BLADE FLATTENING

Wing blade flattening occurs for a second time during stage 5 of wing morphogenesis. It follows blade swelling which occurs during stage 4. Flattening may be initiated by shortening or contraction of the long cell extensions present at the end of stage 4. Perhaps the flattening process is similar to that which occurs during flattening between stages 2 and 3 (see above). Microtubule breakdown might be involved during stage 5 epidermal cell shortening. Some contractile procedure must also presumably be involved to expel haemolymph from

the swollen blade as it flattens.

6 FINAL FLATTENING AND EXPANSION OF THE WING BLADE

During stage 7 the cell bodies of the two epidermal layers once again become separated. However, in this case separation accompanies a flattening of cell bodies as the blade increases in surface area for a final time. The longitudinally oriented microtubules within cell extensions at this stage probably help to form, and maintain, the cell extensions that appear to hold the two epidermal layers apart. The role of microtubules in the formation (Renaud & Swift, 1964; Tilney & Porter, 1967) and maintenance (Tucker, 1979) of elongate cell processes is well documented and they may play a similar role in this case. The function of the cell extensions and their accompanying desmosomes is probably to hold the two surfaces of the wing together during expansion. Similar extensions and desmosomes have been observed in wings of Drosophila (Robertson, 1936; Mandaron, 1970; Fristrom & Fristrom, 1975; Edwards, Milner & Chen, 1978) of Lucilia (Seligman, Filshie, Doy & Crossley, 1975) and of certain aphids (White & Gregory, 1972) during the same or a similar developmental stage. It is interesting to note in the case of aphids, that although they exhibit hemimetabolous development (the wings develop directly from the embryonic buds not from imaginal discs) similar cellular deployments to those utilised by holometabolous insects are used to achieve wing expansion prior to eclosion.

Another role of cell extensions during this stage in wing development may be to separate cell bodies in order to form channels through which air can be pumped at eclosion in order to unfurl the wing.

7 VENATION

From studies of Drosophila pupal wings at critical developmental

stages, it has been suggested that cells on the dorsal surface may induce vein formation in the underlying ventral cells (Lees, 1941; Garcia-Bellido, 1975, 1977; Fausto-Stirling, 1978). Garcia-Bellido (1977), suggests that vein determination is a 2-step process. The approximate location of the veins is first laid down autonomously on both wing surfaces (Sprey & Oldenhave, 1974). However, the final location is determined by interactions between dorsal and ventral surfaces because the cells of the ventral wing surface exhibit non-autonomous behaviour with respect to vein formation. This led Garcia-Bellido,(1977) to conclude that the forces involved in wing flattening and vein formation are probably supracellular and represent the sum of individual cell forces. The intercellular adhesions and cell extensions observed in my examinations may be important in this context.

8 OTHER FACTORS INFLUENCING WING SHAPE

The final wing shape is likely to be the consequence of the combined action of a number of procedures: oriented cell division (Waddington, 1941; Stumpf, 1956), narrowing of vein-forming cells (Waddington, 1941), cell re-arrangement (Fristrom & Fristrom, 1975; Fristrom, 1976; Siegal & Fristrom, 1978; Fristrom, Fekete & Fristrom, 1981), and cell death (Whitten, 1969) as well as events discussed above. Evidence from this study suggests that final overall shape is partially achieved as early as stage 2 when putative prepupal veins are formed. Groups of cells at wing margins and in positions dorsal and ventral to vein-forming lacunae become differentiated by virtue of size and shape from the rest of the epidermis. The cumulative effect of such early local morphological changes (which are restricted to specific wing regions) during the subsequent flattening, expansion, and re-flattening of the wing blade could affect the final wing shape.

Similarly, the formation of the pupal veins during stage 5 appears to contribute to final wing shape. Cells which form veins are narrower, elongate, and more closely packed than those in the remainder of the wing blade which are flattened.

This analysis also shows that during the second phase of wing blade flattening (at stage 5) epidermal cells become arranged in parallel rows. This arrangement is unlike that observed during stage 3 (before swelling occurs). Perhaps after apolysis, highly ordered contraction of the cell extensions and filopodia which are present occurs. This might displace cells slightly and result in the arrangement of cells into parallel rows. Cell re-arrangement has been proposed to explain the generation of anisometric wing shape in Drosophila (Fristrom & Fristrom, 1975; Siegal & Fristrom, 1978; Fristrom, Fekete & Fristrom, 1981). However, no direct evidence about how cell re-arrangement might be achieved and co-ordinated has been obtained in this study or those on Drosophila. If re-arrangement does occur, then some contractile procedure must presumably be involved. Extensive cell migration in Drosophila is unlikely because clonally related cells maintain close proximity and form discrete clonal groups that are 'uninterrupted' by the presence of other cells throughout wing blade morphogenesis (Bryant & Schneiderman, 1969; Bryant, 1970).

9 CUTICULAR DIFFERENTIATION

As in other insects, microtubules and microfilaments are involved in the shape production of hairs and bristles (Lawrence, 1966, for Oncopeltus; Overton, 1967, Perry, 1968, and Reed, Murphy & Fristrom, 1975 for Drosophila; and Locke, 1969 for Calpodes ethlius). The cytoskeletally associated cell shape change activities associated with hair and bristle formation are additional to all those concerned with

cell body shaping and are not involved in overall control of wing shape. However, this illustrates the versatile nature of the wing epithelial cells and also the wide usage of microtubules and microfilaments in cell shape changes.

10 THE FATE OF THE PERIPODIAL MEMBRANE

No peripodial membrane was detected around the wing blade during or after the start of stage 2. Some investigators maintain that the peripodial membrane is shed (Poodry & Schneiderman, 1970; Ursprung, 1972; Milner, 1977). In addition, the wing emerges from the peripodial 'sac' in a proximo-distal direction through the widening lumen of the pedicel or stalk which joins the disc to the larval epidermis (Mandaron & Guillermet, 1977; Schneiderman, 1975). The latter theory is not consistent with observations in this study since the direction of wing outgrowth is in the opposite direction from the location of the external opening of the lumen. It has also been suggested that the peripodial membrane is torn open along a pre-determined line, (Sprey, 1970 ; Sprey & Oldenhave, 1974) is spread laterally, and then fuses with the larval hypodermis (Sprey & Oldenhave, 1974). Those authors who agree that the peripodial membrane is not shed, believe that the peripodial membrane is maintained and comprises as anlagen of adult structures (Sprey & Oldenhave, 1974; Mandaron & Guillermet, 1977). Insufficient evidence has been obtained in this study to substantiate either argument.

11 WING SHAPE CONTROL IN DROSOPHILA AND CALLIPHORA - A COMPARISON

Waddington's (1941) study of Drosophila wing development is the most complete published overall description of dipteran wing morphogenesis to date. It shows that Drosophila wing development involves a series of gross morphological shape changes that occur in conjunction

with a complex sequence of cell shape changes. Examination of Calliphora wing development (this study) has revealed that the sequence of epidermal cell shape changes is virtually identical to that described for Drosophila by Waddington. Certain additional details of the developmental morphology of Drosophila wing discs have emerged since 1941 (reviewed by Poodry, 1980). Cellular events in Drosophila wings during the prepupal period have been examined in some detail. These complement what has been reported above for C. erythrocephala. For example, a change in cell shape, from tall columnar to low columnar (ie. cell flattening) is a feature of wing pouch extension in Drosophila (Auerbach, 1936; Fekete et al., 1975; Poodry & Schneiderman, 1971; Fristrom & Fristrom, 1975). This also occurs in Calliphora (Vijverberg, 1974 a; this study).

Only selected events of metamorphosing Drosophila wing discs have been studied at the ultrastructural level. These reveal similarities between Drosophila and Calliphora wing development that are as follows. Microtubules which are oriented along the lengths of epidermal cells are conspicuous in larval wing discs (Wehman, 1969). As 'evagination' proceeds, microtubules become restricted to cell apices (Fristrom & Fristrom, 1975). Another set of microtubules at a different orientation becomes apparent at a later point. These are aligned parallel to cell surfaces (Wehman, 1969; Fristrom & Fristrom, 1975) and are associated with zonula adhaerens junctions. Wing epithelial cells of 'fully evaginated' discs are drawn out into cytoplasmic extensions which contain longitudinally aligned microtubules (Fristrom & Fristrom, 1975; Edwards, Milner & Chen, 1978). Wehman (1969) observed filopodia close to the basement lamina during prepupal stages of wing development. Hence fine structural changes in cell shaping are probably very similar in Drosophila

and Calliphora during wing morphogenesis. However, a detailed account of the complete fine structural sequence that is related to overall changes in epidermal shaping is not yet available for Drosophila.

Studies of Drosophila wing development have been facilitated by the advent of techniques to culture metamorphosing discs in vitro (see Ashburner & Wright, 1980). The advantage of in vitro study is that metamorphosing discs can be subjected to experimental analysis. Experiments using 'cytoskeletal poisons' complement the theories proposed in this study for wing pouch flattening and extension. They provide support for suggestions that microfilament-mediated contractility and microtubule depolymerisation are necessary. Treatments with microtubule poisons, such as colchicine and colcemid, at concentrations which cause microtubule depolymerisation do not inhibit evagination (Fristrom, 1972; Siegal & Fristrom, 1978). In contrast, treatment with deuterium oxide which promotes microtubule polymerisation, inhibits evagination. The discs of a mutant with abnormally large microtubule numbers/epidermal cell also fail to evaginate, unless colcemid is applied (Fristrom, Fekete & Fristrom, 1981). Treatment with cytochalasin B (which disrupts contractile microfilamentous arrays) reversibly inhibits 'evagination' (Fristrom, 1972; Fekete et al., 1975; Fristrom & Fristrom, 1975). If 'evagination' is dependent on microfilament-mediated contractility as suggested, the effect of cytochalasin B on 'evaginating' wing discs is not surprising.

CHAPTER 5

MICRONUCLEAR ELONGATION IN THE CILIATES PARAMECIUM PRIMAURELIA AND PARAMECIUM TETRAURELIA

INTRODUCTION

A common example of microtubule-associated cell shape change is that of cell elongation. A dramatic example of elongation inside a membrane-bound 'container' is provided by the dividing ciliate micronucleus. The nuclear envelope remains intact throughout micronuclear elongation. The vast increase in micronuclear surface area is accompanied by the elongation of an internal microtubule bundle called a separation spindle. It has been suggested, on the basis of ultrastructural observations, that the elongation of the microtubule bundle is responsible for micronuclear elongation (for example, Tucker, 1967; Davidson & LaFountain, 1976). Paramecium is particularly interesting in that microtubules in the elongating micronucleus have abnormally large diameters (Tucker, 1979; Cohen, Beisson & Tucker, 1980). Certain stages of separation spindle elongation have been examined for a variety of ciliates by other investigators (Jurand & Selman, 1969; Stevenson & Lloyd, 1972; Hauser, 1972; Inaba & Kudo, 1972; Lewis, Witkus & Vernon, 1976; Wolfe, Hunter & St. Adair, 1976; Karadzhan & Raikov, 1977; and see Heath, 1980). However, these include remarkably few assessments of spindle lengths and microtubule diameters at different locations in spindles during different stages of elongation. The possibility that there are structural differences between microtubules at different locations in these spindles or structural changes in spindle microtubules during the course of division cannot be discounted. This chapter deals in detail with these issues for two species in the Paramecium aurelia sibling-species complex (Sonneborn, 1975).

RESULTS

1 PARAMECIUM TETRAURELIA

(a) Metaphase

The metaphase micronucleus is spheroidal in shape (about 4.7 μm in length and about 4.1 μm in equatorial diameter)(Fig. 135). There are many intranuclear microtubules (19 - 24 nm in diameter). As in other ciliates they form a fairly typical mitotic spindle at this stage. Most microtubules run parallel to the longitudinal axis of the nucleus although some others are oriented at right angles to this axis. Figure 135 shows the distribution of chromatin and microtubules at metaphase. Some of the tubules are probably attached to kinetochores; they are associated with chromatin (Fig. 136). Other microtubules terminate at the poles amongst finely fibrous osmiophilic material or at the nuclear envelope (Figs. 137 & 138).

(b) Early separation spindle

After metaphase the micronucleus elongates to form a dumbell-shaped structure. Chromatin is concentrated in the two 'terminal knobs' which are joined by a more slender portion of the nucleus that contains the separation spindle.

When the post-metaphase elongation begins a well-defined separation spindle has formed. The micronuclear length has increased to about 15 μm. Concommitantly the diameter of the micronucleus has decreased to about 2.3 μm in the mid-region (Fig. 139). As the terminal knobs are approached, the micronucleus tapers off (Fig. 140). Micronuclear diameter is smallest at the bases of the terminal knobs (0.4 μm)(Fig. 142). Microtubules (about 24 nm in diameter) and microfilament-like fibrils (about 6 nm in diameter) are conspicuous within the nucleoplasm of terminal knobs (Fig. 141). Cross-sections of micronuclei at this stage

reveal the distribution of microtubules forming separation spindles (Fig. 139). There is a change in microtubule arrangement and size compared with that present during metaphase. One row of microtubules forms an almost continuous 'sheath' just inside the nuclear envelope. Some of these sheath microtubules have a greater diameter (about 26 - 28 nm) than the more centrally positioned microtubules (19 - 24 nm). Short bridges appear to attach the microtubules of the peripheral sheath directly to the nuclear envelope and/or to adjacent sheath microtubules (Fig. 139). More centrally positioned microtubules are arranged into large clusters of varying sizes. These microtubules are from 19 - 24 nm in diameter like those in metaphase micronuclei. Short bridges are sometimes apparent between these tubules.

(c) Late separation spindle

In micronuclei that have reached lengths of 80 - 100 μm, the mid-region of the spindle is about 0.8 μm in diameter whereas at the ends, the spindle diameter is about 0.4 μm. Correlated with this is a variation in microtubule number. The maximum microtubule number/spindle cross-section occurs in the mid-region (about 180 tubules). The number of tubules falls off steadily to about 50 tubules towards the terminal knobs (Figs. 144 & 147). The ordered parallel array of microtubules in the separation spindles permits exact assessments of microtubule number in accurately oriented spindle cross-sections. Attempts were made to obtain accurately oriented spindle cross-sections. Thin cross-sections at selected intervals along the lengths of two micronuclei in the same organism were obtained. Their microtubule distribution profiles were assessed. These show that the mid-region of the spindle contains considerably more tubules than the regions on either side, and also that there is a gradual decrease in microtubule number

from the spindle mid-region to the ends (near the terminal knobs) (Fig. 143). The total number of microtubules at equivalent points along the two different spindles was very similar (Fig. 143).

Not only is there a variability in spindle cross-sectional diameter and microtubule number/cross-section along the length of the micronucleus, but the diameters of the spindle microtubules also vary. In the spindle mid-region, microtubules are predominantly 28 - 31 nm in diameter (Fig. 145). Microtubules of this magnitude are not present in either metaphase or early separation spindles. Interspersed amongst these very large microtubules are microtubules of smaller diameter (mostly about 24 nm). Areas of osmiophilic finely fibrillar material are prevalent between groups of microtubules (Fig. 145). Nearer the ends of the spindle, the microtubules are more closely packed as the micronuclear diameter narrows (Fig. 146). Microtubules of about 28 - 31 nm diameter predominate and the areas of fibrillar intertubule matrix are reduced. At the very ends of spindles, where they meet the terminal knobs, microtubules are predominantly of the 24 nm variety (Fig. 147). Some microtubules extend into the terminal knobs. These microtubules are all about 24 nm in diameter. Dispersed amongst the chromatin and microtubules are microfilamentous strands of about 6 nm diameter (Fig. 148).

2 PARAMECIUM PRIMAURELIA

(a) Late separation spindle

The situation in the elongate micronuclei (about 80 μm) of P. primaurelia is very similar to that described above for P. tetraurelia (Figs. 149 & 150). The diameter of micronuclei varies along the lengths of their spindles. The largest micronuclear diameter is in the spindle mid-region (about 0.8 μm) and tapers off to about 0.4 μm towards each

end of a spindle. The number of spindle microtubules is greatest in the spindle mid-region (about 190 microtubules) and least near each end of the spindle (about 40 microtubules). Microtubule diameter also varies. Microtubules in the spindle mid-region are predominantly about 28 - 31 nm in diameter while those nearer each end of the spindle are predominantly about 19 - 24 nm in diameter. Microtubules of about 19 - 24 nm diameter extend into the chromatin-containing region, and are associated with microfibrils that are about 6 nm in diameter (Fig. 151).

(b) Cold treatment

The sensitivity and lability of spindle microtubules to cold has been well documented (Inoue, 1964; Brinkley & Cartwright, 1970, 1975; Lambert & Bajer, 1977). Not all spindle microtubules react similarly to cold (Brinkley & Cartwright, 1970). It is possible that microtubules with different diameters have different labilities. If this is the case, it would provide further evidence for the presence of two classes of spindle microtubules in the micronucleus. Organisms destined for cold treatment were selected when cleavage furrows were first apparent. They were cooled to $0^{o}C$ and subsequently fixed using the procedure described in the Materials and Methods. Such cold-treated organisms were serially sectioned. All the spindle microtubules persist during cold treatment. Microtubule diameters are either about 31 nm or about 24 nm as in control organisms (compare Figs. 149 & 150 with Figs. 152 & 153). The intranuclear matrix is very densely stained (apart from a few 'empty' spaces; Fig. 152), and is concentrated closely around the spindle microtubules (Fig. 155). Cross-bridges between microtubules are not apparent. Cold-treated organisms have a similar micronuclear organisation to that in control (i.e. untreated) organisms with regard to micronuclear diameter tapering towards the poles, and microtubule numbers

and diameters decreasing towards the poles (Figs. 152-154). Microtubules that are about 24 nm in diameter extend into the terminal knobs as in control organisms. However in cold-treated organisms densely-staining material is clumped around the chromatin and microtubules leaving large electron-lucent regions (Fig. 154). One effect of the dense matrix is to render the cores of microtubules particularly distinct and this highlights the differences in microtubule diameters especially clearly (compare Figs. 155 & 156).

In most cells most spindle microtubules are cold labile. This generalisation may not apply to ciliates. For example, Williams & Williams (1976) subjected dividing Tetrahymena to cold shock that was applied in the same way as that used here for Paramecium. Micronuclear spindles were not examined, but in dividing macronuclei, microtubules persisted.

(c) Final stages of micronuclear elongation

The chromatin-containing terminal knobs begin to separate from the spindle when micronuclei reach lengths of up to 110 µm. The diameters of micronuclei in the spindle mid-region are about 0.6 µm (Fig. 157). Micronuclear diameters taper from the mid-region towards each end of the spindle (Figs. 158 & 159). Near terminal knobs, micronuclear diameters are about 0.4 µm (Fig. 159). In the spindle mid-region there are about 130 microtubules. Most of these are about 31 nm in diameter. The number of microtubules/cross-section decreases on either side of the spindle mid-region as terminal knobs are approached. Sections near terminal knobs show that microtubules are nearly all about 28 - 31 nm in diameter.

DISCUSSION

In his recent review of mitoses in lower eukaryotes, Heath (1980) points out that 'nothing is known about spindle development in Paramecium' nor how microtubules are arranged in the 'entire nucleus'. What has been described are the gross micronuclear shape changes, and it has been established that there are no polar centrioles, the spindle is microtubular, the nuclear envelope remains intact throughout division, and that kinetochores are present (Jurand & Selman, 1969; Stevenson & Lloyd, 1972).

In this analysis, data from micronuclei at metaphase, and early and late stages of anaphase spindle elongation have been compared. Particular attention has been paid to changes in the distribution of microtubules and other cytoskeletal elements within elongating micronuclei. Only the dividing micronucleus of Tetrahymena has been studied in comparable detail (LaFountain & Davidson, 1980).

1 ANAPHASE A - CHROMOSOME TO POLE MOVEMENT

In many mitotic systems, anaphase segregation of chromosomes is thought to involve two distinct motions: the movement of chromosomes from the metaphase plate to the poles (anaphase A), and the further separation of the poles (anaphase B) - i.e. spindle elongation (Inoue, 1976). It has therefore been suggested that more than one motility system may be operating concurrently in some spindles (McIntosh et al., 1976; Sanger, 1977; Cande, 1981).

It has been suggested that actin may be involved in the production of anaphase chromosome movement (Pickett-Heaps, McDonald & Tippit, 1975; Forer, 1976; Pollard, 1976; Sanger & Sanger, 1976). However, a recent study suggests that, at least in some types of cells, only anaphase B,

not anaphase A, requires ATP (Cande, 1982).

In this study, microfilamentous fibres were observed at spindle poles in metaphase micronuclei and also in the terminal knobs during stages in separation spindle elongation. If actinoid and force-generating, these poleward oriented microfilaments might pull on the non-contractile microtubules to draw chromosomes towards the poles. At metaphase some of the microtubules are closely associated with chromosomes and extend into the microfilamentous region near the poles. Microtubules might be connected to chromosomes at kinetochores (as described for P. aurelia by Jurand & Selman, 1969), or via intercalary microfilaments (as described for P. bursaria by Lewis, Witkus & Vernon, 1973). Microtubules could provide a static framework to which the polar microfilaments attach. Possibly these microfilaments pull against the terminal regions of the microtubules.

2 ANAPHASE B - SEPARATION SPINDLE ELONGATION

In the early separation spindle, there is a distinct peripheral sheath of microtubules in addition to the core of more centrally positioned microtubules. This feature has not been previously observed in dividing Paramecium micronuclei. However, it has been reported for dividing micronuclei in one other ciliate (Tetrahymena pyriformis) where the peripheral sheath persists throughout spindle elongation (Davidson & LaFountain, 1976; Wolfe, Hunter & St. Adair, 1976; LaFountain & Davidson, 1979, 1980). It has been suggested that in Tetrahymena increase in spindle length is due to steady polymerization, and consequent elongation of the 150 or so peripheral sheath microtubules which extend along the entire length of the spindle. During P. aurelia early spindle elongation, peripheral sheath microtubules only occur in the spindle mid-region. In P. aurelia, then, the non-sheath microtubules

are also presumably involved. This remains a conjecture since insufficient detail of initial stages of spindle elongation was obtained. The remainder of this discussion is confined to later stages of spindle elongation which have been examined in more detail.

There are two possible ways in which late separation spindle elongation in P. aurelia could be effected.

(a) Microtubule assembly and spindle elongation

One possibility is that continued assembly of peripheral sheath microtubules promotes separation spindle elongation. This has been suggested as a mechanism for micronuclear elongation in Tetrahymena pyriformis (LaFountain & Davidson, 1979). However from evidence obtained in this study, this would mean that in P. aurelia most of the smaller 19 - 24 nm microtubules disassemble (except near the terminal knobs). This would occur in conjunction with further assembly and elongation of the larger sheath microtubules. A situation where one set of microtubules is utilized for initial separation spindle elongation, and is then disassembled as another set of microtubules continues to assemble in the same location for promotion of late separation spindle elongation, would be most unusual.

(b) Intertubule sliding and spindle elongation

The other possibility for late separation spindle elongation is that intertubule sliding occurs. Evidence for sliding between parallel microtubules to promote spindle elongation has been provided by a few other studies (see McIntosh, 1979). Particularly good evidence for this has been obtained from studies of diatom mitosis (Pickett-Heaps, McDonald & Tippit, 1975; Pickett-Heaps & Tippit, 1978; McDonald,

Edwards & McIntosh, 1979). Spindle elongation in Diatoma vulgare is apparently achieved by the sliding apart of two sets of closely overlapping antiparallel microtubules which form the compact spindle microtubule bundle. The number of microtubules/spindle cross-section is halved as this occurs. The present study indicates that a gradual decrease in spindle microtubule number/spindle cross-section occurs during late separation spindle elongation in P. aurelia. Furthermore, cross-bridges or side arms are apparent between microtubules. Microtubules lie parallel to one another, and are mostly packed closely together so that they form a compact bundle. All these factors are consistent with an intertubule sliding mechanism for promotion of spindle elongation. However, if microtubule sliding does occur in P. aurelia, it must be less orderly, or more complex, than that recorded for diatom spindles, as explained above. Furthermore, according to results obtained in this study, microtubule diameters would have to increase during the course of separation spindle elongation. There appears to be no other example of such an unusual situation where an increase in spindle microtubule diameters occurs during spindle elongation.

(c) Microtubule assembly or intertubule sliding?

This study does not permit distinction between the two spindle elongation procedures outlined above. It may be that both procedures are involved to some extent. However, whichever procedure predominates, this study leaves little doubt that separation spindle elongation involves a procedure, or procedures, which have not been previously demonstrated during spindle elongation. If microtubule assembly predominates, then large-scale microtubule disassembly (of the 24 nm tubules) must accompany spindle elongation. If microtubule sliding predominates, and little microtubule disassembly occurs, then most of the 19 - 24 nm microtubules must increase in diameter to 28 - 31 nm.

3 POSSIBLE SIGNIFICANCE OF VARIATION IN MICROTUBULE DIAMETER

In P. aurelia distinct differences in microtubule diameter occur during the process of chromosome separation. These distinct differences were noted among tubules located in different regions of the spindle and in association with different stages of separation spindle elongation. Only one other report of such a phenomenon has been made (Hauser, 1972). Paracineta limbata and Ichthyophtirius multifilius have large microtubules (35 - 40 nm) which appear before smaller microtubules (20 nm). This is in direct contrast to P. aurelia in which the larger microtubules (28 - 31 nm) appear after the smaller microtubules (19 - 24 nm). Large diameter spindle microtubules have previously been reported for P. tetraurelia (31 nm) (Tucker, 1979; Cohen, Beisson & Tucker, 1980) and P. multimicronucleatum (30 nm) (Inaba & Kudo, 1972).

The appearance of 28 - 31 nm microtubules and the simultaneous 'disappearance' of most of the 19 - 24 nm microtubules during spindle elongation is curious. If the smaller microtubules do increase in diameter, then this might occur by changes in the helical arrangement of protofilaments as suggested by Tilney and Porter (1967) for micro- to macro-tubule transitions. The peripheral sheath microtubules (26 - 28 nm) may represent an intermediate stage in this process. Tannic acid staining would show whether the number of protofilaments remains constant or increases.

What is the significance of the finding that, to begin with, the elongating separation spindle in dividing P. aurelia micronuclei consists predominantly of microtubules with diameters of about 24 nm, but subsequently most microtubules have diameters of about 31 nm? Perhaps

this unusual feature has mechanical significance. Presumably 31 nm microtubules are more rigid than 24 nm microtubules. This could be an advantage in a situation where a compact microtubule bundle is involved in pushing chromatin-containing terminal knobs apart over a distance of about 100 μm.

CONCLUDING REMARKS

ORIENTED FIBRE ARRAYS AND SHAPE CONTROL IN CERTAIN NUCLEI, CELLS AND TISSUES - A RESUMÉ

1 DIVERSITY OF SHAPE CHANGES

In this dissertation three shape change situations have been analysed.

The simplest shape change occurs during the elongation of Paramecium micronuclei. A spherical interfission micronucleus becomes dumbell-shaped during cell division. An intranuclear microtubule bundle is mainly responsible.

Growth of the insect ovarian follicles that have been studied involves a fairly simple elongation and tissue shape change from a sphere to a prolate spheroid. In this case spatio-temporally co-ordinated epithelial cell shape changes are involved. There are concommitant changes in the intracellular cytoskeletal organisation of microtubules and microfilaments. In addition, the cells secrete fibres into an extracellular matrix which also apparently plays an important part in shape control and acts in concert with the intracellular fibres. The situation is therefore more complex than that found during micronuclear elongation.

The most complex situation studied occurs during Calliphora wing development. It involves changing from a compact and elaborately folded imaginal disc into a sculptured and highly flattened wing blade. The formation of veins and certain cuticular specialisations further complicates the situation. Follicle growth, and the anisometric expansion of a follicular epithelium, involves relatively simple cell shape changes. Cuboidal cells become columnar and then squamous.

During Calliphora wing morphogenesis, however, a much more complex and exacting sequence of epithelial cell shape changes is necessary to achieve final wing shape. Changes in cell shape are much more radical during wing growth than during ovarian follicle growth. It is not just variations in the shapes of cell bodies that are involved; the outgrowth of long cell extensions and groups of filopodia also takes place at certain points during wing morphogenesis. Two cycles of very marked cell shortening occur with an intervening phase of cell elongation. Cell lengths vary by up to an order of magnitude during some of these changes. Microtubules, microfilaments, filopodia and cell junctions are all employed to generate and/or co-ordinate the complex cell shape ritual.

2 VERSATILITY OF CYTOSKELETAL INVOLVEMENT DURING SHAPE CONTROL

Results from studies by other investigators of microtubule and microfilament involvement during shape control in a variety of situations indicates that these cytoskeletal fibres are both exploited in a very versatile range of ways (see Goldman, Pollard & Rosenbaum, 1976; Dustin, 1978; Roberts & Hyams, 1979). The investigations reported in this dissertation complement these findings. Despite the small sample of shape change situations studied, a wide variety of shape changes occur. Correlated with this, microtubules and microfilaments seem to exhibit a wide range of activities. They are included in fibre arrays that apparently promote elongation, bring about shortening, and resist elongation of cells or parts of cells depending on the situation in question. Descriptions of these activities can be expressed in useful, albeit somewhat colloquial terms, as follows. During shape changes cytoskeletal fibres mainly act as 'active pushers', 'tension transmitters' or 'tension generators' (see Table 3 following).

TABLE 3 FIBRE ACTION DURING SHAPE CONTROL

TYPE OF FIBRE	ACTION		
	ACTIVE PUSHER	TENSION TRANSMITTER	TENSION GENERATOR
MICROTUBULE	Yes*	Yes*	Yes
MICROFILAMENT	Yes*	Yes*	Yes*
EXTRACELLULAR MATRIX FIBRES	No	Yes*	No

* Asterisk denotes that evidence for action has been obtained from studies reported in previous chapters (see text below).

Table 3 emphasises the versatility of microtubule and microfilament action. It is contrasted with the less versatile exploitation of extracellular matrix fibres that are mainly employed to maintain shape rather than to change it; they play no 'active' roles. This is perhaps not surprising, because there is no evidence that extracellular materials can actively generate contractile forces. However, an interesting example of a situation where extracellular matrix fibres apparently act as 'tension transmitters' occurs during anisometric ovarian follicle growth.

Examples obtained in this study which indicate the versatile actions of microtubules and microfilaments are as follows. Microtubules appear to act as 'active pushers' during micronuclear elongation but as 'tension transmitters' during elongation of ovarian follicles. No direct evidence for microtubules acting as 'tension generators' was

obtained in this study. However, studies by other investigators have provided such evidence. For example, microtubules are included in a tension generating system during anaphase chromosome movement (see McIntosh, 1979). Microfilaments appear to act as 'active pushers' during filopodial outgrowth at certain stages in wing development. On the other hand, they seem to play a role as 'tension transmitters' during ovarian follicle growth, and probably act as 'tension generators' in the 'contractile rings' of wing epidermis.

3 NEW ASPECTS OF SHAPE CONTROL

Several previously undetected aspects of the involvement of oriented fibre arrays during shape control have emerged from the investigations reported in this dissertation. These are as follows.

(a) Micronuclear elongation in Paramecium

The overall distribution of microtubules during the elongation of a Paramecium separation spindle has been mapped out for the first time. Elongation involves two types of microtubules with diameters of about 24 nm and 31 nm. Their distribution reveals that spindle elongation is not due to a simple microtubule sliding mechanism.

(b) Ovarian follicle shaping in certain insects

Previous studies of follicle development (Tucker & Meats, 1976; Went, 1978) indicated the involvement of intercellularly aligned microtubules in tension transmission during anisometric follicle growth. This study has shown for the first time that similarly aligned microfilaments may also be involved in follicle shape control. Microfilaments and microtubules can apparently be co-ordinated to produce anisometric follicle growth in P. americana. Microfilaments

alone seem to suffice during follicle shaping in R. prolixus.

Extracellular matrices have not previously been implicated in control of follicle shaping. The follicular epithelium of P. americana secretes a fairly substantial extracellular matrix, the tunica propria. It consists of two separate layers - a fibrous layer and a granular layer. The latter has not been detected before. There are substantial indications that the tunica propria takes over tension transmission from the epithelial cytoskeletal system during the later vitellogenic stages of follicle growth in P. americana.

On the basis of these findings it is argued that the exploitation of oriented fibre arrays may be a widespread feature of follicle shape control during oogenesis in insects generally. Furthermore, evidence for a previously undetected role for follicle cells and their cytoskeletons has been obtained. They may enter a 'post-vitellogenic' phase in which they actively contract. This seems to form part of a mechanism for discharging mature oocytes from ovarioles at the start of oviposition in both of the insects studied. It also presumably brings about shape changes associated with corpus luteum formation.

(c) Wing morphogenesis in Calliphora

Waddington's study (1941) of wing development in Drosophila revealed that wing morphogenesis involves a remarkable sequence of epidermal cell shape changes. However, perhaps surprisingly, there have been no examinations of the complete sequence of fine structural changes involved in the meantime. Nor have there been investigations of how each stage in the sequence of cell shape changes is generated.

The examinations of Calliphora wing development have revealed a

sequence of epidermal cell shape changes which is virtually identical with that described for Drosophila by Waddington. They also reveal the following features.

The assembly of intercellularly aligned microtubule arrays takes place at certain points during wing morphogenesis. Their alignments correlate with directions of cell elongation and/or are related to wing axes. Microfilamentous 'rings' situated at cell apices are also involved in shape control at certain stages. Changing patterns of cell junction arrangement indicate how forces which are generated and/or transmitted by intracellular cytoskeletal arrays may be distributed between cells during the major cell and wing shape changes. A new proposal is advanced for the involvement of filopodia in a 'zipper-like' procedure during the production of the epithelial bilayer at the start of wing pouch flattening.

REFERENCES

AGRELL, I.P.S. (1966) Continuity of the membrane systems in the cells of imaginal discs. Z. Zellforsch. mikrosk. Anat. 72: 22-29.

AGRELL, I.P.S. (1968) Differentiation of the membrane system in cells of imaginal discs. Z. Zellforsch mikrosk. Anat. 88: 365-369.

ANDERSON, E. (1964) Oocyte differentiation and vitellogenesis in the roach Periplaneta americana. J. Cell Biol. 20: 131-155.

ANDERSON, L.M. & TELFER, W.H. (1969) A follicle cell contribution to the yolk spheres of moth oocytes. Tissue and Cell 1: 633-644.

ASHBURNER, M. & WRIGHT, T. (1978) The Genetics and Biology of Drosophila., Vol. 2a. London: Academic Press.

ASHURST, D.E. (1968) The connective tissues of insects. Ann. Rev. Ent. 13: 45-74.

ASHURST, D.E. & CHAPMAN, J.A. (1961) The connective-tissue sheath of the nervous system of Locusta migratoria: an electron microscope study. Quart. J. Micr. Sci. 102: 463-467.

ASHURST, D.E. & COSTIN, N.M. (1974) The development of a collagenous connective tissue in the locust Locusta migratoria. Tissue and Cell 6: 279-300.

AUERBACH, C. (1936) The development of the legs, wings and halteres in wildtype and some mutant strains of Drosophila melanogaster. Trans. Roy. Soc. Edinburgh 58: 787-815.

BAKER, P.C. (1965) Fine structure and morphogenetic movements in the gastrula of the tree frog, Hyla regilla. J. Cell Biol. 24: 95-116.

BAKER, P.C. & SCHROEDER, T.E. (1967) Cytoplasmic filaments and morphogenic movement in the Amphibian neural tube. Devl Biol. 15: 432-450.

BEAULATION, J. (1968) Étude ultrastructurale et cytochemique des glandes prothoraciques et vers à soie aux quatrième et cinquième âges larvaires. 1 La tunica propria et ses relations avec les fibres conjonctives et les hémocytes. J. Ultrastruct. Res. 23: 474-498.

BEHNKE, O. (1970) Microtubules in disk-shaped blood cells. Int. Rev. exp. Path. 9: 1-92.

BEINBRECH, G. (1970) On the function of microtubules during the growth periods of myofibrils in insect flight muscles. Z. Zellforsch. mikrosk. Anat. 109: 138-146.

BELL, W.J. (1969) Continuous and rhythmic reproductive cycle observed in Periplaneta americana. Biol. Bull. 137: 239-249.

BERNFIELD, M.R., COHN, R.D. & BANERJEC, S.D. (1973) Glycosaminoglycans and epithelial organ formation. Am. Zool. 13: 1067-1083.

BERNSTEIN, L.H. & WOLLMAN, S.H. (1976) A circumferential bundle of microfilaments associated with desmosomes near the apex of typical thyroid epithelial cells. J. Ultrastruct Res. 56: 326-330.

BODENSTEIN, D. (1950) The post embryonic development of Drosophila. In Biology of Drosophila (ed. M. Demerec), pp. 275-367. New York: Wiley and Sons.

BONHAG, P.F. (1959) Histological and histochemical studies on the ovary of the american cockroach Periplaneta americana (L). U. Calif. Publs. Ent. 16: 81-124.

BONHAG, P.F. & ARNOLD, W.J. (1961) Histology, histochemistry and tracheation of the ovariole sheaths in the american cockroach Periplaneta americana (L). J. Morph. 108: 107-129.

BRINKLEY, B.R. & CARTWRIGHT, J. (1970) Organization of microtubules in the mitotic spindle: differential effects of cold shock on microtubule stability. J. Cell Biol. 47: 25a.

BRINKLEY, B.R. & CARTWRIGHT, J. (1975) Cold labile and cold stable microtubules in the mitotic spindle of mammalian cells. Ann. N.Y. Acad. Sci. 253: 428-439.

BRYANT, P.J. (1970) Cell lineage relationships in the imaginal wing disc of Drosophila melanogaster. Devl Biol. 22: 389-411.

BRYANT, P.J. & SCHNEIDERMAN, H.A. (1969) Cell lineage growth and determination in the imaginal leg discs of Drosophila melanogaster. Devl Biol. 20: 263-290.

BUNGE, M.B. (1973) The fine structure of nerve fibres and growth cones of isolated sympathetic neurons in culture. J. Cell Biol. 56: 713-735.

BURGESS, D.R. & SCHROEDER, T.E. (1979) The cytoskeleton and cytomusculature in embryogenesis - an overview. Meth. Achiev. exp. Pathol. 8: 171-189.

BURNSIDE, B. (1971) Microtubules and microfilaments in newt neurulation. Devl Biol. 26: 416-441.

BURNSIDE, B. (1973) Microtubules and microfilaments in amphibian neurulation. Am. Zool. 13: 989-1006.

BUXTON, P.A. (1930) Resemblance between a pholcid spider, a tipulid, and a reduviid in Samoa. Proc. Ent. Soc. Lond. 2: 6566.

BYERS, H.R., FUJIWARA, K. & PORTER, K.R. (1980) Visualization of microtubules of cells in situ by indirect immunoflorescence. Proc. Natl. Acad. Sci. (U.S.A.) 77: 6657-6661.

BYERS, B. & PORTER, K.R. (1964) Oriented microtubules in elongating cells of the developing lens rudiment after induction. Proc. Natl. Acad. Sci. U.S.A. 52: 1091-1099.

CANDE, W.Z. (1981) Physiology of chromosome movement in lysed cell models. In International Cell Biology 1980-81. (ed. V.G. Schweiger) pp. 382-391. Berlin: Springer-Verlag.

CANDE, W.Z. (1982) Nucleotide requirements for Anaphase chromosome movements in permeabilized mitotic cells: Anaphase B but not Anaphase A requires ATP. Cell 28: 15-22.

CHANG, M.C. & GOLDMAN, R.D. (1973) The localization of actin-like fibers in cultured neuroblastoma cells as revealed by HMM binding. J. Cell Biol. 57: 867-874.

CHAPMAN, R.F. (1972) The Insects : Structure and Function. (ed. W.S. Bullough) London: English Univ. Press.

CLARKE, M. & SPUDICH, J.A. (1977) Non muscle contractile proteins: The role of actin and myosin in cell motility and shape determination. Ann. Rev. Biochem. 46: 797-822.

CLONEY, R.A. (1966) Cytoplasmic filaments and cell movements: Epidermal cells during ascidian metamorphosis. J. Ultrastruct. Res. 14: 300-328.

CLONEY, R.A. (1972) Cytoplasmic filaments and morphogenesis : effects of cytochalasin B in contractile epidermal cells. Z. Zellforsch. Mikrosk. Anat. 132: 167-192.

COHEN, A.M. & HAY, E.D. (1971) Secretion of collagen by embryonic neuroepithelium at the time of spinal cord-somite interaction. Devl Biol. 26: 578-605.

COHEN, J., BEISSON, J. & TUCKER, J.B. (1980) Abnormal microtubule deployment during defective macronuclear division in a Paramecium mutant. J. Cell Sci. 44: 153-167.

CONKLIN, E.G. (1932) The embryology of Amphioxus. J. Morph. 54: 69-118.

COOKE, P. (1976) A filamentous cytoskeleton in vertebrate smooth muscle fibers. J. Cell Biol. 68: 539-556.

CROSSLEY, A.C.S. (1964) An experimental analysis of the origins and physiology of haemocytes in the blue blowfly Calliphora erythrocephala. J. exp. Zool. 157: 375-398.

DAVEY, K.G. (1965) Reproduction in the insects. London: Oliver & Boyd Ltd.

DAVIDSON, L. & LAFOUNTAIN, J.R. (1976) Preliminary observations on the ultrastructure of the macronuclear amitotic and micronuclear mitotic and meiotic spindle apparatuses in the primitive eukaryote Tetrahymena-pyriformis. J. Protozoology 22: 8A.

DE BIASI, S. & PILOTTO, F. (1976) Ultrastructural study of collagenous structures in some Diptera. J. Submicr. Cytol. 8: 337-345.

DE WILDE, J. & DE LOOF, A. (1974) Reproduction. In The Physiology of Insecta., 2nd edition. (ed. M. Rockstein) New York: Academic Press.

DIPPELL, R.V. (1955) A temporary stain for Paramecium and other protozoa. Stain Technol. 30: 60-71.

DUNLAP-PIANKA, H.L. (1979) Ovarian dynamics in Heliconius butterflies : correlations among daily oviposition rates, egg weights and quantitative aspects of oogenesis. J. Insect Physiol. 25: 741-749.

DUNN, G.A. & HEATH, J.P. (1976) A new hypothesis of contact-guidance in tissue cells. Exp. Cell Res. 101: 1-14.

DUSTIN, P. (1978) Microtubules. New York: Springer-Verlag.

EDELMAN, G.M. (1977) Transmembrane control and surface modulation in animal cells. Prog. Clin. Biol. Res. 17: 467-480.

EDWARDS, J.G. & DYSART, J. McK. (1980) Multicellular cytoskeletons of BHK 21 cells. Cell Biol. Intnl. Rpts. 4: 729.

EDWARDS, J.S., MILNER, M.J. & CHEN, S.W. (1978) Integument and sensory nerve differentiation of Drosophila leg and wing imaginal discs in vitro. Wilhelm Roux's Arch. Devl Biol. 185: 59-77.

FAUSTO-STIRLING, A. (1978) Pattern formation in the wing veins of the fused mutant (Drosophila melanogaster). Devl Biol. 63: 358-369.

FAWCETT, D.W. (1966) An atlas of fine structure. The Cell. Its organelles and inclusions. London: W.B. Saunders Co.

FEKETE, E., FRISTROM, D., KISS, I. & FRISTROM, J.W. (1975) The mechanism of evagination of imaginal discs of Drosophila melanogaster. II Studies on trypsin-accelerated evagination. Wilhelm Roux's Arch. Devl Biol. 178: 123-138.

FISCHMAN, D.A. (1967) An electron microscope study of myofibril formation in embryonic chick skeletal muscle. J. Cell Biol. 32: 557.

FORER, A. (1976) Actin filaments and birefringent spindle fibres during chromosome movements. Cold Spring Harbor Conf. Cell Proliferation 3C: 1273-1293.

FRISTROM, D. (1976) The mechanisms of evagination of imaginal discs of Drosophila melanogaster. III. Evidence for cell rearrangement. Devl Biol. 54: 163-171.

FRISTROM, J.W. (1972) The biochemistry of imaginal disk development. In The Biology of Imaginal Disks., Vol. 5. (eds. H. Ursprung & R. Nöthiger) pp. 109-154. Berlin: Springer-Verlag.

FRISTROM, D.K., FEKETE, E. & FRISTROM, J.W. (1981) Imaginal disc development in a non-pupariating lethal mutant in Drosophila melanogaster. Wilhelm Roux's Arch. Devl Biol. 190: 11-21.

FRISTROM, D. & FRISTROM, J.W. (1975) The mechanism of evagination of imaginal discs of Drosophila melanogaster. 1. General considerations. Devl Biol. 43: 1-23.

FUJITA, S. (1960) Mitotic pattern and histogenesis of the central nervous system. Nature (Lon.) 185: 702-3.

GARCIA-BELLIDO, A. (1975) In Cell Patterning. Ciba Foundation Symp. 29: 161-182.

GARCIA-BELLIDO, A. (1977) Inductive mechanisms in the process of wing vein formation. Wilhelm Roux's Arch. Devl Biol. 182: 93-106.

GARDINER, B.O.C. & MADDRELL, S.H.P. (1972) Techniques for routine and large scale rearing of Rhodnius prolixus Stål (Hemiptera Reduviidae). Bull. ent. Res. 61: 505-515.

GIBBINS, J.R., TILNEY, L.G. & PORTER, K.R. (1969) Microtubules in the formation and development of the primary mesenchyme in Arbacia punctata. I The distribution of microtubules. J. Cell Biol. 41: 201-206.

GOLDMAN, R.D., POLLARD, T.D. & ROSENBAUM, J. (1976) Cell Motility. New York: Cold Spring Harbor.

GRANT, P. (1978) Biology of Developing Systems. New York: Holt, Reinhart & Winston.

GUSTAFSON, T. & WOLPERT, L. (1967) Cellular movement and contact in sea urchin morphogenesis. Biol. Rev. 42: 442-498.

GUTHRIE, D.M. & TINDALL, A.R. (1968) The Biology of the Cockroach. London: Edward Arnold.

HAUSER, M. (1972) The intranuclear mitosis of the ciliates Paracineta limbata and Ichthyophtirius multifiliis. I. Electron microscope observations on pre-metaphase stages. Chromosoma 36: 158-175.

HAY, E.D. (1973) Origin and role of collagen in the embryo. Am. Zool. 13: 1085-1107.

HEATH, I.B. (1980) Variant mitoses in lower eukaryotes - indicators of the evolution of mitosis. Int. Rev. Cytol. 64: 1-80.

HEUBNER, E. & ANDERSON, E. (1970) The effects of vinblastine sulfate on the microtubular organisation of the ovary of Rhodnius prolixus. J. Cell Biol. 46: 191-198.

HEUBNER, E. & ANDERSON, E. (1972 a) A cytological study of the ovary of Rhodnius prolixus. Part I. The ontogeny of the follicular epithelium. J. Morph. 136: 459-494.

HEUBNER, E. & ANDERSON, E. (1972 b) A cytological study of the ovary of Rhodnius prolixus. Part II. Oocyte differentiation. J. Morph. 137: 385-416.

HEUBNER, E. & ANDERSON, E. (1972 c) A cytological study of the ovary of Rhodnius prolixus. Part III. Cytoarchitecture and development of the trophic chamber. J. Morph. 138: 1-40.

HEUBNER, E., TOBE, S.S. & DAVEY, K.G. (1975) Structural and functional dynamics of oogenesis in Glossina austeni : Vitellogenesis with special reference to the follicular epithelium. Tissue and Cell 7: 297-317.

HOFFMAN, P.N. & LASEK, R.J. (1975) The slow component of axonal transport. Identification of major structural polypeptides of the axon and their generality among mammalian neurons. J. Cell Biol. 66: 351.

HOLMES, K.V. & CHOPPIN, P.W. (1968) On the role of microtubules in movement and alignment of nuclei in virus-induced syncytia. J. Cell Biol. 39: 526-543.

HULL, B.E. & STAEHELIN, L.A. (1979) The terminal web. A re-evaluation of its structure and function. J. Cell Biol. 81: 67-82.

HUNDERTMARK, A. (1936) Die Entwicklung der Flügel des Mehlkäfers, Tenebrio molitor, mit besonderer Berücksichtigung der Häutungsvorgänge. Z. Morph. Ökol Tiere 30: 506-543.

INABA, F. & KUDO, N. (1972) Electron microscopy of the nuclear events during binary fission in Paramecium multimicronucleatum. J. Protozool. 19: 57-63.

INOUÉ, S. (1964) Organization and function of the mitotic spindle. In Primitive Motile Systems in Cell Biology. (ed. R.D. Allen and N. Kamiya) pp. 549-598. New York: Academic Press.

INOUE, S. (1976) Chromosome movement by reversible assembly of microtubules. In Cell Motility (eds. R.D. Goldman, T.D. Pollard & J. Rosenbaum) pp. 1317-1328. New York: Cold Spring Harbor.

JURAND, A. & SELMAN, G.C. (1969) The Anatomy of Paramecium aurelia. London: MacMillan.

KARADZHAN, B.P. & RAIKOV, I.B. (1977) Fine structure of the nuclear apparatus of Didinium nasutum (Ciliophora, Gymnostomata) in interphase and during binary fission. Protistologica 13: 15-29.

KARFUNKEL, P. (1974) The mechanism of neural tube formation. Int. Rev. Cytol. 38: 245-271.

KELLY, T.J. & TELFER, W.H. (1979) The function of the follicular epithelium in vitellogenic Oncopeltus follicles. Tissue and Cell 11: 663.

KING, R.C. & AGGARWAL, S.K. (1965) Oogenesis in Hyalophora cecropia. Growth 29: 17-28.

KING, R.C., ROBINSON, A.C. & SMITH, R.F. (1956) Oogenesis in adult Drosophila melanogaster. Growth 20: 121-157.

LAFOUNTAIN, J.R. & DAVIDSON, L.A. (1979) Micronuclear metaphase spindle microtubules in Tetrahymena. Chromosoma (Berl.) 75: 293-308.

LAFOUNTAIN, J.R. & DAVIDSON, L.A. (1980) An analysis of spindle ultrastructure during anaphase of micronuclear division in Tetrahymena. Cell motility 1: 41.

LAMBERT, A.M. & BAJER, A.S. (1977) Microtubule distribution and reversible arrest of chromosome movements induced by low temperature. Cytobiologie 15: 1.

LANGMAN, J., GUERRANT, R.L. & FREEMAN, B.G. (1966) Behaviour of neuroepithelial cells during closure of the neural tube. J. Comp. Neur. 127: 399-412.

LAWRENCE, P.A. (1966) Development and determination of hairs and bristles in the milkweed bug, Oncopeltus fasciatus (Lygaeidae, Hemiptera). J. Cell Sci. 1: 475-498.

LEES, A.D. (1941) Operations on the pupal wing of Drosophila melanogaster. J. Genet. 42: 115-142.

LEWERENZ, G. (1961) Untersuchungen über Wachstum und Struktur der im Thoraxbereich liegenden Imaginalscheiben von Calliphora erythrocephala MEIG. (Diptera, Muscidae). Dt. Ent. Z. 8: 222-249.

LEWIS, L.M., WITKUS, E.R. & VERNON, G.M. (1976) The role of microtubules and microfilaments in the micronucleus of Paramecium bursaria during mitosis. Protoplasma 89: 203-219.

LOCKE, M. (1969) The structure of an epidermal cell during the development of the protein epicuticle and the uptake of moulting fluid in an insect. J. Morph. 129: 7-40.

LOCKE, M. & HUIE, P. (1972) The fiber components of insect connective tissues. Tissue and Cell 4: 601-612.

LOCKE, M. & HUIE, P. (1981 a) Epidermal feet in pupal segment morphogenesis. Tissue and Cell 13: 787-803.

LOCKE, M. & HUIE, P. (1981 b) Epidermal feet in insect morphogenesis. Nature 293: 733.

MAA, W.C. & BELL, W.J. (1977) An endogenous component of the mechanism controlling the vitellogenic cycle in the american cockroach. J. Insect Physiol. 23: 895-897.

MADHAVAN, M.M. & SCHNEIDERMAN, H.A. (1977) Histological analysis of the dynamics of growth of imaginal discs and histoblast nests during the larval development of Drosophila melanogaster. Wilhelm Roux's Arch. Devl Biol. 180: 269-305.

MANDARON, P. (1970) Développement in vitro des disques imaginaux de la Drosophile. Aspects morphologiques et histologiques. Devl Biol. 22: 298-320.

MANDARON, P. (1971) Sur le mécanisme de l'evagination des disques imaginaux chez le Drosophile. Devl Biol. 25: 581-605.

MANDARON, P. (1974) Sur le mécanisme de l'evagination de disques inaginaux de Drosophile cultivés in vitro: effects de diverses substances affectant la membrane cellulaire. Wilhelm Roux's Arch. Devl Biol. 175: 49-63.

MANDARON, P. & GUILLERMET, C. (1977) Analyse microcinématographique de l'evagination des disques d'aile et de patte de Drosophile cultives in vitro. Compte Rendus Acad. Sci. Paris. Series D. 287: 257-260.

McDONALD, K.L. EDWARDS, M.K. & McINTOSH, J.R. (1979) Cross-sectional structure of the central mitotic spindle of Diatoma vulgare. Evidence for specific interactions between antiparallel microtubules. J. Cell Biol. 83: 443-461.

McGREGOR, H.C. & STEBBINGS, H. (1970) A massive system of microtubules associated with cytoplasmic movement in telotrophic ovarioles. J. Cell. Sci. 6: 431-449.

McINTOSH, J.R. (1979) Cell Division. In Microtubules. (eds. K. Roberts & J.S. Hyams) pp. 381-442. London: Academic Press.

McINTOSH, J.R., CANDE, W.Z., LAZARIDES, E., McDONALD, K. & SNYDER, J.A. (1976) Fibrous elements of the mitotic spindle. Cold Spring Harbor Conf. Cell Proliferation 3C: 1261-1272.

MESSIER, P.E. (1978) Microtubules, interkinetic nuclear migration and neurulation. Experimentia 34: 289-296.

MILNER, M.J. (1977) The time during which β-ecdysone is required for the differentiation *in vitro* and *in situ* of wing imaginal discs of *Drosophila melanogaster*. Devl Biol. 56: 206-212.

NAGELE, R.G. & LEE, H. (1979) Ultrastructural changes in cells associated with interkinetic nuclear migration in the developing chick neuroepithelium. J. exp. Zool. 210: 89-106.

NORTHCOTE, D.H. (1971) Organisation of structure, synthesis and transport within the plant during cell division and growth. In *Control mechanisms of growth and differentiation*. Symp. Soc. Exp. Biol. 25. Cambridge: Cambridge Univ. Press.

OCKLEFORD, C.D. (1974) Cytokinesis in the heliozoan *Actinophrys sol*. J. Cell Sci. 16: 499-517.

OCKLEFORD, C.D. & TUCKER, J.B. (1973) Growth, breakdown, repair and rapid contraction of microtubular axopodia in the heliozoan *Actinophrys sol*. J. Ultrastruct.Res. 44: 369-387.

OVERTON, J. (1967) The fine structure of developing bristles in wild-type and mutant *Drosophila melanogaster*. J. Morph. 122: 367-380.

PEARCE, T.L. & ZWAAN, J. (1970) A light and electron microscopic study of cell behaviour and microtubules in the embryonic chick lens using colcemid. J. Embryol. exp. Morph. 23: 491-507.

PERRY, M.M. (1968) Further studies on the development of the eye of *Drosophila melanogaster*. I. The Ommatidia. J. Morph. 124: 249-262.

PETERS, W. (1965) Die Sinnesorgane an der Labellen von *Calliphora erythrocephala* Mg. (Diptera). Z. Morph. Ökol. Tiere 55: 259-320.

PICKETT-HEAPS, J.D., McDONALD, K.L. & TIPPIT, D.H. (1975) Cell division in the pennate diatom *Diatoma vulgare*. Protoplasma 86: 205-242.

PICKETT-HEAPS, J.D. & TIPPIT, D.H. (1978) The diatom spindle in perspective. Cell 14: 455-467.

POLLARD, T.D. (1976) Cytoskeletal functions of cytoplasmic contractile proteins. J. Supramol. Struct. 5: 317-334.

POLLARD, T.D. & WEIHING, R.R. (1974) Actin and myosin and cell movement. Crit. Rev. Biochem. 2: 1-65.

POODRY, C. (1980) Imaginal discs. Morphology and development. In The Genetics and Biology of Drosophila., Vol. 2d (eds. M. Ashburner & T. Wright). London: Academic Press.

POODRY, C.A. & SCHNEIDERMAN, H.A. (1970) The ultrastructure of the developing leg of Drosophila melanogaster. Wilhelm Roux's Arch. Devl Biol. 166: 1-44.

POODRY, C.A. & SCHNEIDERMAN, H.A. (1971) Intercellular adhesivity and pupal morphogenesis in Drosophila melanogaster. Wilhelm Roux's Arch. Devl Biol. 168: 1-9.

RAFF, E.C. (1979) The control of microtubule assembly in vivo. Int. Rev. Cytol. 59: 1-96.

RAKIC, P. (1972) Mode of cell migration to the superficial layers of fetal monkey neocortex. J. comp. Neurol. 145: 61-84.

RAVEN, P. (1961) Oogenesis: The storage of developmental information. London: Pergamon Press.

REED, C.T., MURPHY, C. & FRISTROM, D. (1975) The ultrastructure of the differentiating pupal leg of Drosophila melanogaster. Wilhelm Roux's Arch. Devl Biol. 178: 285-302.

RENAUD, F.L. & SWIFT, H. (1964) The development of basal bodies and flagellae in Allomyces arbusculus. J. Cell Biol. 23: 339-354.

REVEL, J.P. & BROWN, S.S. (1976) Cell junctions in development, with particular reference to the neural tube. Cold Spring Harbor Symp. Quant. Biol. 40: 443.

REYNOLDS, E.S. (1963) The use of lead citrate at high pH as an electron-opaque stain in electron microscopy. J. Cell. Biol. 17: 208-212.

ROBERTS, K. & HYAMS, J.S. (1979) Microtubules. London: Academic Press.

ROBERTSON, C.W. (1936) The metamorphosis of Drosophila melanogaster including an accurately timed account of the principal morphological changes. J. Morph. 59: 351-399.

SANGER, J.W. (1977) Nontubulin molecules in the spindle. In Mitosis: Facts and Questions. (eds. M. Little, N. Paweletz, C. Petzett, H. Ponstingl, D. Schroeder and H.-P. Zimmerman) pp. 98-120. Berlin: Springer-Verlag.

SANGER, J.W. & SANGER, J.M. (1976) Actin localization during cell division. In Cell Motility. (eds. R.D. Goldman, T.D. Pollard & J. Rosenbaum) pp. 1295-1316. New York: Cold Spring Harbor.

SAUER, M.E. (1936) The interkinetic migration of embryonic epithelial nuclei. J. Morph. 60: 1-11.

SAUER, M.E. & WALKER, B.E. (1959) Radioautographic study of interkinetic nuclear migration in the neural tube. Proc. Soc. Exp. Biol. Med. 101: 557-560.

SAUNDERS, J.W. (1966) Death in embryonic systems. Science 154: 604-612.

SCHLOTTMAN, L.L. & BONHAG, P.F. (1956) Histology of the ovary of the adult mealworm Tenebrio molitor L. (Coleoptera, Tenebrionidae) Univ. Calif. Publs. Ent. 11: 351-394.

SCHLÜTER, J. (1933) Die Entwicklung der Flügel bei der Schlupfwespe Habrobracon juglandis Ash. Z. Morph. Ökol. Tiere 27: 488-517.

SCHNEIDERMAN, H.A. (1975) New ways to probe pattern formation and determination in insects. In Insect Development. Symp. Roy. Entom. Soc. Lon. 8 (ed. P.A. Lawrence) London: Blackwell Scientific Publ.

SCHROEDER, T.E. (1970) Neurulation in Xenopus laevis. An analysis and model based upon light and electron microscopy. J. Embryol. exp. Morph. 23: 427-462.

SCHROEDER, T.E. (1976) Actin in dividing cells: Evidence for its role in cleavage but not mitosis. In Cell Motility (eds. R.D. Goldman, T.E. Pollard & J. Rosenbaum) pp. 265-278. New York: Cold Spring Harbor.

SELIGMAN, I.M., FILSHIE, B.K., DOY, F.A. & CROSSLEY, A.C. (1975) Hormonal control of morphogenetic cell death in the wing hypodermis in Lucilia cuprina. Tissue and Cell 7: 281-296.

SIEGAL, J.G. & FRISTROM, J.W. (1978) The biochemistry of imaginal disc development. In Genetics and Biology of Drosophila., Vol. 2a (eds. M. Ashburner & T. Wright) London: Academic Press.

SINGH, T. (1958) Ovulation and corpus luteum formation in Locusta migratoroides (Reiche and Fairmaine) and Schistecerca gregaria (Forskål). Trans. Roy. Entom. Soc. Lond. 110: 1-20.

SMITH, D.S. (1968) Insect cells. Their structure and function. Edinburgh: Oliver and Boyd.

SMITH, D.S. & TREHERNE, J.E. (1963) Functional aspects of the organisation of the insect nervous system. In Advances in Insect Physiology 1 (eds. J.W.L. Beament, J.E. Treherne and V.B. Wigglesworth) London: Academic Press.

SONNEBORN, T.M. (1975) The Paramecium aurelia complex of 14 sibling species. Trans. Am. microsc. Soc. 94: 155-178.

SPOONER, B.S. (1975) Microfilaments, microtubules and extracellular materials in morphogenesis. Bioscience 25: 440-450.

SPOONER, B.S. & WESSELS, N.K. (1972) An analysis of salivary gland morphogenesis. Role of cytoplasmic microfilaments and microtubules. Devl Biol. 27: 38-57.

SPREY, Th. E. (1970) Morphological and histochemical changes during the development of some of the imaginal disks of Calliphora erythrocephala. Neth. J. Zool. 20: 253-257.

SPREY, Th. E. (1971) Cell death during the development of the imaginal disks of Calliphora erythrocephala. Neth. J. Zool. 21: 221-264.

SPREY, Th. E. & OLDENHAVE, M. (1974) A detailed organ map of the wing disk of Calliphora erythrocephala. Neth. J. Zool. 24: 291-310.

STEBBINGS, H. & BENNETT, C.E. (1975) The sleeve element of microtubules. In: Microtubules and Microtubule Inhibitors. (eds. M. Borgers & M. de Brabander) pp. 35-45. Oxford: Elsevier.

STEINBERG, M.S. (1970) Does differential adhesion govern self-assembly processes in histogenesis? Equilibrium configurations and the emergence of a hierarchy among populations of embryonic cells. J. exp. Zool. 173: 395-434.

STEVENSON, I. & LLOYD, F.P. (1972) Ultrastructure of nuclear division in Paramecium aurelia. III. Meiosis in the micronucleus during conjugation. Aust. J. Biol. Sci. 25: 775-779.

STUMPF, H. (1956) Die Richtungen der Teilungspindeln auf dem puppen Flügel von Drosophila im Verlaufe der Mitosenperiode. Bio. Zbl. 75: 17-27.

TILNEY, L.G. (1968) The assembly of microtubules and their role in the development of cell form. Devl Biol. Suppl. 2: 63-102.

TILNEY, L.G. & GIBBINS, J.R. (1969) Microtubules in the formation and development of the primary mesenchyme in Arbacia punctulata. II. An experimental analysis of their role in development and maintenance of cell shape. J. Cell Biol. 41: 227-250.

TILNEY, L.G. & PORTER, K.R. (1967) Studies on the microtubules in Heliozoa. II The effect of low temperatures on these structures in the formation and maintenance of the axopodia. Cell. Biol. 34: 327-343.

TRELSTAD, R.L., HAY, E.D. & REVEL, J.P. (1967) Cell contact during early morphogenesis in the chick embryo. Devl Biol. 16: 78-106.

TUCKER, J.B. (1967) Changes in nuclear structure during binary fission in the ciliate Nassula. J. Cell Sci. 2: 481-498.

TUCKER, J.B. (1968) Fine structure and function of the cytopharyngeal basket in the ciliate Nassula. J. Cell Sci. 3: 493-514.

TUCKER, J.B. (1974) Microtubule arms and cytoplasmic streaming and microtubule bending and stretching of intertubule links in the feeding tentacle of the suctorian ciliate Tokophyra. J. Cell. Biol. 62: 424-437.

TUCKER, J.B. (1979) Spatial organisation of microtubules. In Microtubules (eds. K. Roberts & J.S. Hyams) pp. 315-357. London: Academic Press.

TUCKER, J.B. (1981) Cytoskeletal co-ordination and intercellular signalling during metazoan embryogenesis. J. Embryol. exp. Morph. 65: 1-25.

TUCKER, J.B. & MEATS, M. (1976) Microtubules and control of insect egg shape. J. Cell Biol. 71: 207-217.

ULLMANN, S.L. (1973) Oogenesis in Tenebrio molitor. J. Embryol. exp. Morph. 30: 179-217.

URIBE, C. (1925) On the biology and life history of Rhodnius prolixus Stahl. J. Parasitol. 13: 129-137.

URSPRUNG, H. (1972) The fine structure of imaginal disks. In The biology of imaginal disks. (eds. H. Ursprung & R. Nöthiger) New York: Springer Verlag.

VAN RUITEN, Th. M. & SPREY, Th. E. (1973) Ultrastructure of the developing leg disc of Calliphora erythrocephala. Z. Zellforsch. mikrosk. Anat. 147: 373-400.

VIJVERBERG, A.J. (1974a) Change in the shape of wing imaginal discs of Calliphora erythrocephala. Meigen Neth. J. Zool. 24: 89-91.

VIJVERBERG, A.J. (1974b) A cytological study of the proliferating patterns of imaginal discs of Calliphora erythrocephala Meigen during larval and pupal development. Neth. J. Zool. 24: 171-217.

WADDINGTON, C.H. (1941) The genetic control of wing development in Drosophila. J. Genet. 41: 75-139.

WARREN, R.H. (1974) Microtubular organisation in elongating myogenic cells. J. Cell Biol. 63: 550-566.

WEHMAN, H.J. (1969) Fine structure of Drosophila wing imaginal discs during early stages of metamorphosis. Wilhelm Roux's Arch. Devl Biol. 163: 375-390.

WEIHING, R.R. (1979) The cytoskeleton and plasma membrane. Meth. Achiev. exp. Pathol. 8: 42-109.

WENT, D.F. (1978) In vitro culture of eggs and embryos of the viviparous paedogenic gall midge Heteropeza pygmaea. J. exp. Zool. 177: 301-312.

WESSELS, N.K. & COHEN, J.H. (1968) Effects of collagenase on developing epithelia in vitro : lung, ureteric bud, and pancreas. Devl Biol. 18: 294-309.

WESSELS, N.K. & EVANS, J. (1968) Ultrastructural studies of early morphogenesis and cytodifferentiation in the embryonic mammalian pancreas. Devl Biol. 17: 413-446.

WESSELS, N.K., SPOONER, B.S., ASH, J.F., BRADLEY, M.O., LUDUENA, M.A., TAYLOR, E.L., WRENN, J.T. & YAMADA, K.M. (1971) Microfilaments in cellular and developmental processes. Science (New York) 171: 135-143.

WHITE, D.F. & GREGORY, J.M. (1972) Juvenile hormone and wing development during the last larval stages in aphids. J. Insect Physiol. 18: 1599-1619.

WHITTEN, J.M. (1969) Cell death during early morphogenesis : Parallels between insect limb and vertebrate limb development. Science 163: 1456-1457.

WILLIAMS, N.E. & WILLIAMS, R.J. (1976) Macronuclear division with and without microtubules in Tetrahymena. J. Cell Sci. 20: 61-77.

WOLFE, J., HUNTER, B. & ST. ADAIR, W. (1976) A cytological study of micronuclear elongation during conjugation in Tetrahymena. Chromosoma 55: 289.

WRENN, J.T. & WESSELS, N.K. (1970) Cytochalasin B. Effects upon microfilaments involved in morphogenesis of estrogen-induced glands of oviduct. Proc. Natl. Acad. Sci. 66: 904-908.

WRIGLEY, N.G. (1968) The lattice spacing of crystalline catalase as an internal standard of length in electron microscopy. J. Ultrastruct. Res. 24: 454-464.

YAMADA, K.M., SPOONER, B.S. & WESSELS, N.K. (1971) Ultrastructure and function of growth cones and axons of cultured nerve cells. J. Cell Biol. 49: 614-635.

YAMASAKI, T. & NARAHASHI, T. (1959) Effects of potassium and sodium ions on the resting and action potentials of the giant axons of the cockroach. Nature 182: 1805.

ZWAAN, J., BRYANT, Ph.R. & PEARCE, T.L. (1969) Interkinetic nuclear migration during the early stages of lens formation in the chick embryo. J. Embryol. exp. Morph. 21: 71-83.

ACKNOWLEDGEMENTS

My sincere thanks go to my parents, Mr. and Mrs. C.E. Franklin, and to my husband, Dr. T.J. Mathews, for financing my research and for their moral support. Sincere thanks also to my supervisor, Dr. J.B. Tucker, for his enthusiastic support, help, encouragement and inspiration and for permitting me to include one of his unpublished photographs of an early P. tetraurelia separation spindle.

My thanks also to Mr. J.B. Mackie and Mr. D.L.J. Roche for technical assistance, to Dr. J. Beisson, Mr. J. Stevenson and Miss C. McTavish for supplying certain organisms, and to Mrs. A. Rogers for typing this dissertation.

KEY TO ABBREVIATIONS

b	cytoplasmic 'blebs'
Ba	bacteroids
bl	basement lamina
Br	bristles
C	cuticle
CB	cell body
ch	vitellogenic channel
CR	chromatin
Cs	cellular strand
d	desmosome
E	cell extension
Er	endoplasmic reticulum
F	fibres/fibrous layer
FC	follicle cell
Fi	filopodia
g	gap junction
Gl	glycogen
GP	growth phase
Gr	granules/granular layer
H	haemocyte
L	lamina
Li	lipid droplet
La	lattice spacing
m	membrane
ma	macula adhaerens junction
Mc	mitochondrion
mf	microfilaments
Mi	mitotic figure
mt	microtubules
Ms	muscle elements
Mv	microvilli
My	myelin figure
N	nucleus
Ne	nuclear envelope
O	oocyte

Os	ovariole sheath
p	projection/cell process
Pc	wing pouch
PM	peripodial membrane
Po	promyoblasts
R	region
Ri	ridge
S	'spaces'
Sc	sheath cell
sd	septate desmosome
SN	sensory nerve
T	trachea
Tc	trichome
Ti	trichogen cell
tp	tunica propria
To	tormogen cell
Tr	tracheole
V	vein
WE	wing epithelium
WM	wing margin
WT	wing tip
z	zonula adhaerens junction

FIGURE 1

Schematic diagram showing the organisation of the ovariole of P. americana. The diagram compares the follicle numbering system and the growth phase system with the ovariole regions classification. The most mature follicle is termed follicle number one. Follicles are numbered in increasing numerical magnitude from follicle 1 to the germarium. Growth phase 1 includes meiotic events in the germarium. Growth phase 2 refers to the change in follicle size and shape from spherical to disc-shape. Follicle elongation takes place during the third, fourth and fifth growth phases. The terminal filament (TF)and the germarium (Ge) are indicated.

Figure 1

Ovariole Organisation

Vitellogenesis	Previtellogenesis			Ge	TF
Region 5	Region 4		R.3	R.2	R.1
Growth phase 5	G.p. 4	G.p. 3	G.p. 2	G.p.1	

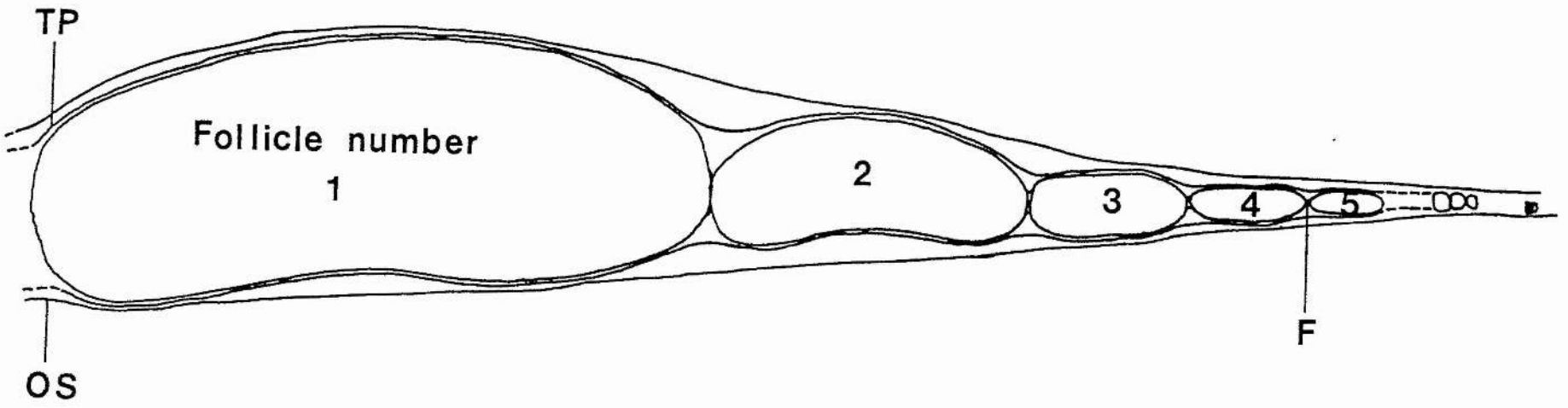

FIGURE 2

The relationship between the diameters (measured at their widest points and at right angles to the longitudinal axis of the ovariole) and lengths of cockroach follicles 1-5 in 75 ovarioles is shown. The shoulders of the computed regression lines (arrows) indicate significant differences. This reveals the three growth phases 3-5 that account for most of the anisometric growth of follicles and oocytes. The relationship in length between follicles 1-5 is also compared. The blackened areas denote the range of lengths exhibited by follicles 1-5 (Fol. 1-5). For example, follicle 1 ranges between lengths of 1,200-2,400 µm in growth phase 4 and lengths of 2 400-4 100 µm in growth phase 5 whereas follicle 2 exhibits lengths of 1,000-2,400 µm in growth phase 4 and does not enter growth phase 5.

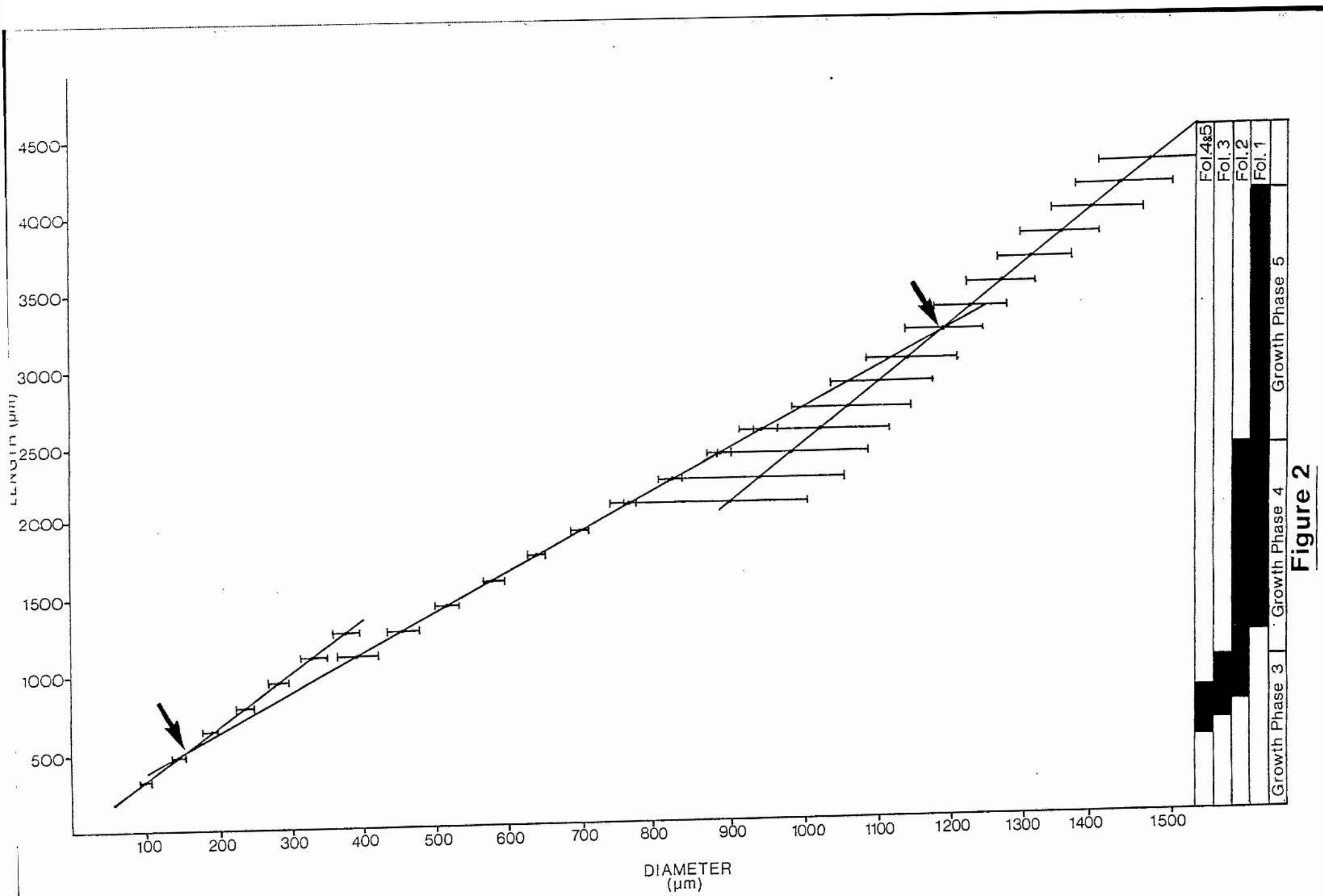
4500
4000
3500
3000
2500
2000
1500
1000
500
100
200
300
400
500
600
700
800
900
1000
1100
1200
1300
1400
1500
DIAMETER
(μm)
Fol.4&5
Fol.3
Fol.2
Fol.1
Growth Phase 5
Growth Phase 4
Growth Phase 3

Figure 2

FIGURE 3

The basis of the cockroach follicle numbering system and growth phases 3-5 is shown in terms of positioning in ovariole regions 4-5 at different points in the vitellogenic cycle. A shows the situation immediately after ovulation and D just prior to ovulation with intervening stages B and C completing the sequence.

Figure 3

Relative changes in follicle size and shape

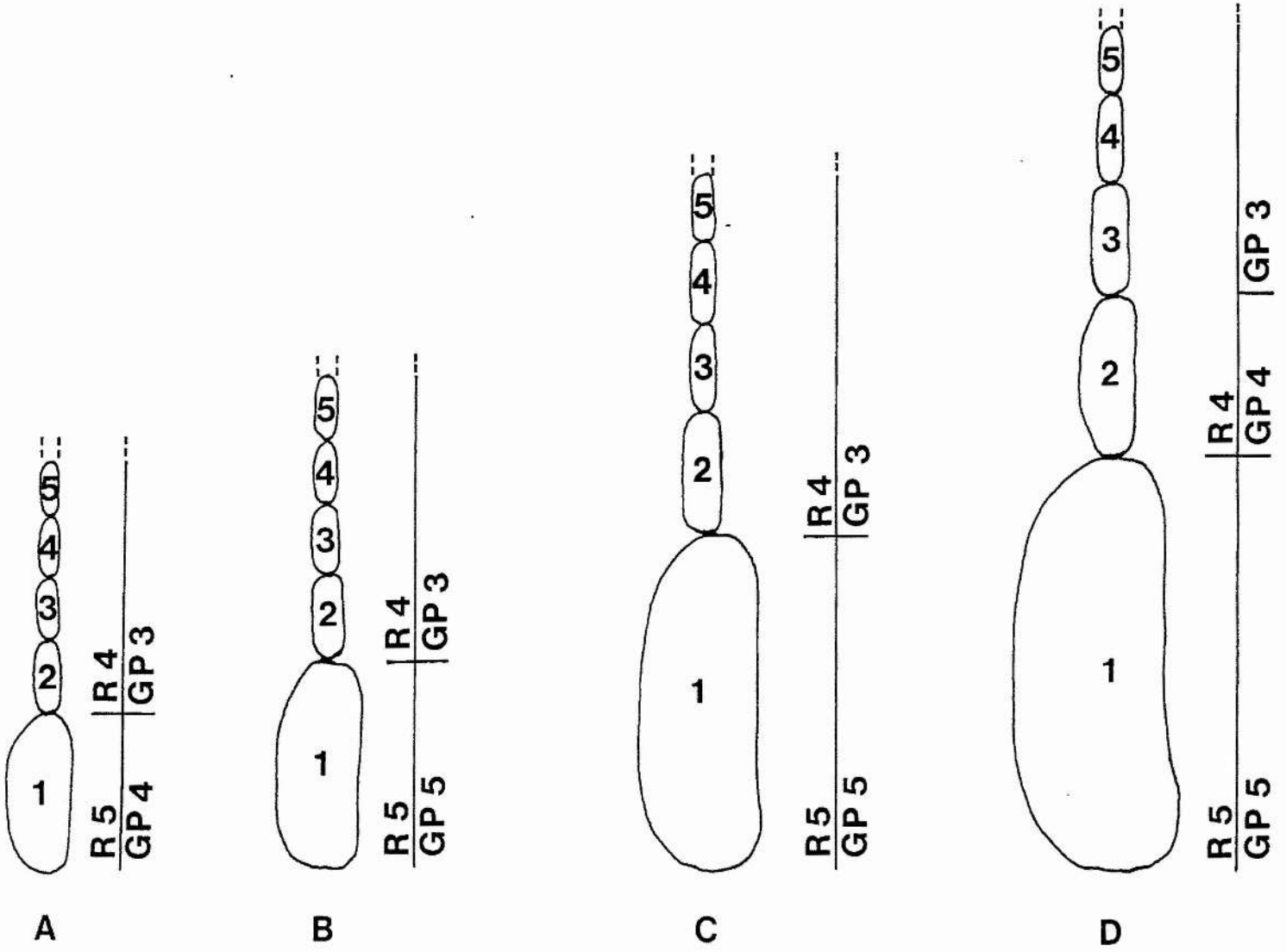

FIGURE 4

Part of the outer surface of the ovariole sheath surrounding an ovariole of P. americana freshly isolated in saline. The anastomosing aggregates of interconnected cells of the sheath are shown. Cells are variable in shape and are connected by cellular strands. Tracheal branches and tracheoles ramify amongst the cells. Nomarski interference contrast. X 120. Bar = 100 µm.

FIGURE 5

Section through part of a cockroach ovariole sheath. A group of sheath cells, including a tracheolar cell, are surrounded by an extracellular lamina (L). Sheath cells contain endoplasmic reticulum, glycogen, lipid droplets and mitochondria. X 3,800. Bar = 5 µm.

4

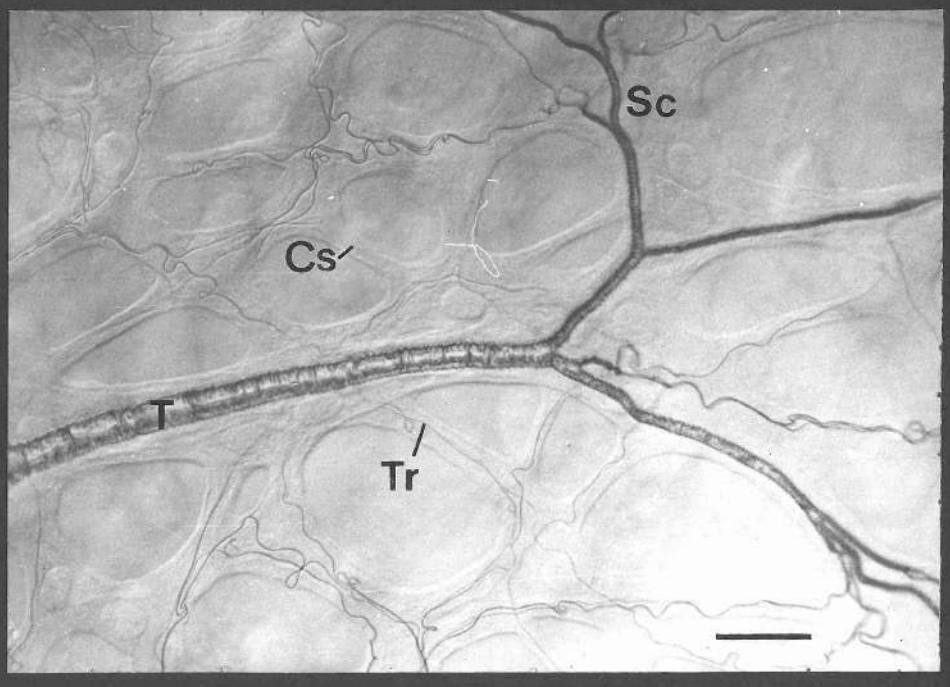

5

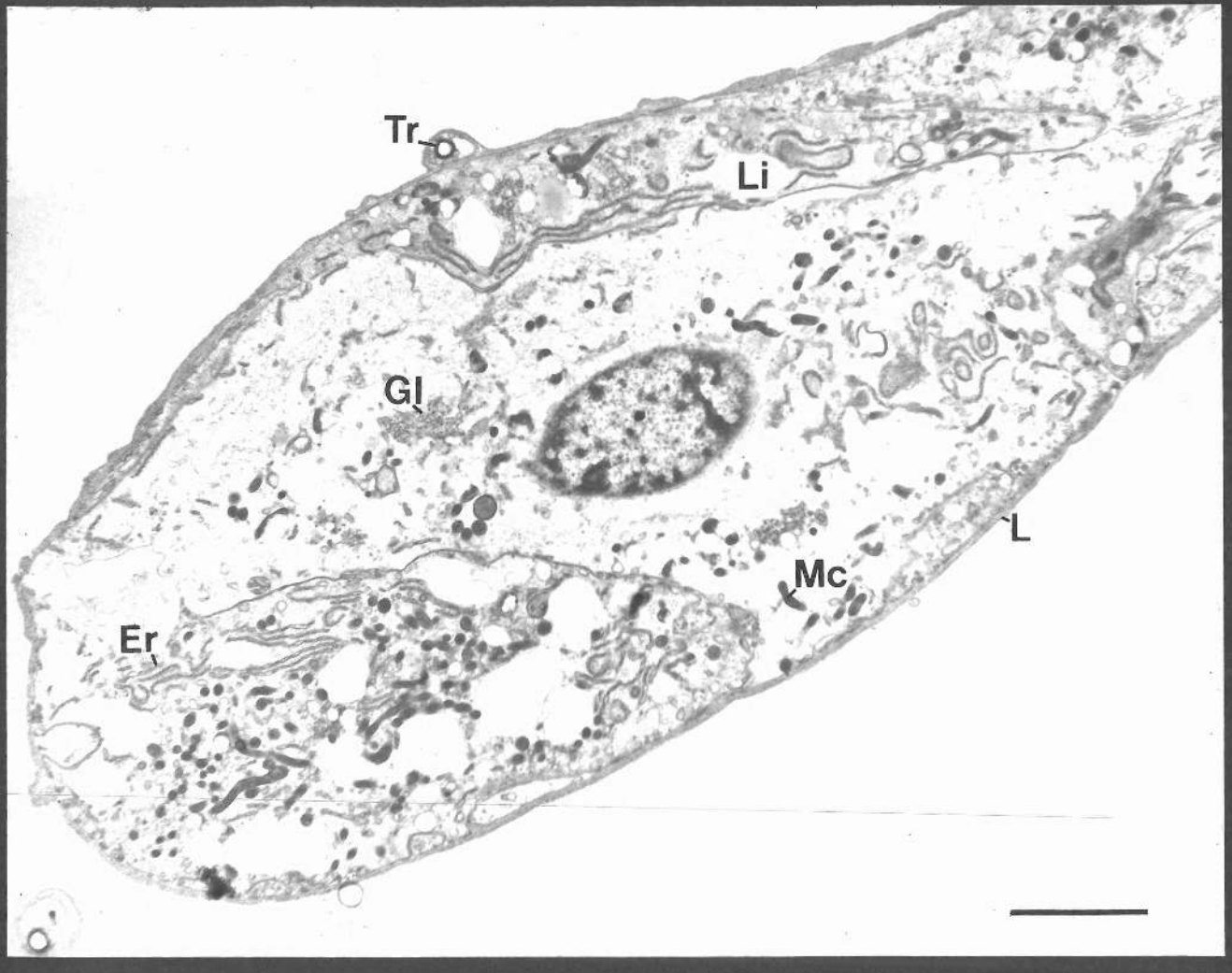

FIGURE 6

Section through part of the ovariole sheath of a cockroach. The cells comprising the ovariole sheath contain microtubules. These are of variable orientation. X 35,000.

FIGURE 7

Part of the outer surface of a cockroach follicle cell and its tunica propria. The section is perpendicular to the outer surface of, and parallel to the polar axis of, the follicle. Circumferentially oriented microtubules and bundles of microfilaments are clustered near the cell surface and close to the cell boundaries at the level of apical desmosomes. A circumferentially oriented process from one cell extends into a surface depression in an adjacent cell. Microtubules extend along the interior of the interdigitation. X 51,900.

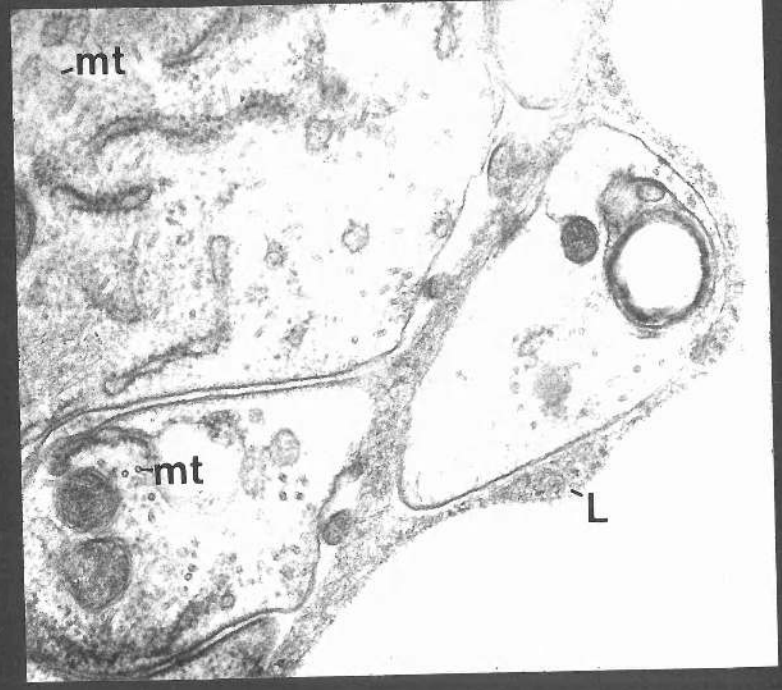

(7)

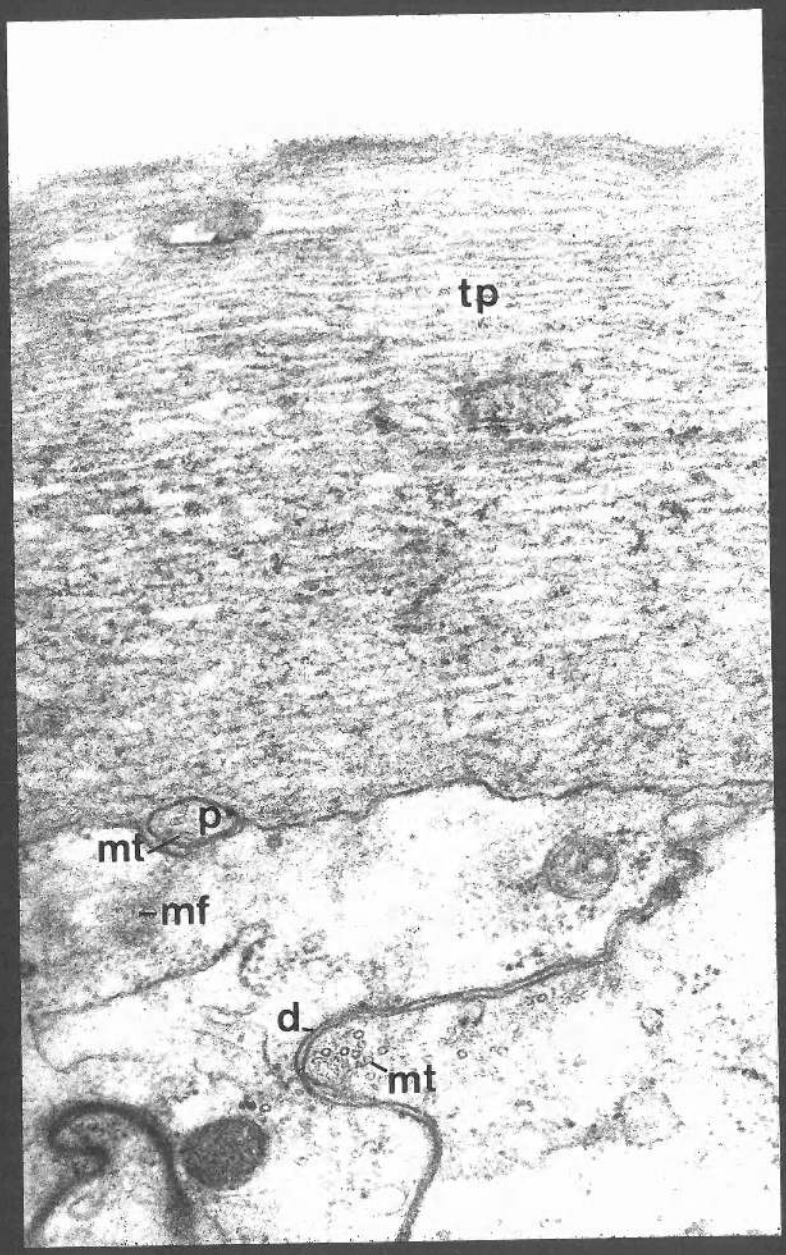

FIGURE 8

Section grazing through part of the outer surface of a P. americana follicle cell during growth phase 3. Microtubules and microfilaments are closely associated with apical desmosomes. X 72,500.

FIGURE 9

Section through part of a P. americana follicular epithelium where adjacent cells meet. Microtubules run alongside the lateral follicle cell membranes at right angles to the oocytes' polar axis. X 63,600.

8

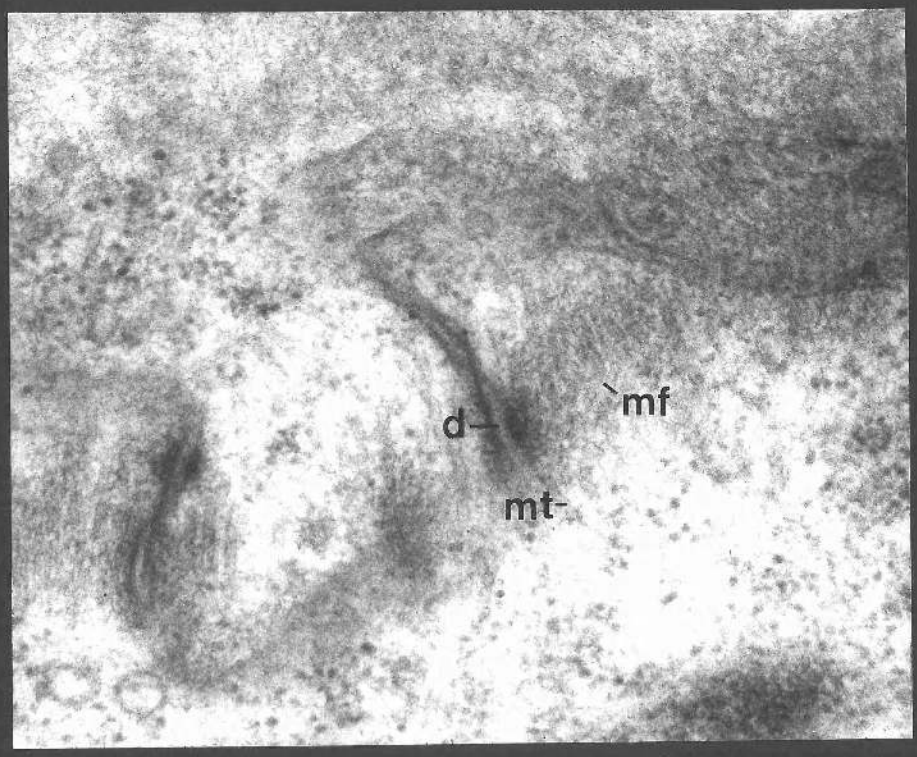

9

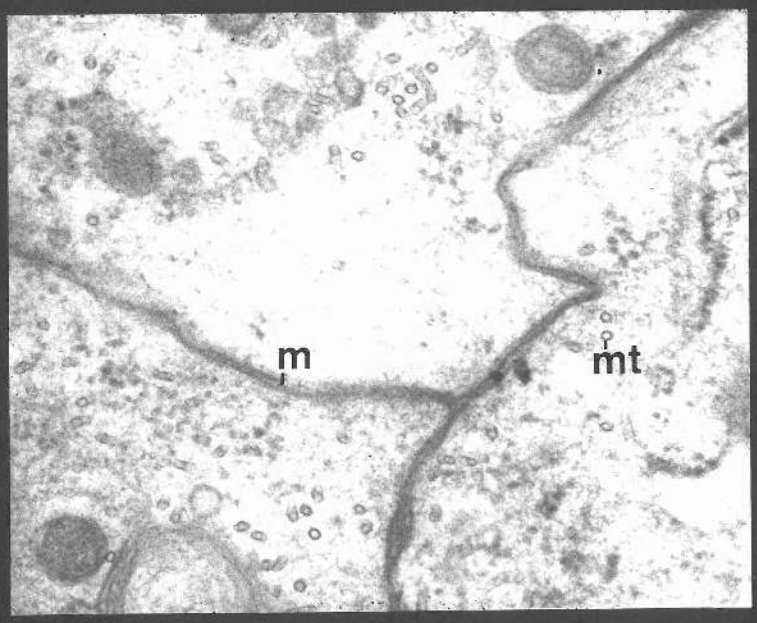

FIGURE 10

Section grazing through part of a P. americana follicle cell during growth phase 4. Circumferentially arranged microfilaments and microtubules are grouped directly beneath the follicle cell outer surface. X 63,600.

FIGURE 11

Part of the outer surface of a P. americana follicle during growth phase 4. The section is perpendicular to the outer surface and parallel to the polar axis of the follicle. Circumferentially oriented microtubules and microfilaments are clustered together near the cell surface. Circumferentially oriented microfilaments appear to be joined to desmosomes. X 116,600.

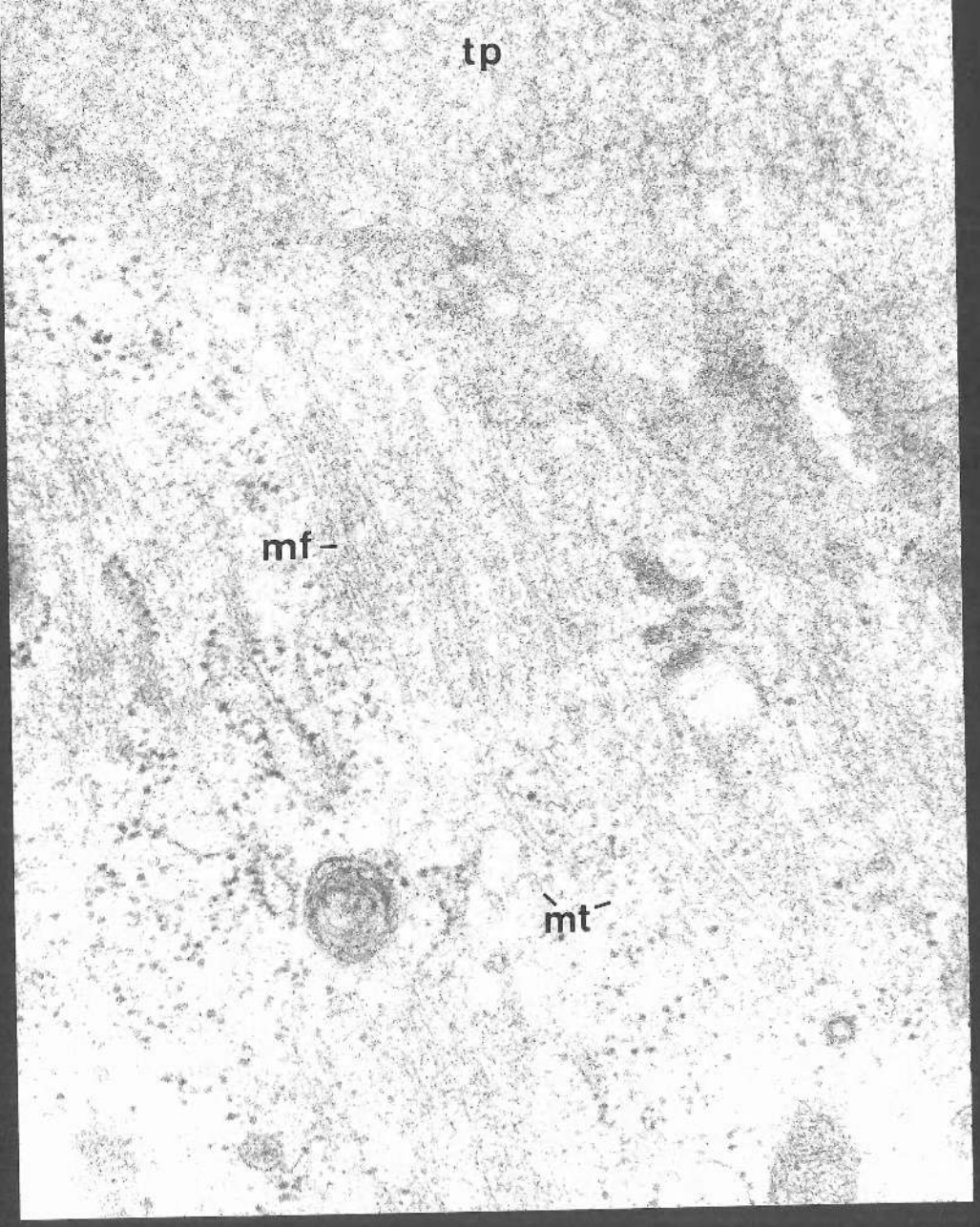

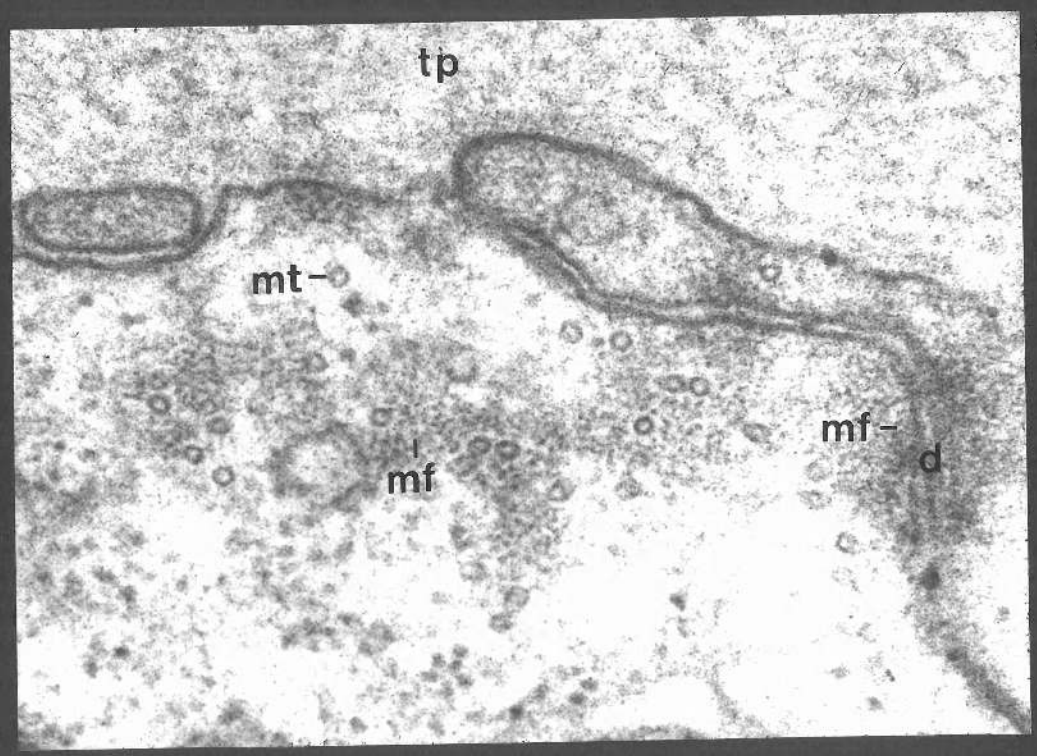

11

FIGURE 12

Section grazing through part of the outer surface of a P. americana follicle during growth phase 4. Circumferentially oriented microfilaments of adjacent cells appear to be connected to apical desmosomes. X 63,600.

FIGURE 13

Section grazing through part of the outer surface of a P. americana follicle as in Fig. 14. Circumferentially oriented microfilament bundles are joined to apical desmosomes and connect to lateral membranes of adjacent follicle cells thus providing an interconnected network of filaments throughout the follicular epithelium. X 17,200. Bar = 1 μm.

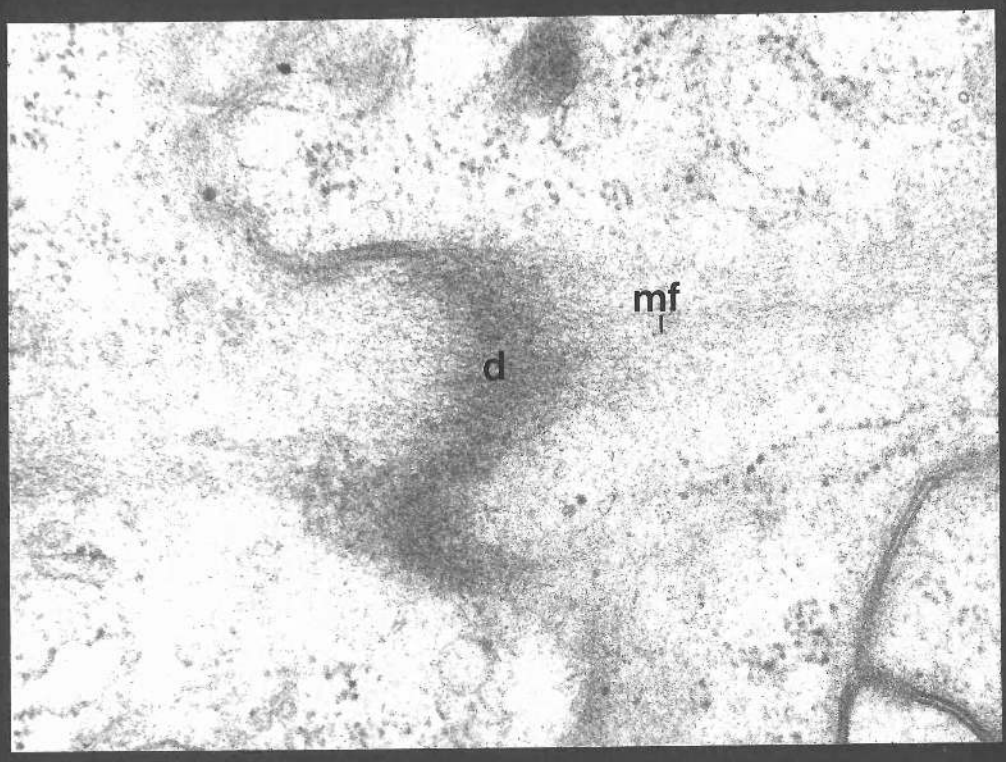
mf
d

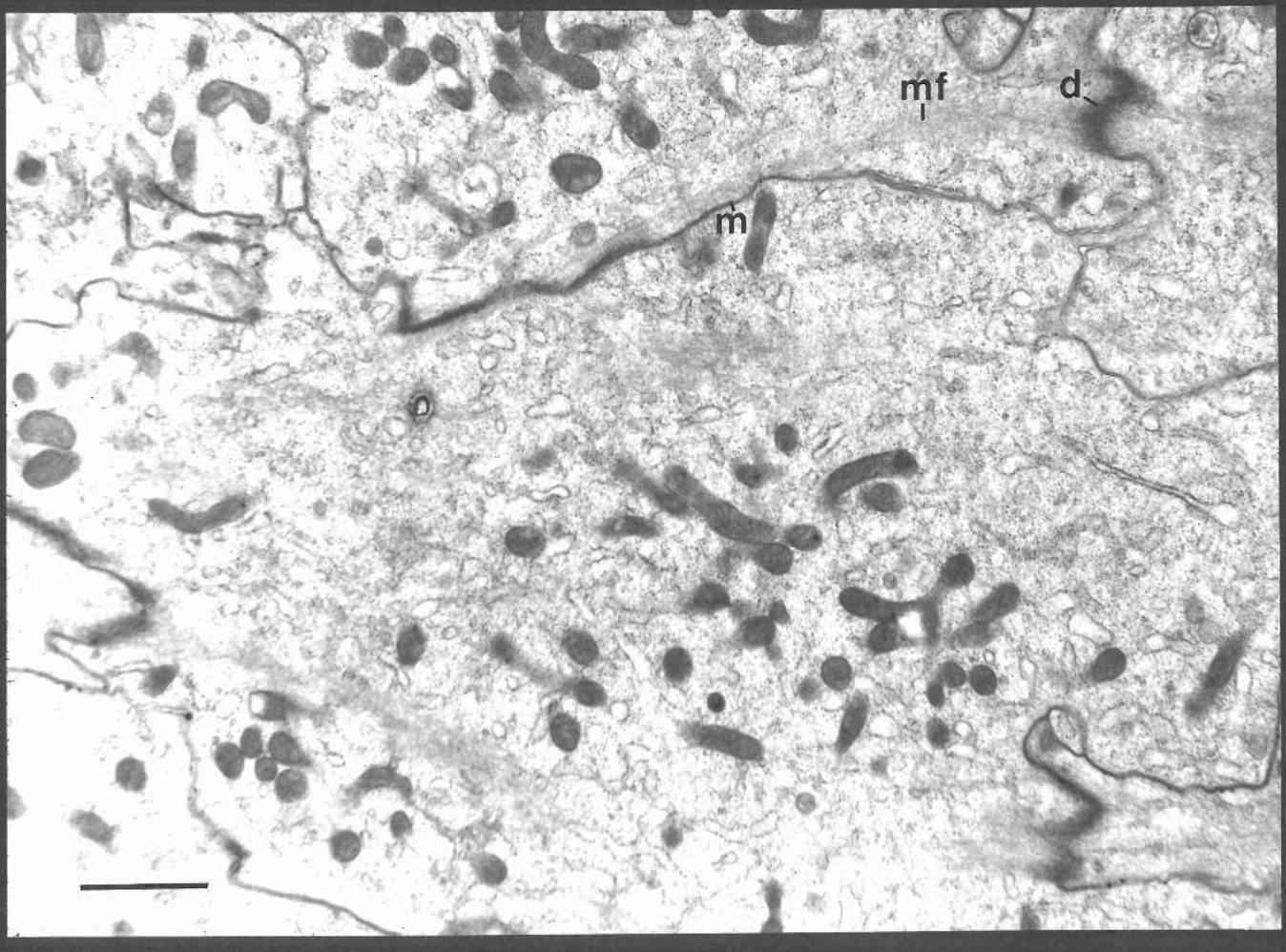
mf
d
m

FIGURE 14

Section grazing through part of the outer surface of a P. americana follicle during growth phase 5. Vitellogenic channels develop at points where 3 cells meet. Channels are filled with flocculent material. Microfilaments and microtubules extend along the sides of developing channels. X 19,600.

FIGURE 15

Section through a portion of a P. americana follicle during stage 5. The section is perpendicular to the outer surface and the polar axis of the follicle. Part of a vitellogenic channel is shown. The extent of detachment of the follicle cell from the tunica propria during vitellogenic channel formation is evident. X 9,300.

FIGURE 16

Section perpendicular to the outer surface of a P. americana follicle during growth phase 5. Microvilli are mostly withdrawn from follicle cell bases. The space thus created between follicle cell and oocyte is filled with flocculent electron lucent material. Bacteroids often occur within this space. X 42,400.

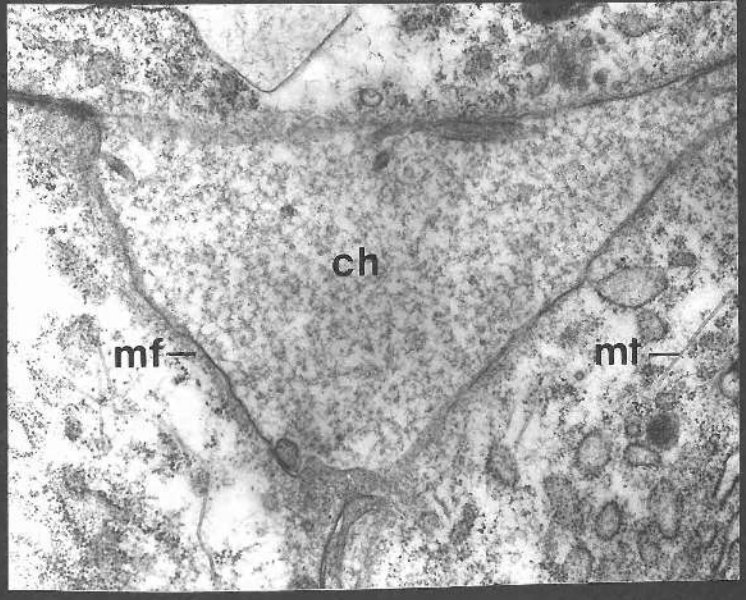

14

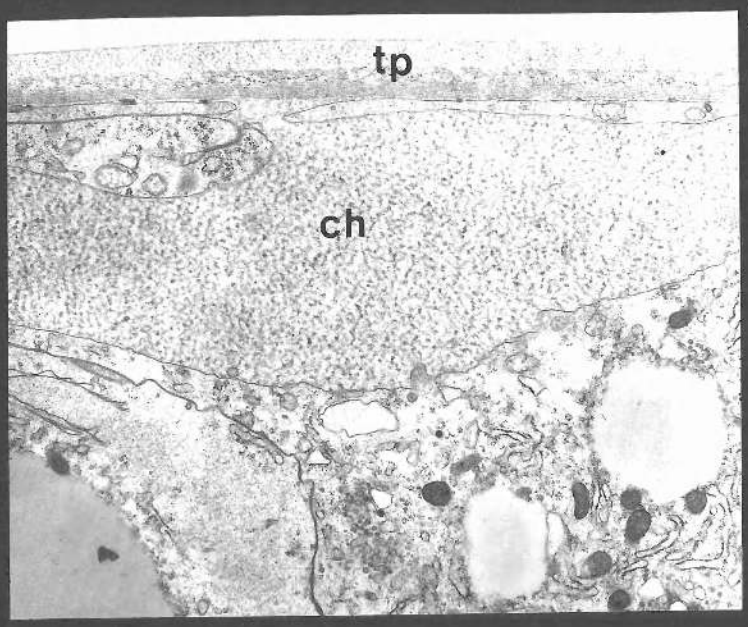

15

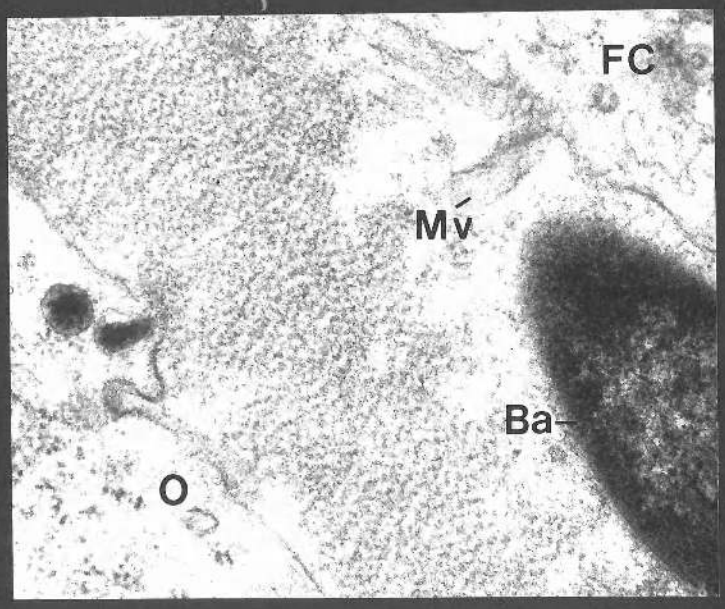

16

FIGURE 17

Section through part of a cockroach follicle near its outer surface at a region where two cells meet. The plane of the section is oriented perpendicular to the outer surface of the follicle and the follicle's polar axis. Follicle cells become detached from the tunica propria during the formation of channels. The tunica propria is differentiated into an outer granular and an inner fibrous layer. X 63,600.

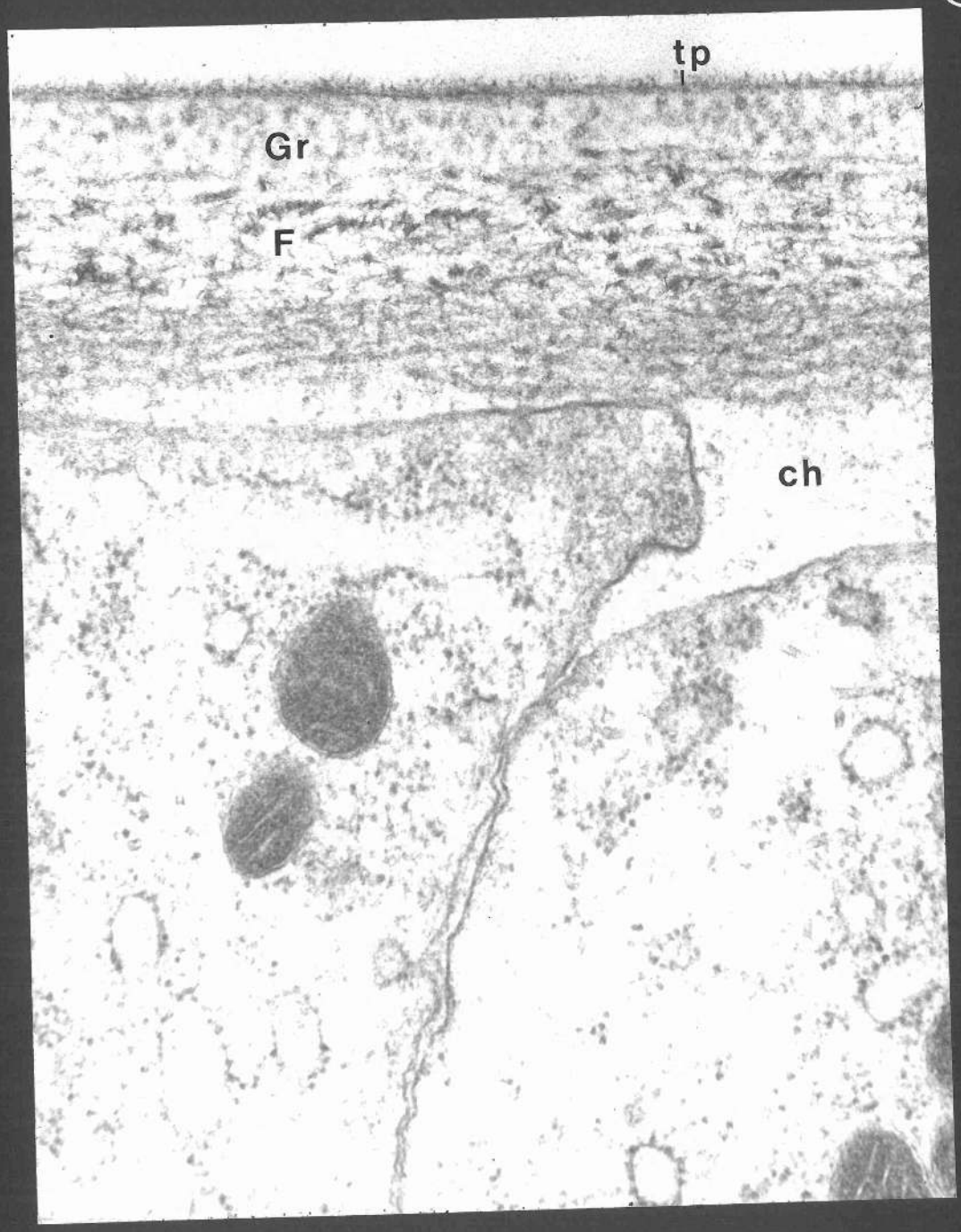
tp
Gr
F
ch

FIGURE 18a

Section grazing through part of the tunica propria of a cockroach follicle during growth phase 3. A layer of the laminated tunica propria is shown to illustrate that the tunica propria really is laminated in composition and contains no fibres. X 63,600.

FIGURE 18b

Section perpendicular to the outer surface of a cockroach follicle during growth phase 3. The layered or laminated appearance of the tunica propria is evident. X 63,600.

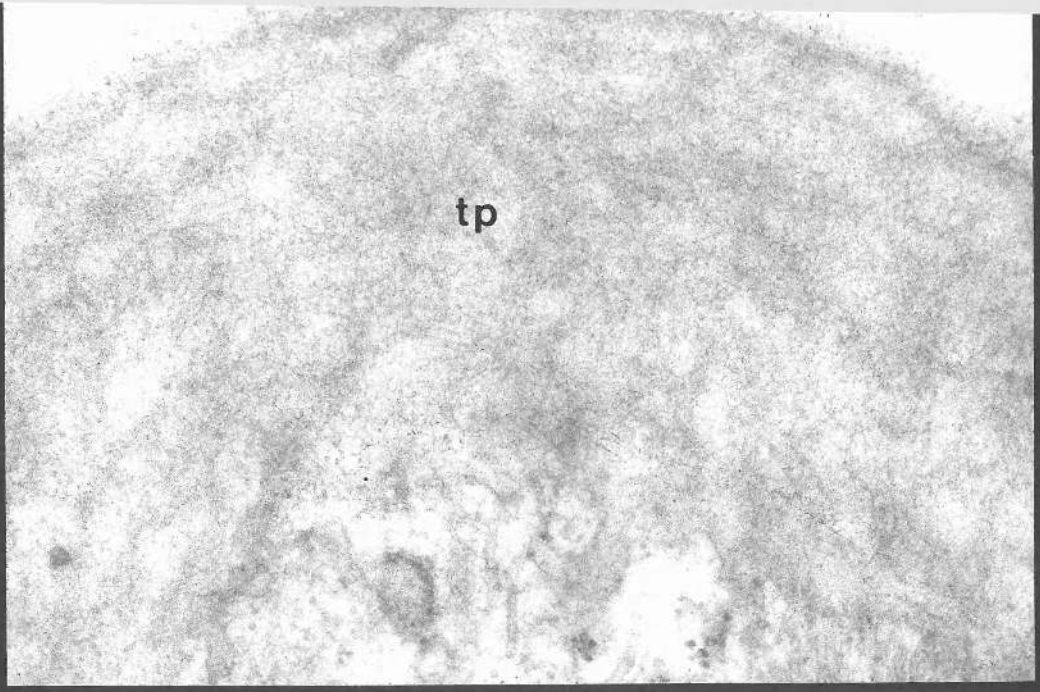

(18b)

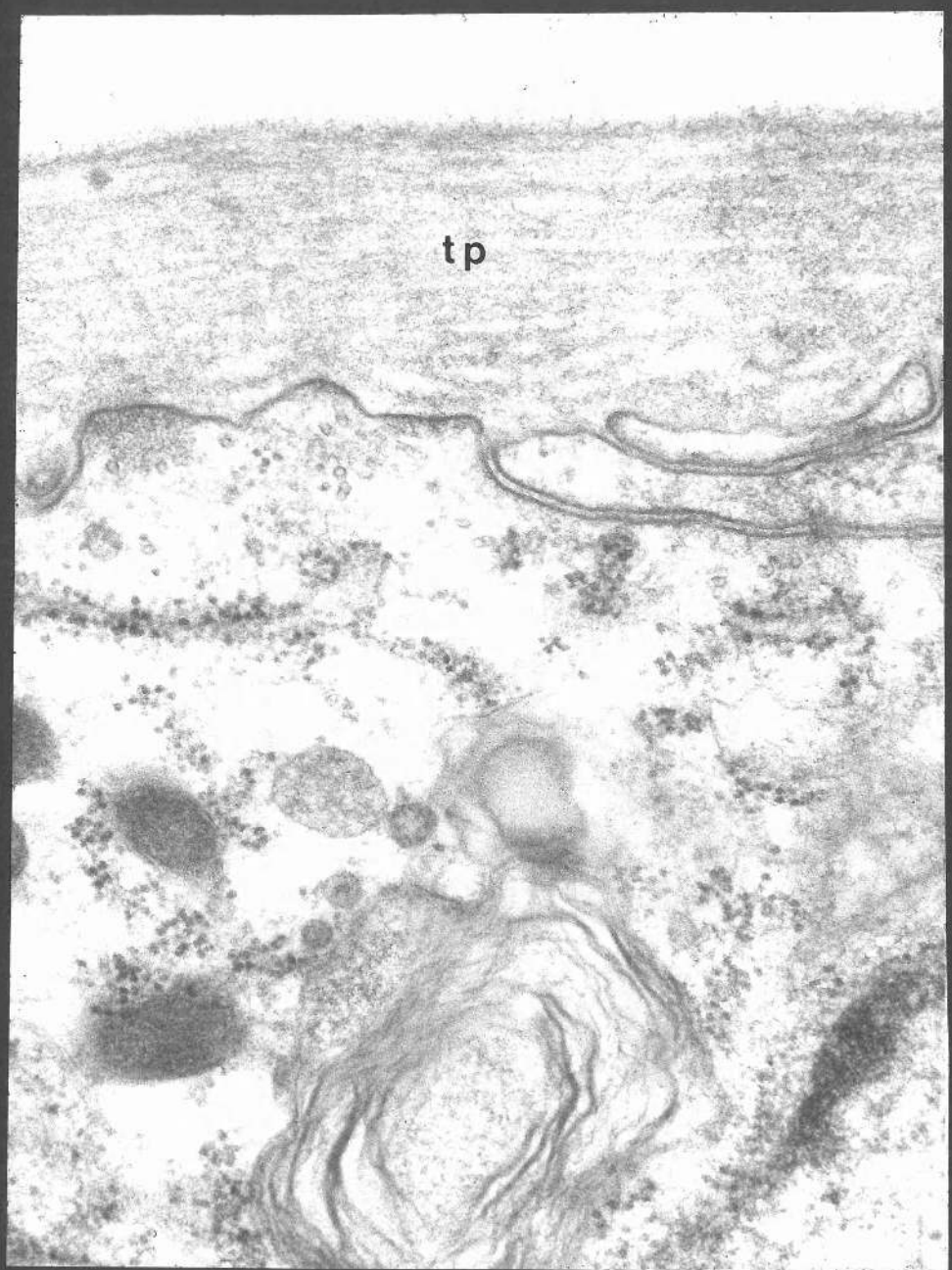

FIGURE 19

Part of the outer surface of a cockroach follicle cell and its tunica propria during growth phase 4. The section is parallel to the outer surface and parallel to the polar axis of the follicle. Figure 19 shows that there is an increase in tunica propria thickness from growth phase 3 (Fig. 18a) to growth phase 4. Fibrous elements are embedded within the tunica propria (arrows). Microtubules and microfilaments are clustered directly beneath the follicle cell outer surface close to a desmosome. X 63,600.

FIGURE 20

Section grazing through part of the tunica propria of a P. americana follicle during growth phase 4. Circumferentially oriented fibres within the tunica propria are shown. Most of the fibres have diameters of 12-14 nm (short arrows). Others are grouped in bundles up to 30 nm in diameter (long arrows). X 63,600.

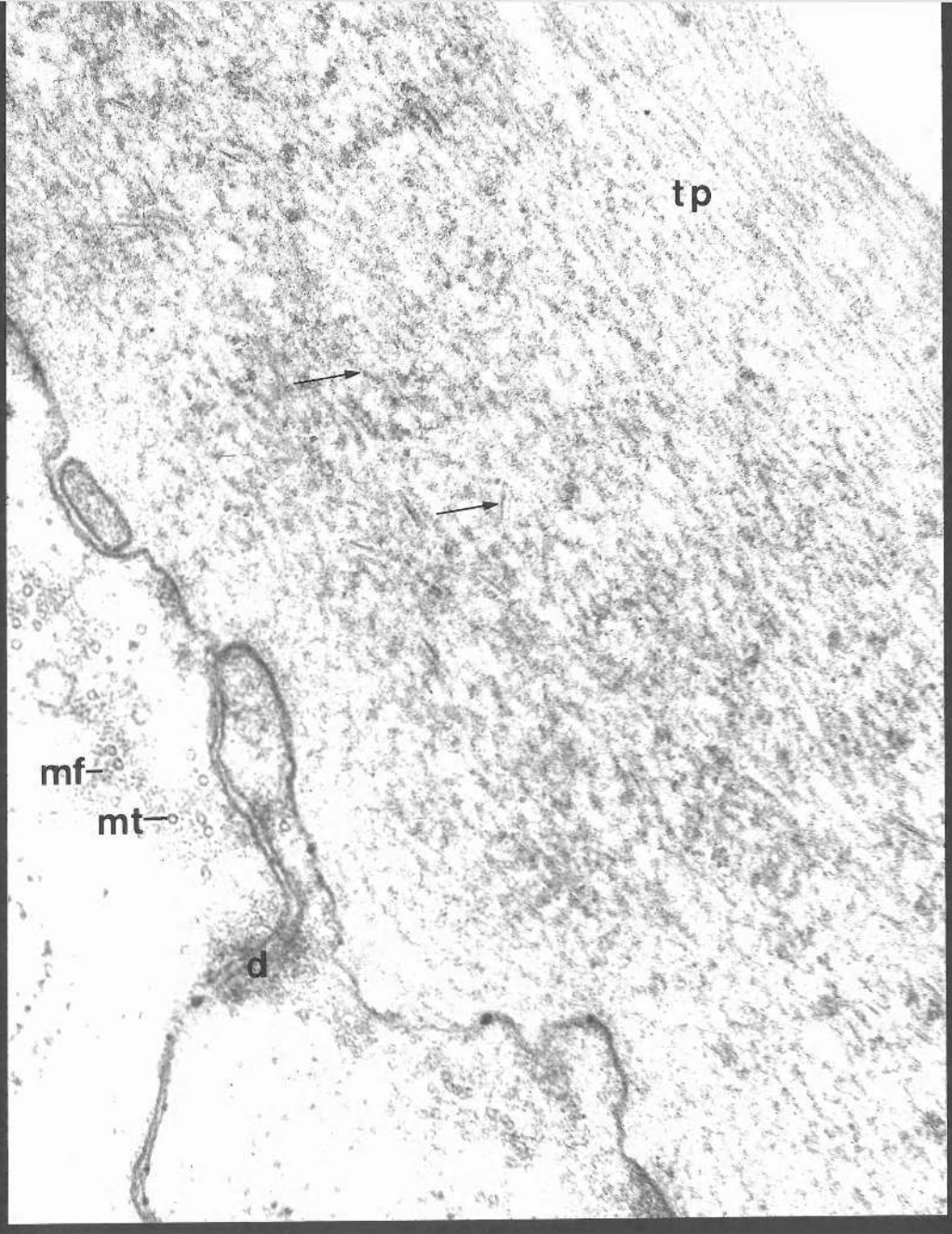

2u

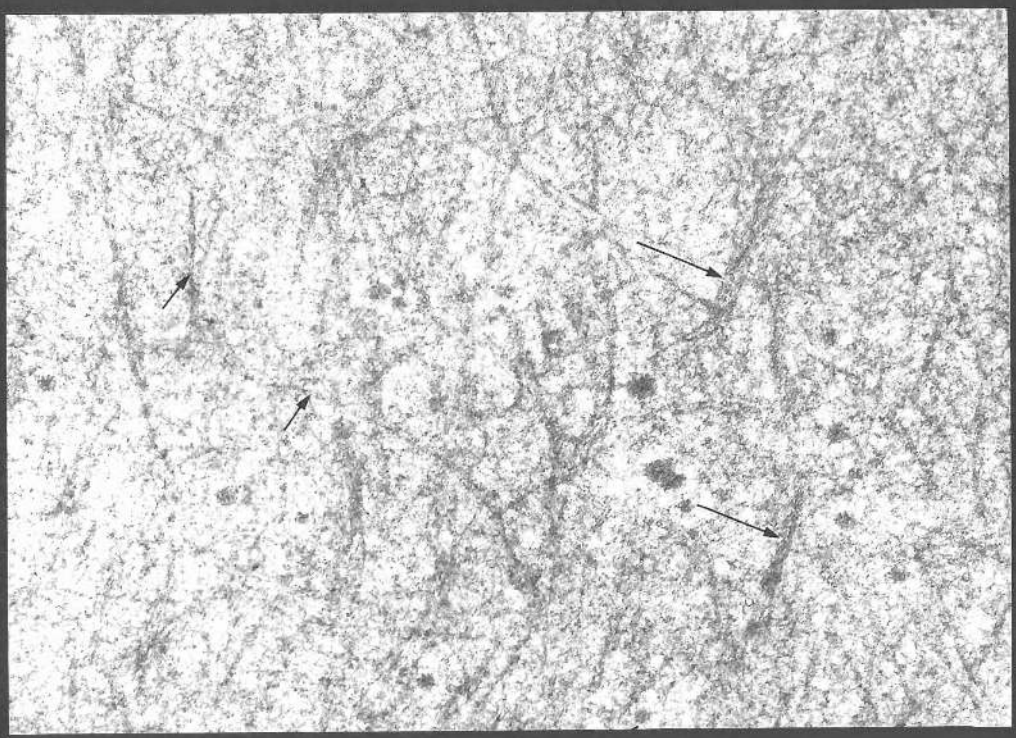

FIGURE 21a

Section grazing through part of the tunica propria of a P. americana follicle during growth phase 5. Two layers, an outer granular layer, and an inner fibrous layer are evident. The granular layer consists of granules 25-30 nm in diameter. The fibrous layer consists of small fibres of 12-14 nm in diameter (short arrows) and larger fibres of up to 36 nm in diameter. Some of the larger fibres have a cross-banded appearance (double arrow). X 63,600.

FIGURE 21b

Section through part of the tunica propria of a P. americana follicle during late growth phase 5. The section is perpendicular to the outer surface and perpendicular to the polar axis of the follicle. The cross-banded appearance of the tunica propria fibres is clearly apparent. X 116,600.

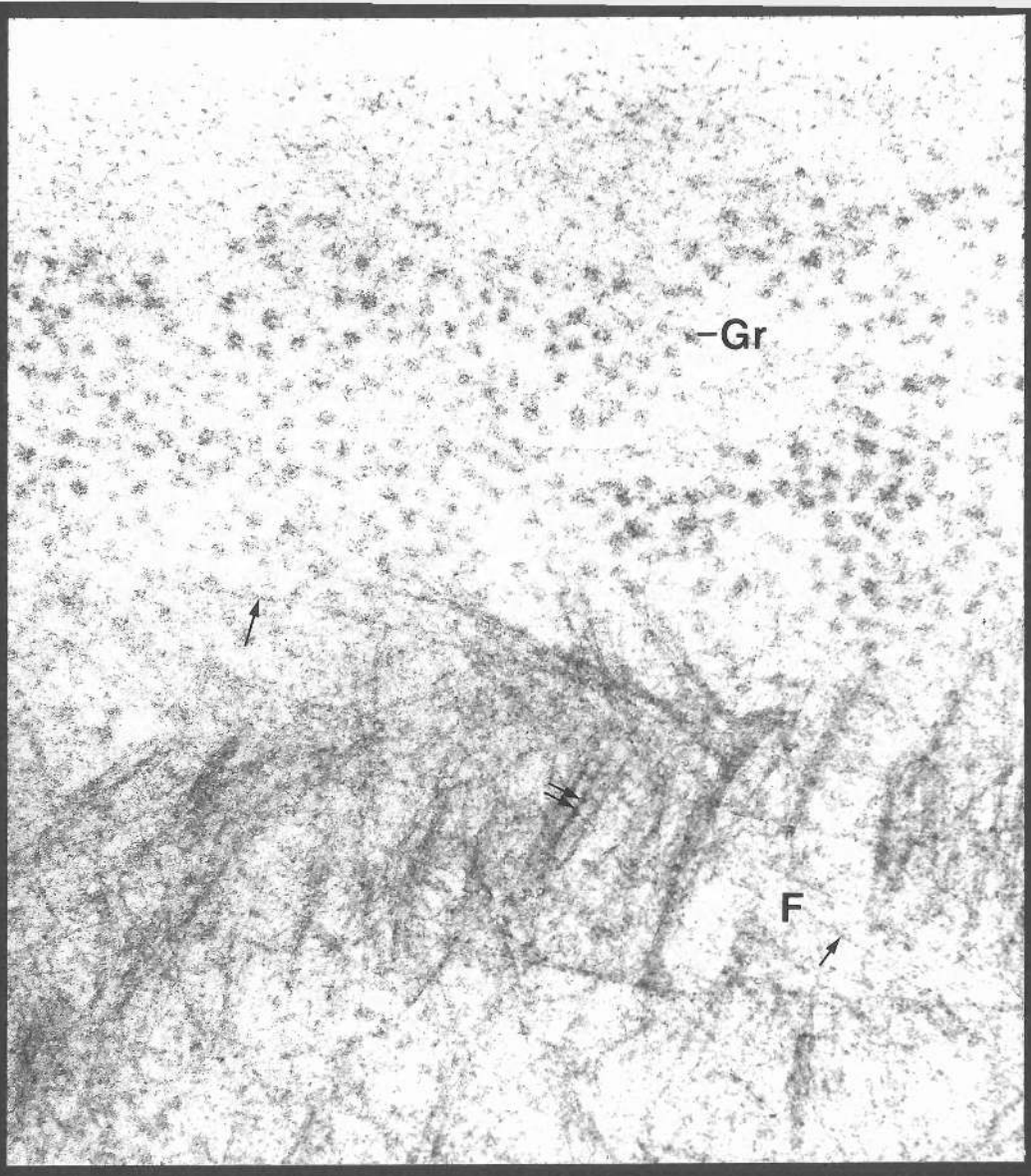

21b

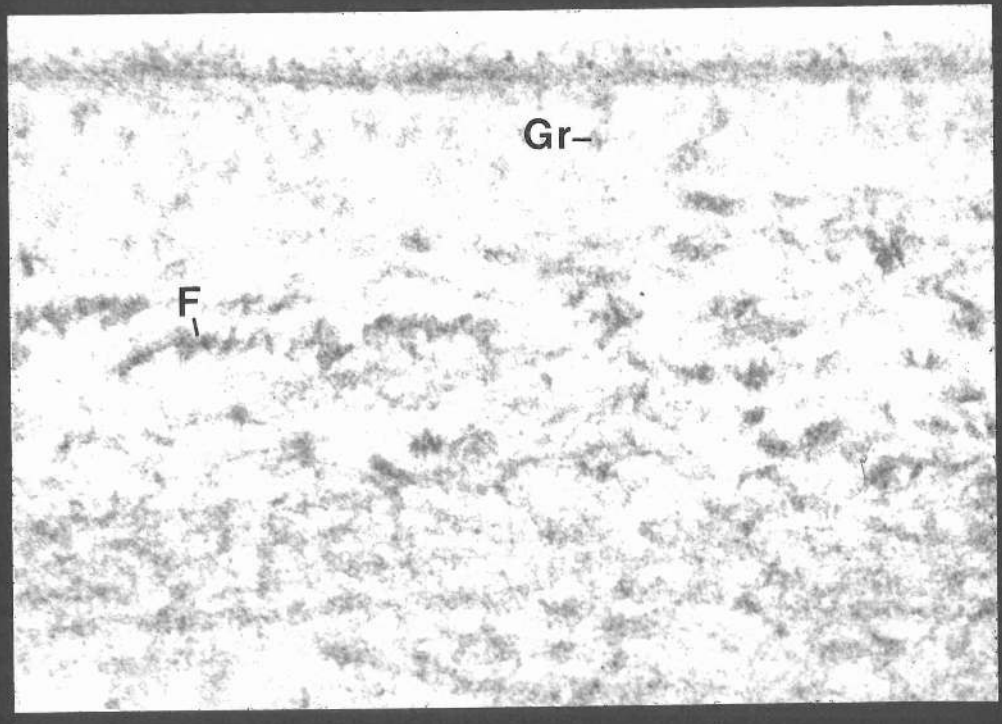

FIGURE 22

Section grazing through the outer surface of two adjoining epithelial plug cells. Circumferentially oriented microtubules and microfilaments are clustered at the apices of these cells. X 28,200.

FIGURE 23

Section through part of an epithelial plug of a cockroach ovariole. The section is parallel to the long axis of the ovariole. Many microtubules run parallel to the longitudinal axes of epithelial plug cells alongside the lateral membranes of the cells. Some tubules meet the lateral membranes at various points (arrows). Adjacent cells are often joined by septate desmosomes. X 35,000.

FIGURE 24

Section through part of an epithelial plug cell showing the large numbers of microtubules which run parallel to the longitudinal axis of the cell. The section is at right angles to the long axis of the ovariole. X 39,100.

FIGURE 25

Section through two adjacent epithelial plug cells showing microtubules which meet the lateral membranes of these cells. Section orientation as in Fig. 24. X 47,000.

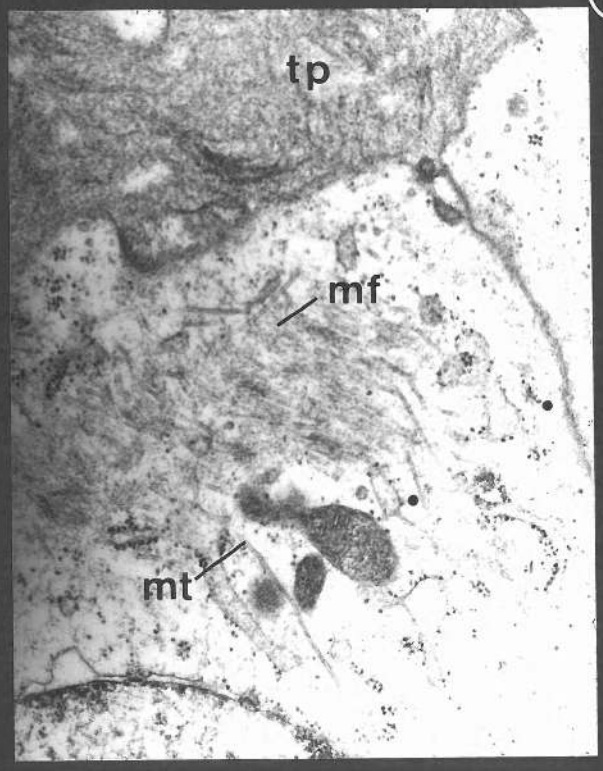
22
tp
mf
mt

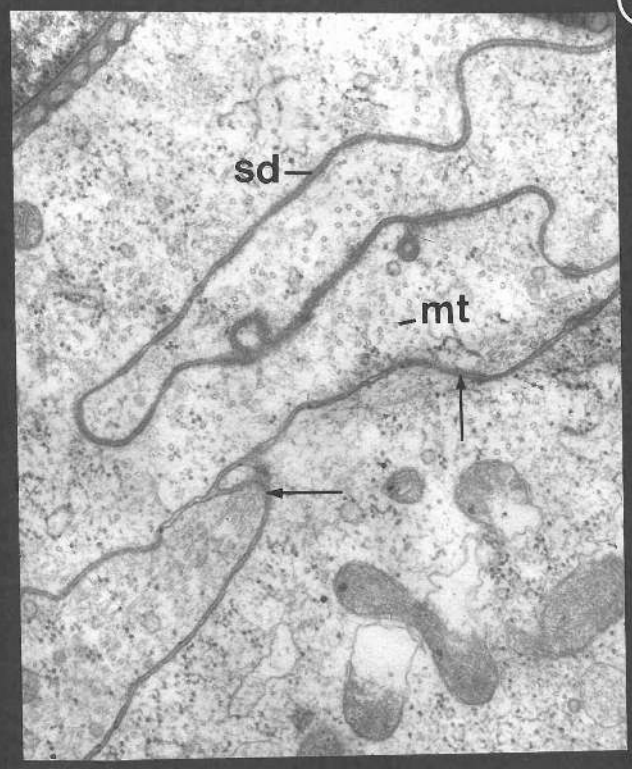
23
sd
mt

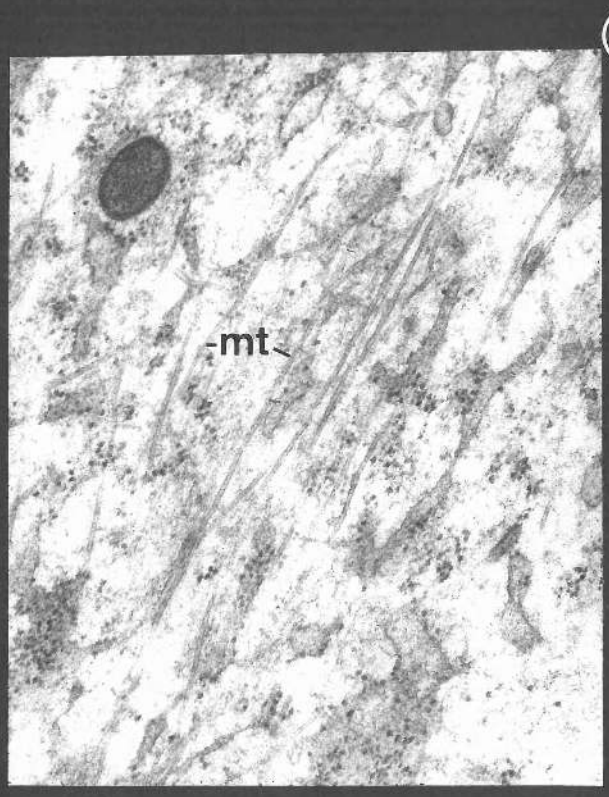
24
mt

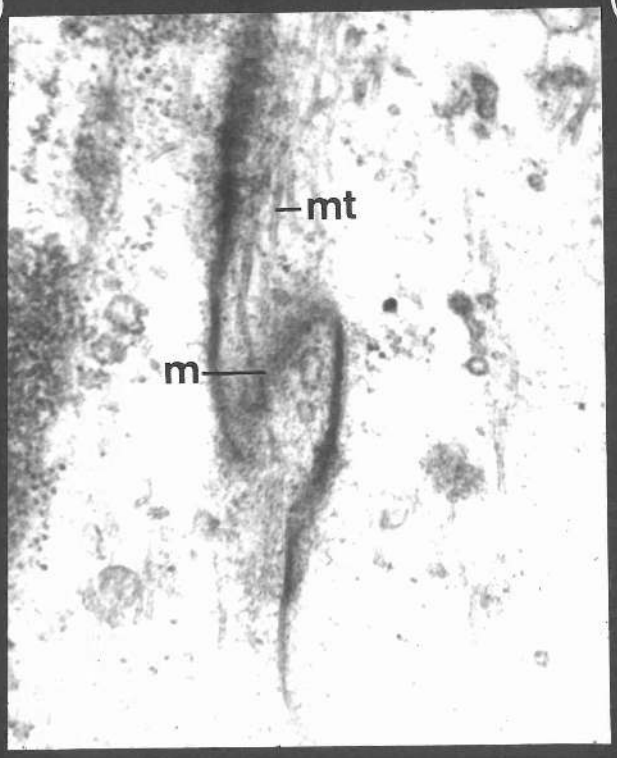
mt
m

FIGURE 26

Schematic diagram showing the 'follicle-tunica' sequence of cockroach follicles during growth phases 3-5. The arrangement of desmosomes, microfilaments, microtubules, fibres and granules are portrayed as they would be revealed at an edge formed by a cut parallel to the plane of the epithelium and parallel to the follicles' polar axis. For clarity, the microvilli which project from the inner surfaces of the cells have been omitted. Interdigitating cell processes and all the organelles shown are represented as disproportionately large structures with respect to cell size.

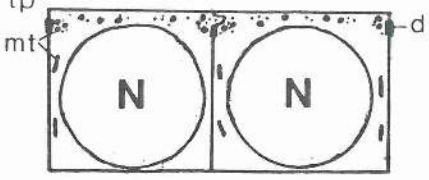

GP 3

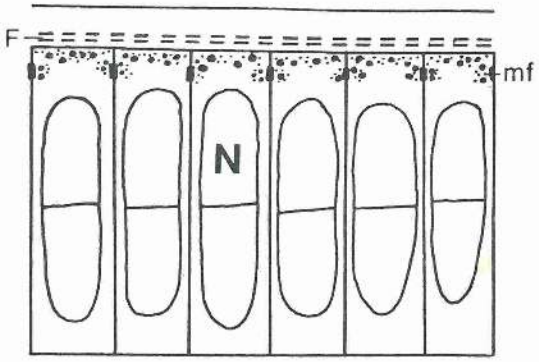

GP 4

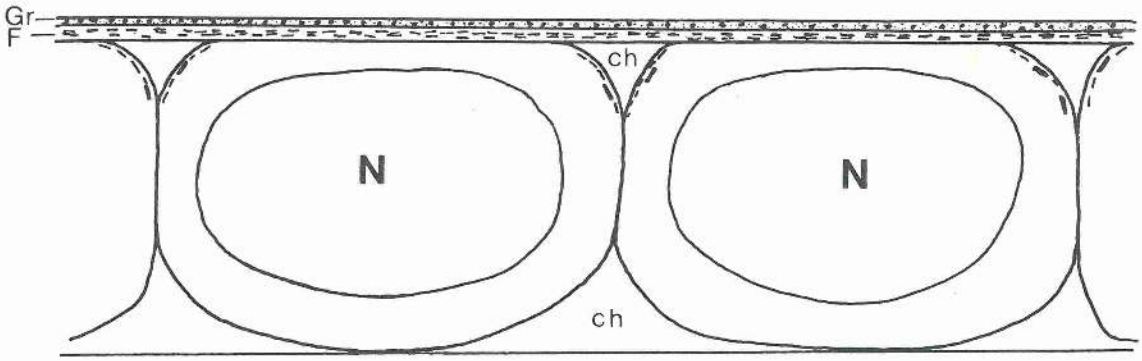

GP

Figure 26

P.americana 'follicle-tunica' sequence

FIGURE 27

The basis of the follicle numbering system and growth phases 1 and 2 is shown in terms of positioning in the ovariole at different points in the vitellogenic cycle of R. prolixus. A shows the situation immediately after ovulation and C just prior to ovulation with intervening stage B completing the sequence. The terminal filament (TF) and the tropharium (T) are indicated. (CH) indicates chorion formation, (V) indicates vitellogenic follicles and (PV) indicates previtellogenic follicles.

A

V	PV	T	TF
GP 2	GP 1		

B

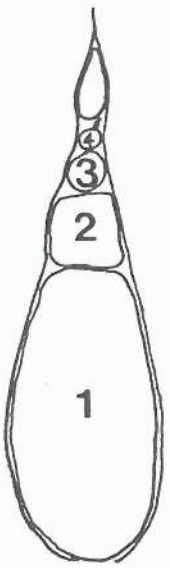

V	PV	T	TF
GP 2	GP 1		

C

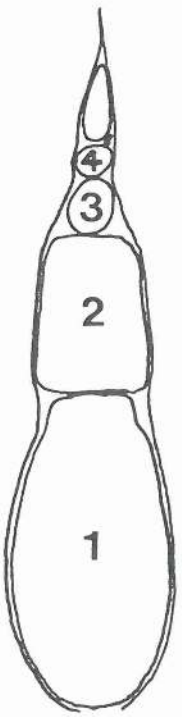

CH	V	PV	T	TF
GP 2		GP 1		

FIGURE 28

The relationship between the diameters (measured at their widest points and at right angles to the longitudinal axis of the ovariole) and lengths of R. prolixus follicles in a large sample of ovarioles is shown. The shoulder of the computed regression lines (arrow) indicates a significant difference. This reveals the two growth phases 1-2 that account for most of the anisometric growth of follicles. The relationship in length between follicles 1-4 is also compared. The blackened area denotes the range of lengths exhibited by follicles 1-4.

Figure 28

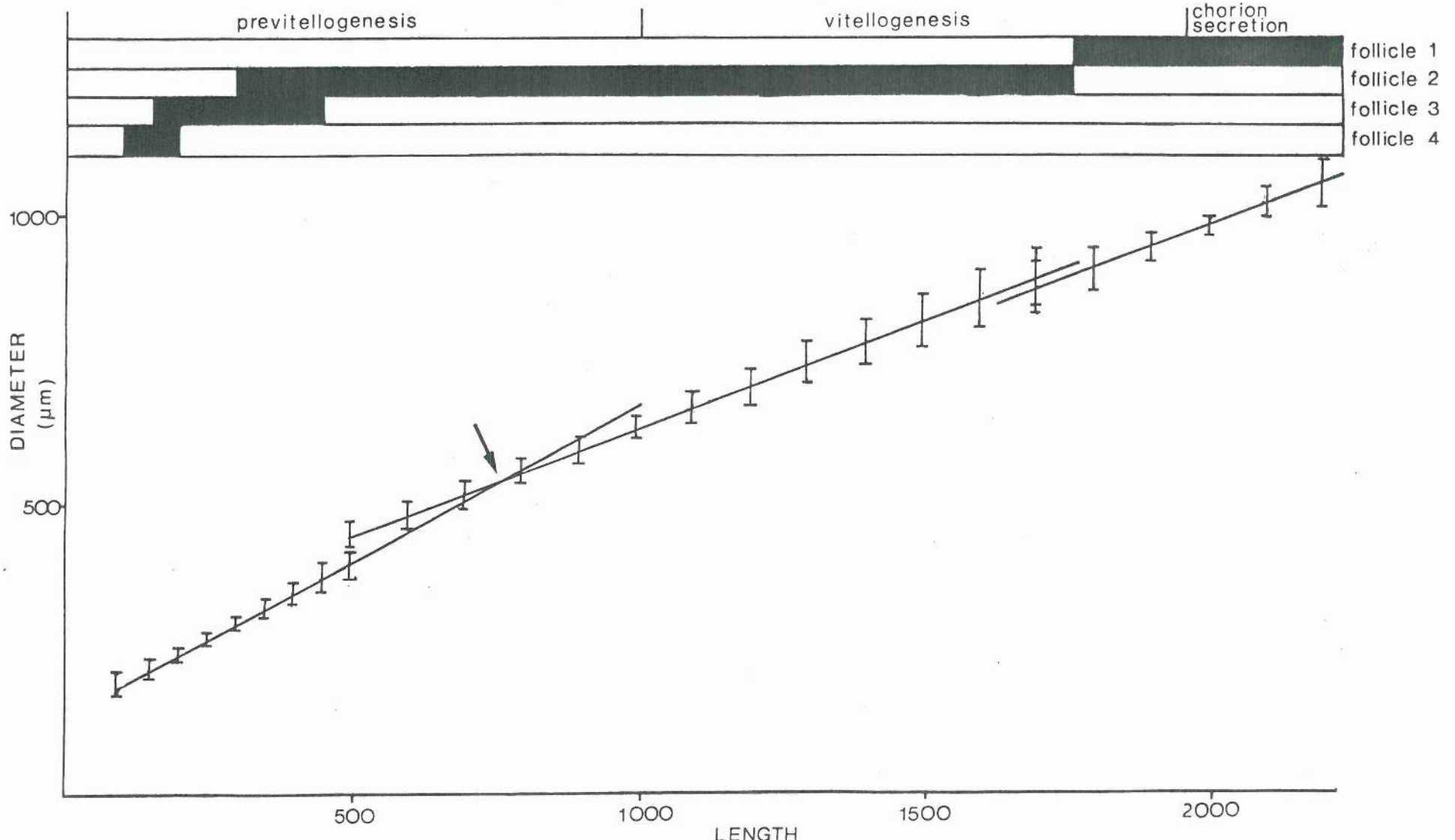
previtellogenesis
vitellogenesis
chorion secretion
follicle 1
follicle 2
follicle 3
follicle 4
1000
500
DIAMETER (µm)
500
1000
1500
2000
LENGTH

FIGURE 29

Section through part of a R. prolixus follicle during early previtellogenic growth. The plane of the section is oriented perpendicular to the surface and to the polar axis of the follicle. Circumferentially oriented fibrous elements are evident within the tunica propria on the side of the tunica propria nearest the follicle cells (arrow). Also shown are circumferentially oriented microfilament bundles which are closely grouped near the follicle cell surface. X 58,300.

FIGURE 30

Section through part of an R. prolixus follicle during late previtellogenesis. Section orientation as in Fig. 29. The thickness of the tunica propria is reduced compared with its thickness during early previtellogenesis (compare with Fig. 29). Circumferentially oriented fibres are evident. The fibres are grouped into bundles 25-30 nm in diameter on the side of the tunica propria nearest follicle cells (arrow). Part of the ovariole sheath and its external lamina lie close to the tunica propria. X 58,700.

FIGURE 31

Section through part of a R. prolixus follicle during vitellogenesis. The tunica propria is further reduced in thickness compared with its thickness during previtellogenic growth. Fibrous elements occur within the tunica propria as during previtellogenic growth (arrow). The ovariole sheath lies very close to the tunica propria and contains muscular elements and microtubules. X 58,700.

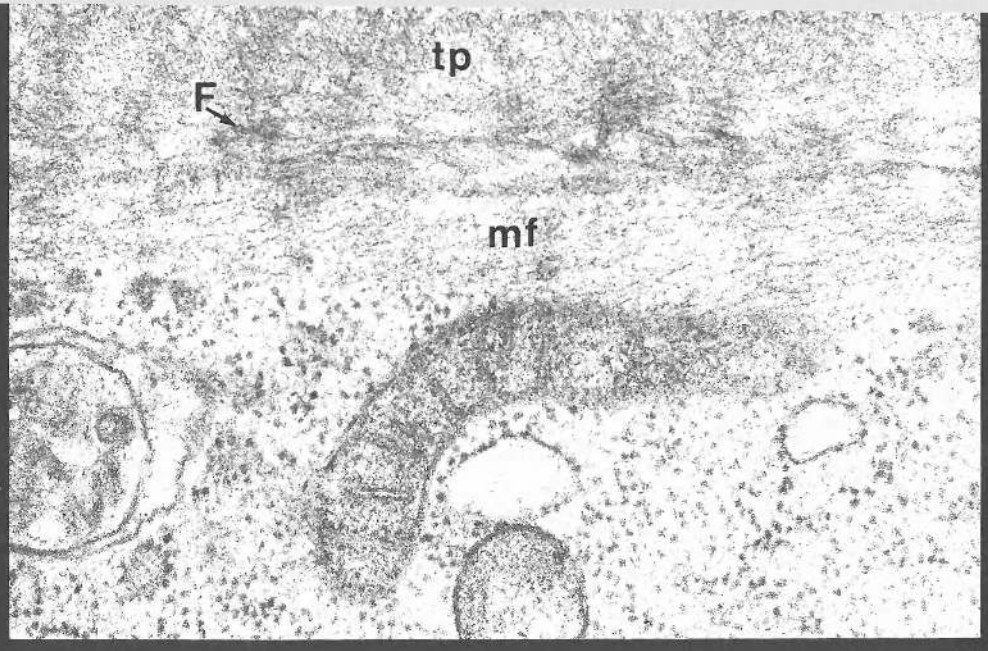

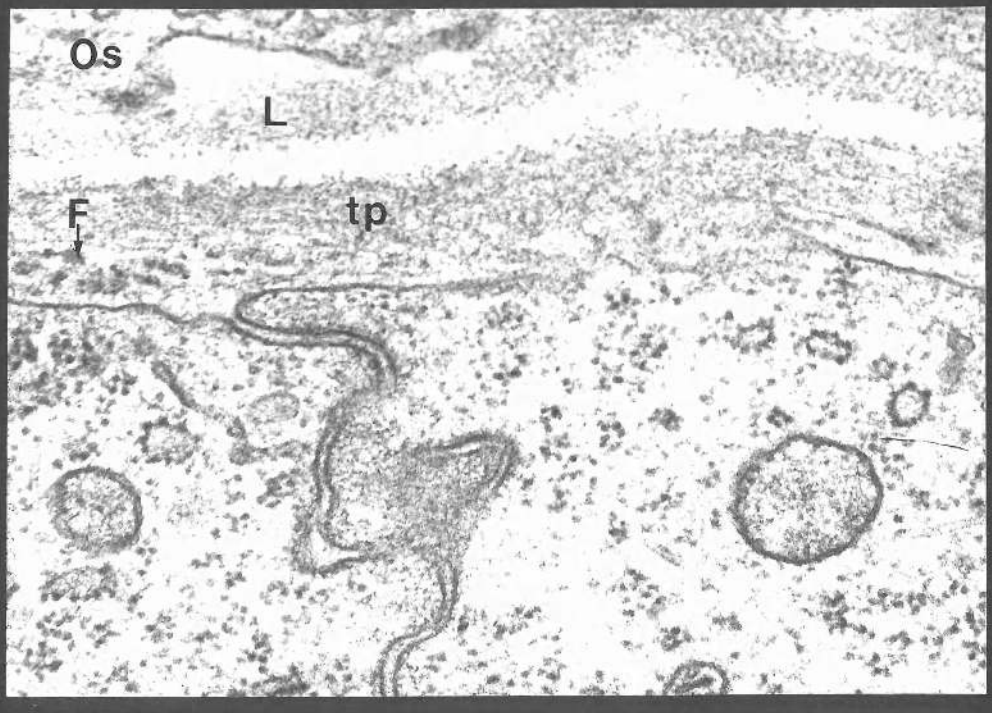

30

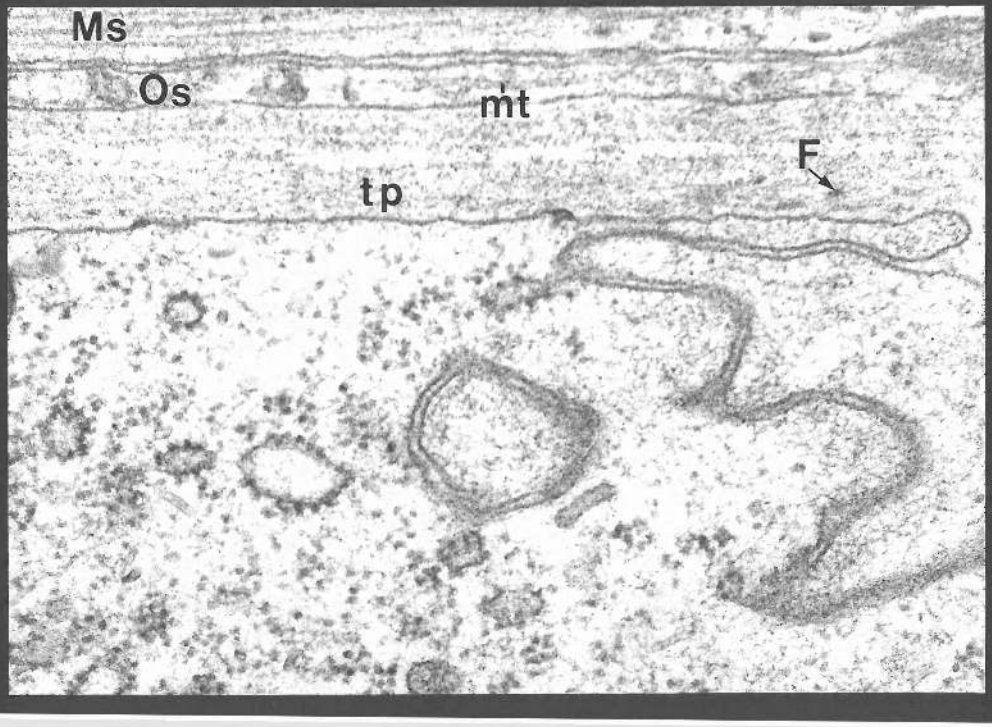

31

FIGURE 32

Section grazing through a follicle of R. prolixus during pre-vitellogenesis. Circumferentially oriented fibres are grouped on the side of the tunica nearest follicle cells. Some fibres occur 'singly' (short arrow) while others are grouped into bundles up to 30 nm in diameter. Circumferentially arranged microtubules and microfilaments are clustered directly beneath the follicle cell surface. X 82,900.

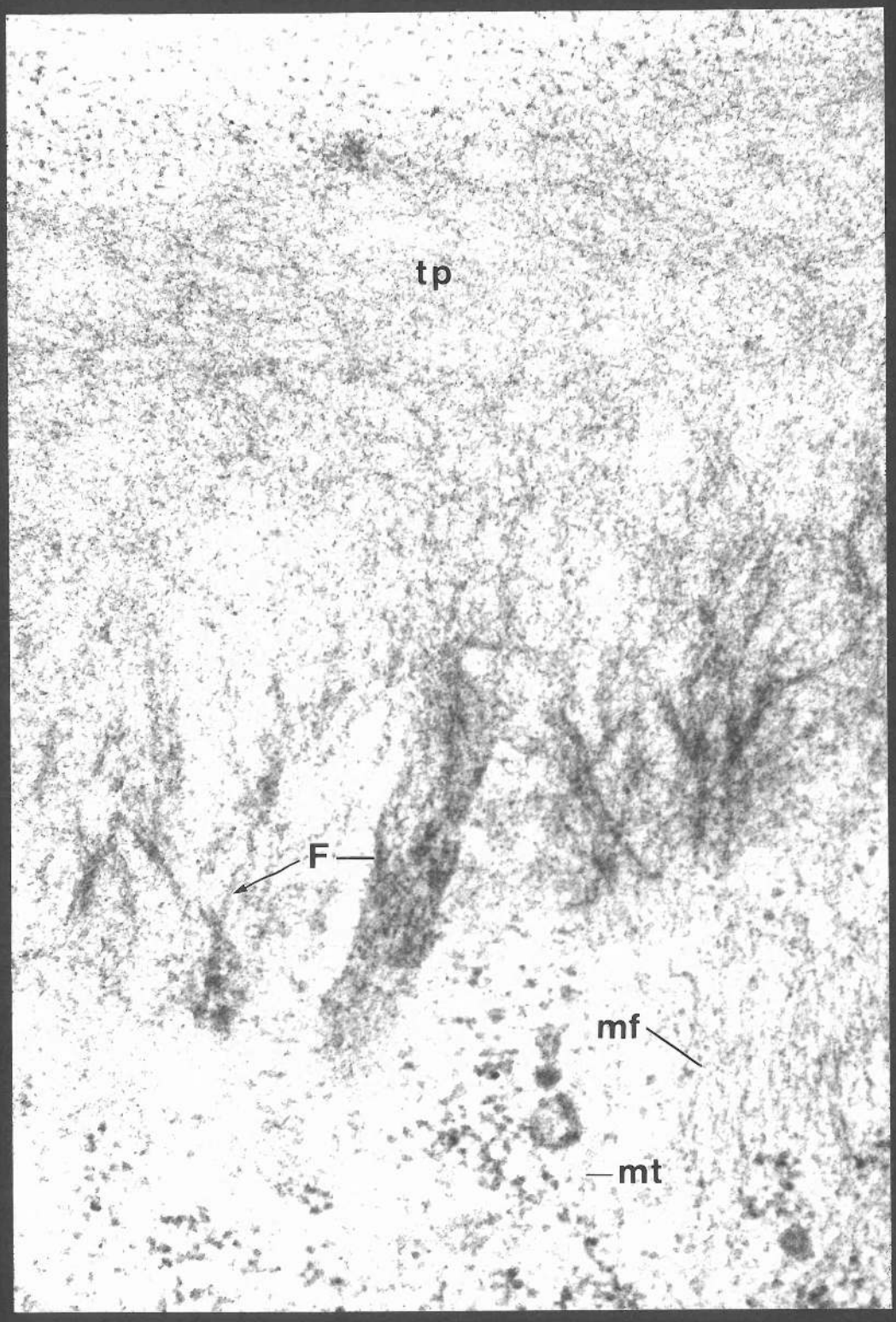
tp
F
mf
mt

FIGURE 33

Section grazing through part of a follicle of R. prolixus during vitellogenesis. Most of the fibrous elements of the tunica propria are arranged circumferentially on the side of the tunica nearest follicle cells. The fibres are grouped into bundles up to 30 nm in diameter. Others are smaller measuring 12-14 nm in diameter. X 90,100.

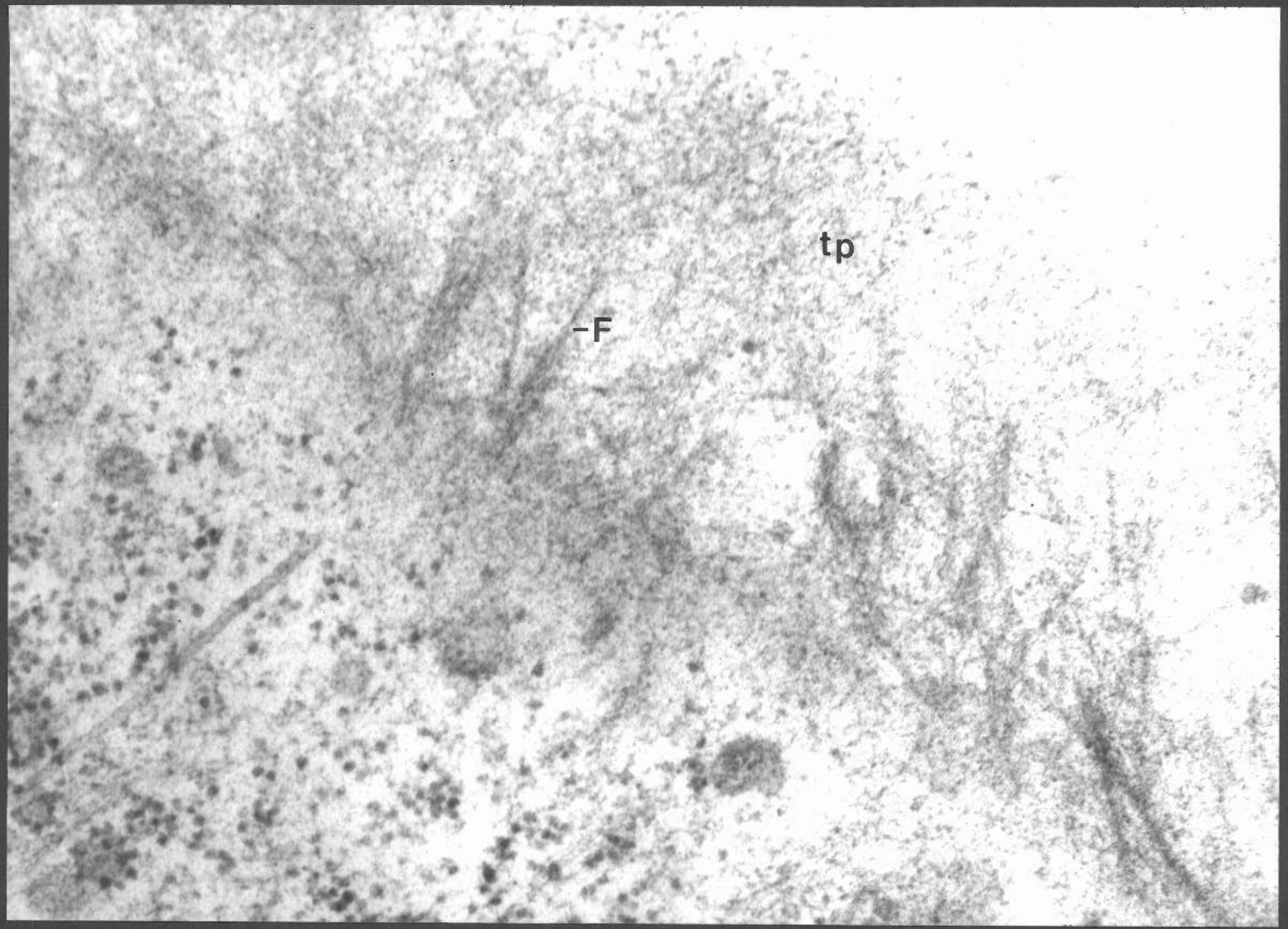
tp
-F

FIGURE 34

Part of two adjacent follicle cells of a R. prolixus follicle during previtellogenesis. Microtubules run parallel to the long axes of cells (as indicated by the arrow) at right angles to the polar axis of the follicle. X 87,000.

FIGURE 35

Section grazing through the outer surface of two adjacent R. prolixus follicle cells during previtellogenesis. A filopodial process from one cell (FC1) extends into a space between the cells FC1 and FC2. Microfilament bundles extend along the interior of the filopodium. X 37,100.

34

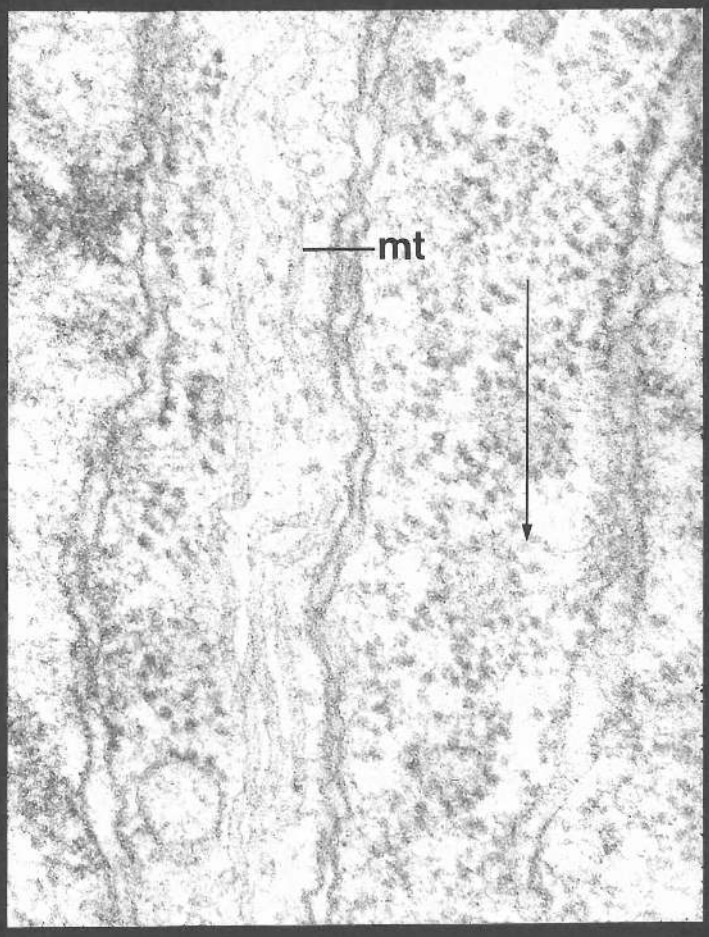

35

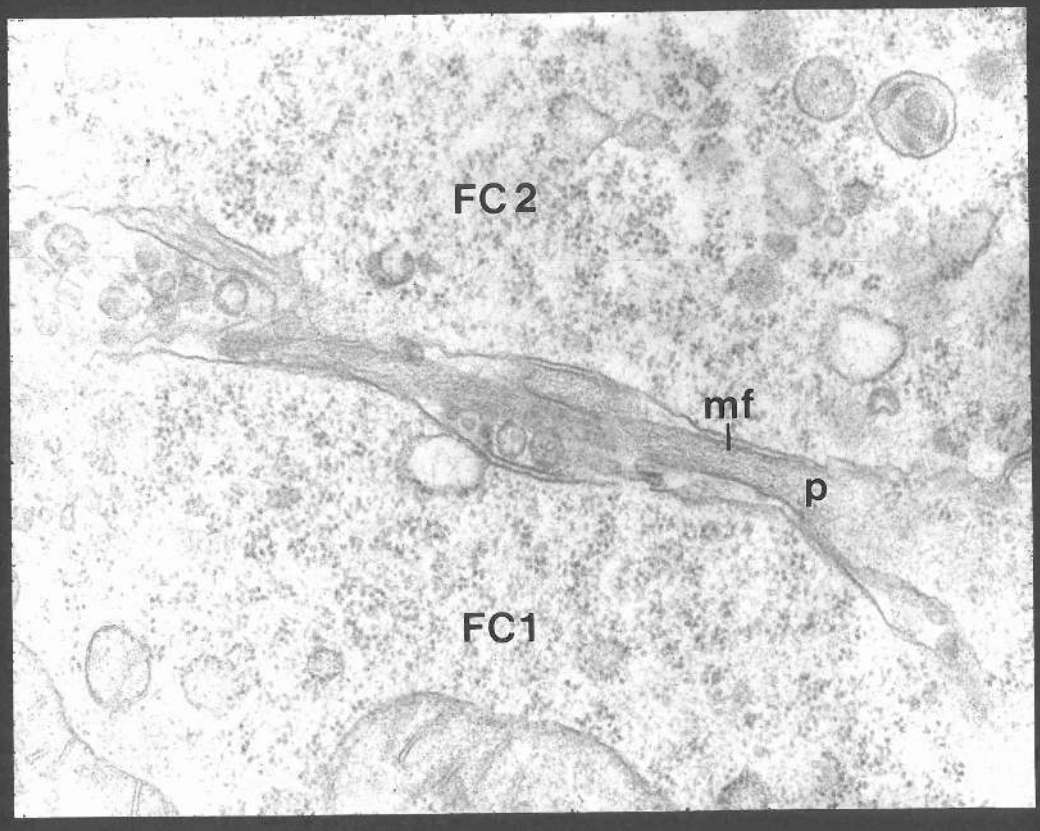

FIGURE 36

Section through part of the basal surface of two adjacent R. prolixus follicle cells during previtellogenesis. The plasma membranes of adjacent cells are connected by septate desmosomes, gap junctions and zonulae adhaerentes junctions. Circumferentially oriented microfilaments are clustered around the zonulae adhaerens junction. The plane of the section is oriented perpendicular to the outer surface of and parallel to the polar axis of the follicle. X 87,000.

FIGURE 37

Part of the basal surface of a R. prolixus follicle during early previtellogenesis. The section is oriented perpendicular to the outer surface and to the polar axis of the follicle. Circumferentially oriented microfilament bundles extend across a follicle cell at the level of zonulae adhaerentes. X 39,200.

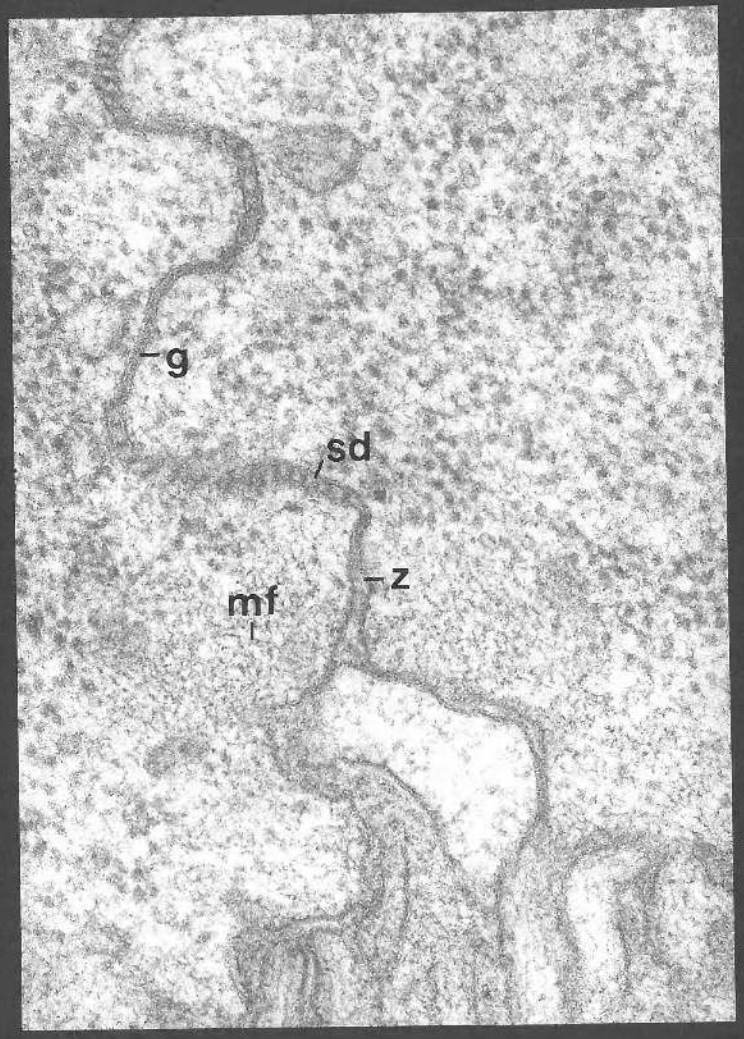

37

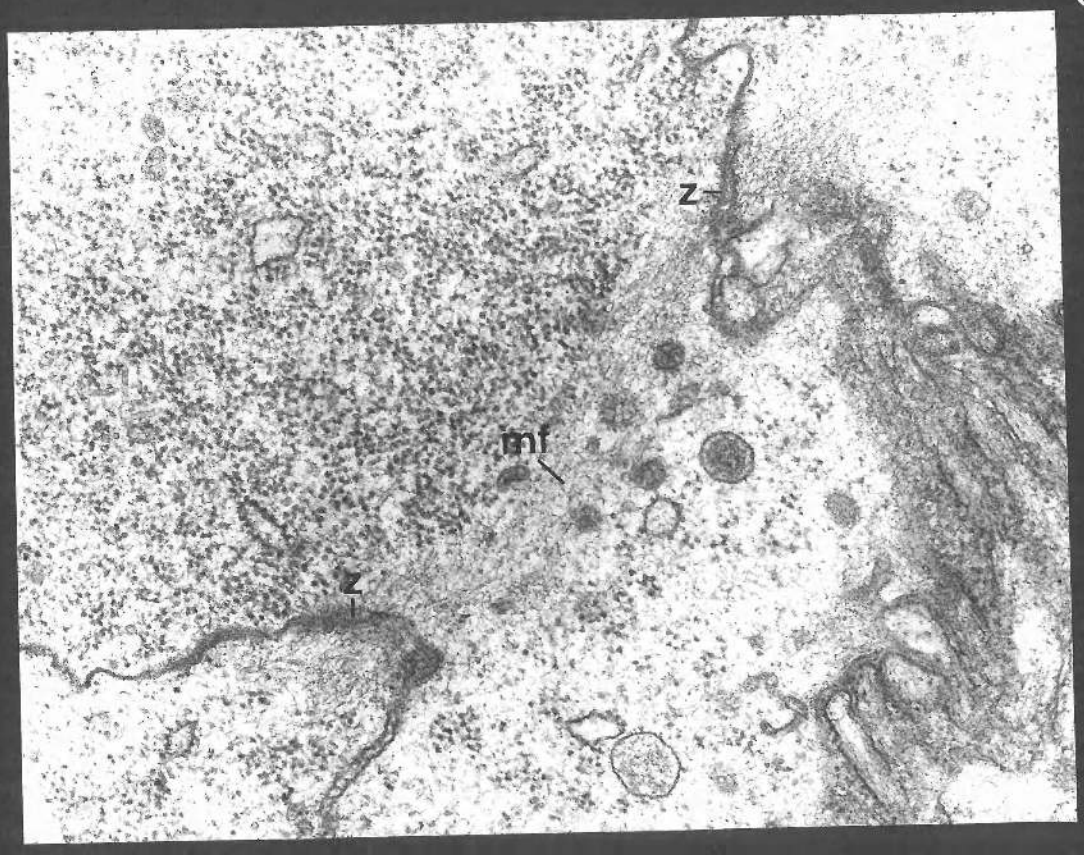

FIGURE 38

Section through part of the basal surface of a R. prolixus follicle during late previtellogenesis. The section was cut perpendicular to the outer surface and to the polar axis of the follicle. Follicle cell boundaries are 'peaked' and the positions of microfilament bundles that extend from 'peak' to 'peak' are also shown (compare Fig. 37). X 12,000. Bar = 1 µm.

38

FIGURE 39

Section cut parallel to the outer surface and to the polar axis of a R. prolixus follicle during vitellogenesis. The section is at the level of the follicle cell nuclei. Vitellogenic channels occur between follicle cells. X 8,700. Bar = 2 μm.

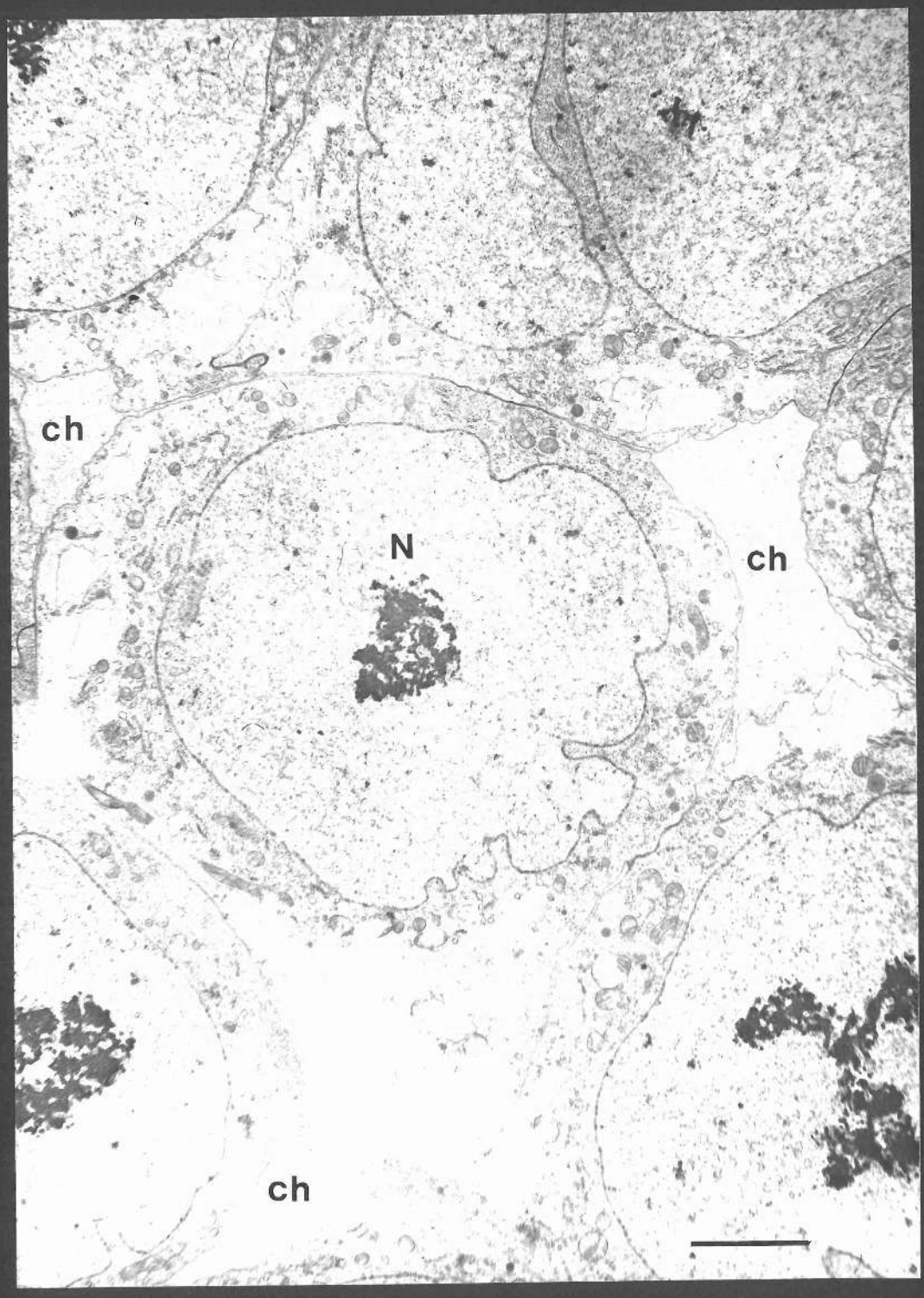
ch
N
ch
ch

FIGURE 40

Part of the outer surface of a R. prolixus follicle during vitellogenesis showing a portion of one of the vitellogenic channels. The section orientation is perpendicular to the outer surface and the polar axis of the follicle. X 12,500. Bar = 1 μm.

FIGURE 41

Part of the basal surface of a R. prolixus follicle during vitellogenesis. A portion of one of the vitellogenic channels is shown where it approaches the oocyte surface. Section orientation as in Fig. 40. X 14,000. Bar 1 μm.

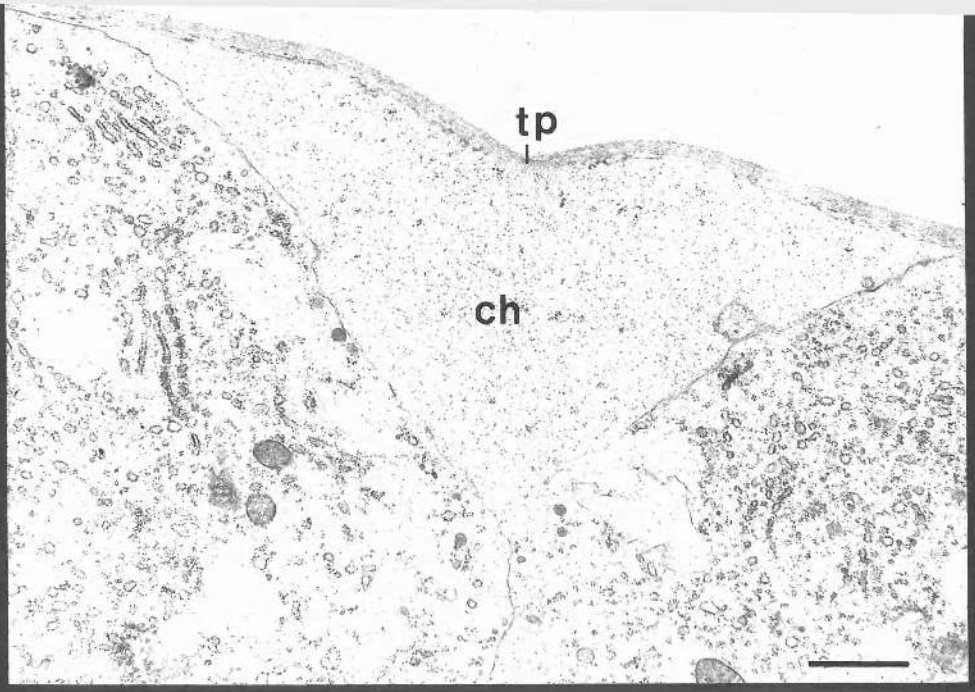

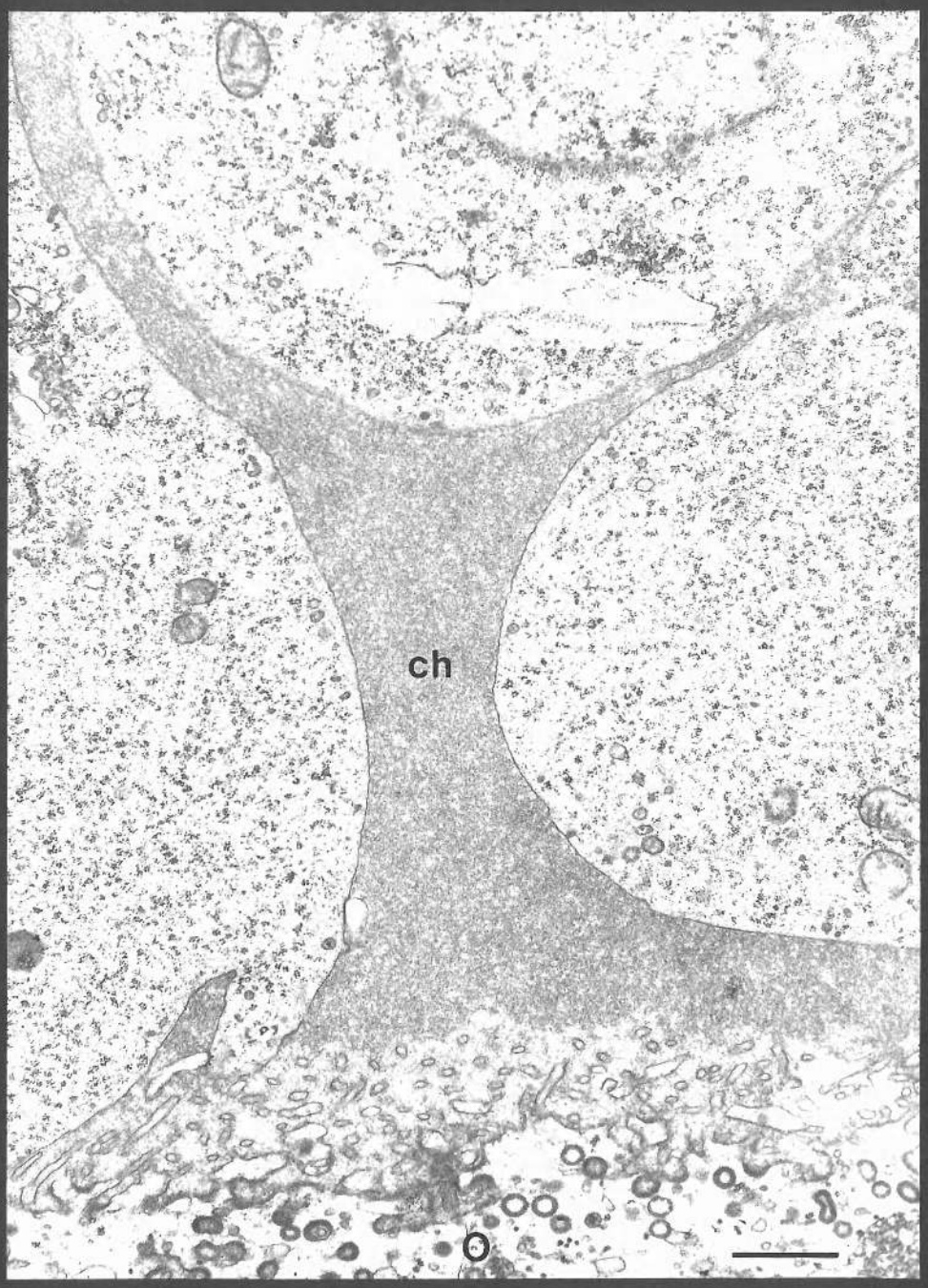

41

FIGURE 42

Section grazing through part of a R. prolixus follicle during vitellogenesis showing part of a vitellogenic channel. Channels form at points where three follicle cells meet. Bundles of microfilaments follow the margins of the channel along cell membranes at the sides of the follicle cells. Microtubules occur alongside channels. X 31,000.

FIGURE 43

Section grazing through a region of a R. prolixus follicle during vitellogenesis. A vitellogenic channel separates two follicle cells. Microfilament bundles within the follicle cells run alongside the channels. X 43,000.

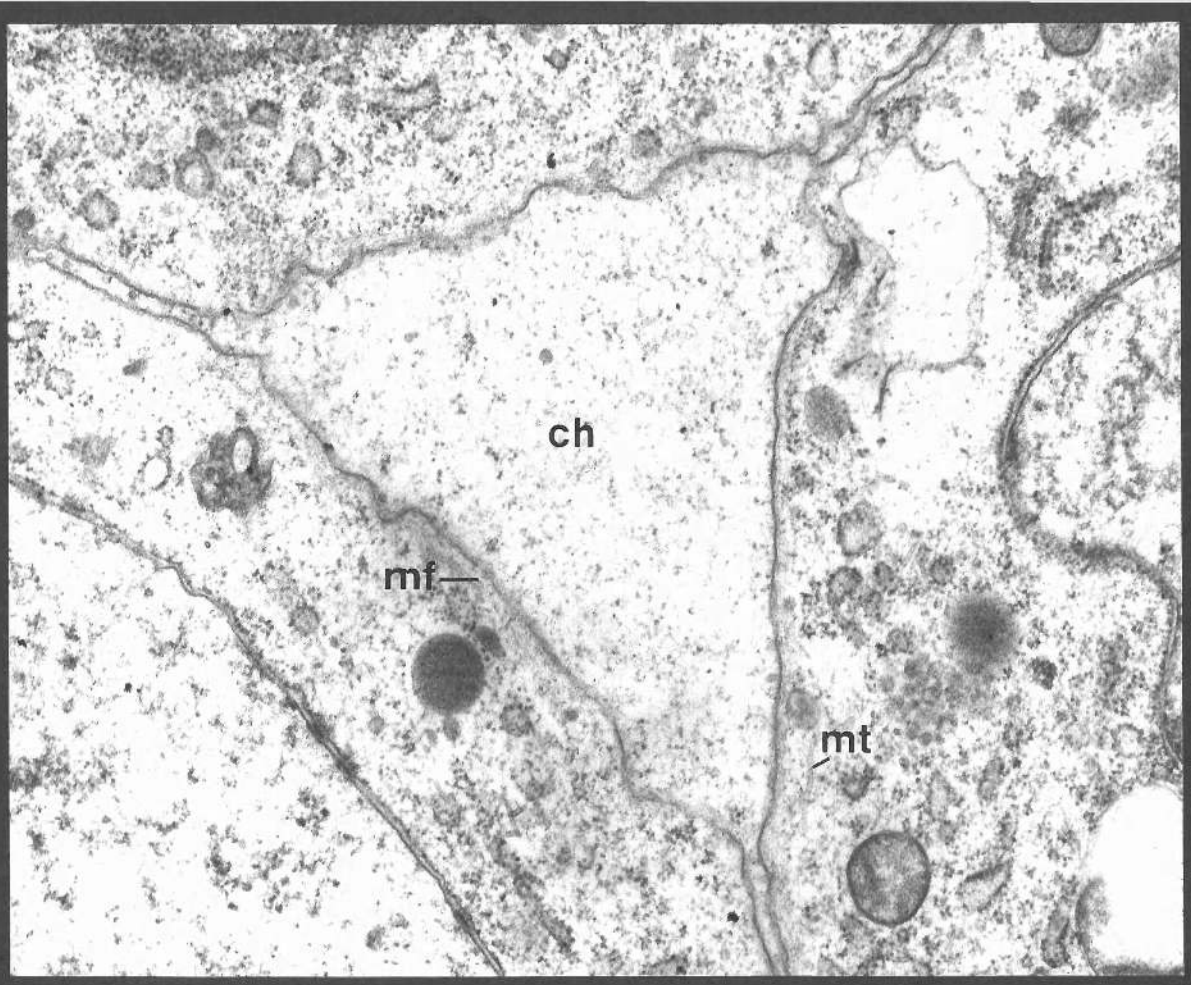

43

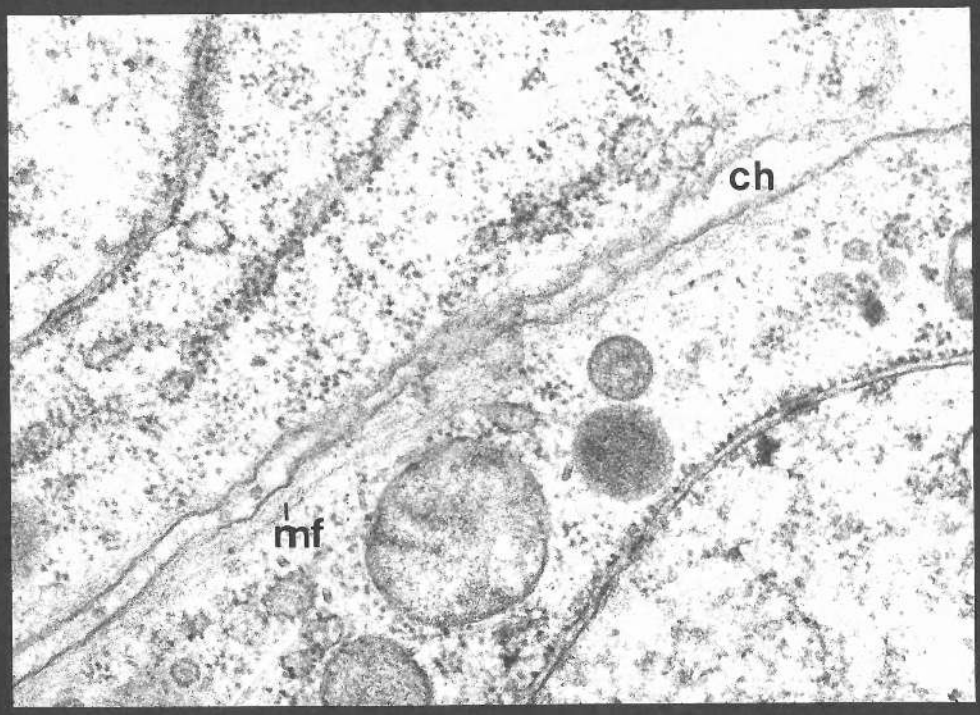

FIGURE 44

Section grazing through the outer surface of a R. prolixus follicle during vitellogenesis. Filopodial projections from follicle cell outer surfaces approach the tunica propria and extend into surface depressions in adjacent cells. Bundles of microfilaments extend along the interiors of these projections. Circumferentially arranged fibrous elements occur within the tunica propria. X 37,100.

FIGURE 45

Section of a R. prolixus follicle showing the inner surfaces of two adjacent follicle cells. A filopodial projection from the inner surface of one follicle cell is shown. Microfilament bundles extend along the interior of the projection. X 43,000.

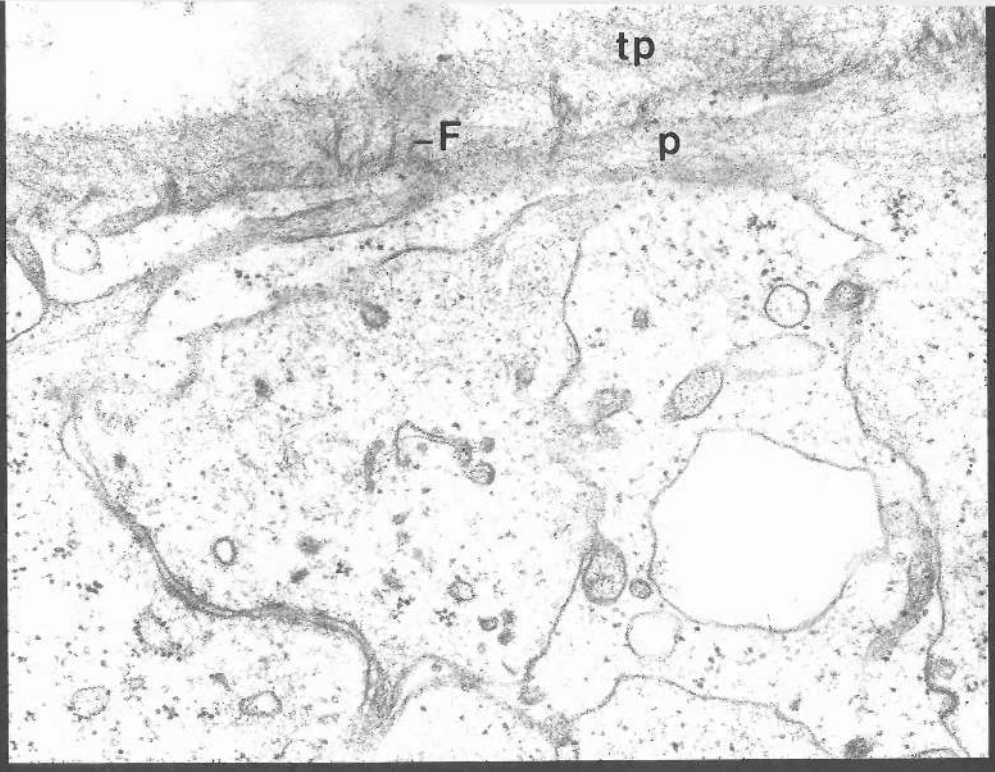

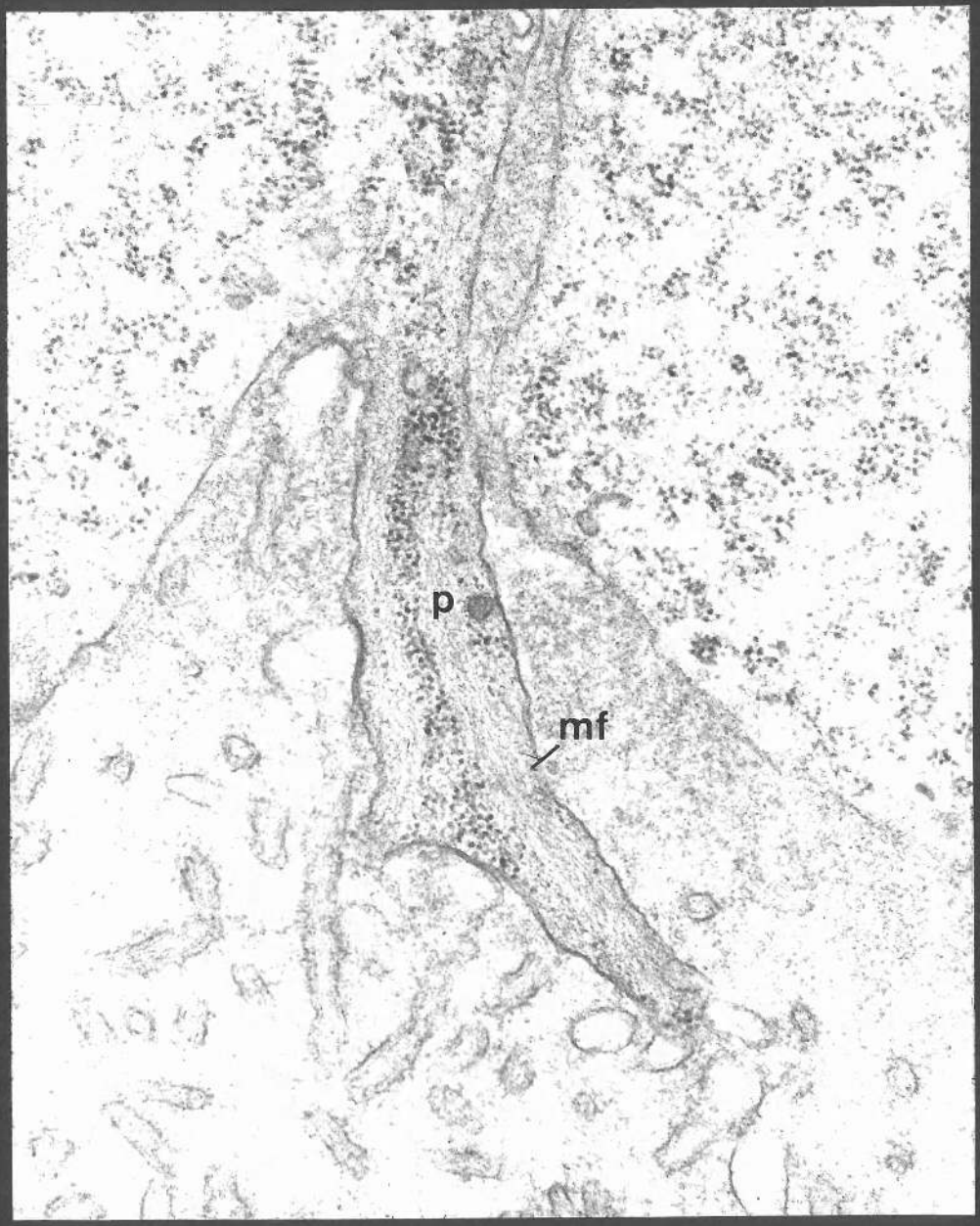

45

FIGURE 46

Diagrammatic representation showing the cytodifferentiation of follicle cells during follicle growth. A shows the cytoarchitecture of follicle cells during early previtellogenesis, B shows the situation during late previtellogenesis and C the situation during vitellogenesis.

R. PROLIXUS CYTODIFFERENTIATION DURING FOLLICLE GROWTH

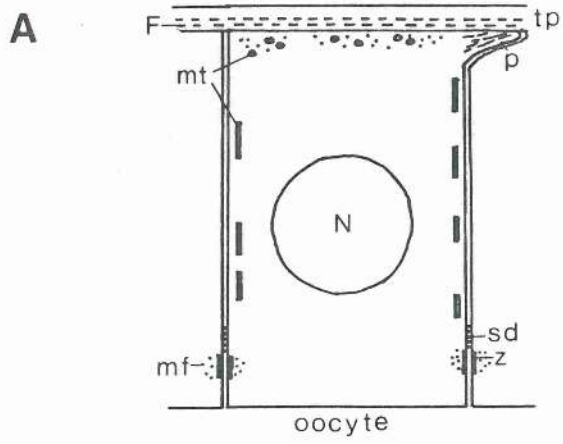

FIGURE 47

Section through the ovariole sheaths of a R. prolixus ovariole. The irregularly-shaped sheath cells lie very close to the follicle and its tunica propria. Muscle elements can be seen within a myoepithelial sheath cell. X 58,700.

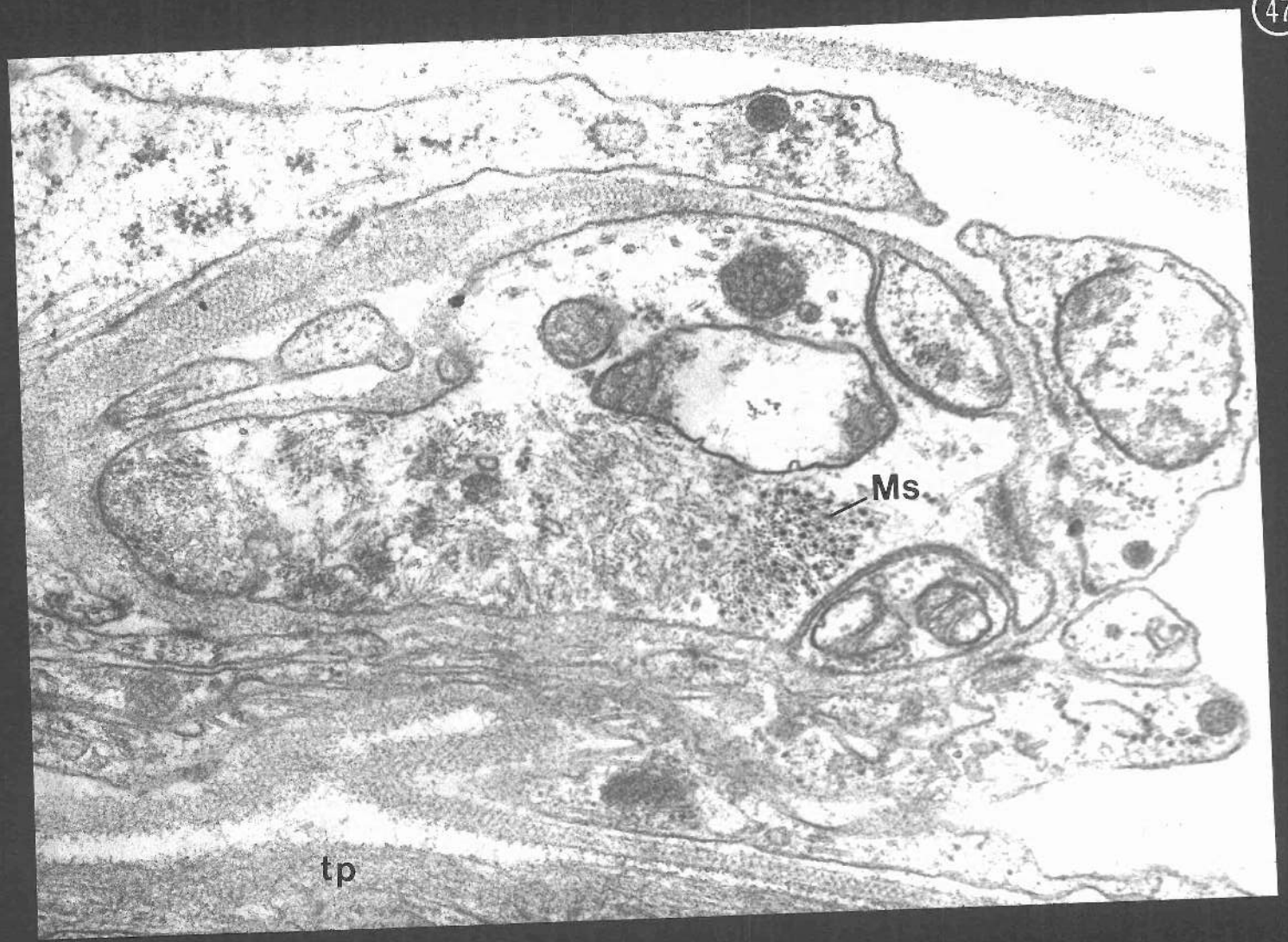
Ms
tp

FIGURE 48

Shows the inner surfaces of two adjacent follicle cells of R. prolixus at their junction with the oocyte. The follicle cell membranes are very convoluted and interdigitate with adjacent cells. X 47,000.

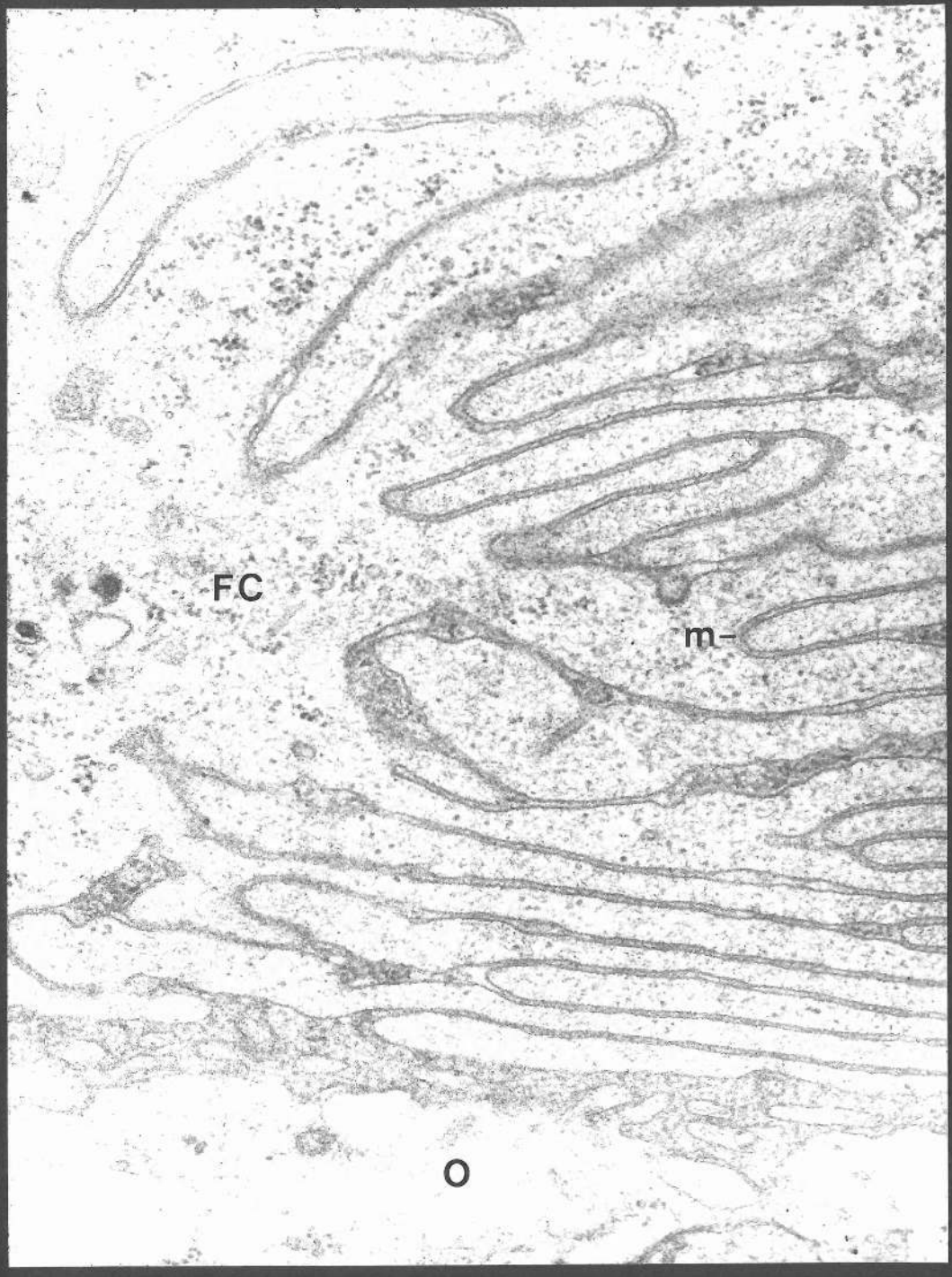
FC
m
O

FIGURE 49

Section grazing through the outer surface of a P. americana follicle cell during post-vitellogenesis. Circumferentially oriented microtubules occur directly beneath the outer surface of the follicle cell. X 58,700.

(49)

FIGURE 50

Part of the corpus luteum of P. americana showing tunica propria and part of the outer surfaces of two follicle cells. The tunica propria is highly folded and consists of an outer granular layer and an inner fibrous layer. Circumferentially arranged bundles of microfilaments and groups of microtubules occur just beneath the outer surfaces of the follicle cells. X 16,500.


Gr
F
mf
mt

FIGURE 51

Section through part of the tunica propria of a R. prolixus corpus luteum. Fibrous elements of the inner surface of the tunica are shown.

X 47,700.

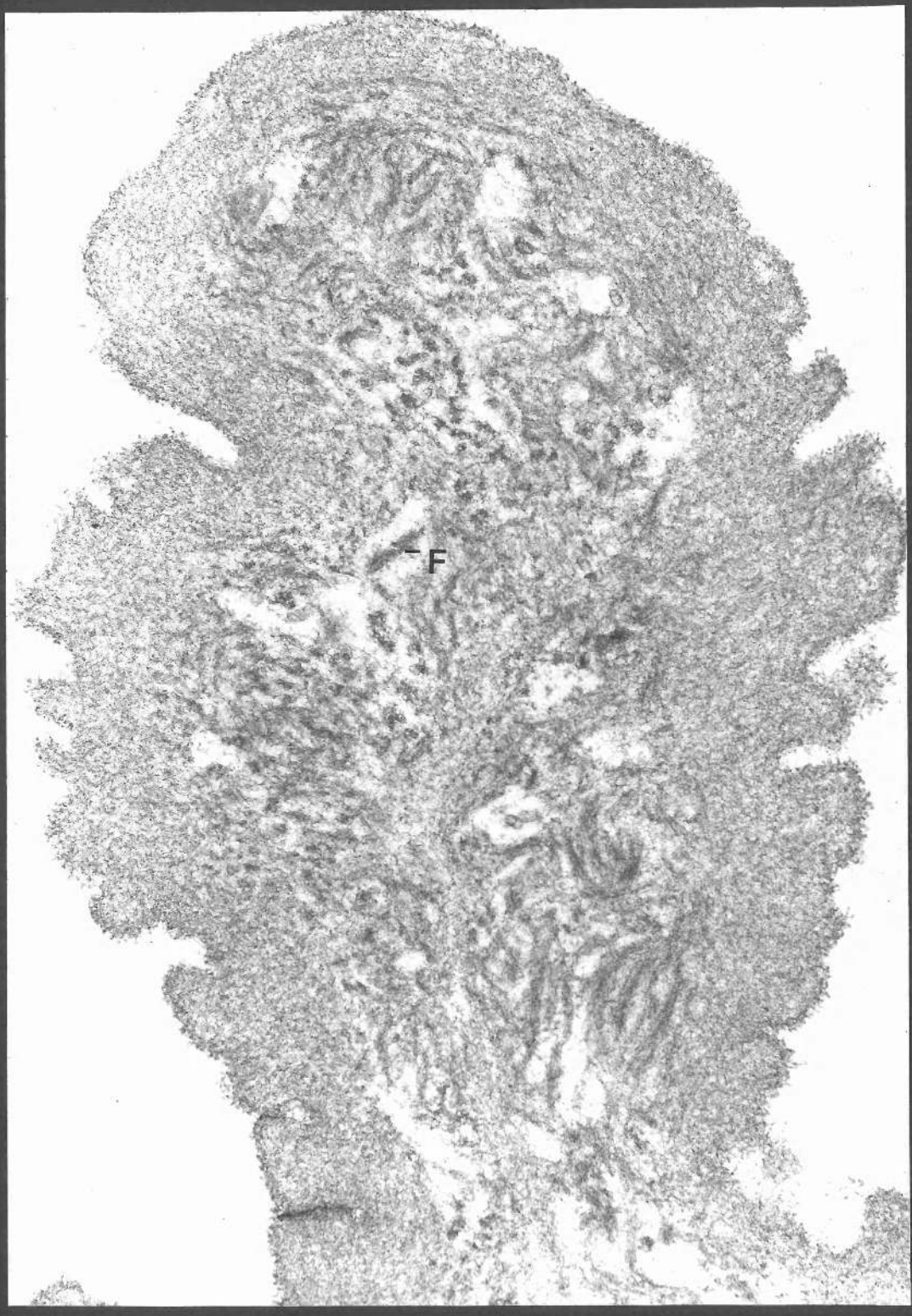
F

FIGURE 52

Section through part of a R. prolixus corpus luteum. Secondary foldings in the tunica propria are shown. X 4,300.

FIGURE 53

Section through part of the tunica propria of a P. americana corpus luteum. Secondary foldings in the tunica propria are shown as well as the outer granular and inner fibrous layers of the tunica. X 12,700.

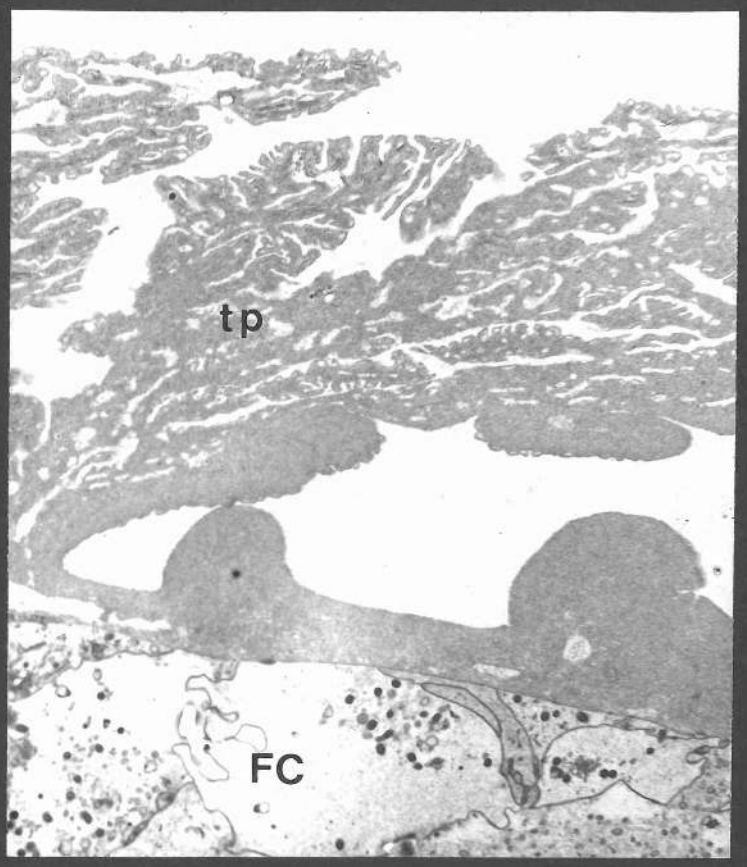

52

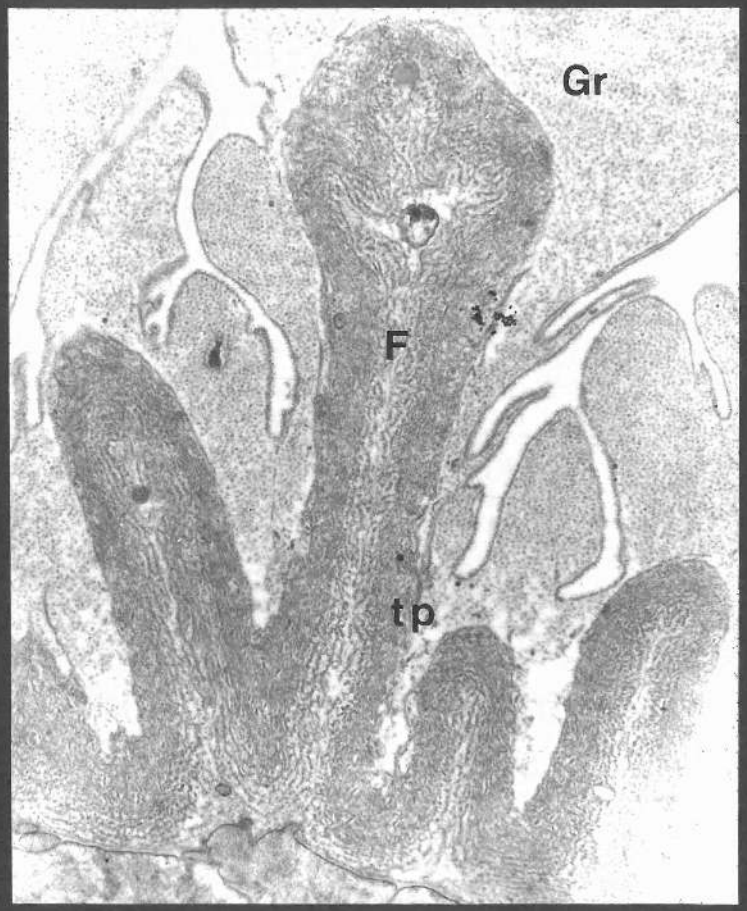

53

FIGURE 54

Section through part of the tunica propria of a cockroach corpus luteum showing degeneration of the granular layer. Some granules showing no signs of degeneration are also shown. X 29,700.

FIGURE 55

Myelin figures within the cytoplasm of a P. americana corpus luteum follicle cell are shown. X 21,000.

54

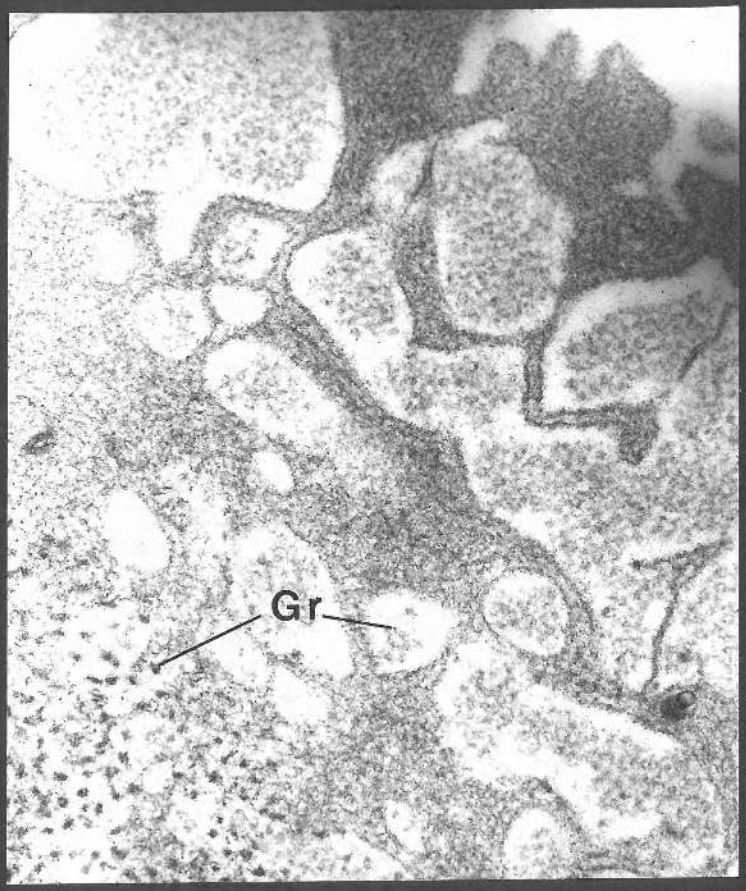

55

FIGURE 56

Section through part of the follicular epithelium of a R. prolixus corpus luteum. The section is oriented perpendicular to the long axis of the ovariole. Many microtubules run parallel to the long axis of the follicle cell. X 47,000.

FIGURE 57

Section through part of the follicular epithelium of a P. americana corpus luteum showing the many microtubules which run parallel to the long axis of each cell. Section orientation as in Figure 56. X 41,300.

FIGURE 58

Part of the outer surface of a follicle cell of a P. americana corpus luteum. Many circumferentially oriented microtubules and microfilaments occur directly beneath the outer surface of the follicle cell. The section is oriented parallel to the long axis of the ovariole. X 42,400.

FIGURE 59

Part of the outer surface of a R. prolixus corpus luteum showing tunica propria and the outer surfaces of follicle cells. A bundle of microfilaments occurs directly beneath the outer surface of a follicle cell. Fibrous elements are evident within tunica propria. X 47,000.

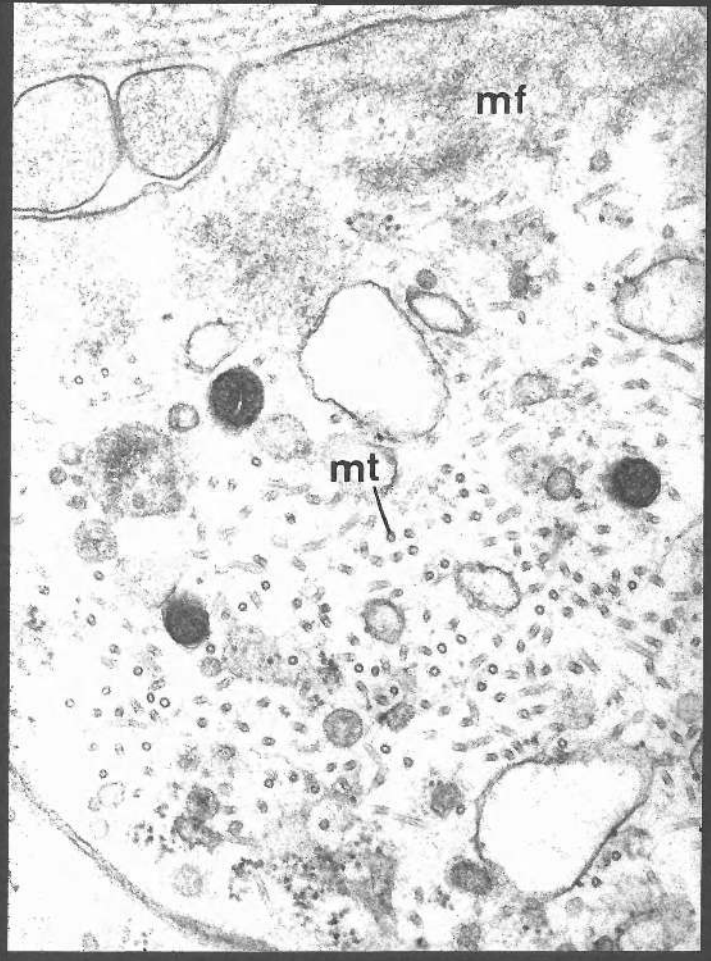

59

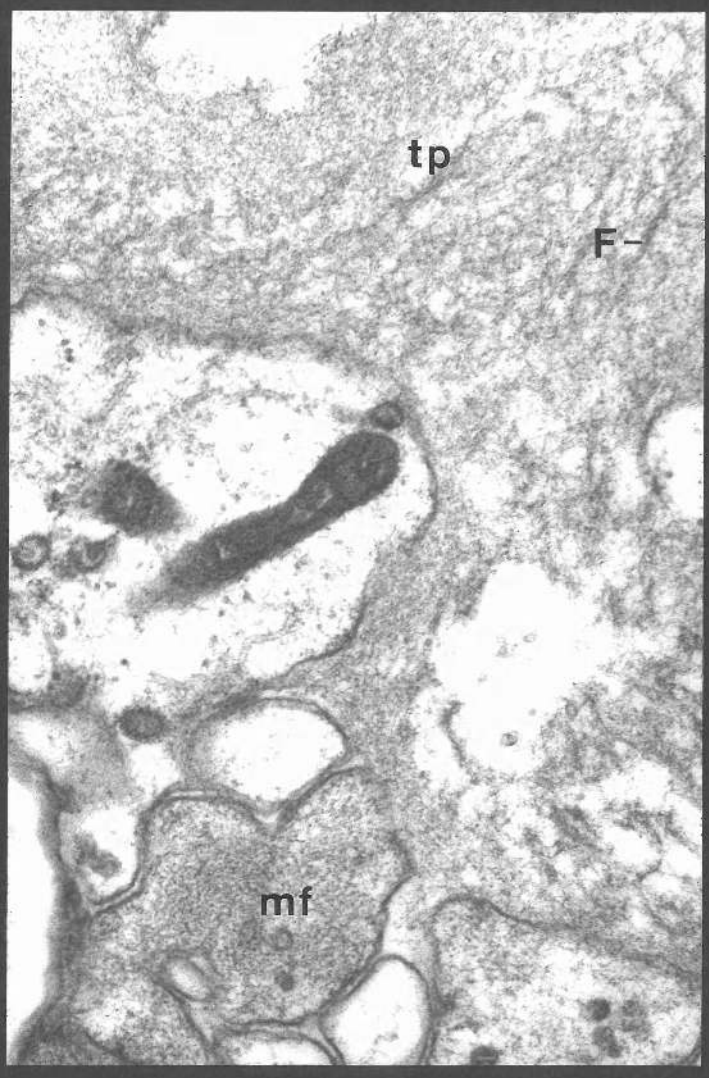

FIGURE 60

A diagrammatic representation of follicle cells and tunica propria showing their organisation during post-vitellogenesis (prior to ovulation) and after ovulation (corpus luteum formation) in both P. americana and R. prolixus. A represents the situation prior to ovulation and B represents the situation after ovulation.

R. prolixus

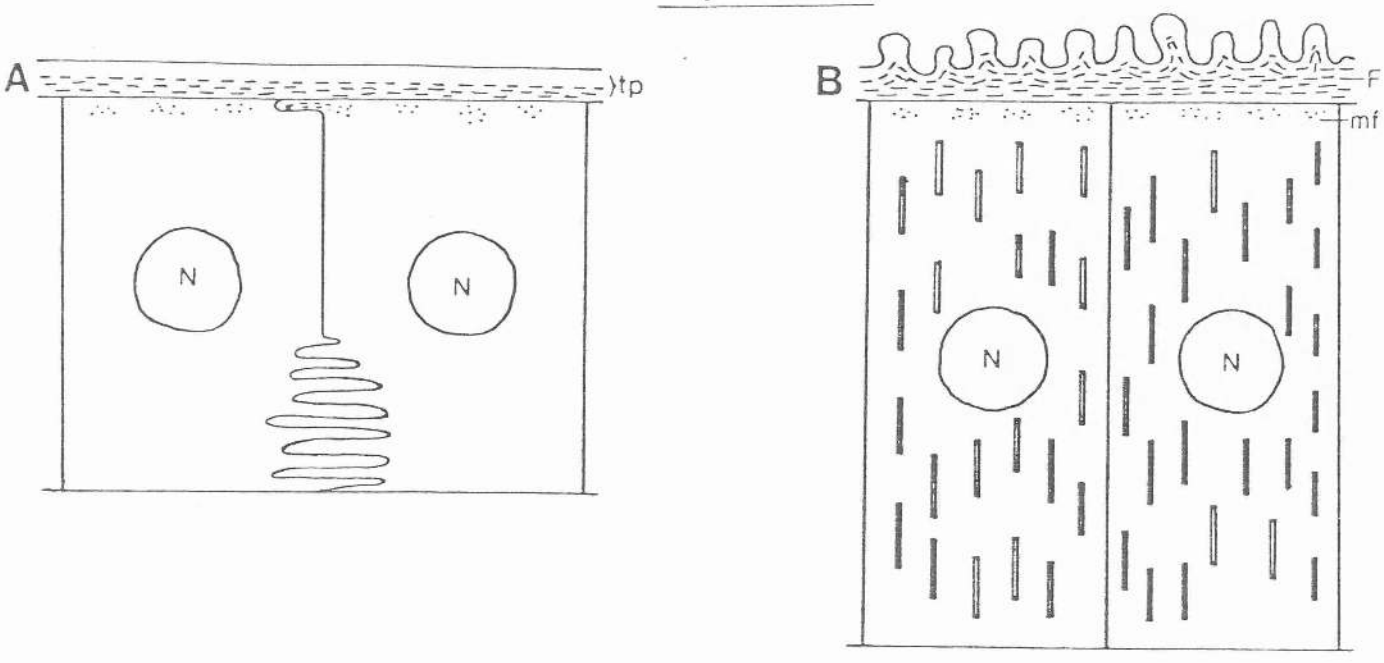

P. americana

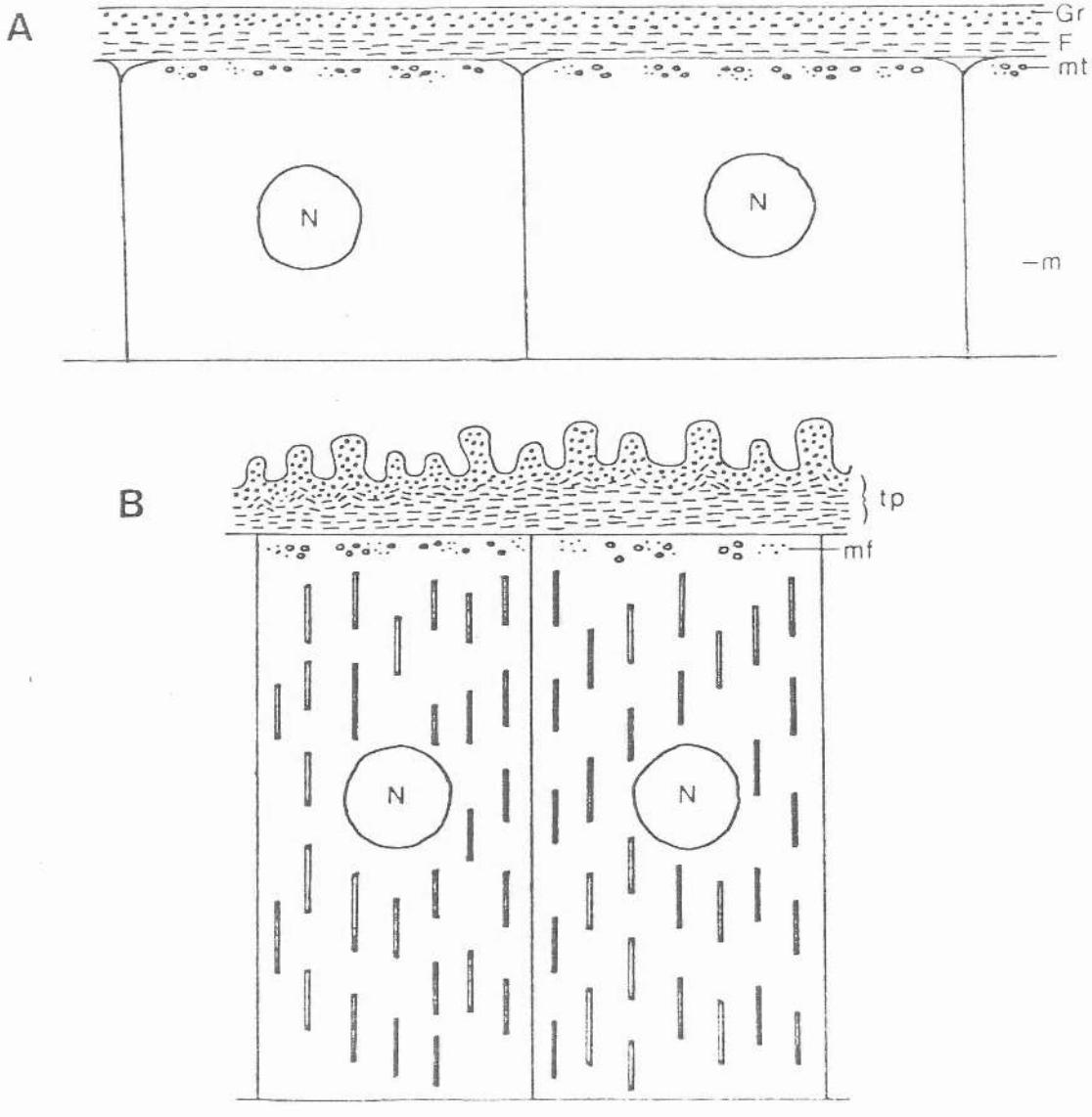

FIGURE 61

An imaginal disc of C. erythrocephala freshly isolated in saline. At the start of puparium formation the imaginal disc is folded in this manner. The arrow indicates the region of the wing pouch. Tracheae supply the imaginal disc with oxygen. X 25.

FIGURE 62

Median longitudinal section through an imaginal disc during Stage 1. The section is stained with methylene blue. Three main parts can be distinguished. The proximal part of the wing disc (Pr) consists of epidermis and promyoblasts and will form the dorsal thorax. The middle part consists of epidermis, with promyoblasts only at the proximal side, and will form the articulating part of the wing. The distal part of the wing disc (D) consists only of epidermis and will form the wing blade and the lateral imaginal thorax (Sprey, 1970). The peripodial membrane and the wing blade epidermis are indicated. The two epidermal layers of the distal portion of the wing disc can be distinguished. At the most distal part of the distal portion, the two epidermal layers are closely juxtaposed to form an epidermal bilayer which becomes the wing tip. More proximally the two epidermal layers approach one another but are not yet juxtaposed. X 55.

FIGURE 63

Median longitudinal section through a methylene blue stained C. erythrocephala wing imaginal disc during a later stage of Stage 1 than Figure 62. The two epidermal layers of the distal portion of the wing imaginal disc are closely juxtaposed to form an epidermal bilayer which constitutes the wing blade. More proximally the epidermal layers are not yet juxtaposed. This region will become the articulating part of the wing. Promyoblasts are also shown. X 55.

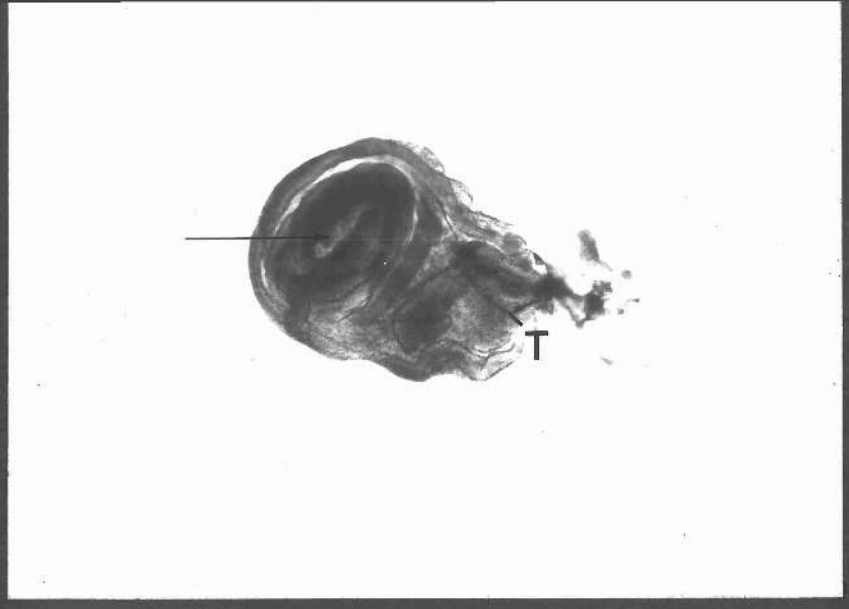

62

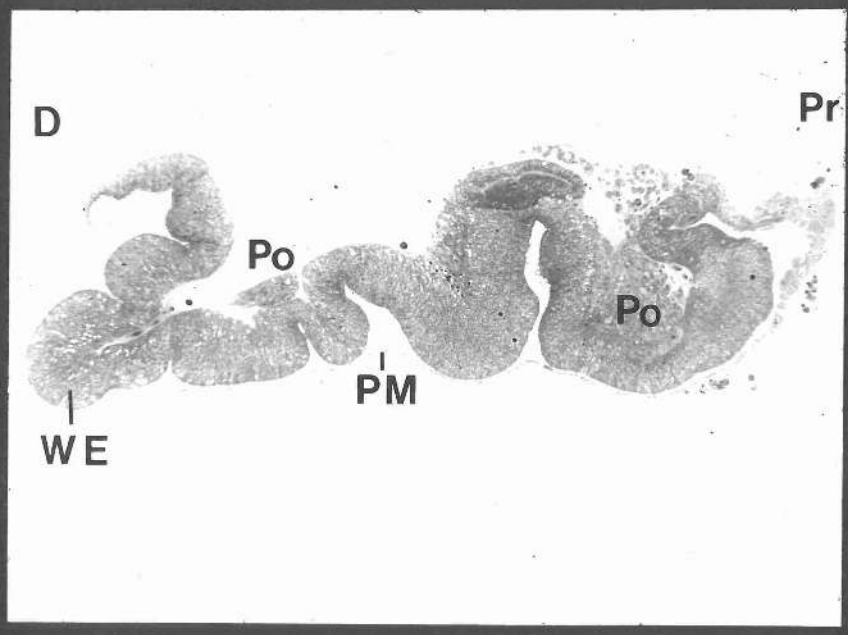

63

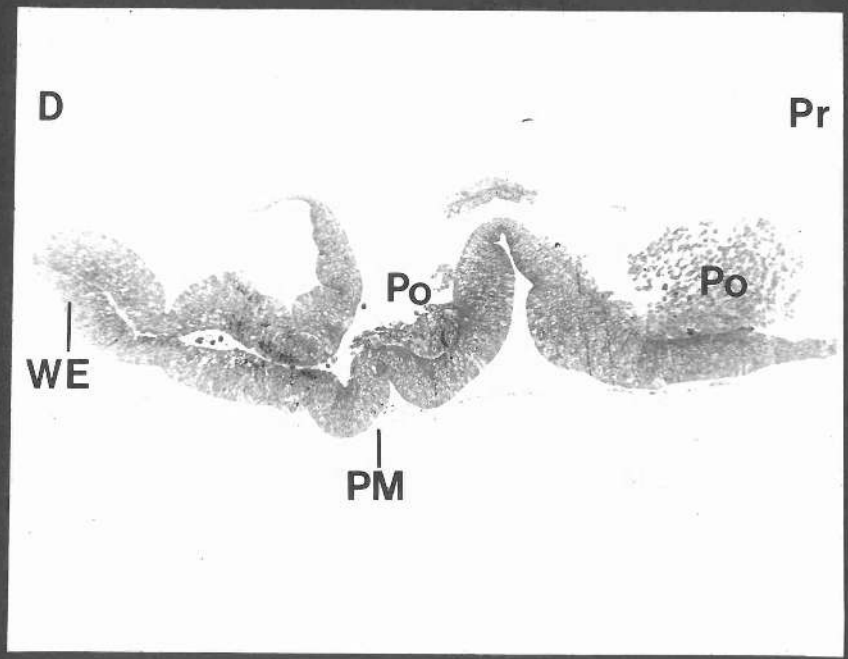

FIGURE 64

Diagrammatic representation of the 'evagination' of a C. erythrocepala wing disc. The arrows indicate directions of growth. A represents the third instar resting period. B represents the situation at puparium formation (0 hours). The wing disc has become more folded in a characteristic manner. The wing pouch now formed from the formation of a second cross ridge protrudes into the peripodial cavity in a distal direction. C represents a wing imaginal disc at about 4 - 6 hours after puparium formation. The wing pouch protrudes further into the peripodial cavity and a bilayer is created at the most distal region of the disc. D represents the final growth during Stage 1 where the epidermal layers are juxtaposed to form a bilayer which becomes the wing blade.

A

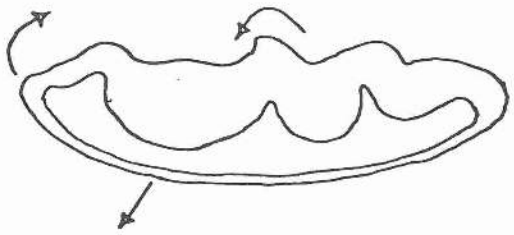

D Pr

B

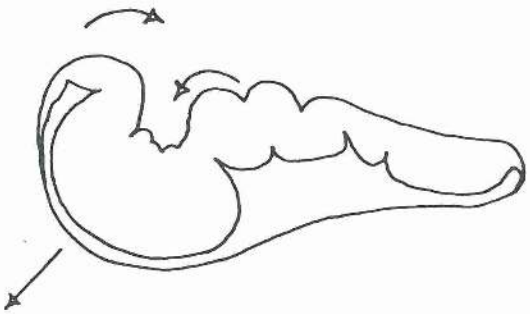

C

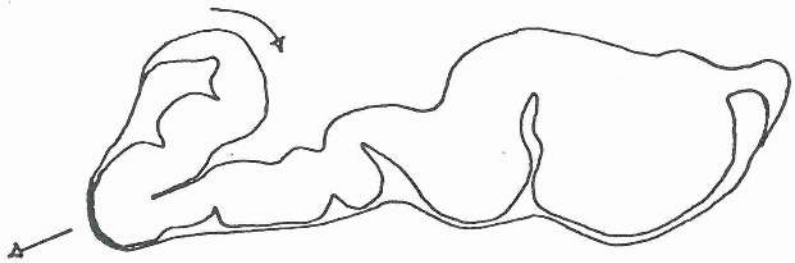

D

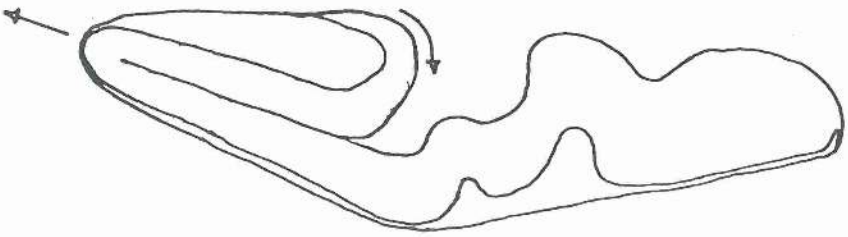

FIGURE 65

Frontal view of an imaginal disc of C. erythrocephala freshly isolated in saline 6 hours after puparium formation. The wing pouch is evident. Compare with C of Figure 64. Note also the peripodial membrane.
X 25.

FIGURE 66

Frontal view of a wing imaginal disc of C. erythrocephala freshly isolated in saline 14 hours after puparium formation. The wing pouch extends further into the peripodial cavity than earlier on during Stage 1 (Fig. 65). Compare D of Figure 64 which represents the lateral median view of a similar wing disc. X 25.

FIGURE 67

Lateral median section through the wing pouch of a C. erythrocephala wing imaginal disc during Stage 1. The section is stained with methylene blue. The wing tip has formed from the apposition of the two epithelial layers. Where the two epithelial layers become juxtaposed at their bases, the presumptive dorsal and ventral layers of the wing blade are created beginning at the putative wing tip. As the epithelial layers come together, haemocytes become trapped between them. Epithelial cells are highly vacuolar. 'Blebs' of cytoplasm occur at cell apices. The peripodial membrane cells are squamous in shape and abutt against the wing tip (arrow). X 230.

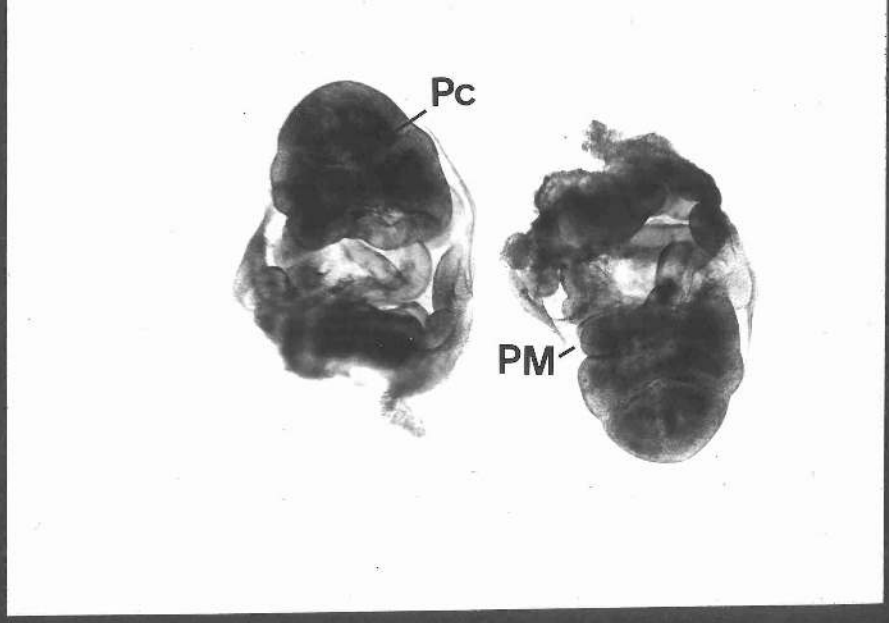

66

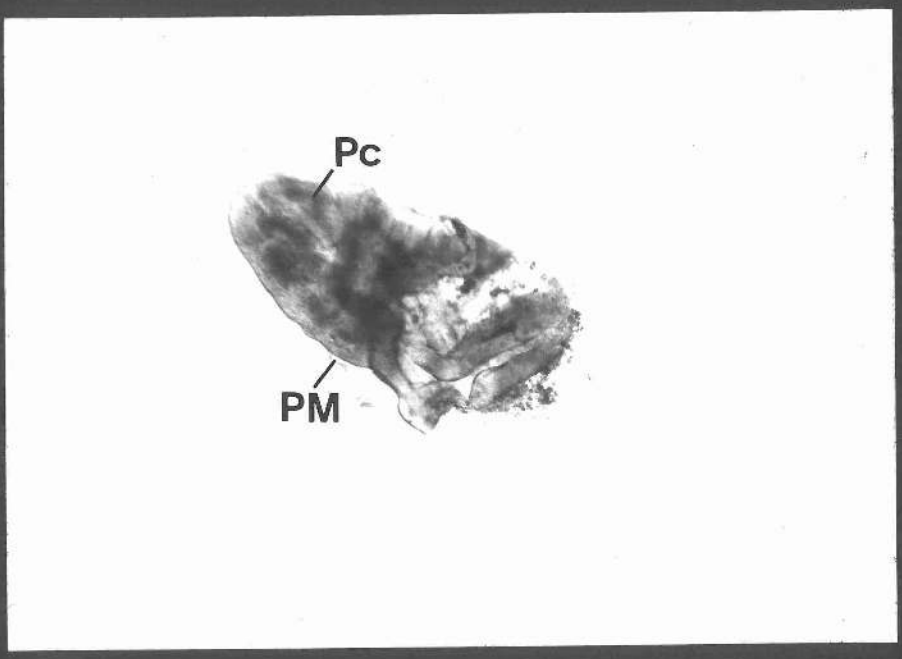

67

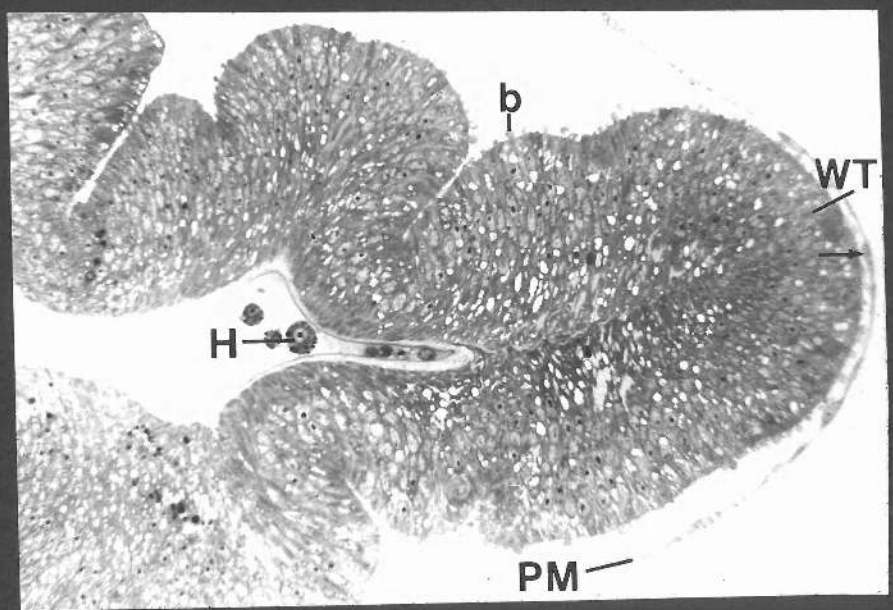

FIGURE 68

A C. erythrocephala wing imaginal disc freshly isolated in saline showing how the developing wing blade has twisted on its axis so that the wing blade now lies in a cephalo-caudal direction (indicated by arrows) with respect to the larval body. X 25.

FIGURE 69

Basal view of a C. erythrocephala wing freshly isolated in saline 21 hours after puparium formation. There is no distinguishable peripodial membrane. X 25.

FIGURE 70

Transverse section through a Stage 2 C. erythrocephala wing blade. The lacunae of the presumptive prepupal veins can be distinguished. Dorsal and ventral epithelial layers are juxtaposed at their bases except over the vein lacunae. Haemocytes occur within vein lacunae. X 200.

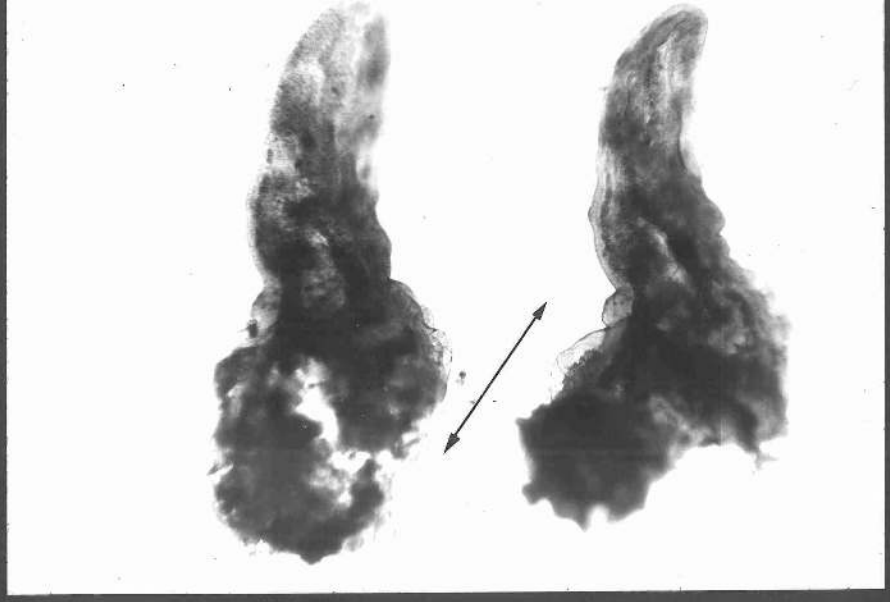

69

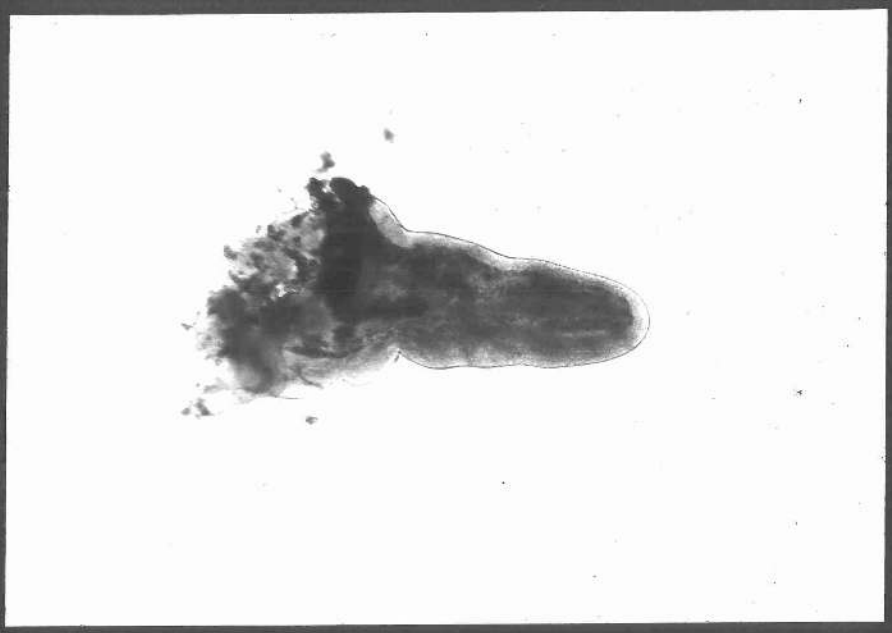

70

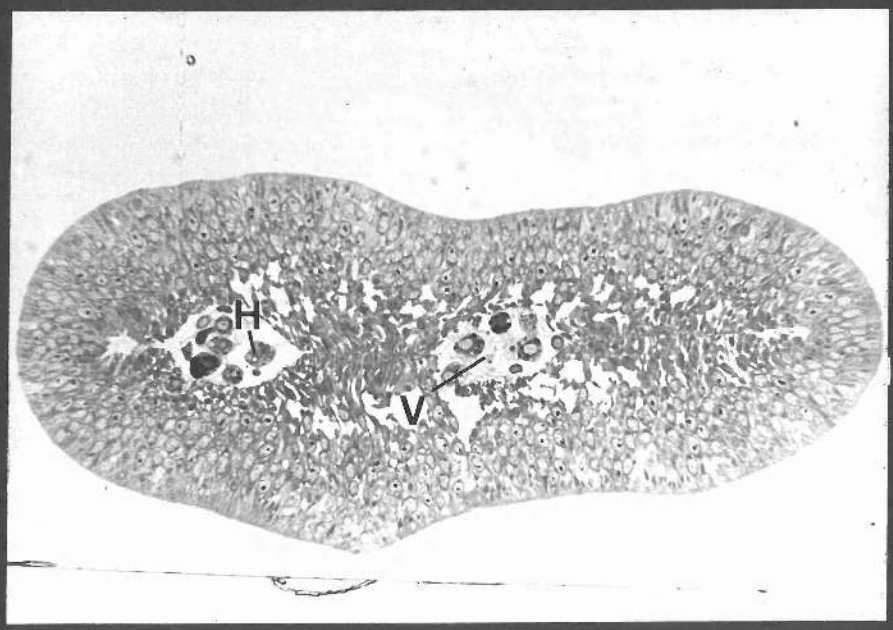

FIGURE 71

Basal view of a C. erythrocephala wing freshly isolated in saline 26 hours after puparium formation (Stage 3). Note the increase in wing width and especially length (See Fig. 69). The prepupal veins can be distinguished (arrows). X 25.

FIGURE 72

Basal view of a C. erythrocephala wing freshly isolated in saline 38 hours after puparium formation (Stage 4). The swollen spongy nature of the wing is apparent. X 25.

71

72

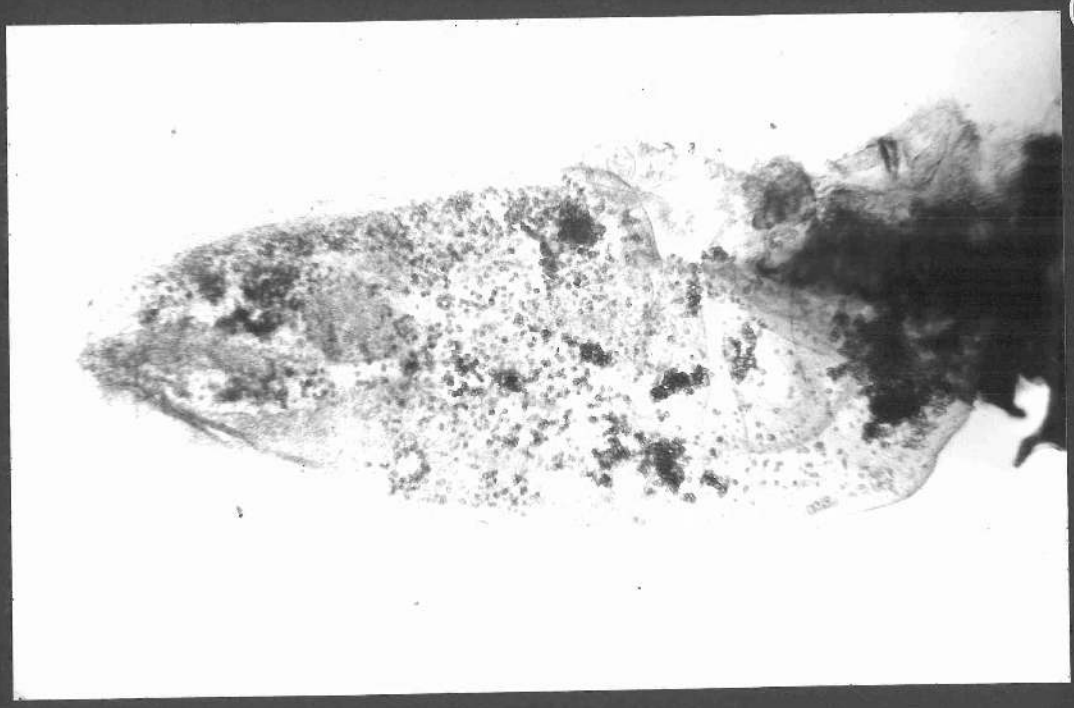

FIGURE 73

Ventral view of a C. erythrocephala wing freshly isolated in saline 52 hours after puparium formation (Stage 5). The wing lies within the pupal cuticle. X 25.

FIGURE 74

Dorsal view of a C. erythrocephala wing freshly isolated in saline 90 hours after puparium formation (Stage 5). The wing lies within the pupal cuticle. The pupal veins are clearly apparent and the outline of the wing is slightly sculptured. X 25.

FIGURE 75

Lateral view of a C. erythrocephala wing blade 5 days after puparium formation (Stage 7). The wing is folded in a characteristic manner within the pupal cuticle. Bristles are apparent (arrow). X 25.

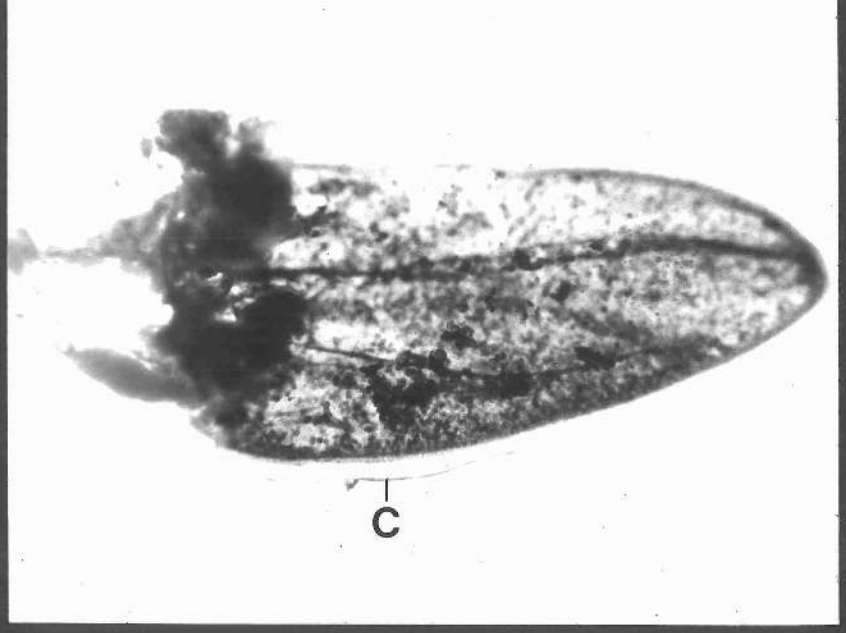

74

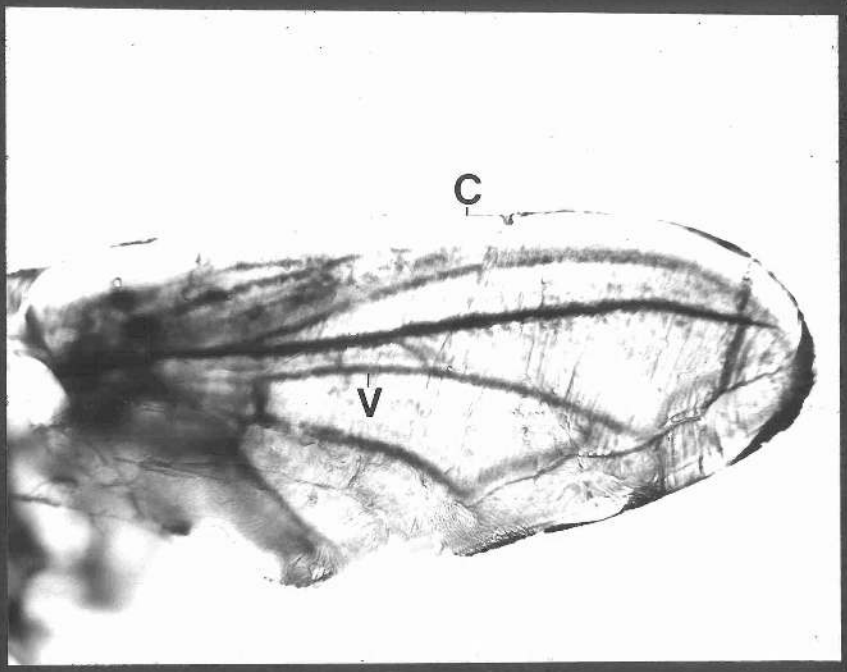

75

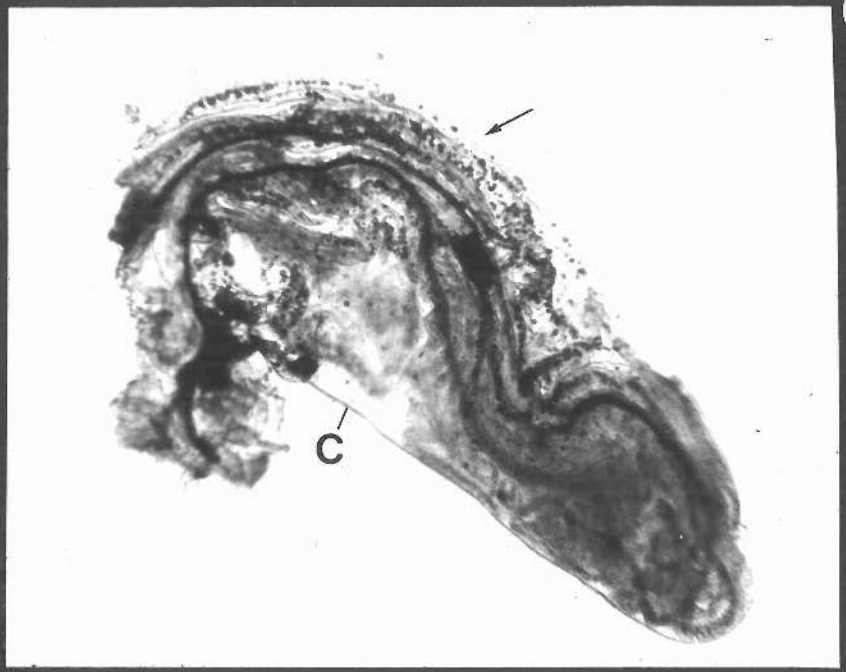

FIGURE 76

Dorsal view of an adult C. erythrocephala wing mounted in euparol. Note the large size of the wing as compared with the size of the wing pouch in Figure 61. Note also the trichomes and bristles. X 25.

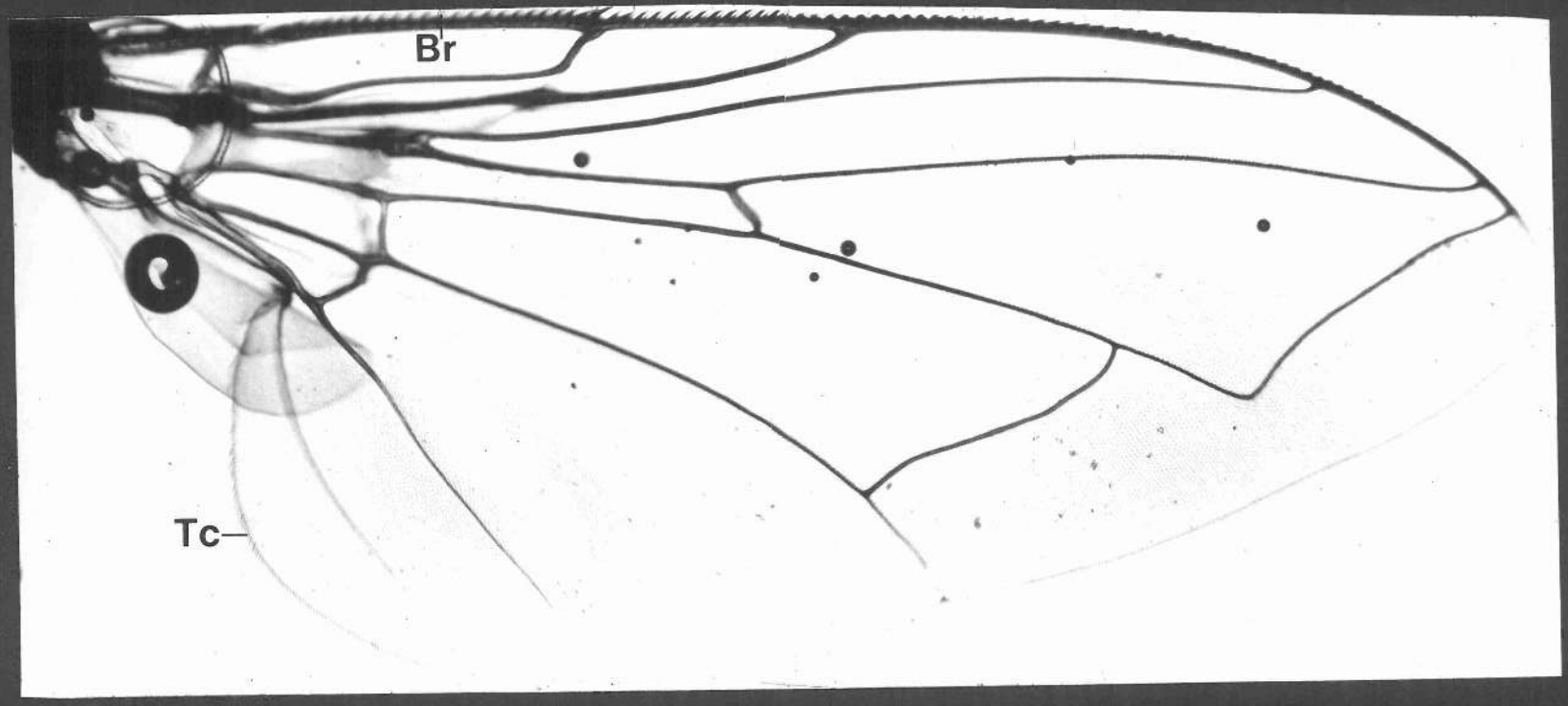
Br
Tc

FIGURE 77

Diagrammatic representations of wings and parts of wings describing the terminology used in this Chapter. Proximal (Pr) indicates the portion of wing blade nearest the larval or pupal body whilst distal (D) indicates that portion furthest away from the larval or pupal body. Anterior (A) indicates that part of the wing blade nearest the cephalic region of the animal whilst posterior (P) indicates that side nearest the animal's caudal region. Transverse or cross-section (T/S) indicates a section cut at right angles to the proximo-distal wing axis. Longitudinal section (L/S) indicates a section cut parallel to the proximo-distal wing axis along the mid-line. Margin (M) indicates the edges of the flattened wing blade except the most distal edge which is the wing tip (WT). Apex indicates the cuticle-bearing surface of an epidermal cell while base indicates the side of an epidermal cell nearest the basement lamina and/or haemolymph. Thickness indicates the distance of an epidermal layer from apex to base.

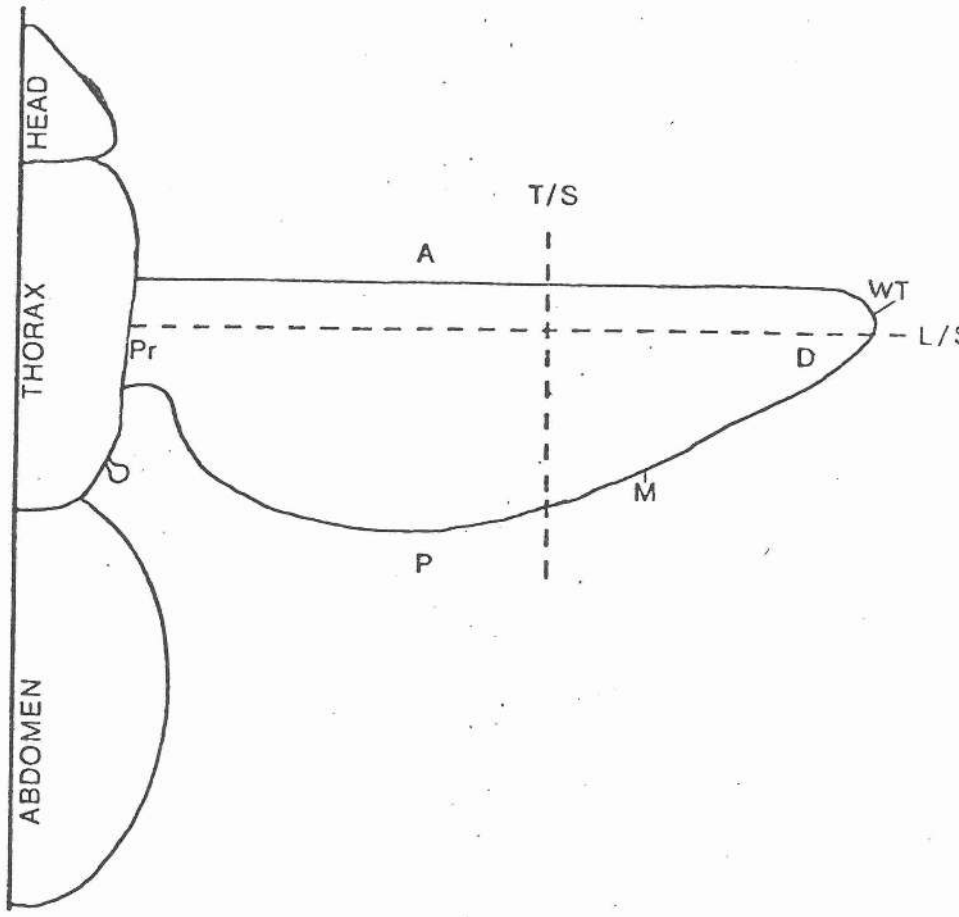
HEAD
THORAX
ABDOMEN
T/S
A
WT
L/S
Pr
D
M
P

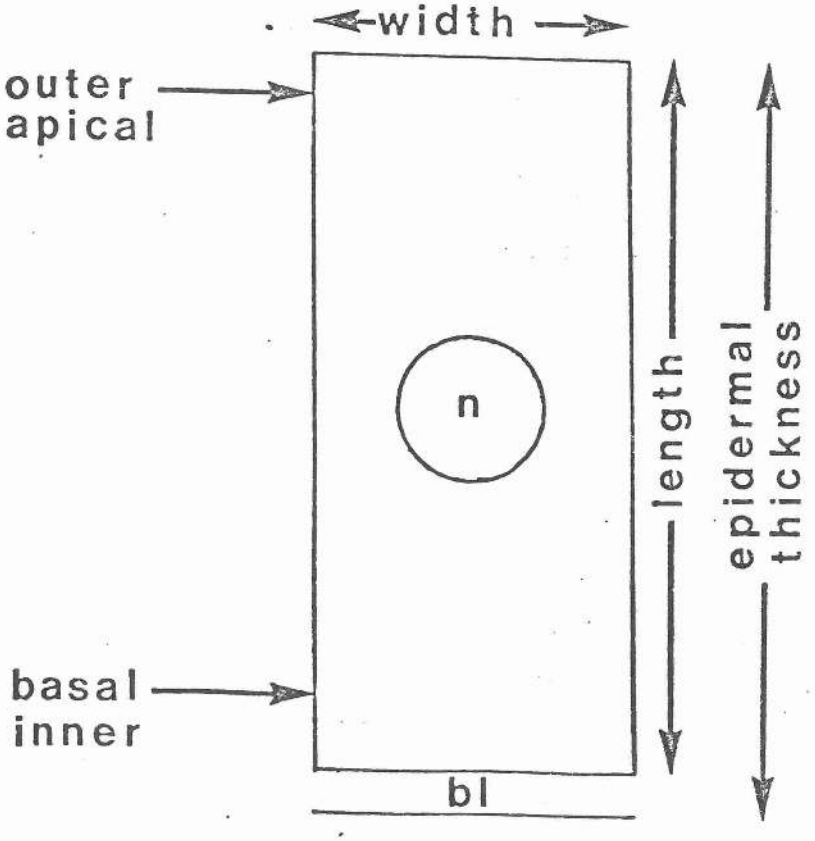
width
outer
apical
basal
inner
n
length
epidermal
thickness
bl

FIGURE 78

Longitudinal section of the tip of a Stage 1 C. erythrocephala wing imaginal disc stained with methylene blue and arranged in a pseudostratified layer. Individual epidermal cells are spindle-shaped. The portion of each cell at the level of the nucleus is the widest region of the cell (arrow). Above and below the nucleus in each cell are long cell extensions (double arrow). In contrast, epidermal cells of the peripodial membrane are squamous in shape and are arranged in a single layer. X 1,200.

FIGURE 79

Longitudinal section of the most distal part of a C. erythrocephala wing imaginal disc stained with methylene blue. Mitoses are frequent but are confined to the apical region of the epidermal layers (arrows). Cells undergoing mitosis are 'rounded up'. X 1,300.

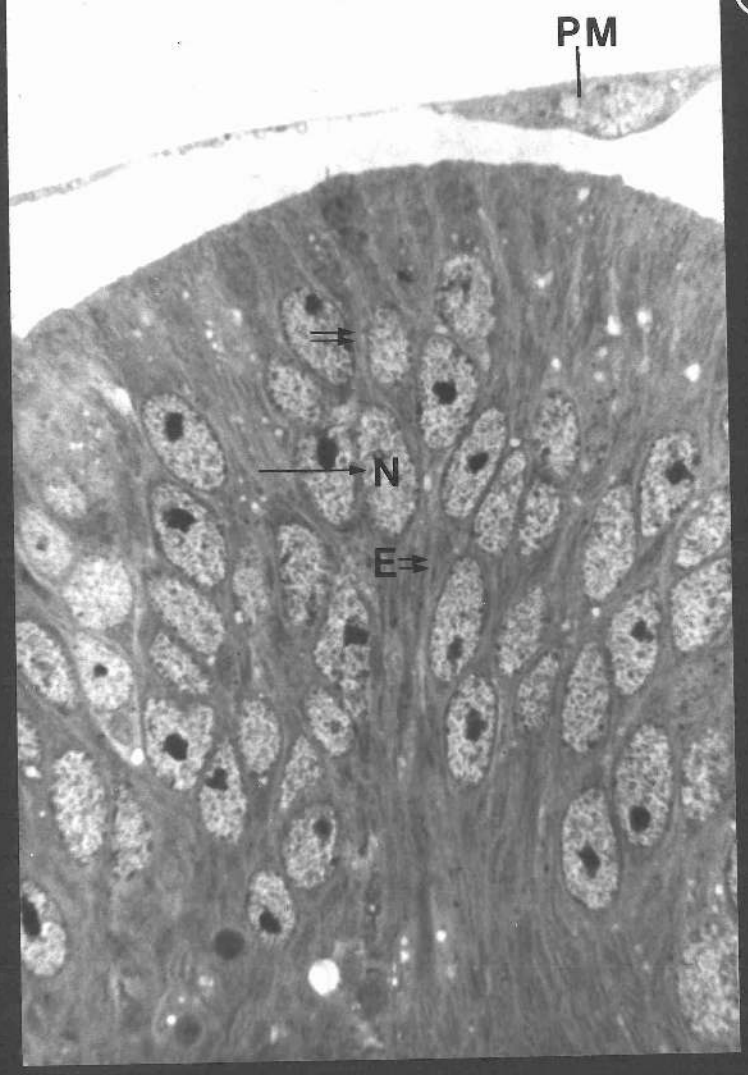

79

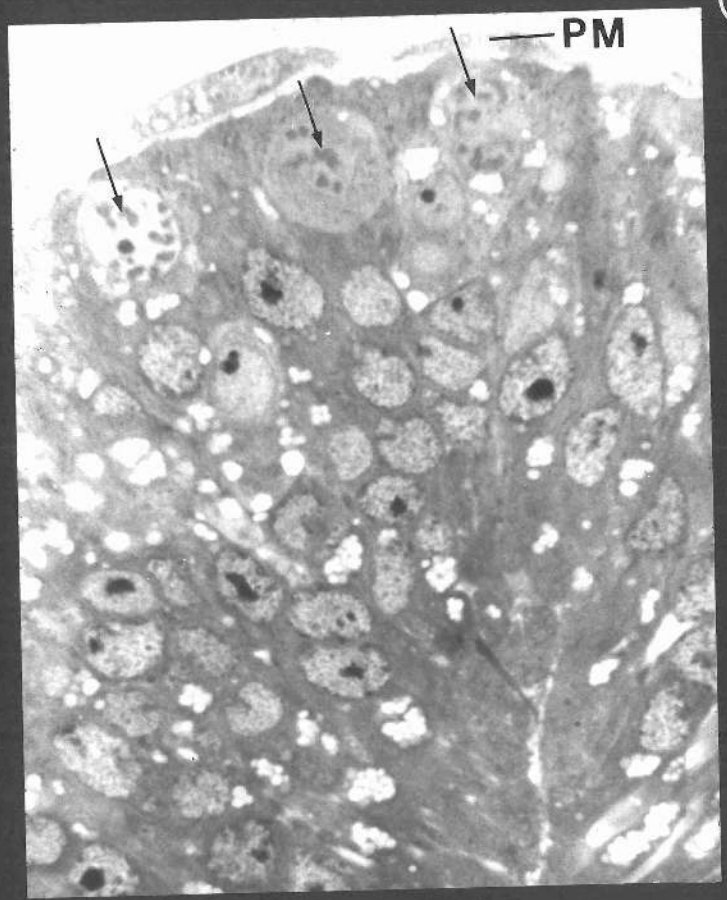

FIGURE 80

Longitudinal section through part of a Stage 1 C. erythrocephala wing imaginal disc stained with methylene blue. Filopodial cell extensions project from cell bases and interdigitate with adjacent epidermal cell filopodia or with dorsal or ventral epidermal layers. X 1,700.

FIGURE 81

Part of cell extensions of a Stage 1 C. erythrocephala wing disc. Microtubules are abundant within cell extensions and run parallel to the long axis of each epidermal cell. Note that the mitochondrion is also oriented parallel to the cells' long axis. X 54,000.

80

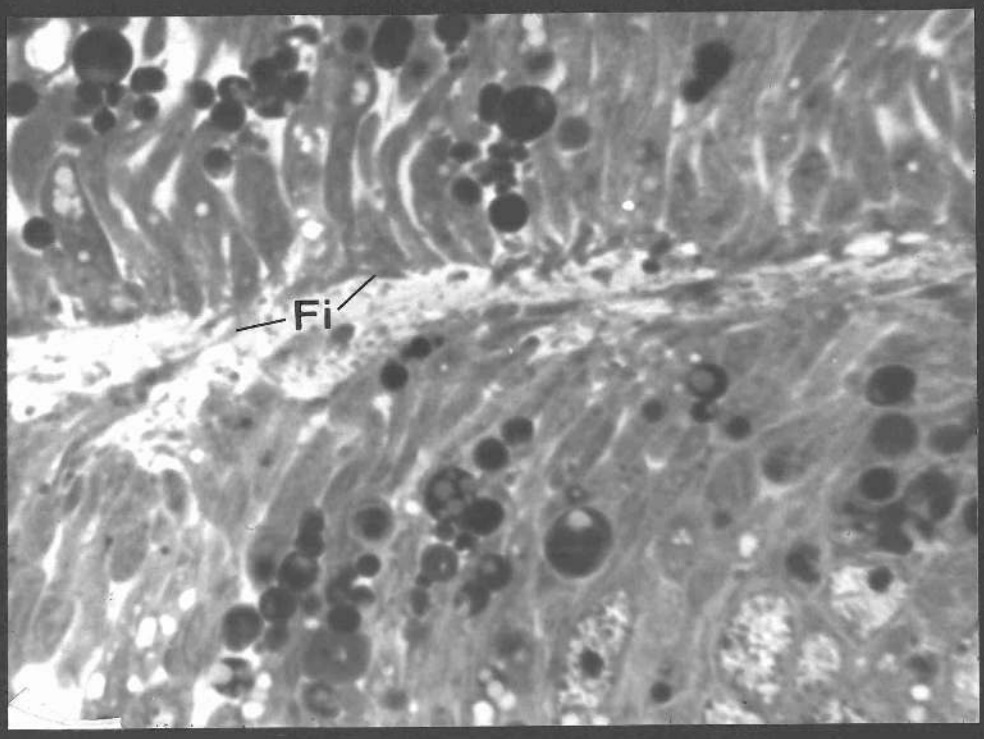

81

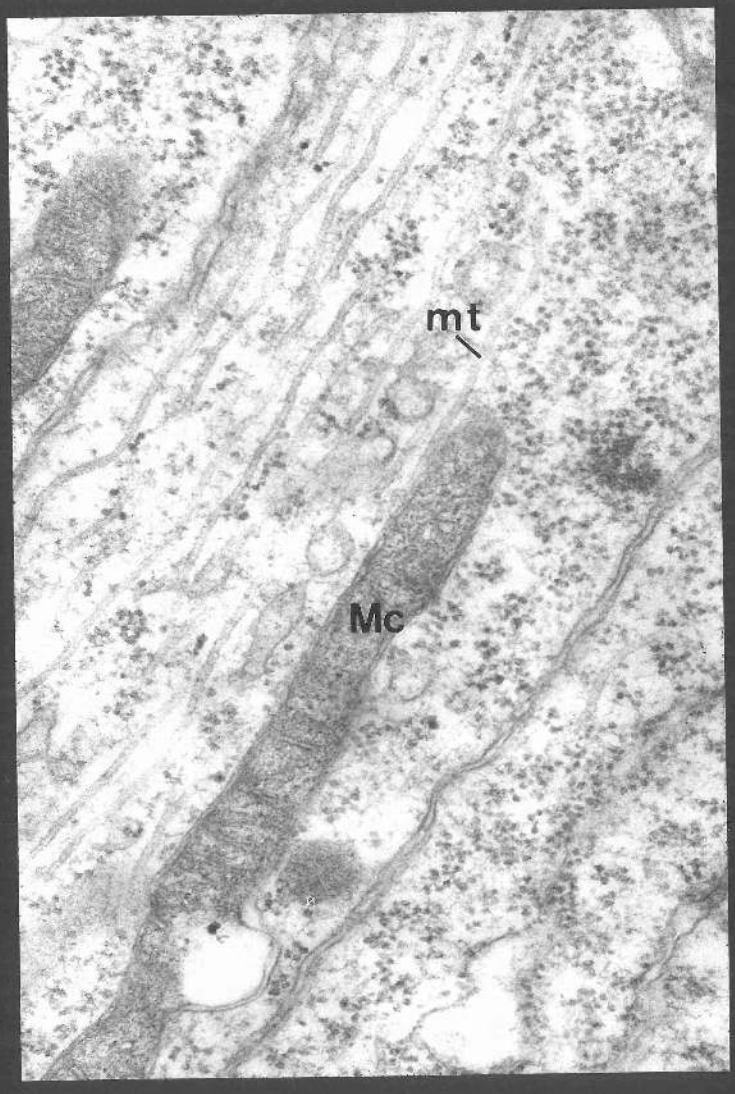

FIGURE 82

A portion of the apical part of an epidermal layer of a C. erythrocephala wing disc during Stage 1. Adjacent cells are joined by zonula adhaerens junctions. A projection from one cell extends into a surface depression in an adjacent cell. Some microtubules extend into the projection. A 'bleb' of cytoplasm occurs at the cell apex. X 29,000.

FIGURE 83

Feulgen stained preparation of a Stage 1 C. erythrocephala wing imaginal disc to show cell proliferation. Mitotic cells are 'rounded up' and confined to cell apices. Spindle axes are predominantly oriented parallel to the proximo-distal wing axis. X 1,300.

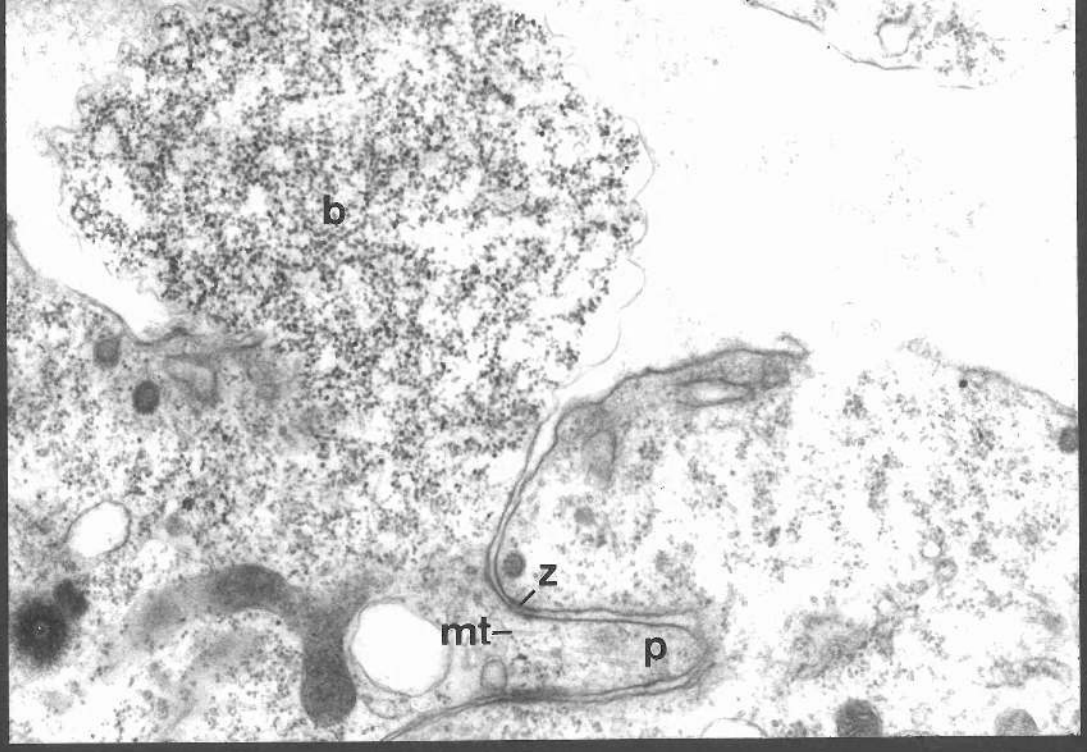
b
z
mt–
p

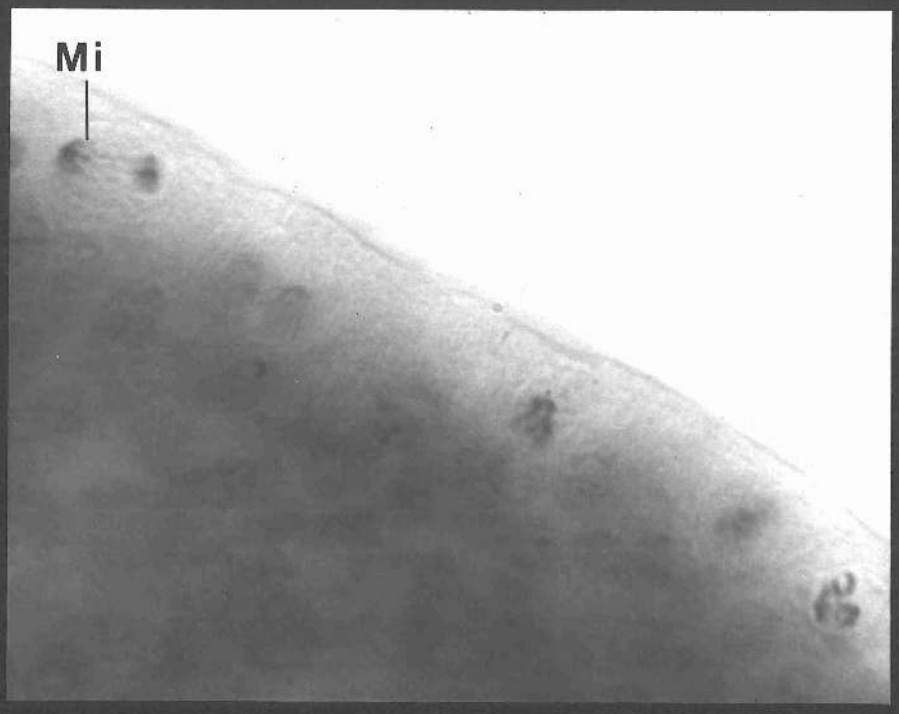
Mi

FIGURE 84

Longitudinal section of part of the basal region of a Stage 1 C. erythrocephala wing imaginal disc epidermis in a region where the two epidermal layers closely approach one another but are not yet juxtaposed. Filopodia extend from each cell into the basement lamina. Filopodia contain microfilaments which extend along their lengths. X 39,100.

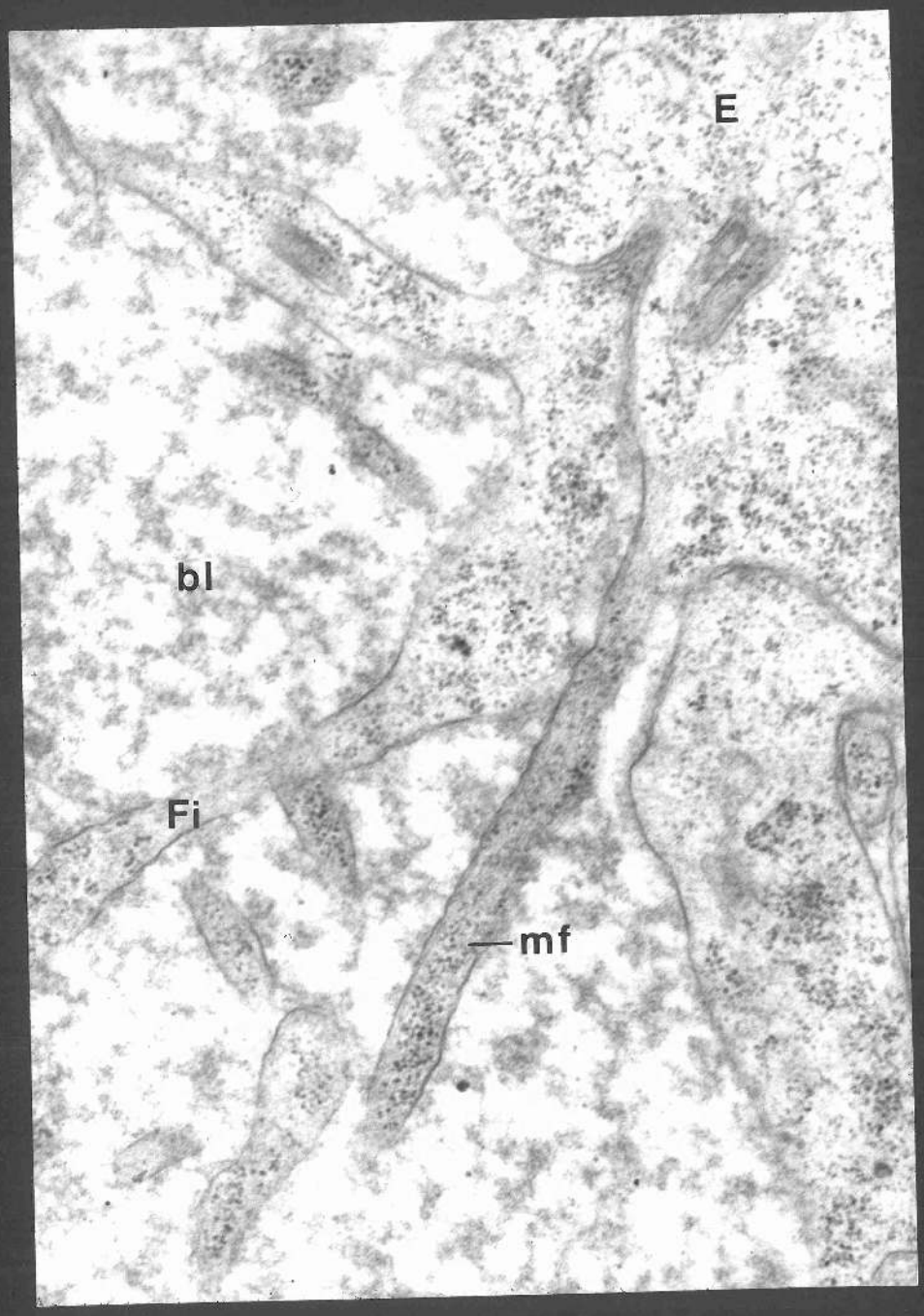
E
bl
Fi
mf

FIGURE 85

Longitudinal section through a C. erythrocephala wing imaginal disc during Stage 1. Haemocytes become trapped between the two epidermal layers as they approach one another to form the dorsal and ventral wing surfaces. X 1,300.

FIGURE 86

Transverse section through a C. erythrocephala wing blade during Stage 2. The two epidermal layers are basally connected. Individual epidermal cells are spindle shaped with the nucleus constituting the widest part of each cell. Cells are closely packed at the apex of the epidermal layers whereas large intercellular spaces occur at the base of the epidermal layers. X 1,300.

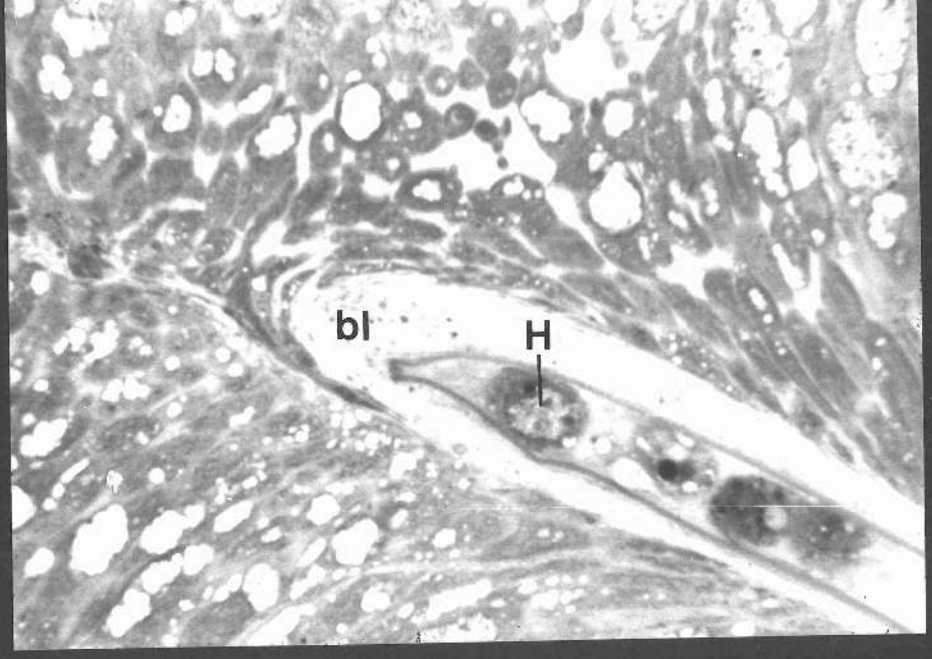

86

FIGURE 87

Transverse section through a Stage 2 C. erythrocephala wing blade showing part of an epidermal cell extension. Many microtubules run parallel to the long axis of the cell. X 54,000.

FIGURE 88

Transverse section through a Stage 2 C. erythrocephala wing blade showing a portion of the apical part of an epidermal layer. Zonula adhaerentes connect adjacent cells. Microfilaments and microtubules are closely associated with these junctions. Microvilli occur along the apical surface. Each microvillus contains microfilaments which extend along its interior. Epicuticle deposition has begun (arrow) and extends from one microvillus tip to another. X 53,000.

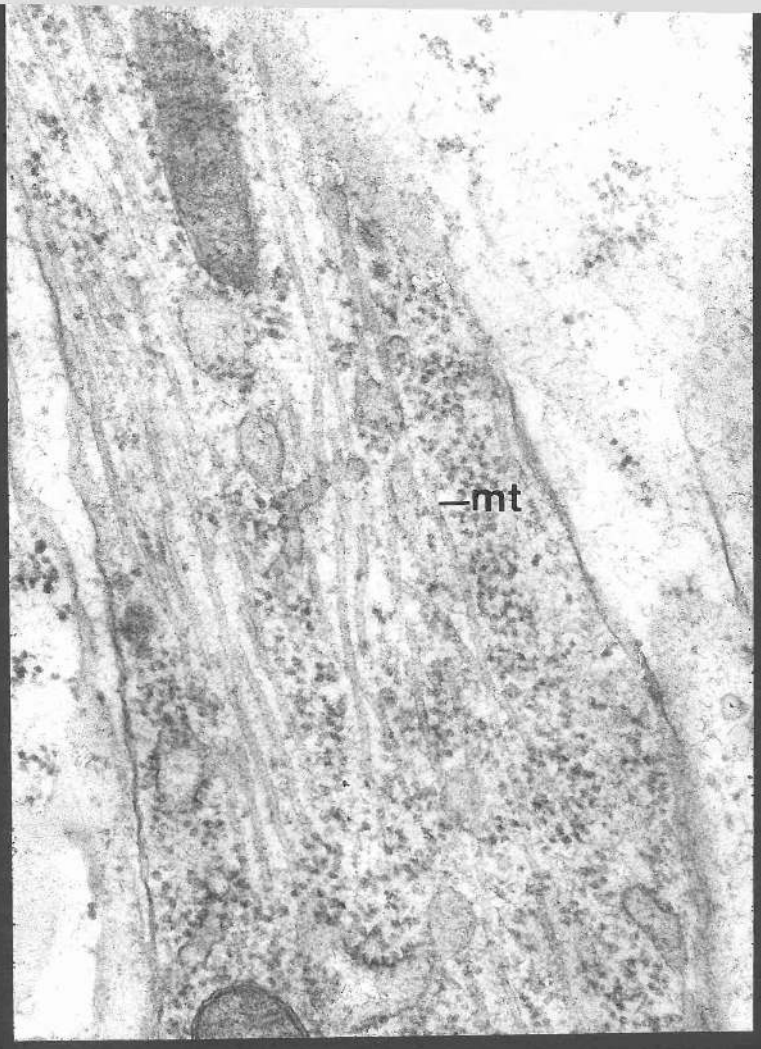

88

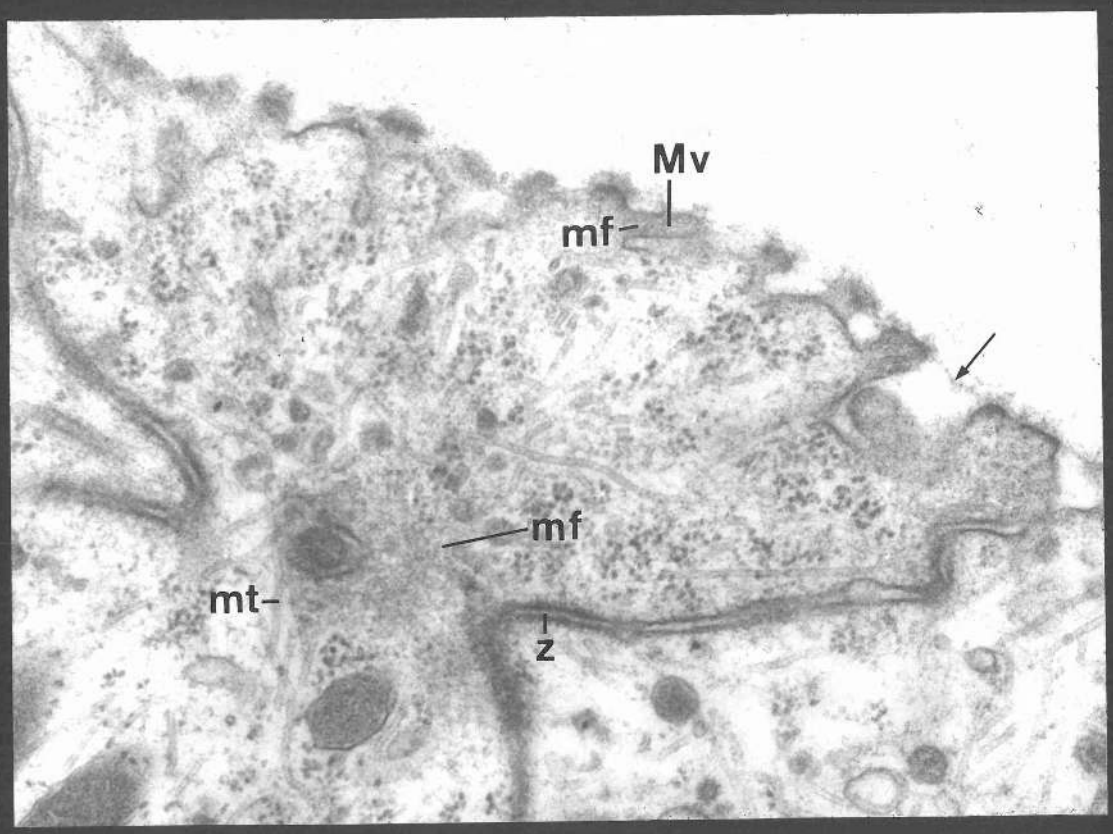

FIGURE 89

Transverse section through a Stage 2 C. erythrocephala wing blade showing part of the apical regions of two adjacent epidermal cells. Microfilaments are closely associated with a zonula adhaerens junction and appear to extend right around the perimeters of the apical region of each cell. Microtubules occur in close association with the zonula adhaerentes. Basal to the zonula adhaerens is a gap junction. X 69,600.

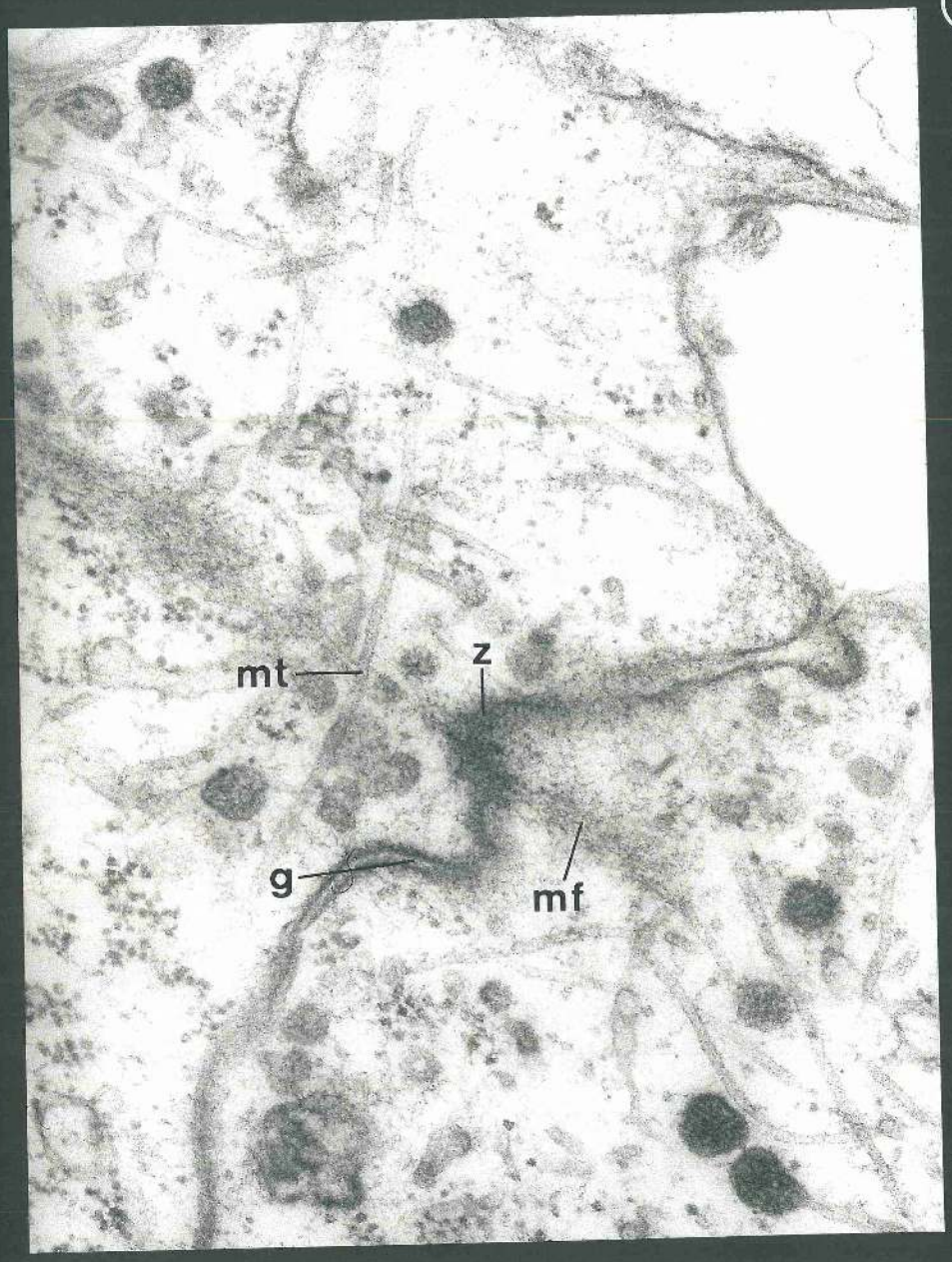
mt
z
g
mf

FIGURE 90

Transverse section through a Stage 2 C. erythrocephala wing blade showing the bases of dorsal and ventral epidermal layers. Filopodia protrude from epidermal cell bases and interconnect with filopodia from an opposing cell or an adjacent cell (arrows). Desmosomal plaques often connect dorsal and ventral epidermal cells. X 12,000. Bar = 1 μm.

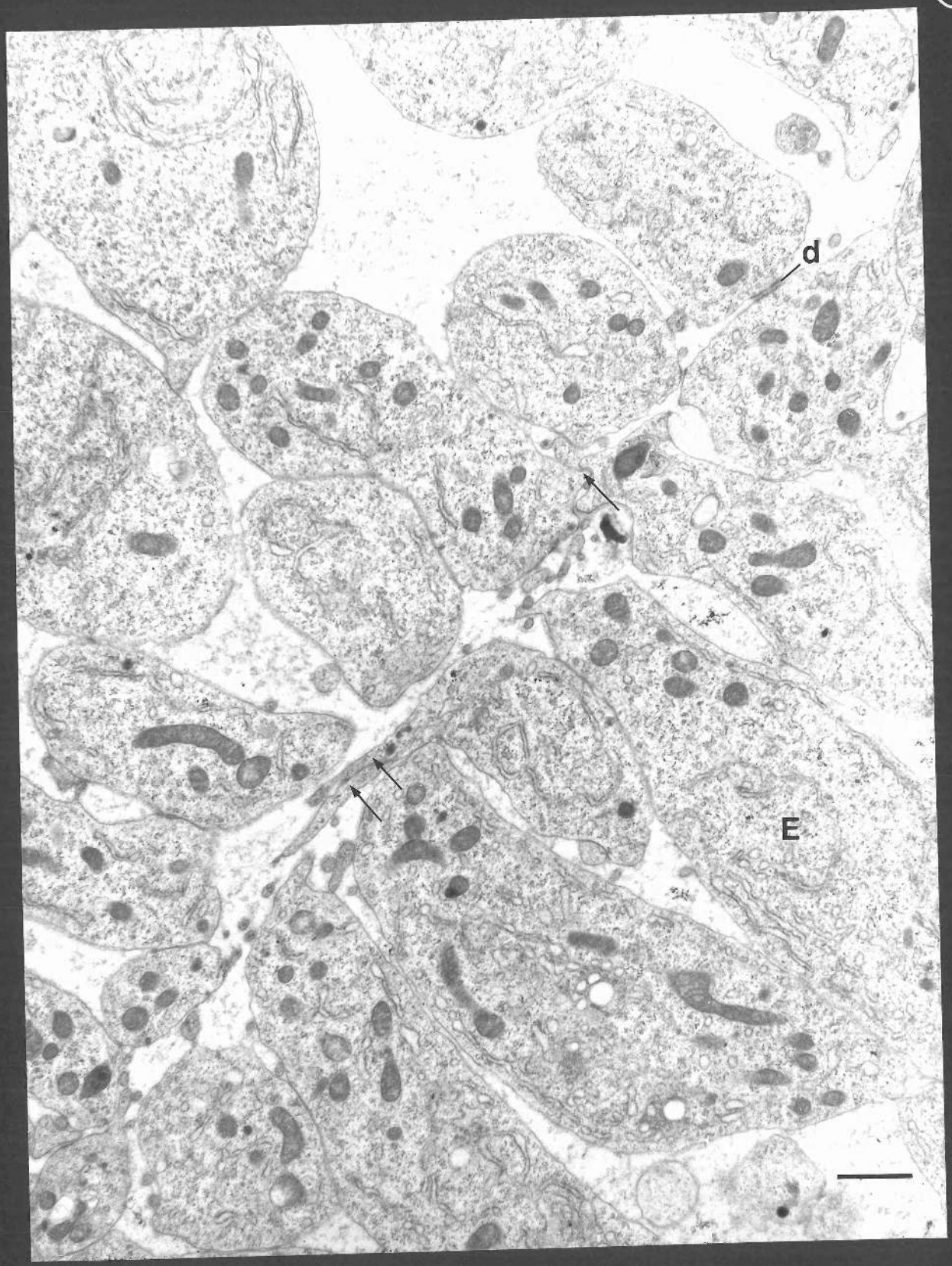
d
E

FIGURE 91

Transverse section through filopodia at the base of epidermal cells of a Stage 2 C. erythrocephala wing blade. Many microtubules occur within the filopodia. The tubules extend along the long axes of the filopodia. X 52,000.

FIGURE 92

Transverse section of epidermal cell bases of a Stage 2 C. erythrocephala wing blade. Cells of dorsal and ventral epidermal layers are connected at intervals by desmosomal plaques along their basal surfaces. X 31,300.

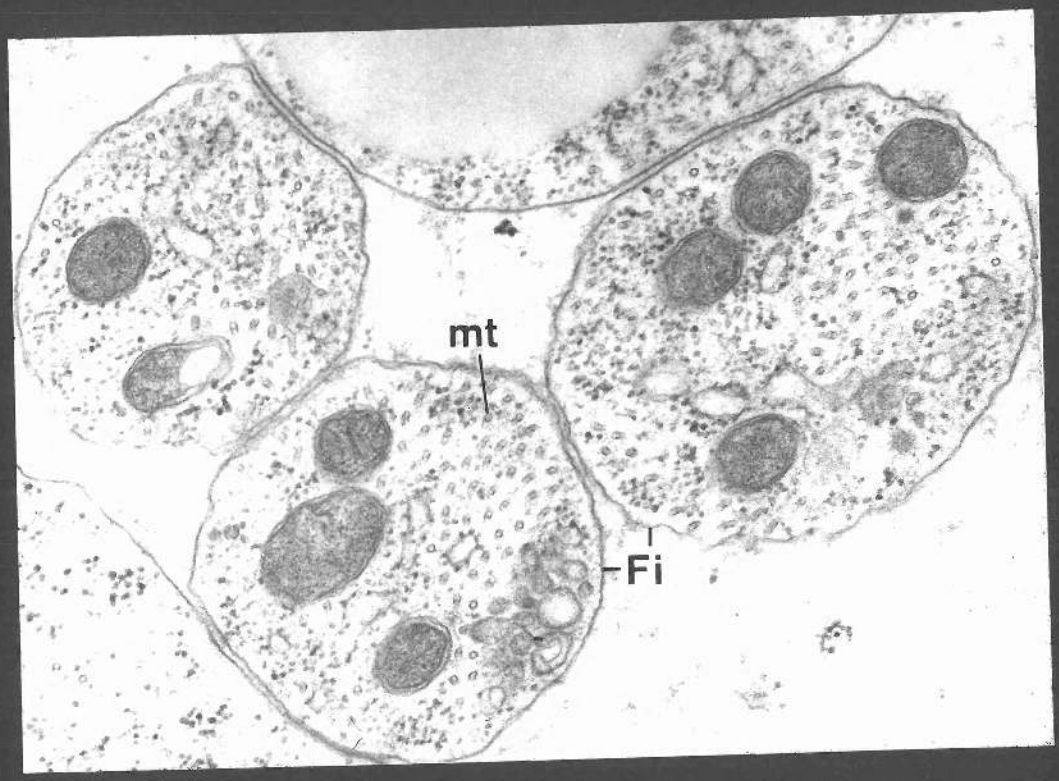
mt
Fi

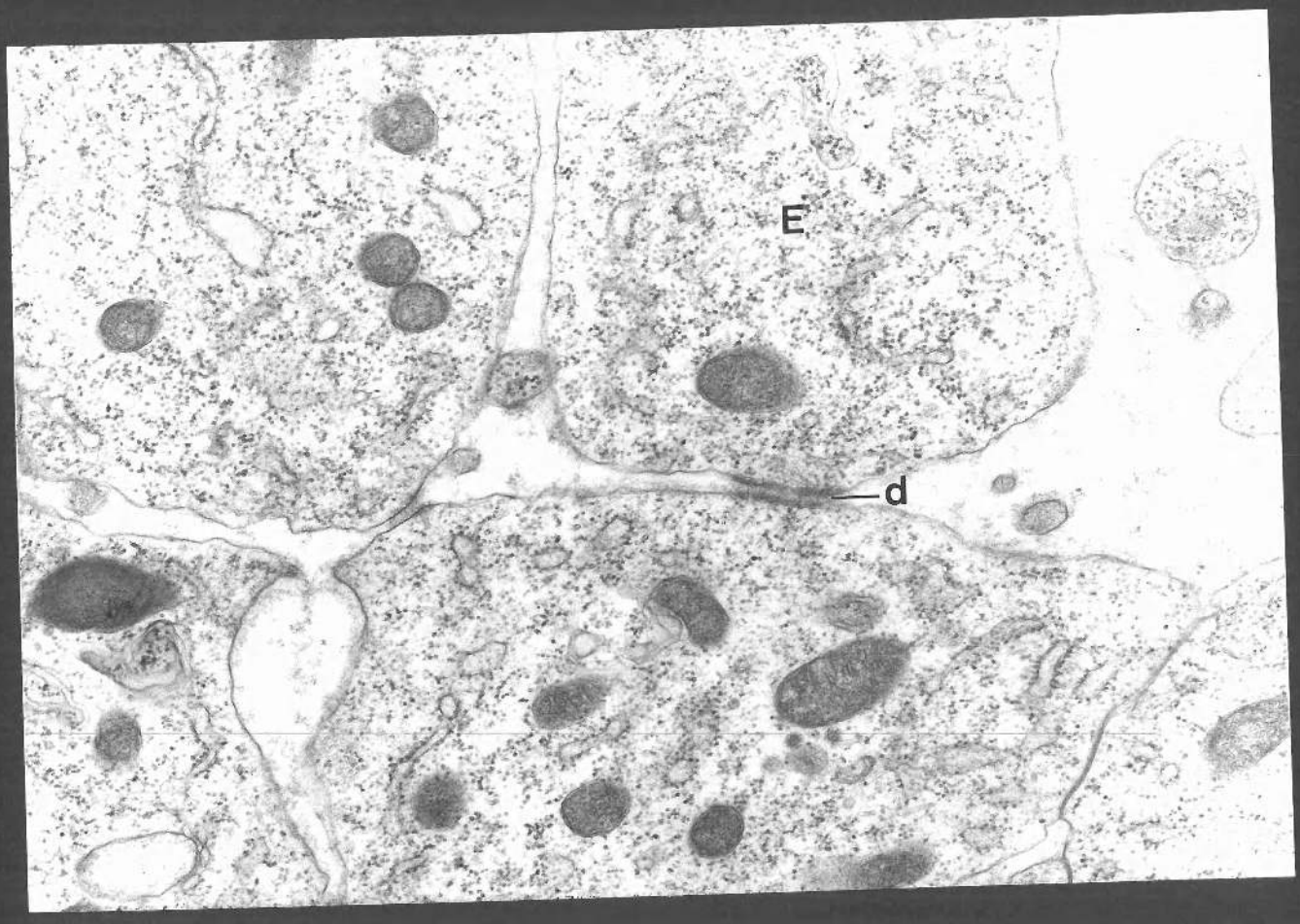
E
d

FIGURE 93

Transverse section of part of a Stage 2 C. erythrocephala wing blade in a region directly above a vein lacuna. Most nuclei of cells which are dorsal to the lacuna are concentrated in the basal half of cells so that cell extensions apical to the nucleus are longer than those basal to it. Cells undergoing mitosis are 'rounded up' and are apically situated in the epidermis (arrow). X 1,400.

FIGURE 94

Transverse section through the vein lacuna region of a Stage 2 C. erythrocephala wing blade. Haemocytes occur within the lacuna. Most of the basal cell extensions of epidermal cells of dorsal and ventral wing epidermal layers interdigitate with adjacent cells. Some basal cell extensions extend around the lacuna (arrow). X 1,000.

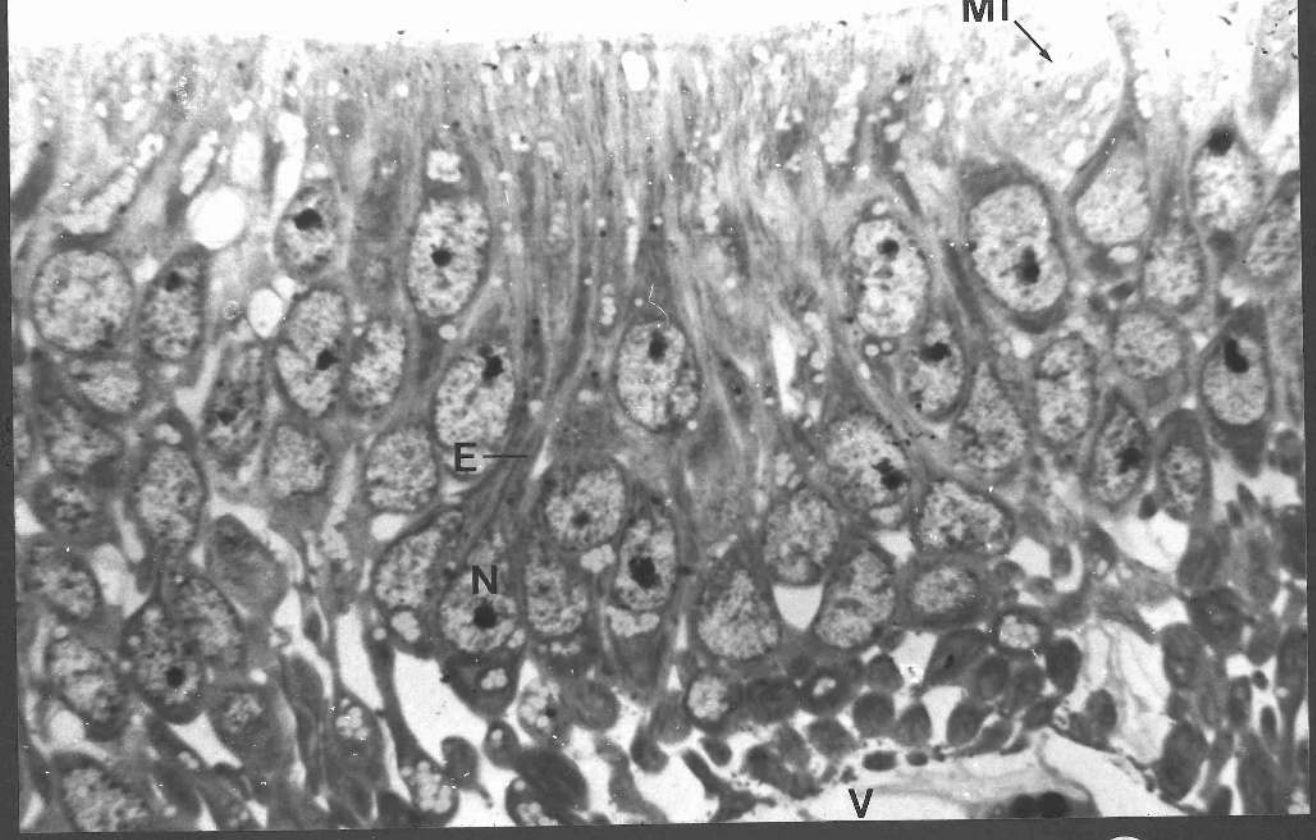

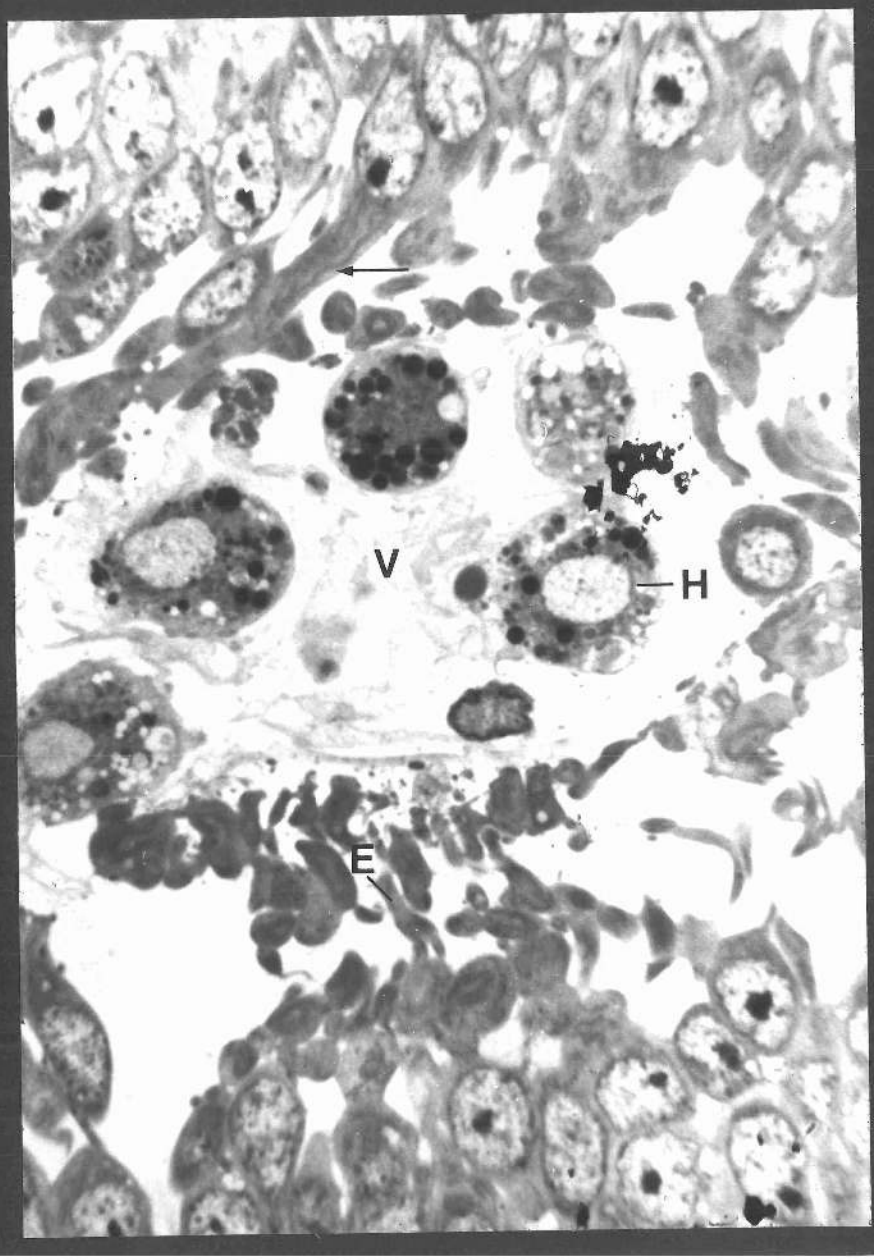

94

FIGURE 95

Transverse section through the margin of a Stage 2 C. erythrocephala wing blade. Epidermal cells are wide at their apices and narrow at their bases. X 1,000.

FIGURE 96

Longitudinal section through a Stage 1 C. erythrocephala wing blade showing part of the wing margin epidermal layers. Cell apices of adjacent cells interdigitate and are joined by septate desmosomes. X 36,000.

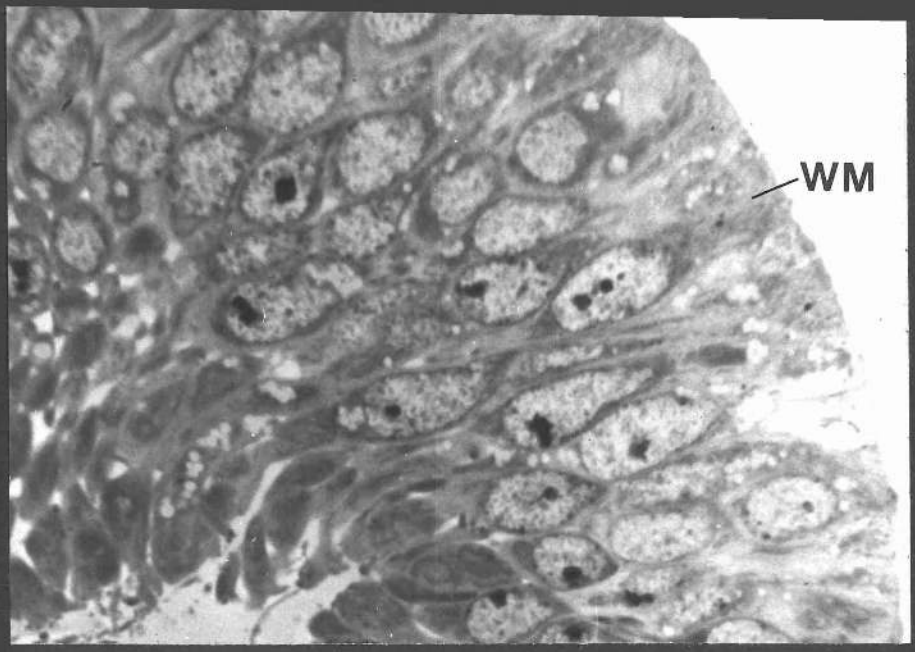
WM

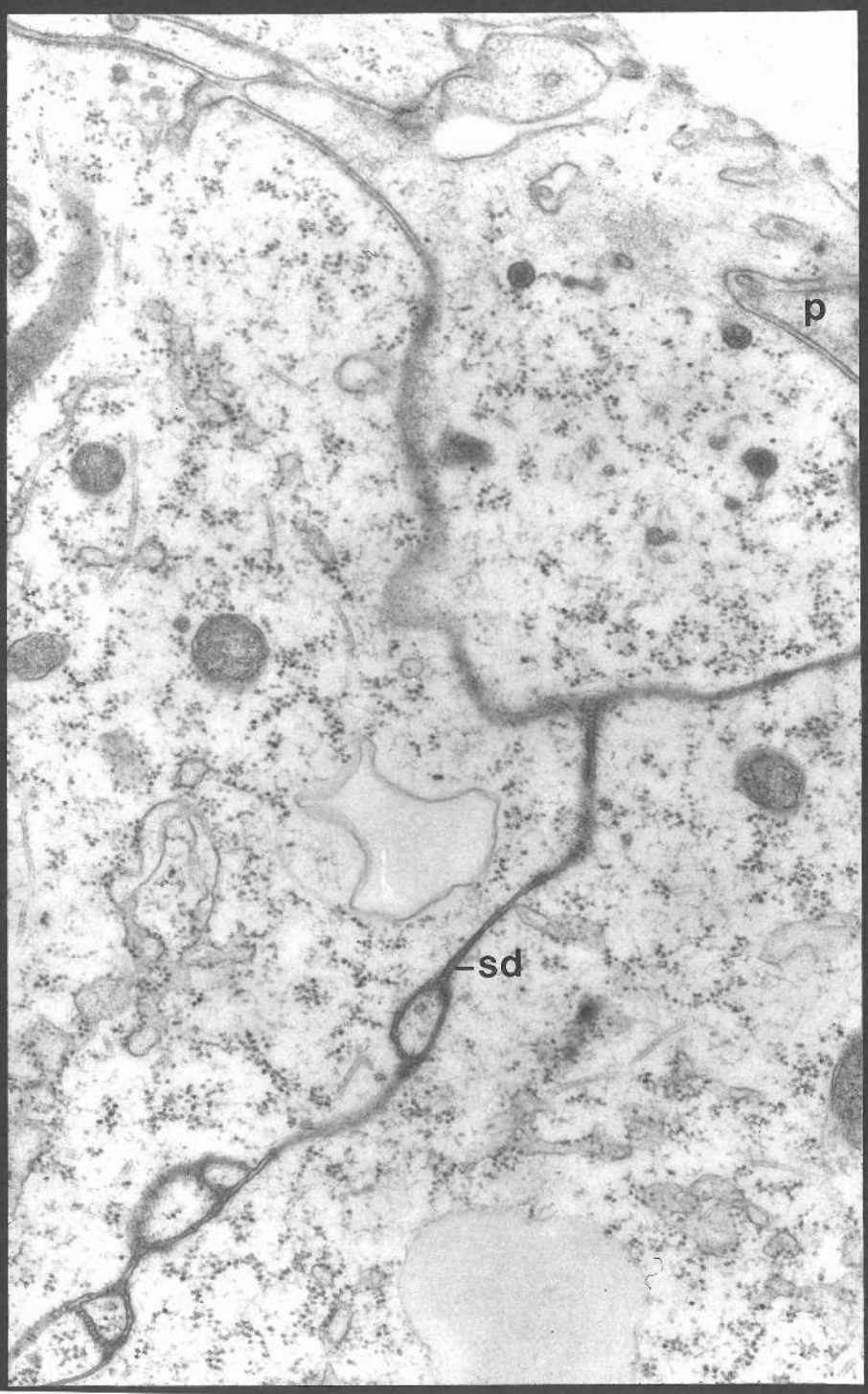
p
sd

FIGURE 97

Transverse section of a Stage 3 C. erythrocephala wing blade. The wing blade is dorso-ventrally flattened. Epidermal cells of dorsal and ventral epidermal layers are juxtaposed at their bases, and adjacent cells are not pseudostratified. The outer or apical surfaces of epidermal cells are convex except at wing margins. The prepupal veins are apparent. X 100.

FIGURE 98

Transverse section through part of a Stage 3 C. erythrocephala wing blade. Cells of dorsal and ventral epidermal layers are juxtaposed at their bases. The nuclei of dorsal or ventral epidermal cells are all arranged in a single layer. The apex of each cell is convex (arrow). A haemocyte is located between adjacent cells of one epidermal layer. X 1,000.

FIGURE 99

Transverse section through the wing margin of a Stage 3 C. erythrocephala wing blade. The apices of cells at the wing margin are smooth and flat whereas those adjacent to the margin are convex. X 1,000.

97

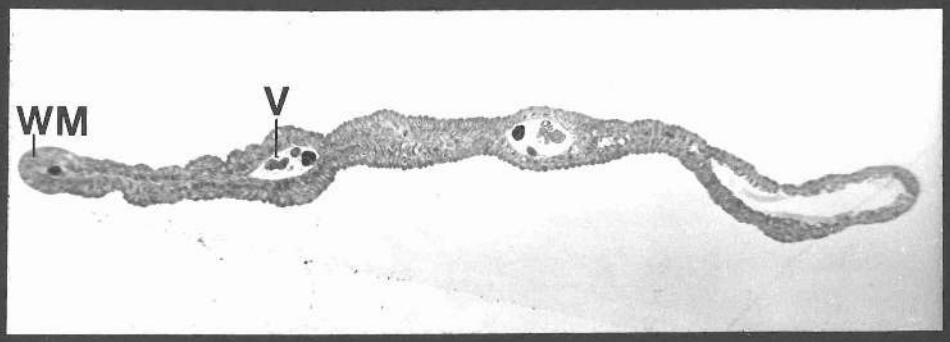

98

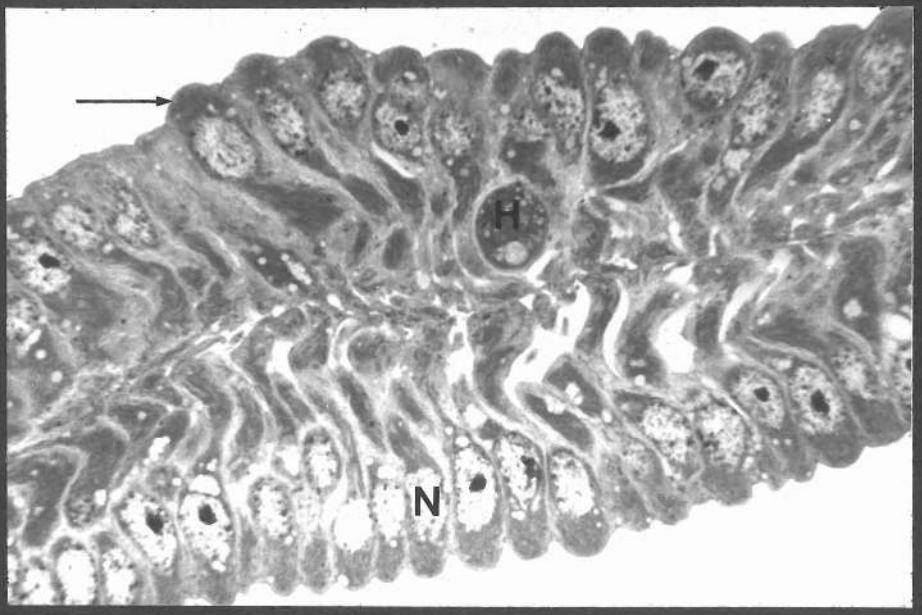

99

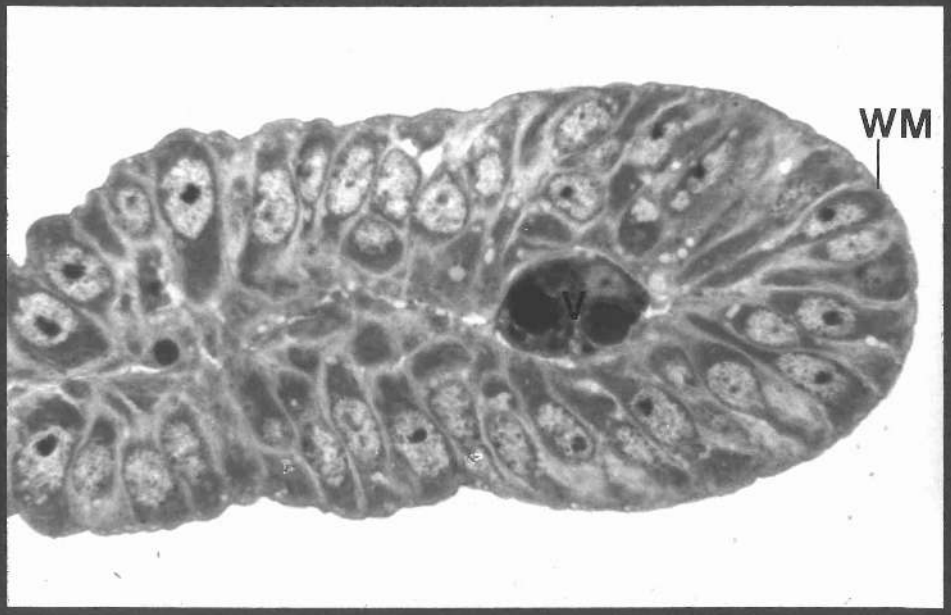

FIGURE 100

Scanning electron micrograph of the surface of a Stage 3 C. erythrocephala wing blade. The cell surfaces are convex and ridged and each cell is usually more elongate in a direction parallel to the proximo-distal wing axis. X 4,000. Bar = 5 μm

FIGURE 101

Longitudinal section through the apex of an epidermal cell of a Stage 3 C. erythrocephala wing blade. The outer surface of the cell is convex and ridged. Many microtubules are situated within the apical part of the cell. Most microtubules are oriented perpendicular to the proximo-distal wing axis. Cuticle deposition is shown. X 47,000.

FIGURE 102

Transverse section through the prepupal vein area of a Stage 3 C. erythrocephala wing blade showing the arrangement of epidermal cells dorsal and ventral to a prepupal vein. Basal cell extensions from epidermal cells extend around the vein. X 1,000.

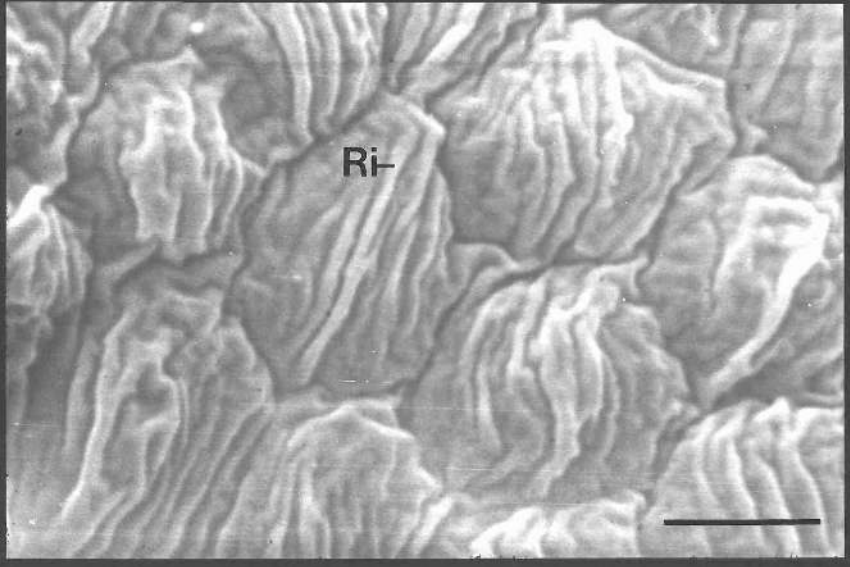

101

102

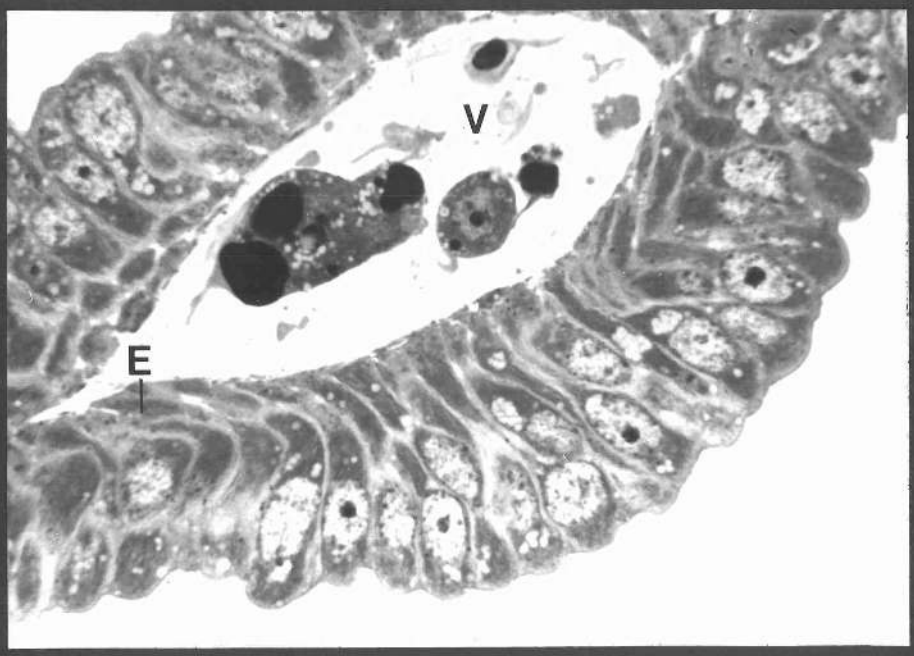

FIGURE 103

Transverse section through filopodia at the bases of epidermal cells shown in Figure 102. Many microtubules extend along the long axes of the filopodia. X 50,900.

FIGURE 104

Transverse section of a Stage 3 C. erythrocephala wing blade showing the bases of dorsal and ventral epidermal layers which are interconnected by means of desmosomal plaques. X 47,000.

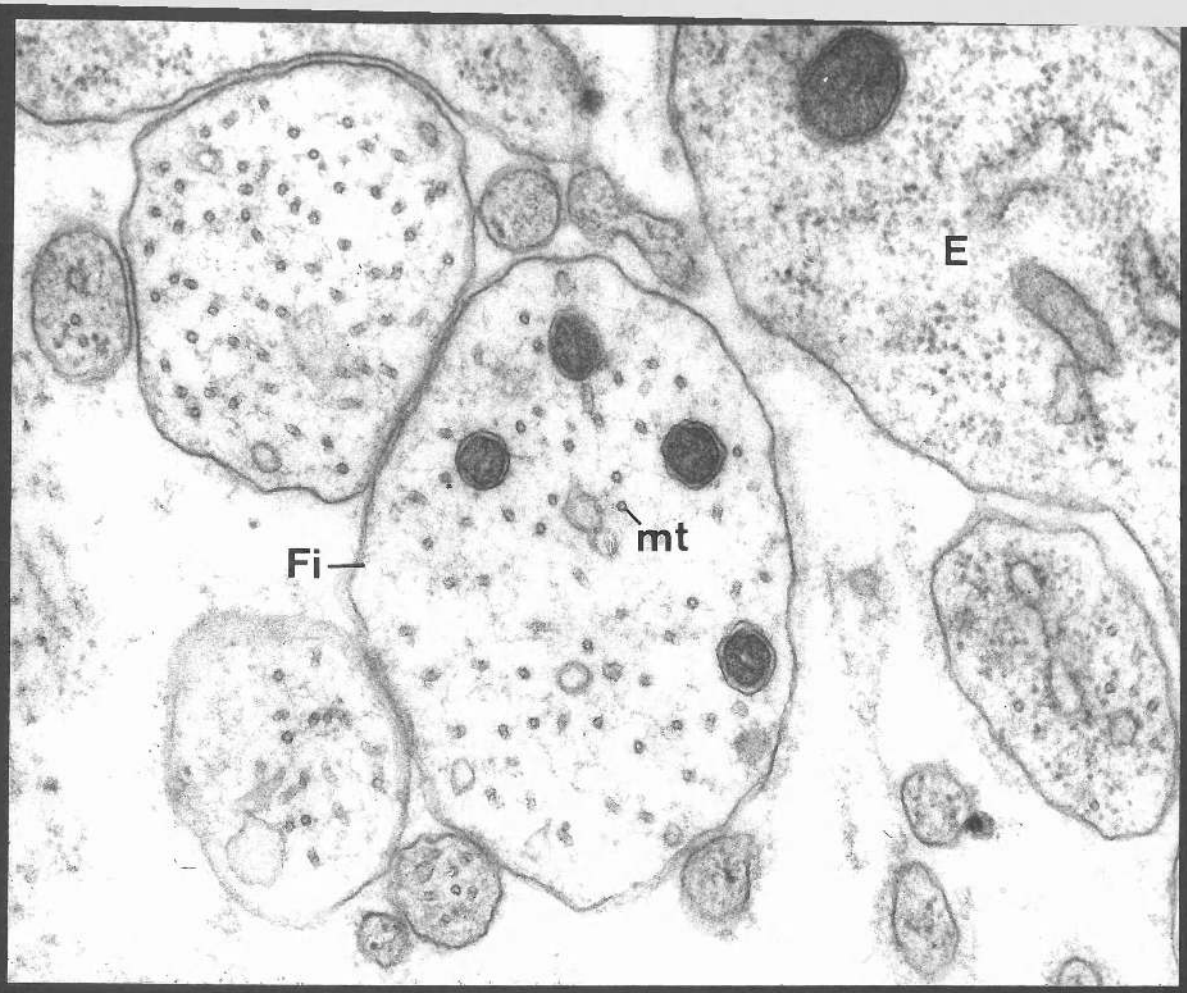
E
mt
Fi

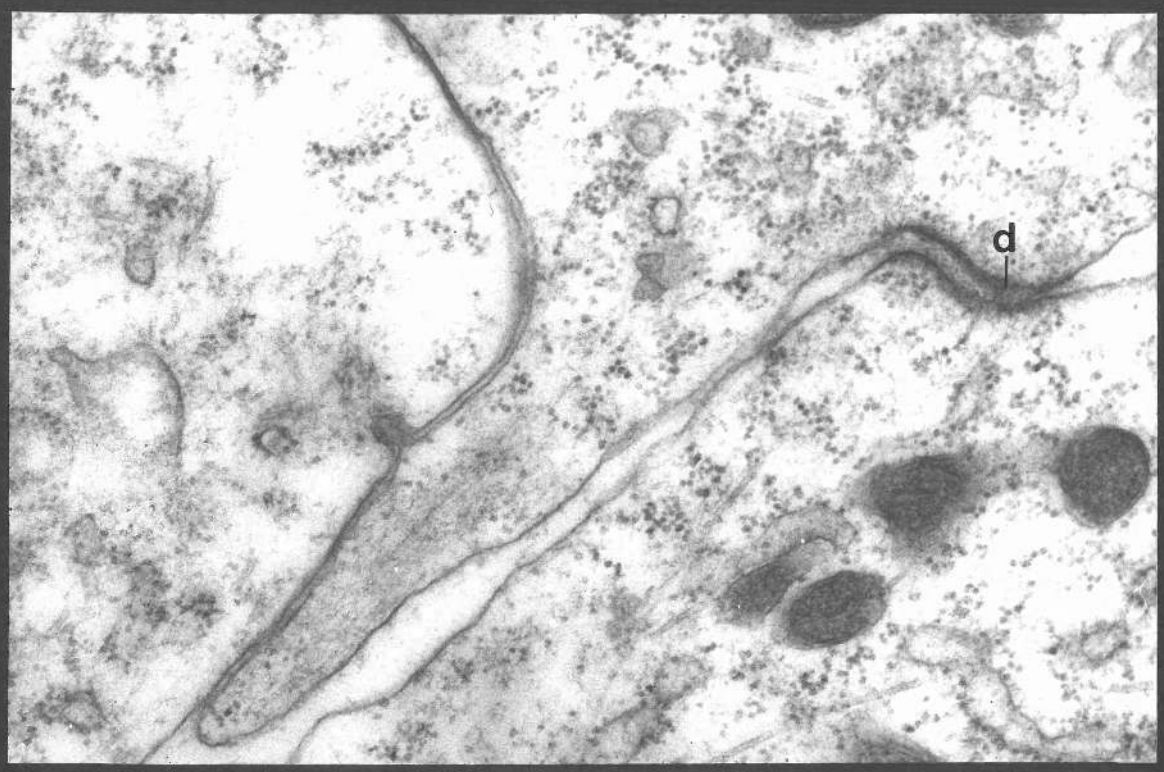
d

FIGURE 105

Feulgen stained preparation of part of a C. erythrocephala Stage 2 wing blade showing nuclear size and packing. X 1,400.

FIGURE 106

Feulgen stained preparation of part of a C. erythrocephala Stage 3 wing blade showing the increased nuclear size. X 1,400.

105

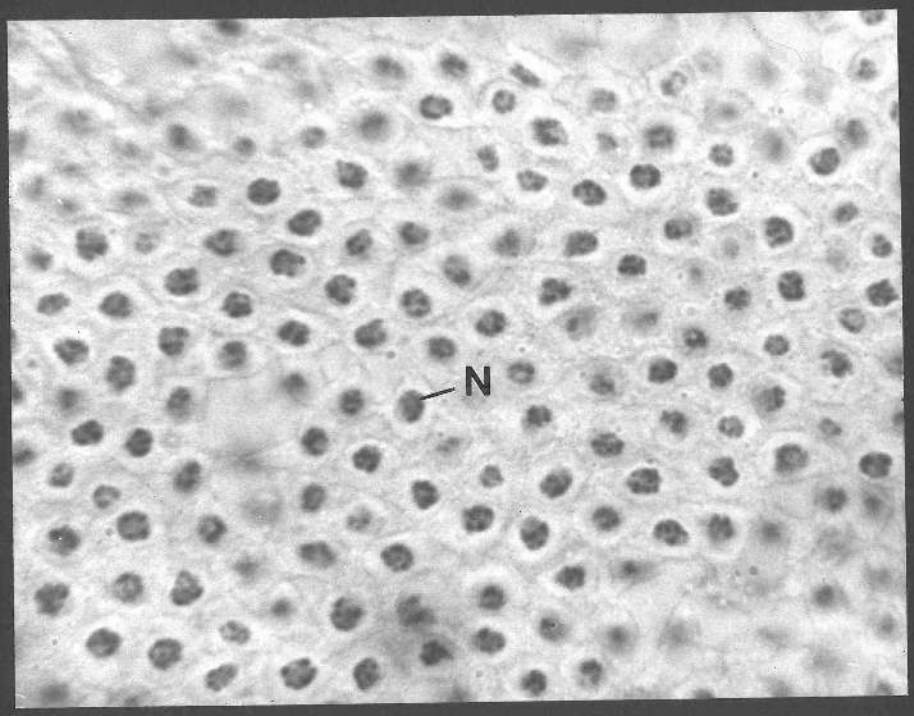

106

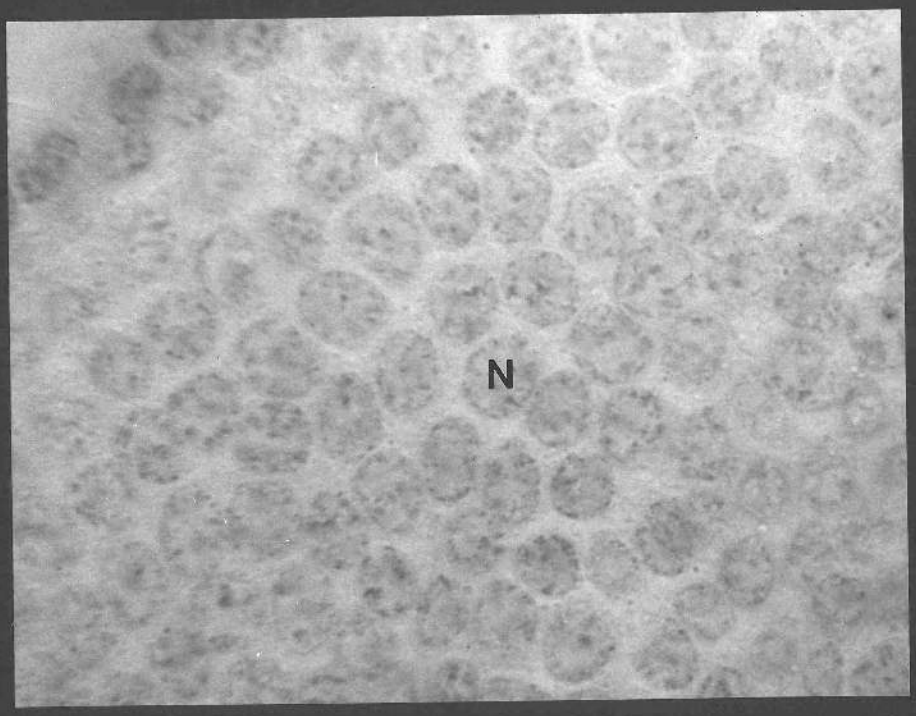

FIGURE 107

Transverse section of a methylene blue stained Stage 4 C. erythrocephala wing blade. Cell bodies lie directly beneath the pupal cuticle. Cell bodies of dorsal and ventral epidermal layers are separated from one another. At the wing margin, a cell extension projects from each cell body. These cell extensions appear to connect midway across the wing blade. X 180.

FIGURE 108

Lateral view of part of an unfixed Stage 4 C. erythrocephala wing blade freshly isolated in saline. Cell bodies are arranged directly beneath the pupal cuticle. Below each cell body a long cytoplasmic extension projects into the wing interior. Adjacent cell extensions lie parallel to one another and are connected to one another at various points by filopodia, X 1,200.

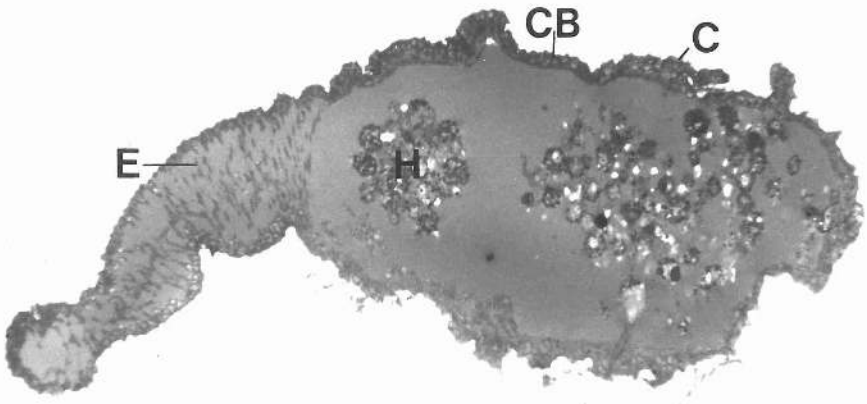

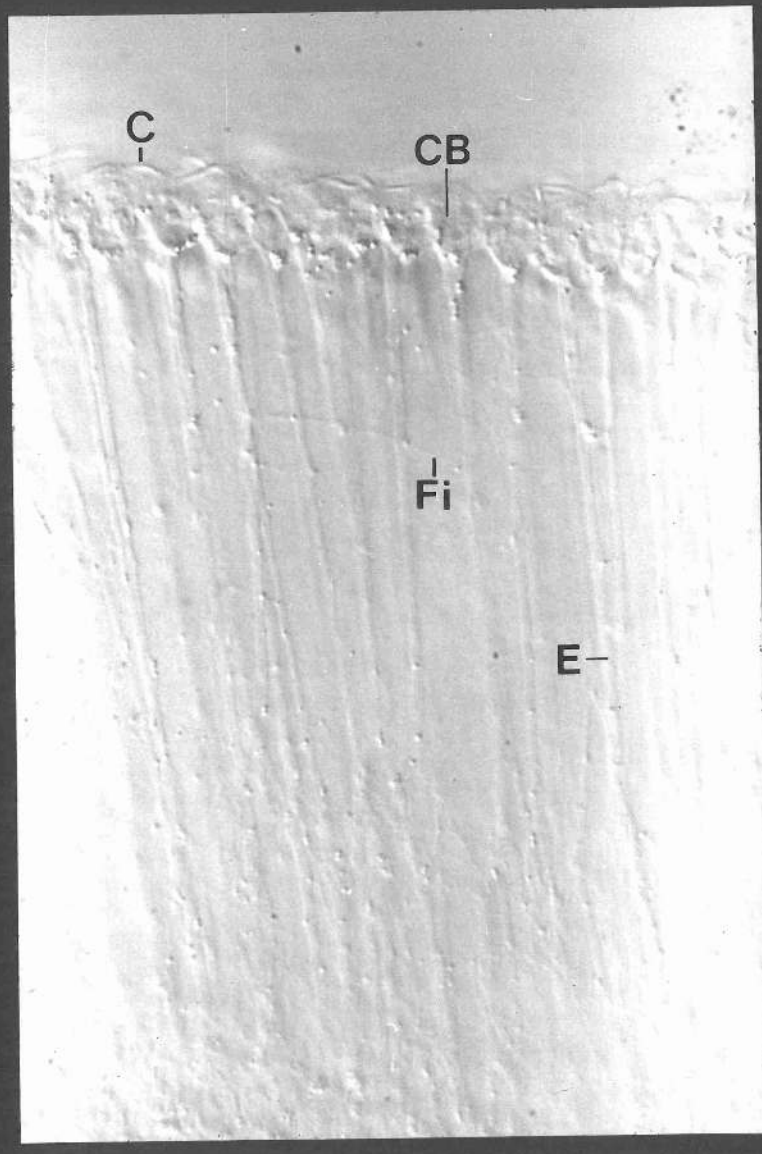

108

FIGURE 109

Methylene blue stained transverse section of part of a wing margin of a Stage 4 C. erythrocephala wing blade. Cell bodies of both dorsal and ventral epidermal layers are arranged in single layers beneath the shed pupal cuticle. Cell extensions project from cell bodies into the interior of the wing blade and connect midway. Filopodia connect adjacent cell extensions at various points along their lengths. X 1,400.

FIGURE 110

Methylene blue stained transverse section of part of a Stage 4 C. erythrocephala wing blade in a region of maximum swelling. Some cell extensions below cell bodies appear to connect to haemocytes. A filopodium connects one cell extension to another. The pupal cuticle is attached to the apical surfaces of epidermal cells. X 1,400.

109

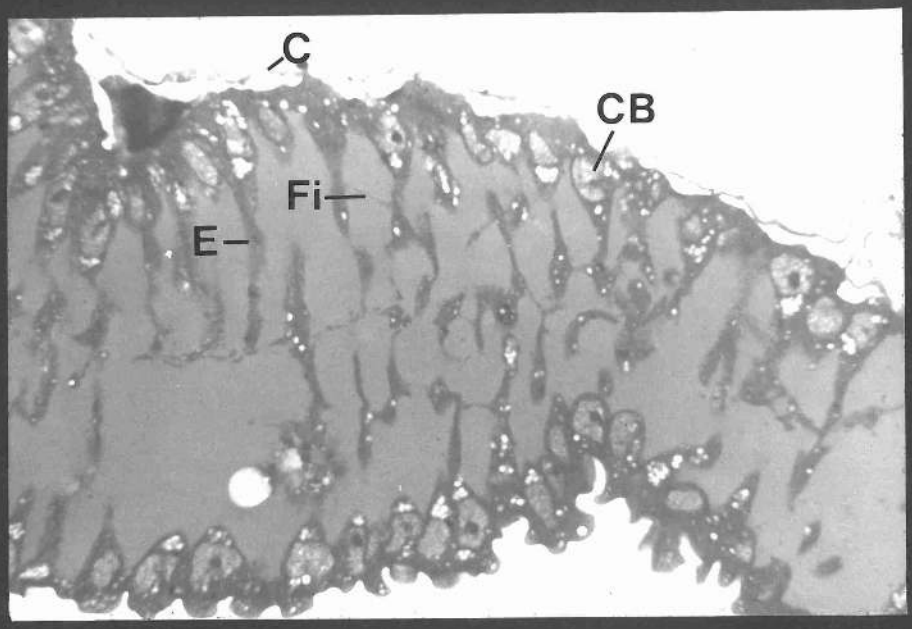

110

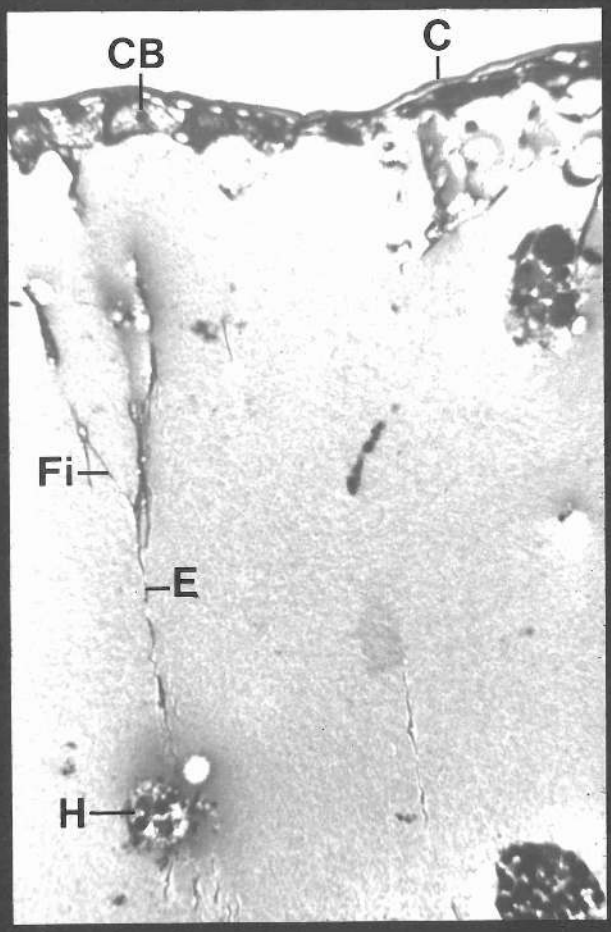

FIGURE 111a

Transverse section through part of a Stage 5 C. erythrocephala wing blade. Epidermal cells in intervein regions are columnar in shape except over veins (Fig. 117) and at wing margins (Fig. 119). Nuclei all occur at one level within dorsal and ventral epidermal layers. Trichomes are apparent at cell apices, and bristles at the wing margin. The entire wing blade lies within the pupal cuticle. The wing blade has a spongy appearance. X 200.

FIGURE 111b

Transverse section through part of the intervein region of a Stage 5 C. erythrocephala wing blade. Dorsal and ventral epidermal cells are columnar in shape. Dorsal and ventral epidermal layers are connected at epidermal cell bases. All nuclei are at one level within each epidermal layer. Trichomes project from cell apices. X 1,400.

111a

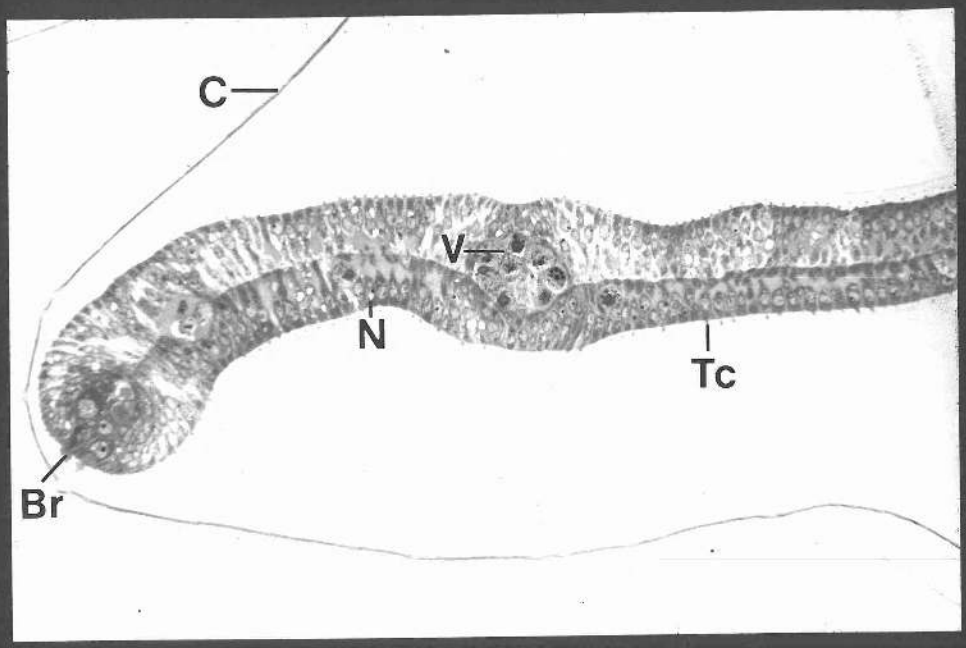

111b

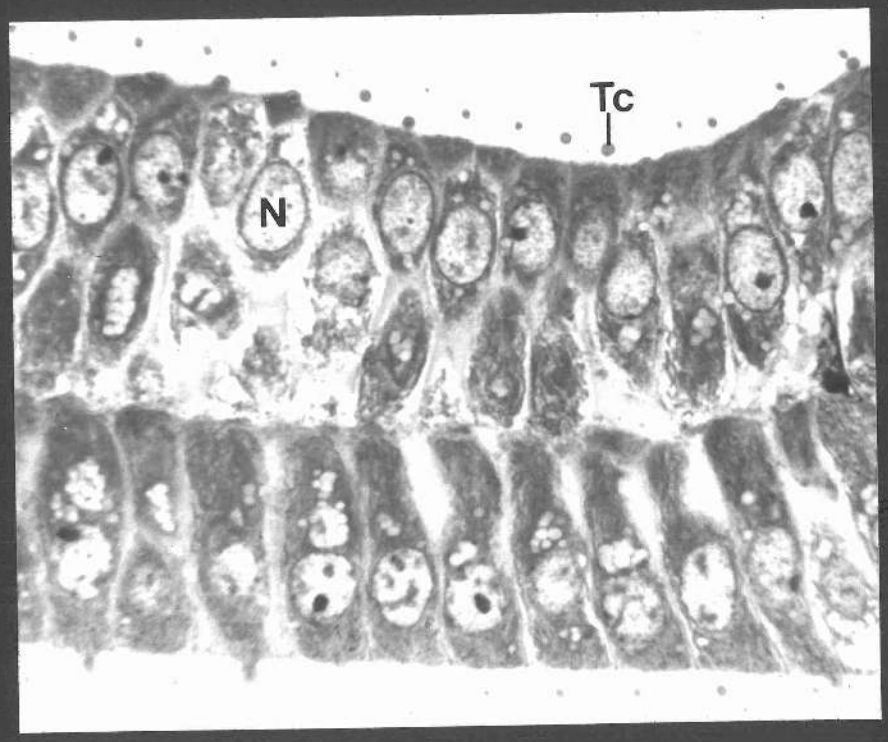

FIGURE 112

Feulgen stained preparation of a Stage 5 C. erythrocephala wing blade showing the nuclear arrangement in an intervein region. Nuclei are arranged in parallel rows. X 1,400.

FIGURE 113

Transverse section of part of the apices of two adjacent Stage 5 C. erythrocephala wing blade epidermal cells. Adjacent cells are anchored at their apices by maculae adhaerentes. X 64,700.

FIGURE 114

Transverse section of two interconnecting dorsal and ventral Stage 5 C. erythrocephala wing blade epidermal cells. The epidermal cells are connected at their flattened bases by a zonulae adhaerens junction. X 47,000.

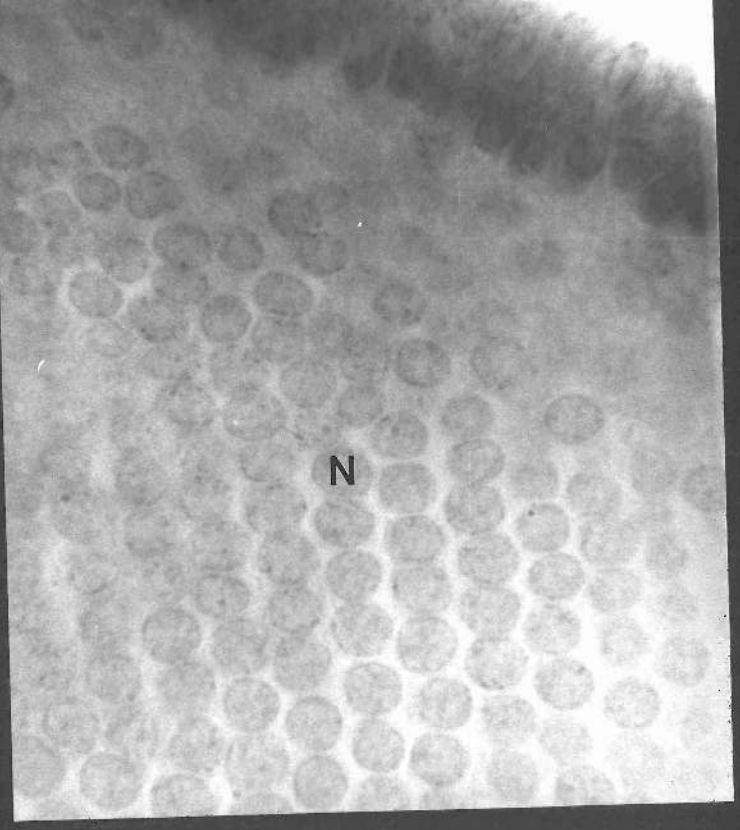

113

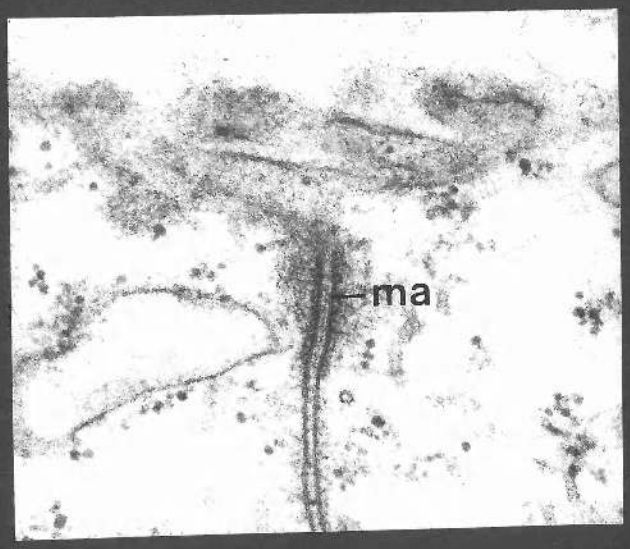

114

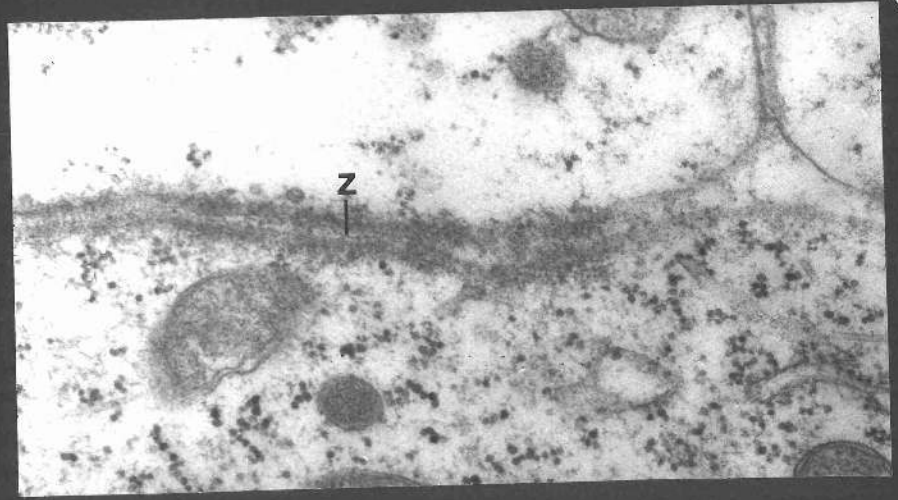

FIGURE 115

Transverse section through a portion of the basal part of the epidermal layers of a Stage 5 C. erythrocephala wing blade. A pocket of haemolymph (Poc) projects between two adjacent cells. Dorsal and ventral wing epidermal layers are connected by zonulae adhaerentes junctions. X 24,700.

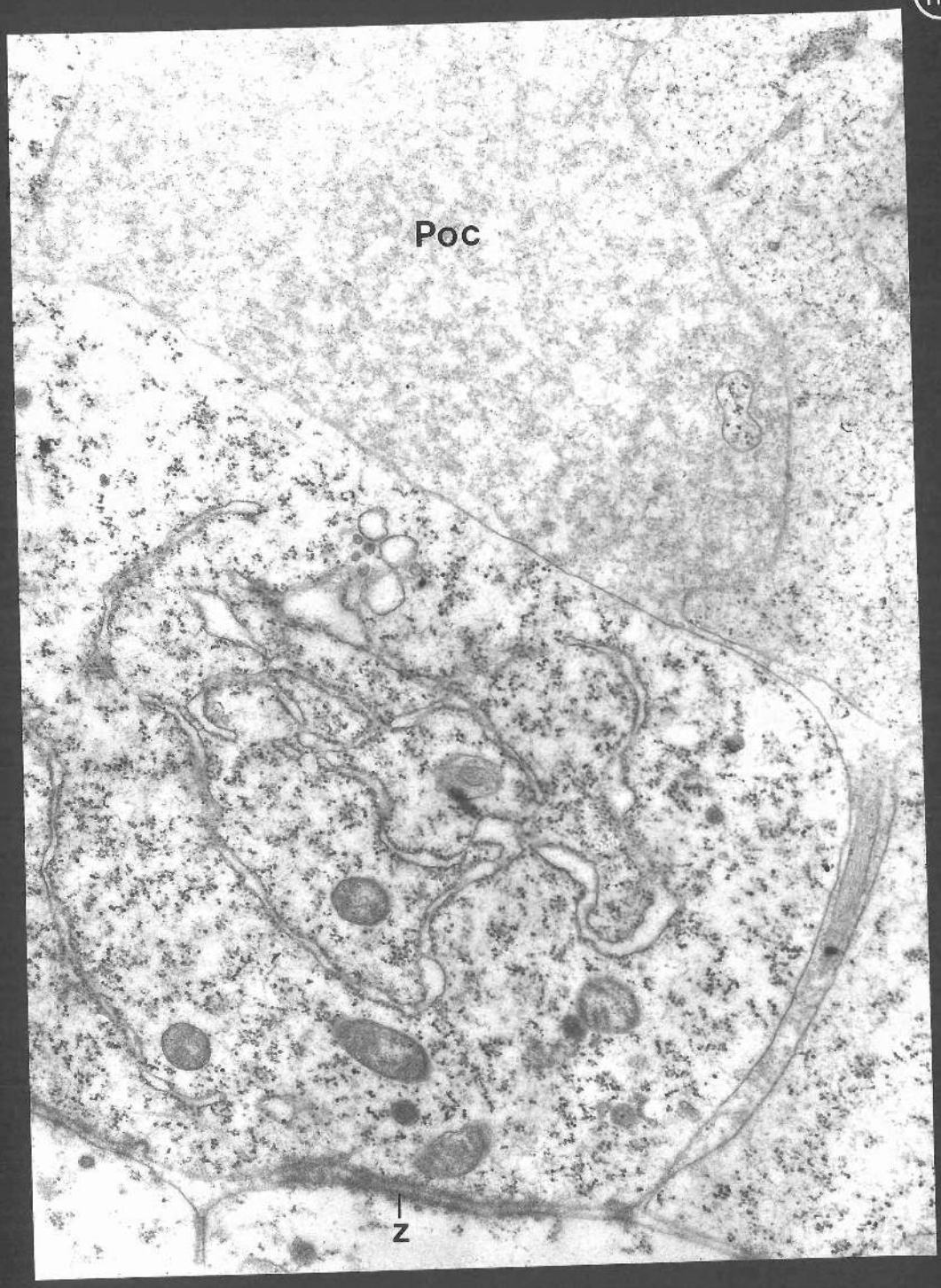
Poc
Z

FIGURE 116

Methylene blue stained transverse section of part of a Stage 5 C. erythrocephala wing blade. A haemocyte is apparent between epidermal cells (arrow). A pupal vein can be distinguished. Haemocytes, tracheae and tracheoles occur within the vein. X 1,200.

FIGURE 117

Transverse section of a methylene blue stained Stage 5 C. erythrocephala wing blade showing a pupal vein. Epidermal cells dorsal and ventral to the vein have long cell extensions basal to the nucleus. These cell extensions extend around the vein. Haemocytes occur within the vein. X 1,200.

116

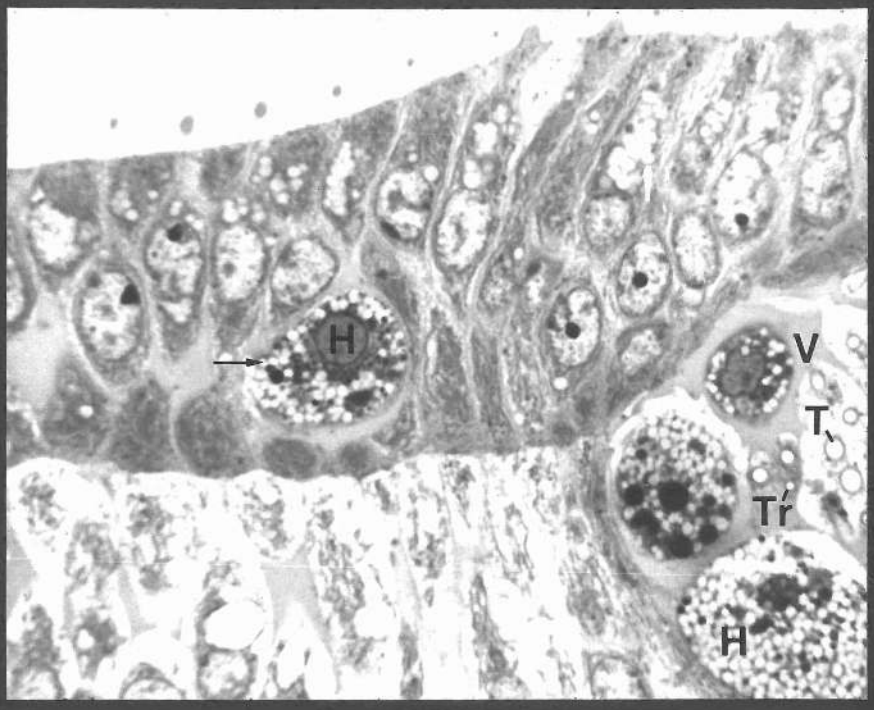

117

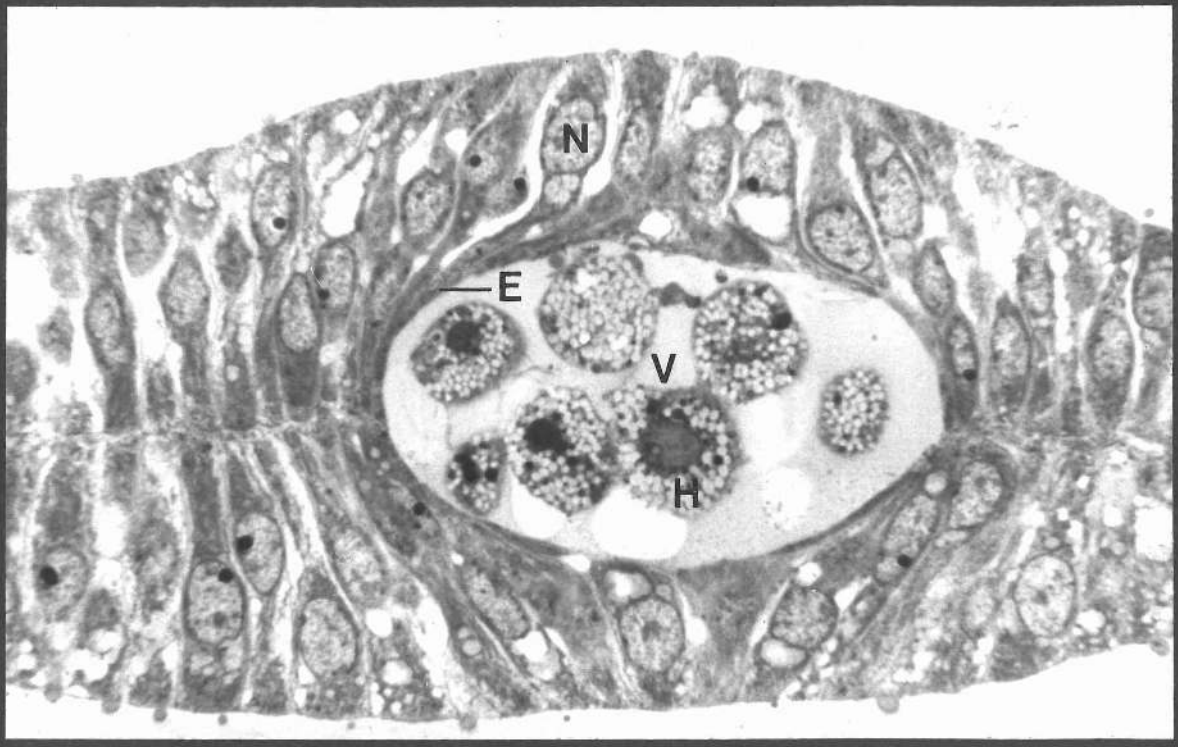

FIGURE 118

Transverse section through cell extensions of Stage 5 C. erythrocephala wing blade epidermal cells in a vein region where adjacent cell bases are connected. Microtubules run along the lengths of the filopodia. X 38,800.

FIGURE 119

Transverse section of the posterior wing margin of a Stage 5 C. erythrocephala wing blade. Cells of the posterior wing margin are arranged in a pseudostratified epithelial layer. Trichomes and bristles are apparent as are the trichogen and tormogen cells associated with bristle development. These cells have larger nuclei than the surrounding cells. The sensory nerve can also be distinguished (arrow). Epidermal cells surrounding the bristle-associated cells are narrow and have cell extensions which run around the bristle-associated cells in order to maintain a connection with dorsal or ventral epidermal layer. The wing blade is enclosed within its pupal cuticle. X 1,200.

118

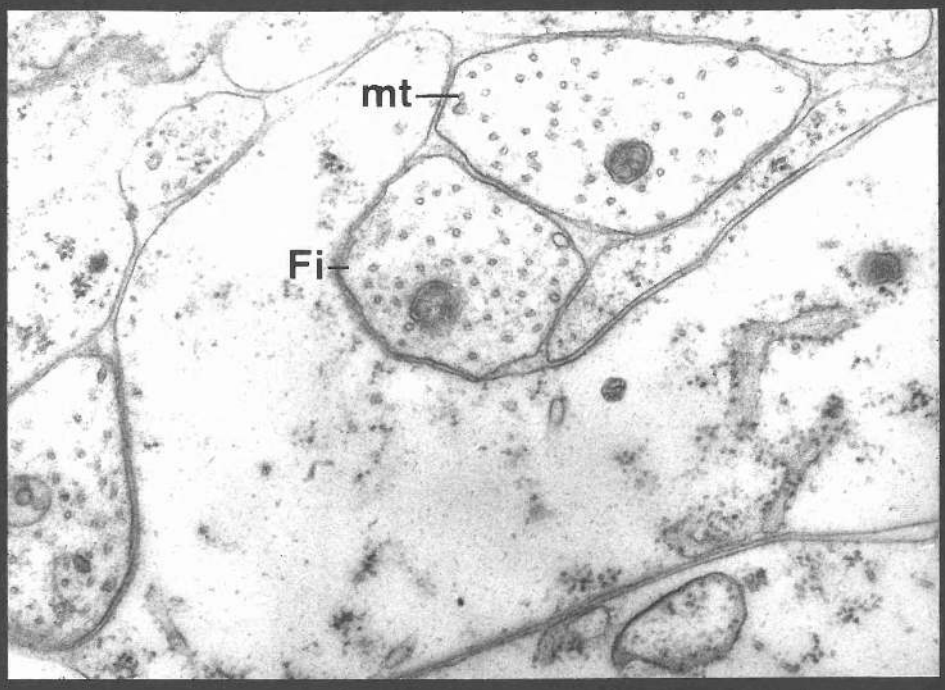

119

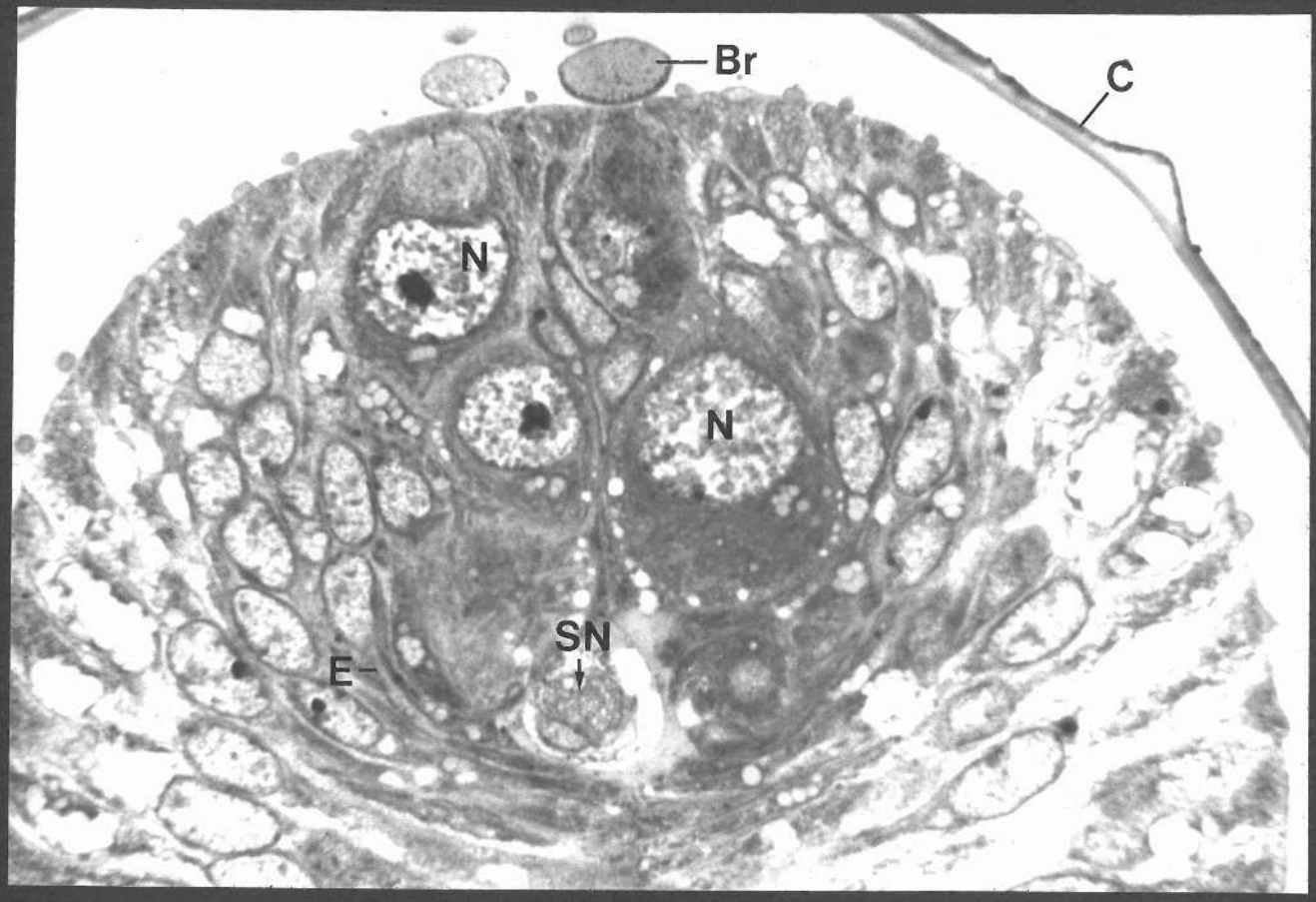

FIGURE 120

Dorsal view of an unfixed C. erythrocephala wing blade mounted in euparol showing the arrangement and spacing of trichomes and bristles. X 600.

FIGURE 121

Feulgen stained preparation showing part of a C. erythrocephala wing blade. Nuclei of trichome-bearing epidermal cells are shown. Nuclei are packed closer together over veins as compared with inter-vein regions. X 1,300.

120

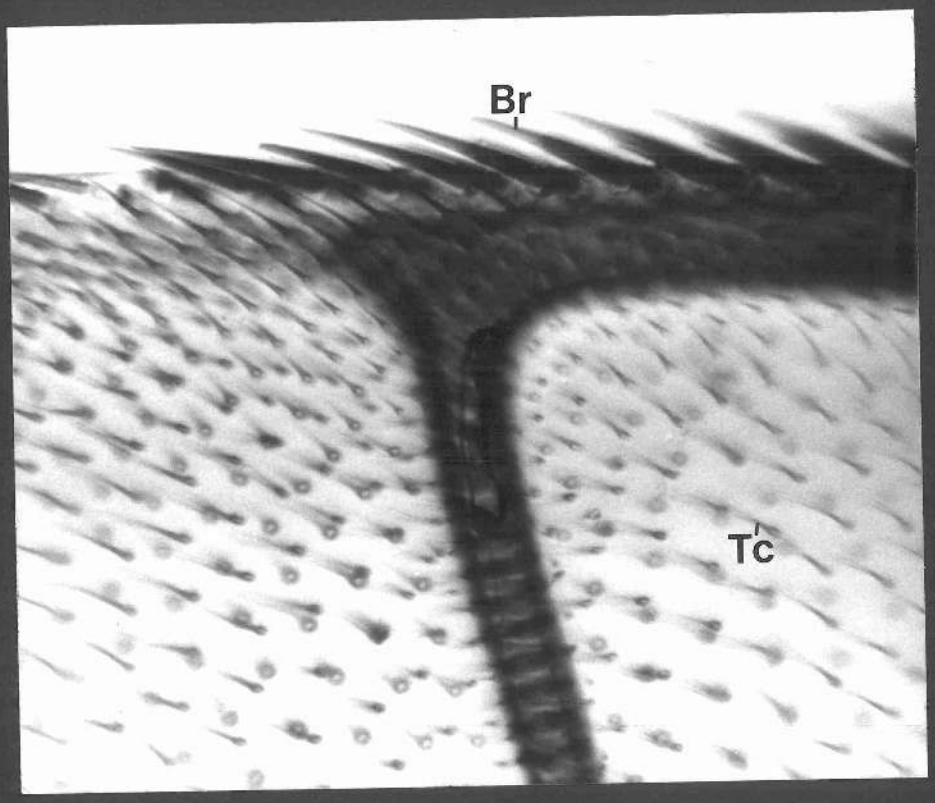

121

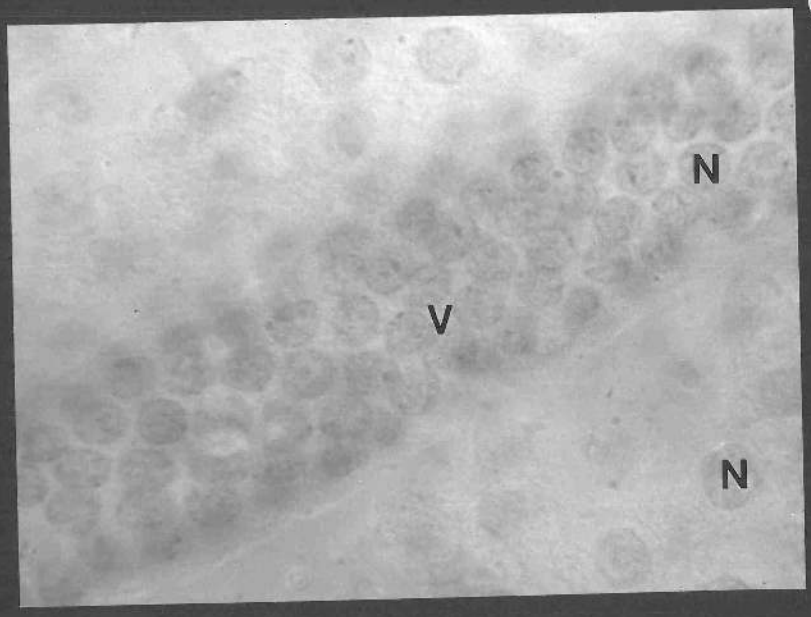

FIGURE 122

Longitudinal section through a trichome of a C. erythrocephala wing blade. The trichome grows out from a single epidermal cell. Microfilaments and microtubules occur at the base of the trichome and extend into the trichome around the border and at the tip of the trichome. X 38,300.

FIGURE 123

Feulgen stained preparation of part of a C. erythrocephala wing blade showing the nuclear arrangement of trichome and bristle-associated cells. Nuclei of trichogen and tormogen cells (arrows) are larger than nuclei of trichome-bearing epidermal cells (double arrow). X 1,400.

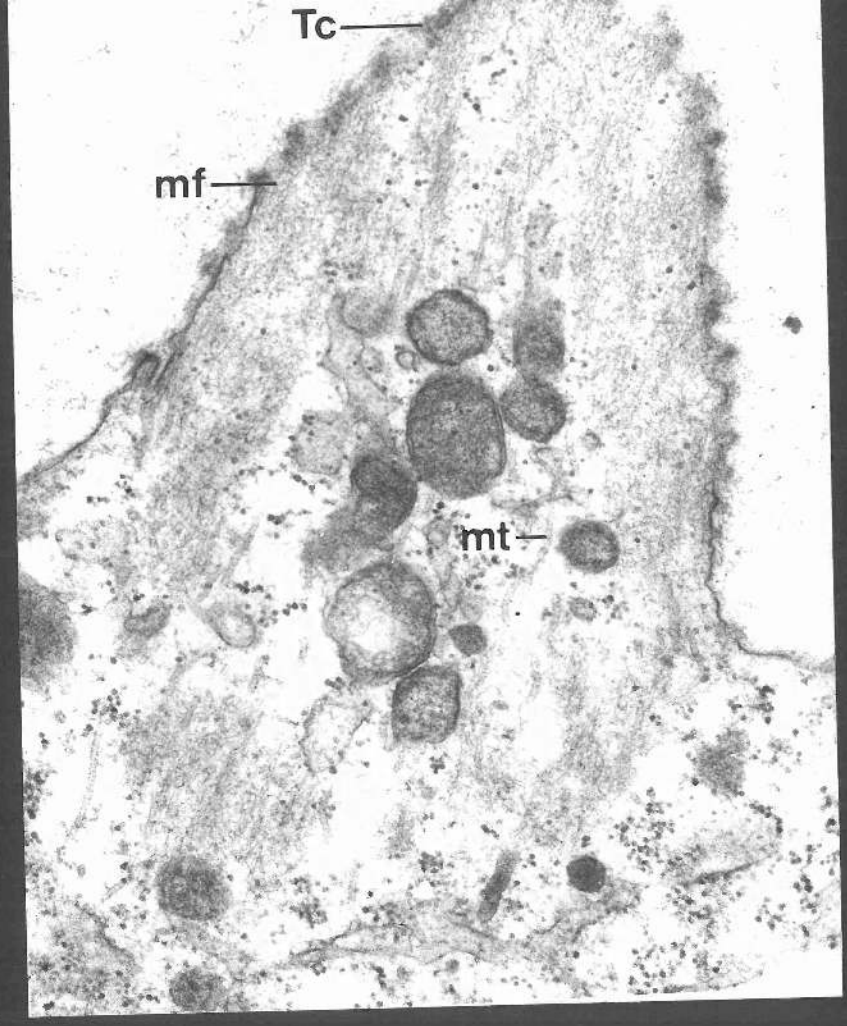

123

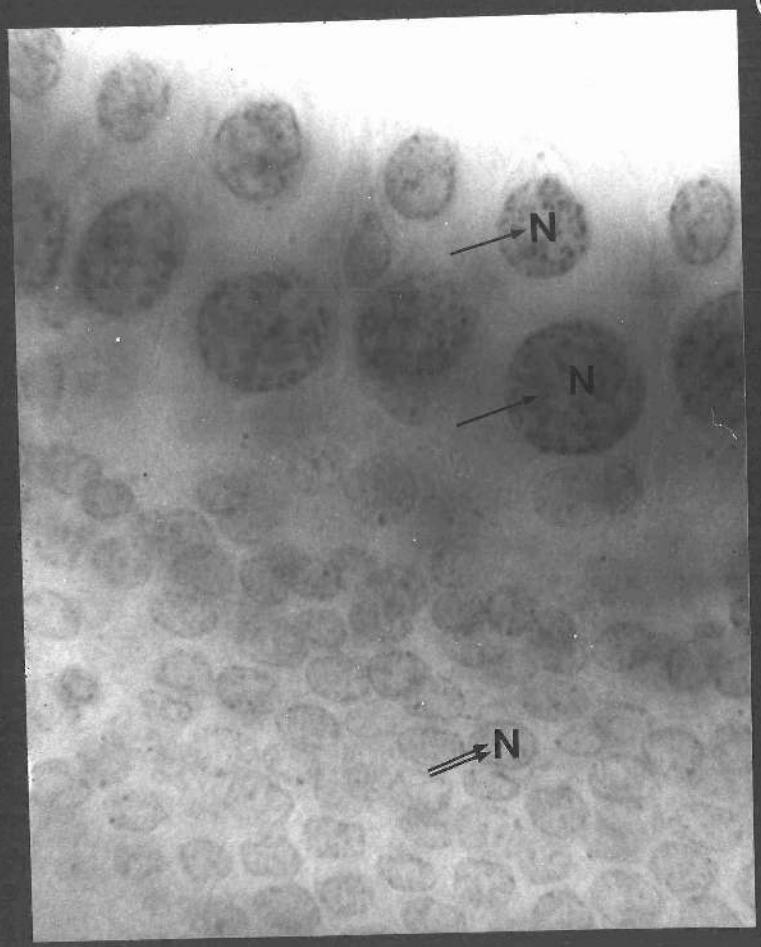

FIGURE 124

Transverse section through a bristle of a C. erythrocephala wing blade anterior margin. Microtubules are abundant within the bristle shaft whereas other organelles are sparce. Microfilaments are grouped into bundles of a characteristic size and shape and are evenly spaced around the bristle shaft margin. X 45,000.

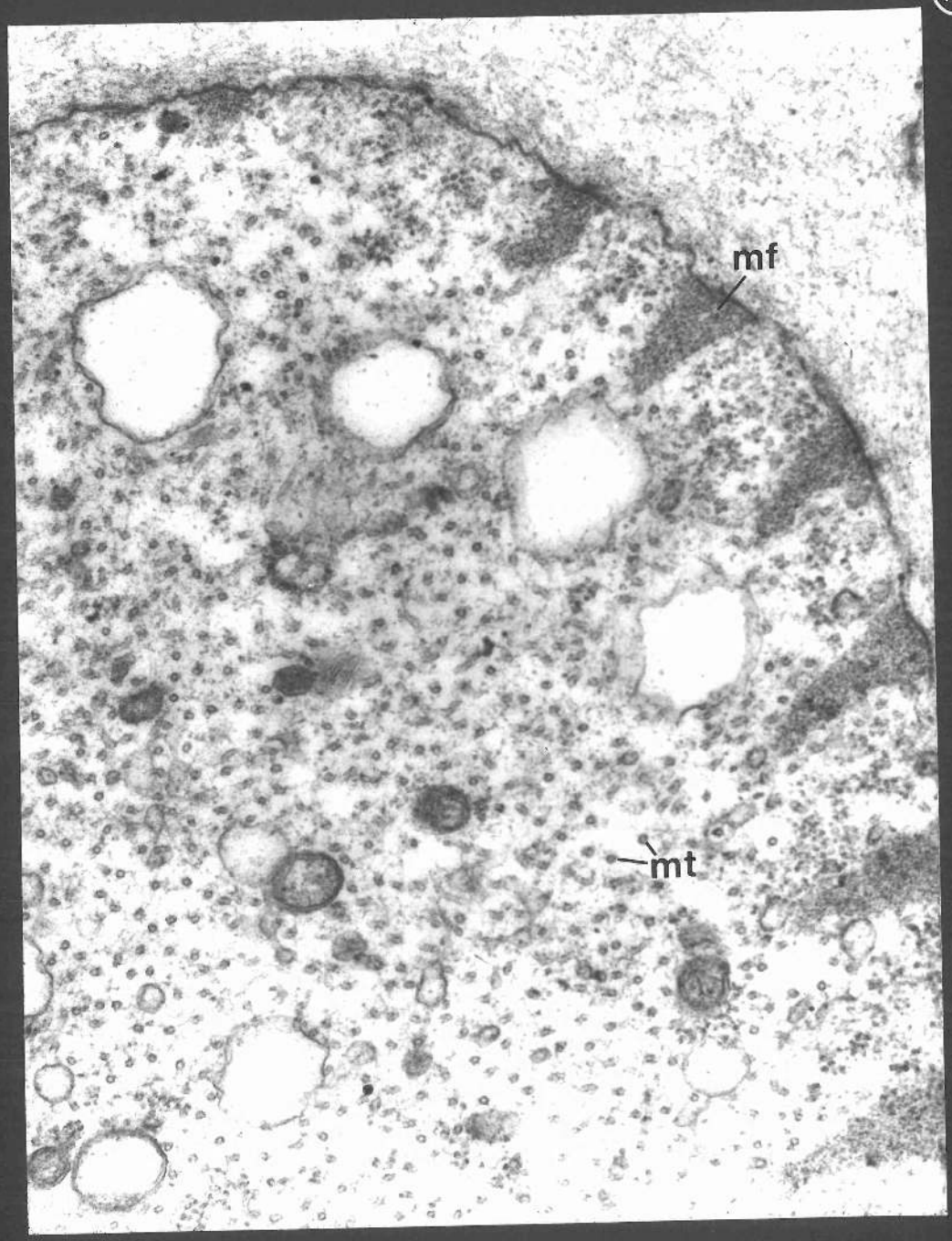
mf
mt

FIGURE 125

Transverse section through a C. erythrocephala anterior wing margin bristle. Ridges of cuticle surround the bristle shaft. Microtubules abound within the bristle shaft but microfilaments are absent. X 51,000.

FIGURE 126

Part of the anterior wing margin of C. erythrocephala mounted in euparol showing a concentrated array of bristles which exhibit cuticular ridges when examined electron microscopically (Fig. 125). X 1,000.

125

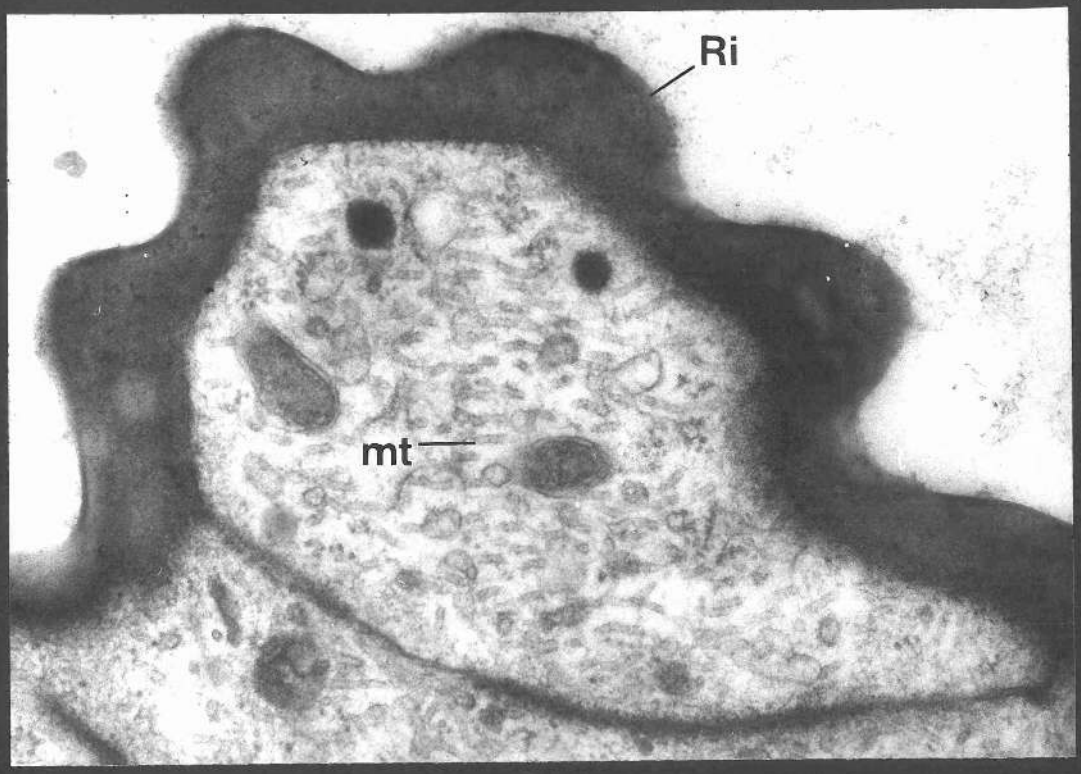

126

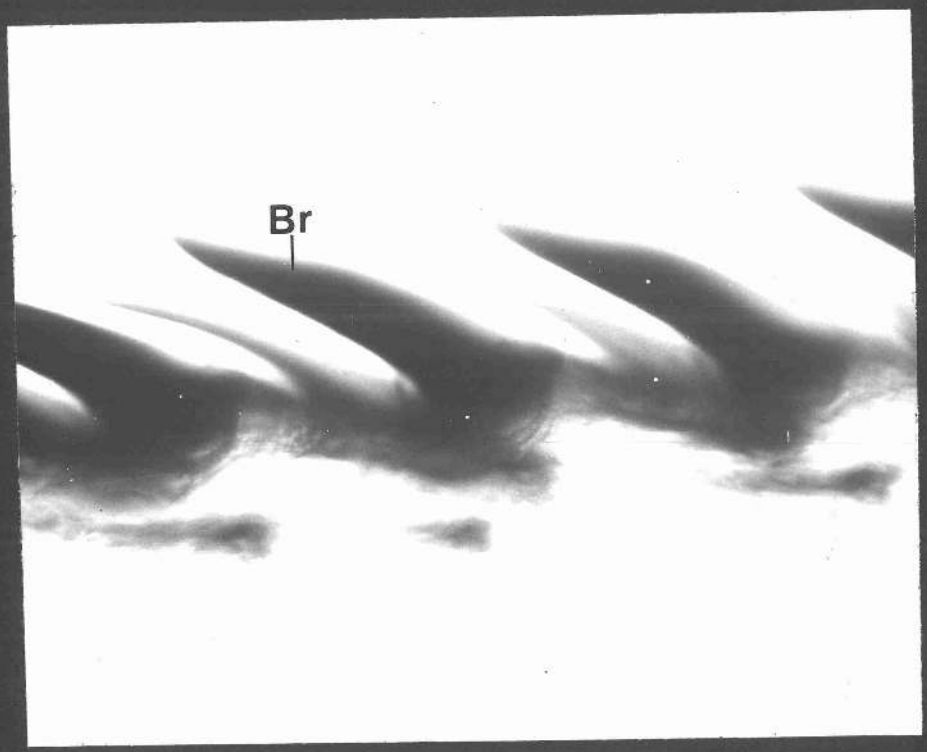

FIGURE 127

Transverse section of part of the intervein region of a Stage 7 C. erythrocephala wing blade. Epidermal cell bodies are squamous in shape. Cell extensions project from cell bodies into the wing interior and extend into a complicated series of filopodial processes. X 1,400.

FIGURE 128

Transverse section through a Stage 7 C. erythrocephala wing blade showing part of the apices of two adjacent cells. The cells are apically connected by a zonulae adhaerens junction. Microtubules are apparent beneath the cells' outer surface. The extent of adult cuticle deposition is shown. X 58,000.

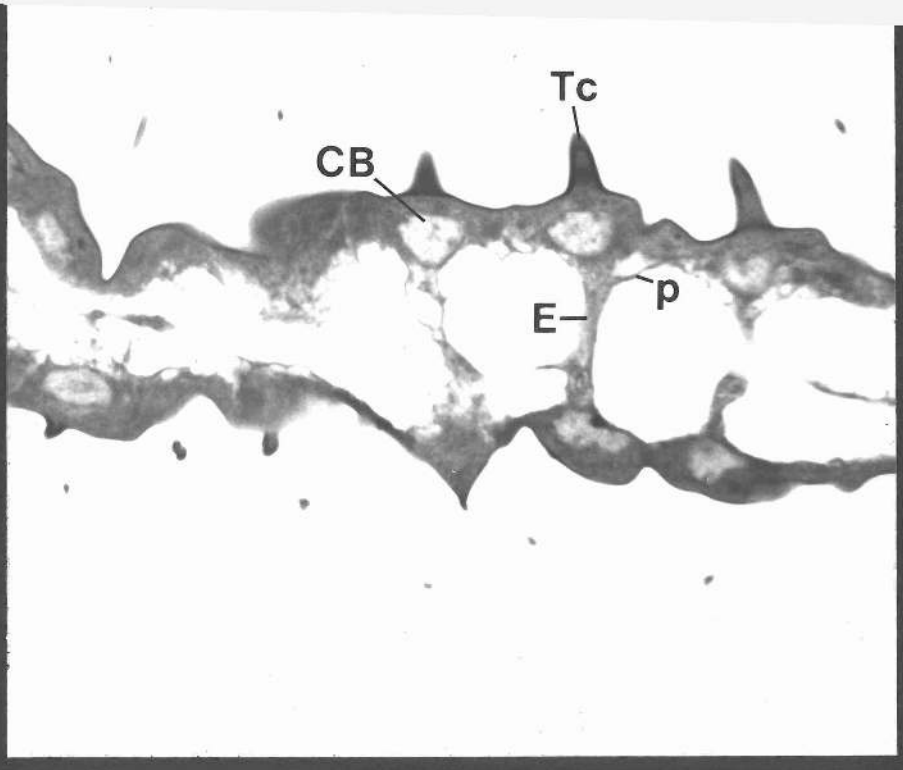

128

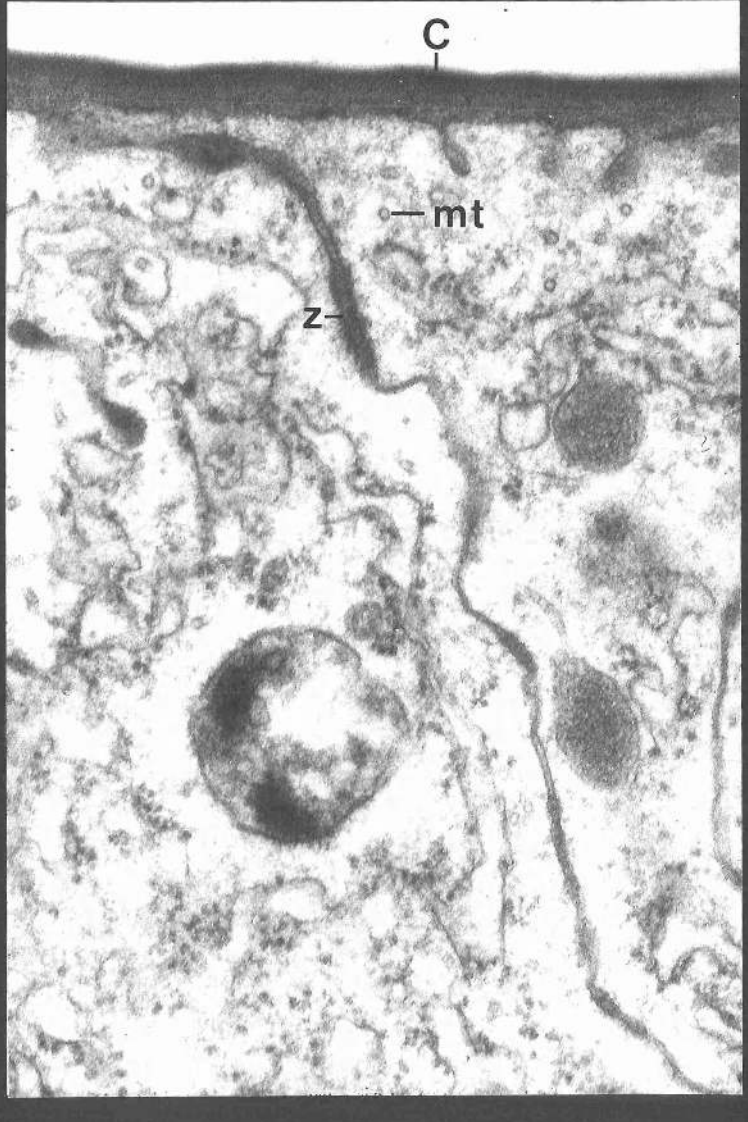

FIGURE 129

Longitudinal section of two adjoining cell extensions which project from the bases of cell bodies of a Stage 7 C. erythrocephala wing blade. Numerous microtubules extend along the interior of the cell extension. One cell extension is connected to a cell process of an adjacent cell extension by means of a three-layered intercellular cementing material (arrows). X 50,000.

FIGURE 130

Longitudinal section of two structures (arrows) which connect adjacent cell processes similar to those shown in Figure 129. The three-layered nature of the intercellular cementing material is shown. X 68,000.

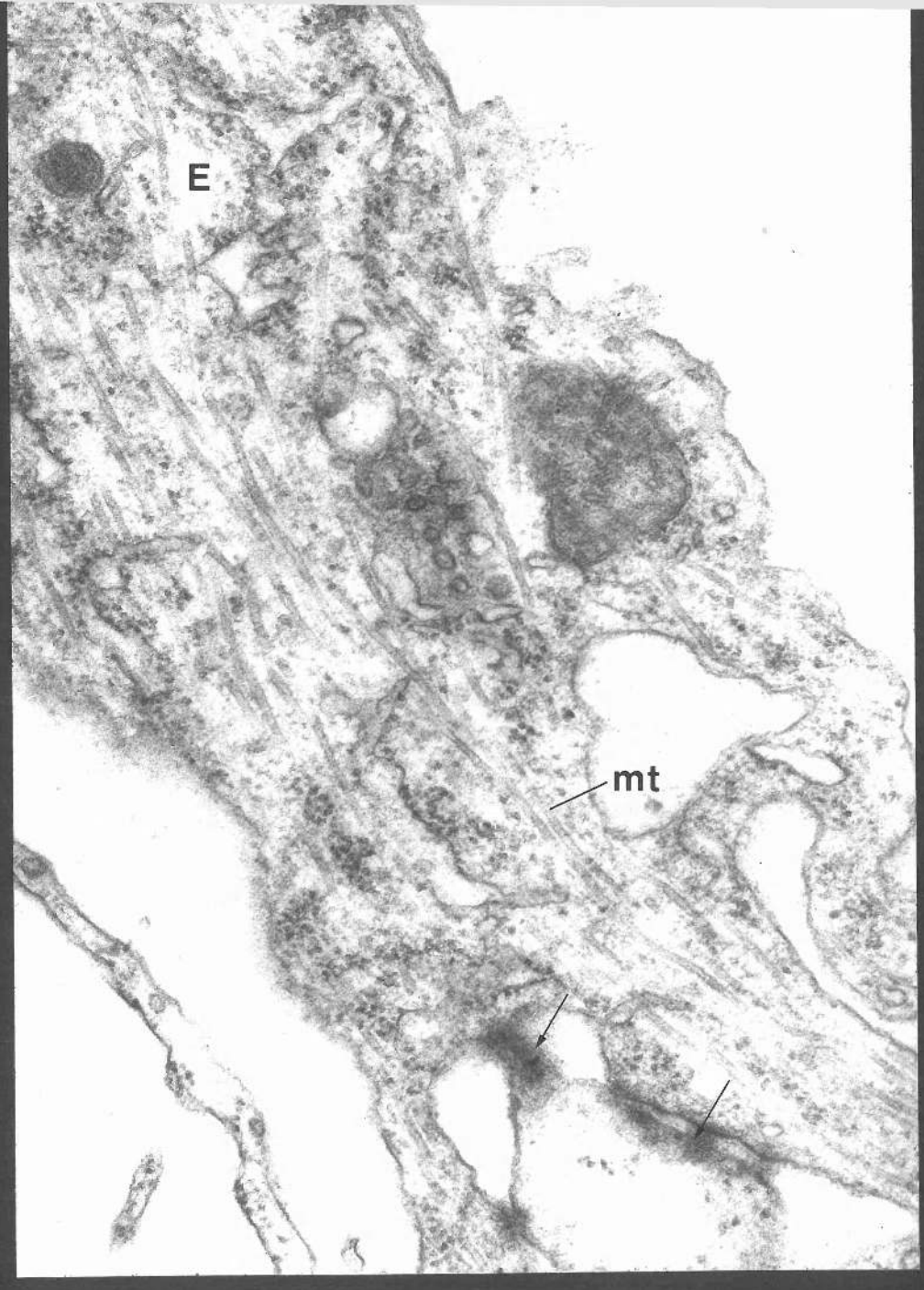

130

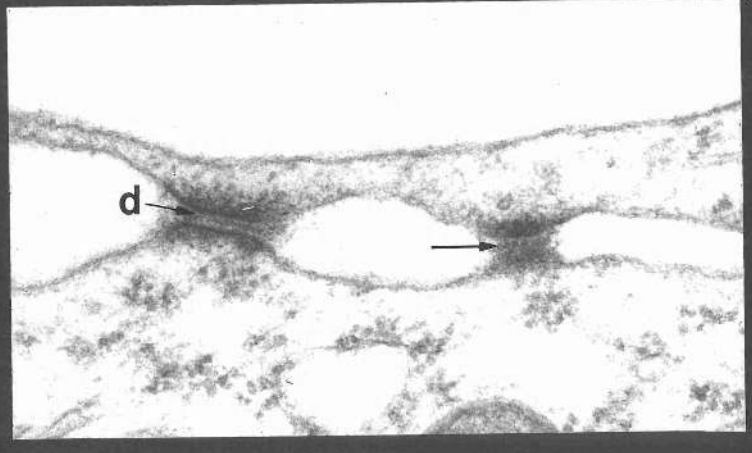

FIGURE 131

Transverse section of the anterior margin of a Stage 7 C. erythrocephala wing blade. Due to the large nature of the bristle-associated trichogen and tormogen cells the other epidermal cells of the wing margin are stacked. Trichomes and bristles can also be distinguished. X 1,400.

FIGURE 132

Transverse section through the posterior margin of a Stage 7 C. erythrocephala wing blade. Epidermal cells of the posterior wing margin are stacked, whereas more anteriorly the epidermal cells are arranged in single layers. No bristles are borne on the posterior wing margin. Only trichomes occur. X 1,400.

(131)

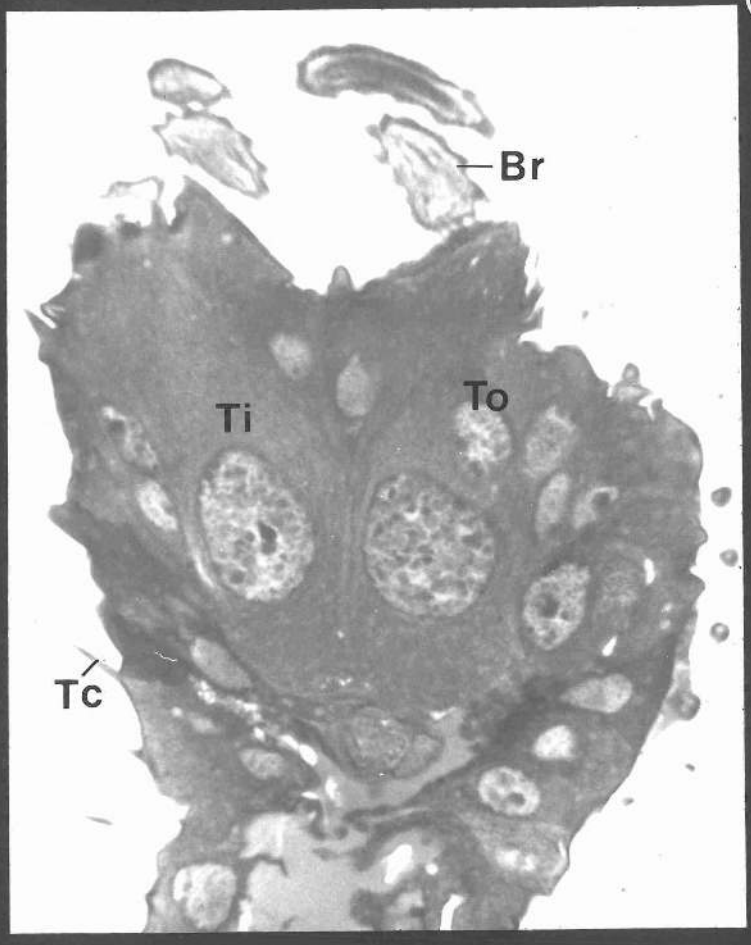

(132)

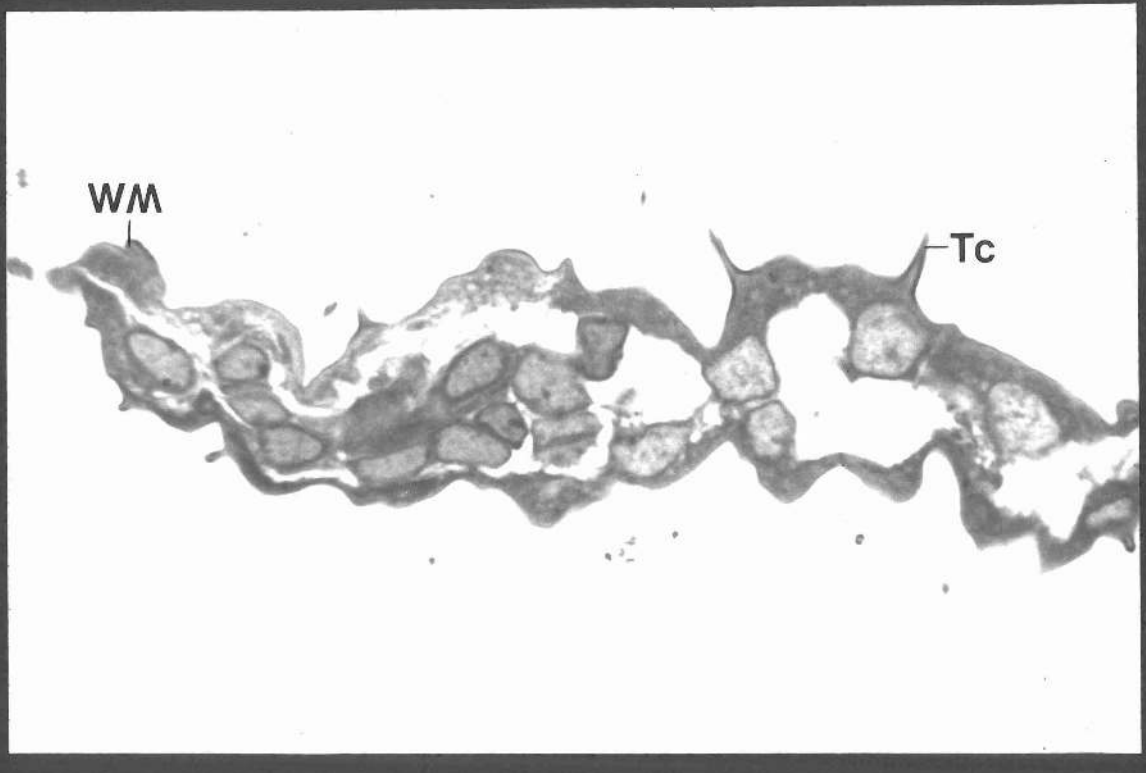

FIGURE 133

Transverse section through part of a Stage 7 C. erythrocephala wing blade. A vein containing haemocytes is shown. Epidermal cells dorsal and ventral to the vein are narrower than the adjacent intervein cells and do not have basal cell extensions, except at vein margins. Instead, adjacent cells are attached at their bases by interdigitating filopodia. X 1,800.

FIGURE 134

Transverse section through a Stage 7 C. erythrocephala wing blade showing the apical surface of an intervein epidermal cell. Microtubules are abundant just beneath the outer surface of the cell. Adult cuticle deposition is shown. X 65,700.

(133)

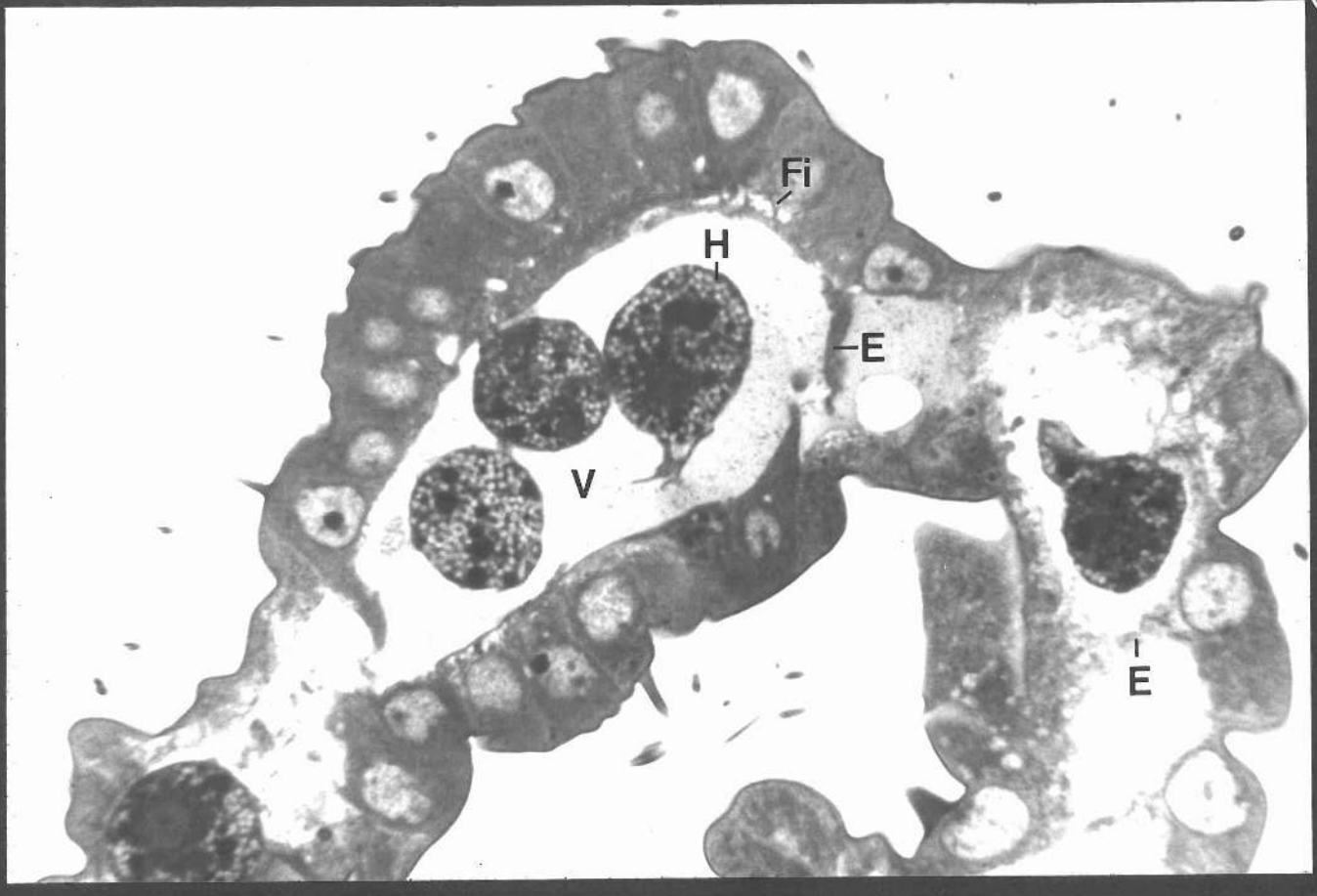

(134)

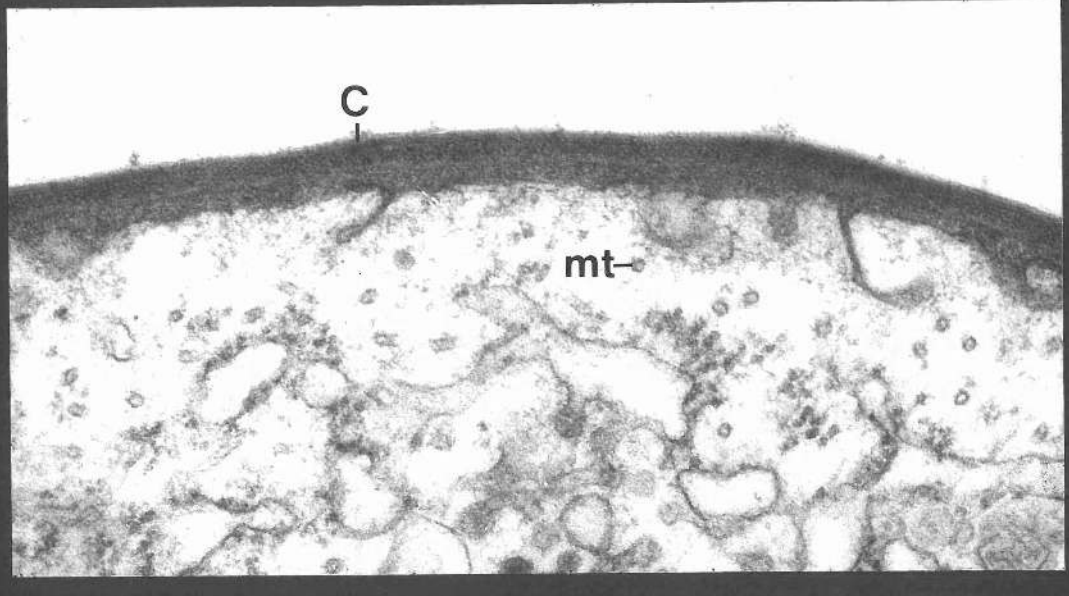

FIGURE 135

Longitudinal section through a P. tetraurelia metaphase micronucleus showing the distribution of chromatin and microtubules. Most microtubules run parallel to the longitudinal axis of the micronucleus (arrow) although others are oriented at right angles to this axis. The nuclear envelope is intact. X 29,800.

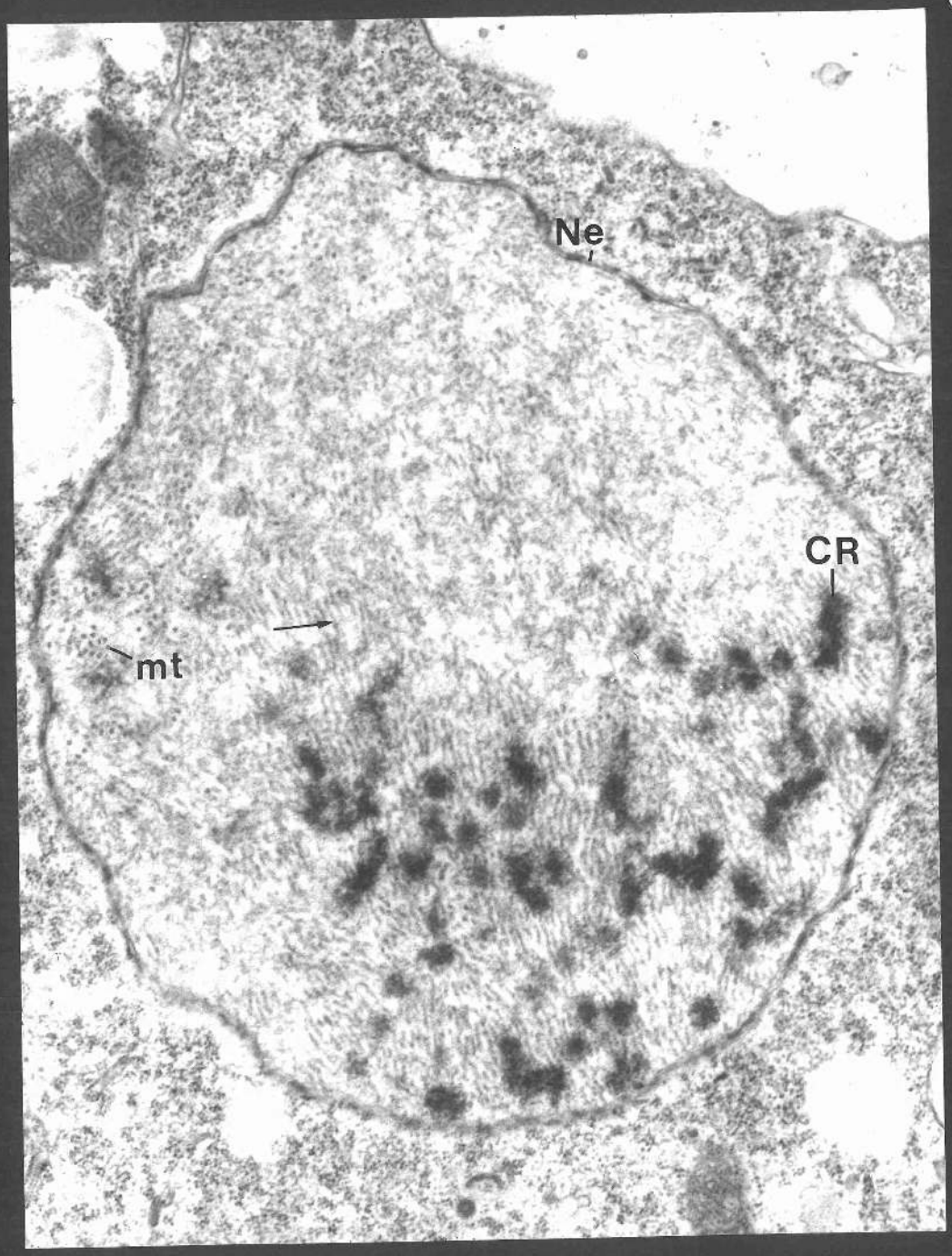
Ne
CR
mt

FIGURE 136

Longitudinal section of part of a P. tetraurelia metaphase micronucleus showing the close association of microtubules with chromatin. Microtubules appear to be attached to the chromatin at various instances (arrows). Note that the intranuclear microtubules have the same size (24 nm) diameter as the cytoplasmic microtubules (double arrow). X 76,900.

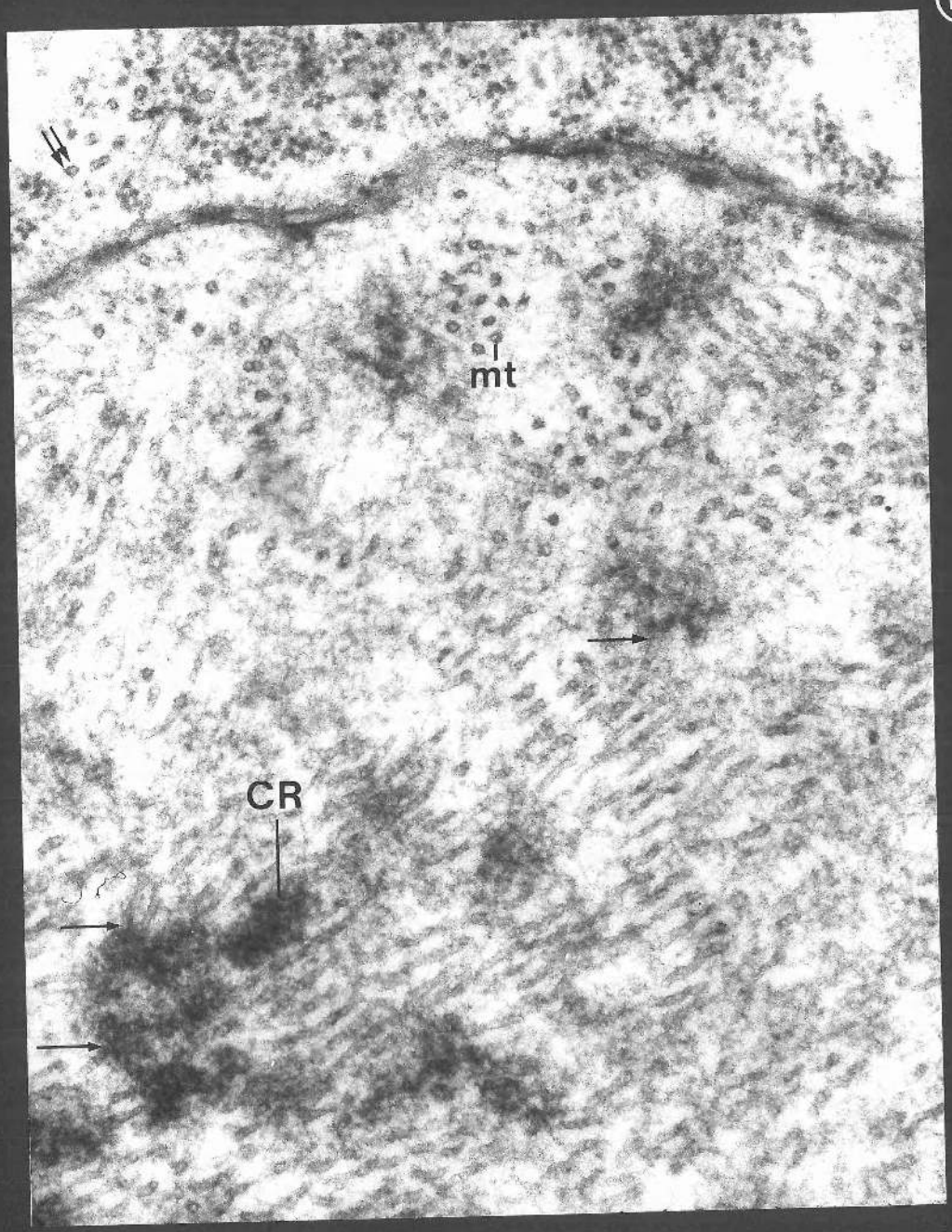
mt
CR

FIGURE 137

Section grazing through a pole of a P. tetraurelia micronucleus. Microtubules terminate at the pole amongst finely fibrous material. X 76,900.

FIGURE 138

Longitudinal section through part of a P. tetraurelia micronucleus. Many microtubules are closely associated with chromatin. Many microtubules terminate at the nuclear envelope (arrows). X 76,900.

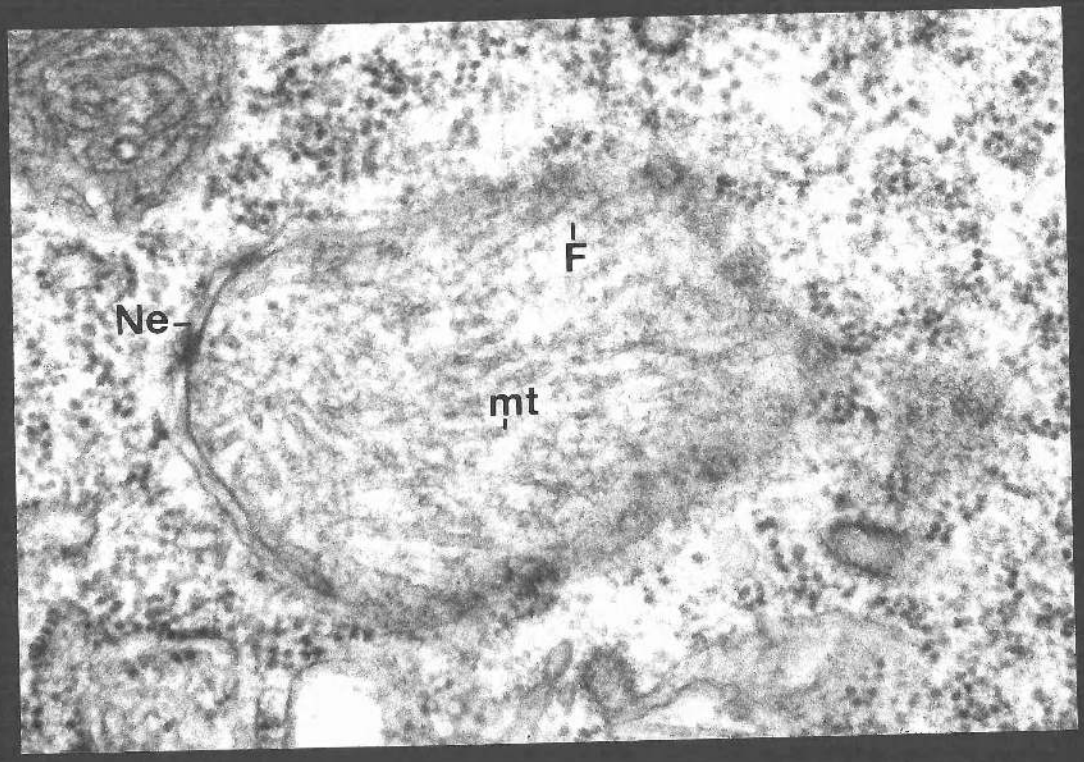
F
Ne
mt

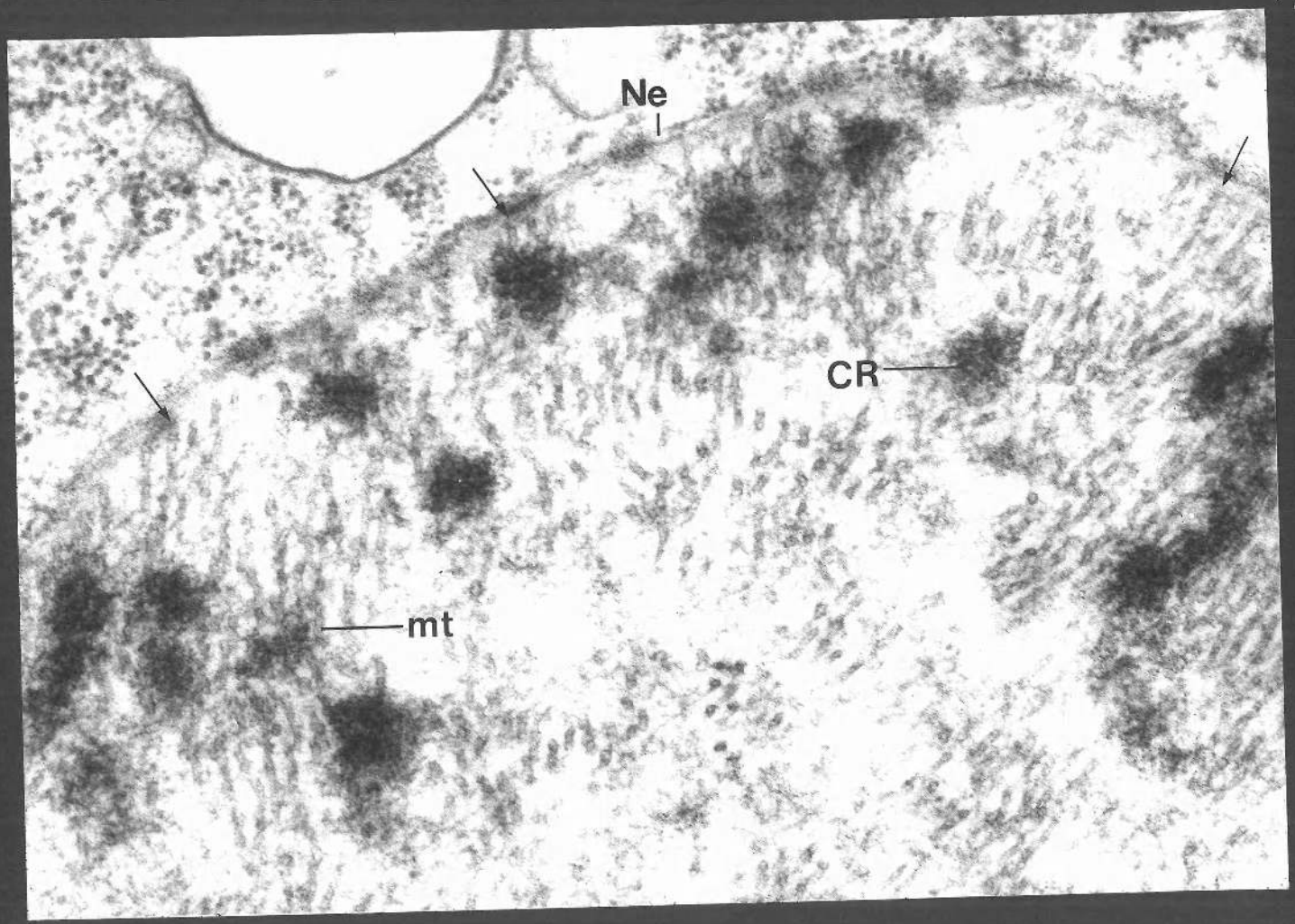
Ne
CR
mt

FIGURE 139

Cross-section through the mid-region of an early P. tetraurelia micronuclear separation spindle. Spindle tubules are abundant within the micronucleus. Some microtubules form a complete row directly beneath the nuclear envelope. These tubules have a slightly greater diameter (24 - 26 nm) than the more centrally positioned microtubules (19 - 24 nm). Compare these peripheral microtubules with the 24-diameter cytoplasmic microtubule (arrow). Note the short bridges between tubules and between tubules and the nuclear envelope (double arrows). The nuclear matrix is finely fibrous in appearance. X 76,900.

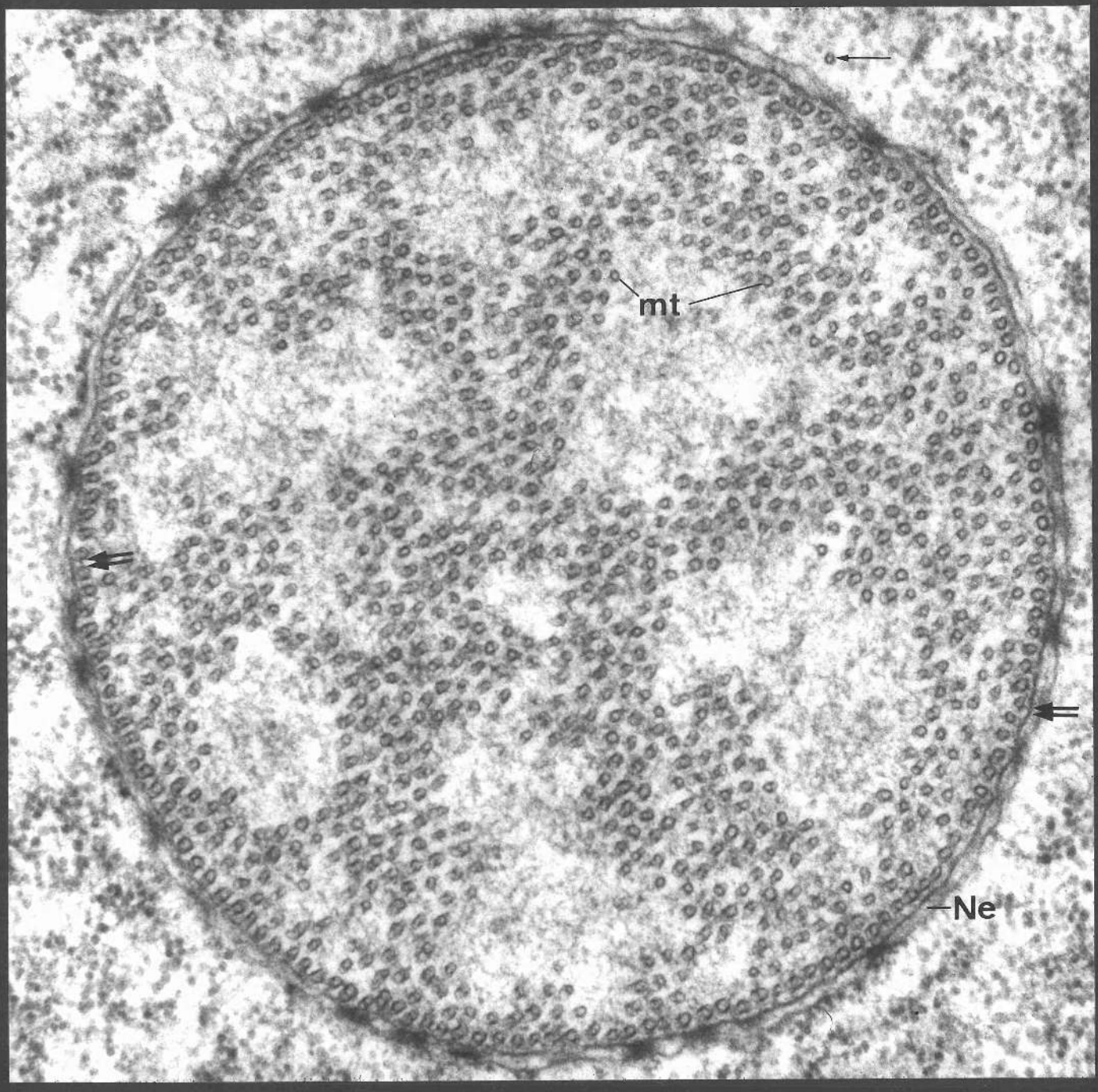
mt
Ne

FIGURE 140

Slightly oblique
A cross-section through a region near the terminal knob of an early P. tetraurelia micronuclear separation spindle. The diameter of the micronucleus is smaller than the mid-region diameter (compare with Figure 139). The nuclear envelope is intact. X 76,900.

FIGURE 141

Section grazing through the polar region of an early P. tetraurelia micronucleus. Microfilament-like fibrils are conspicuous within the nucleoplasm. X 56,000.

140

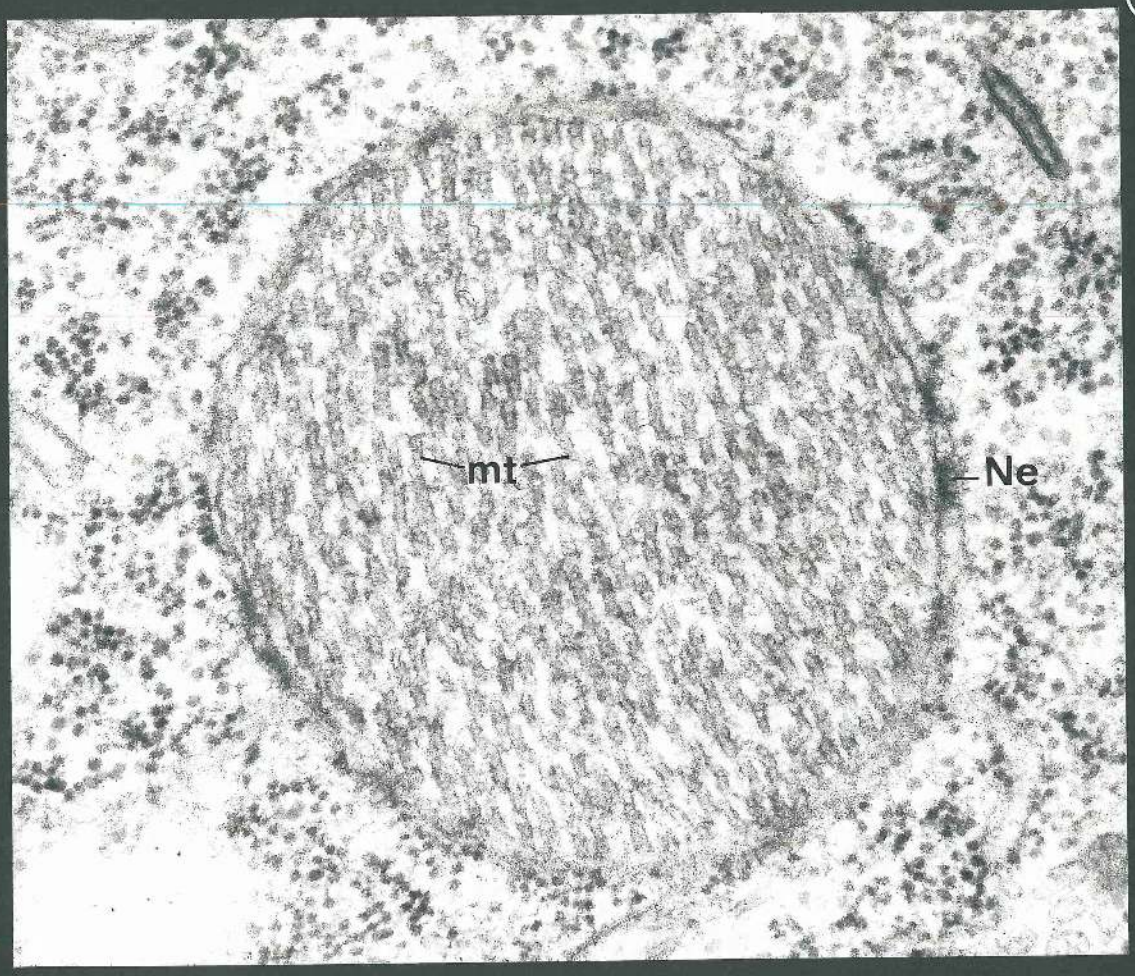

141

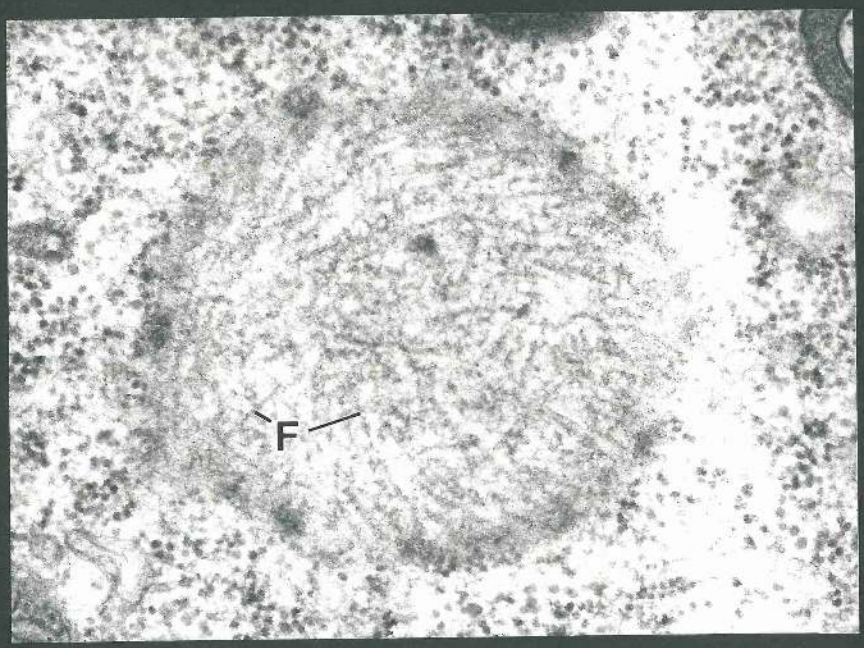

FIGURE 142

Section through the polar region of an early P. tetraurelia micronuclear separation spindle. The diameter of the separation spindle as it meets the chromatin-containing terminal knob is even smaller than in Figure 140. Microtubules extend into the chromatin-containing region and are closely associated with chromatin (arrow). More conspicuous are microfilament-like fibrils which abound amongst the chromatin. X 76,900.

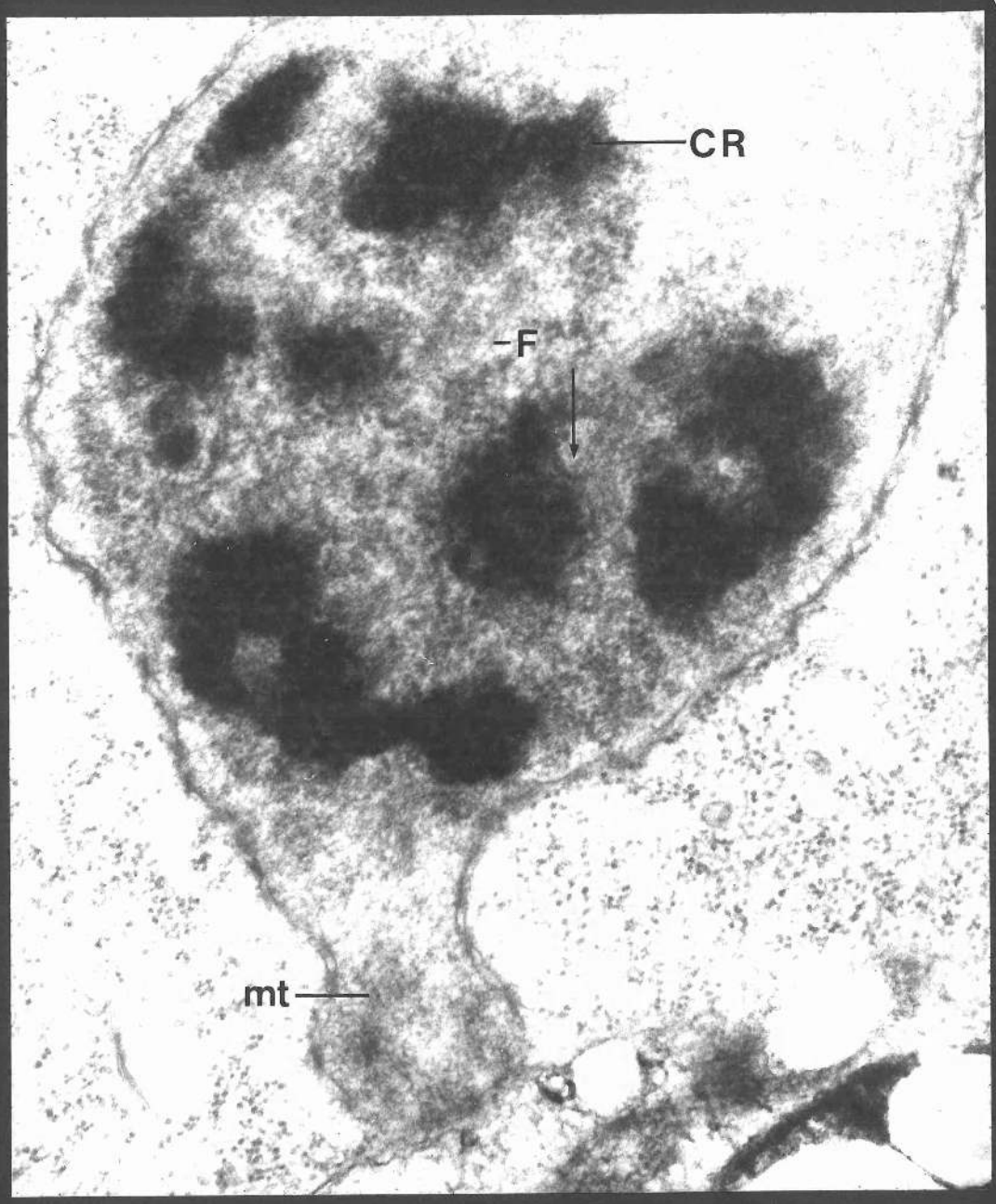
CR
F
mt

FIGURE 143

Changes in the number of microtubules per cross-section at 5 μm intervals along the lengths of two P. tetraurelia late separation spindles from the same organism. Each point on the graph represents a value taken from a single micronucleus. In each micronucleus represented, the number of microtubules per cross-section is greatest in the separation spindle mid-region and least nearest the poles. There is no sharp decrease in microtubule number. Instead there is a gradual decrease in microtubule number from the spindle mid-region towards the terminal knobs. The number of microtubules per cross-section at equivalent points along the lengths of the two different spindles is similar.

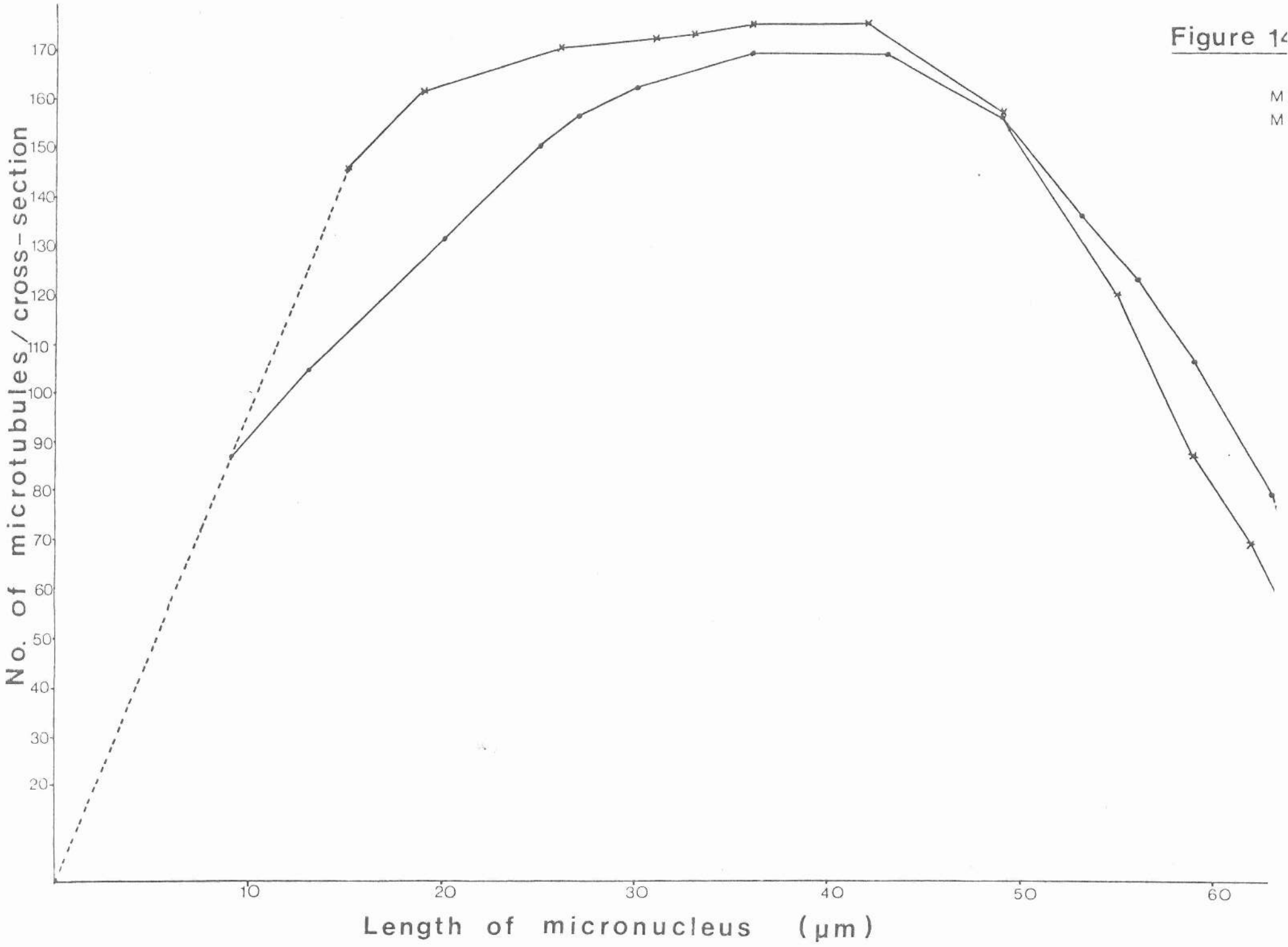
Figure 14
M
M
No. of microtubules / cross-section
170
160
150
140
130
120
110
100
90
80
70
60
50
40
30
20
10
20
30
40
50
60
Length of micronucleus (μm)

FIGURE 144

Cross-section through the mid-region of two P. tetraurelia late separation spindles. Most of the spindle tubules have diameters in the range of 28 - 31 nm. Compare microtubule and micronuclear size with Figure 139. The nuclear envelope is intact. X 76,900.

FIGURE 145

Enlarged cross-section of the mid-region of a P. tetraurelia micronuclear separation spindle. Nearly all of the microtubules have diameters of about 31 nm. Some microtubules form a complete row directly beneath the nuclear envelope. Short bridges link adjacent microtubules (arrow) and also link microtubules to the nuclear envelope (double arrow). The nucleoplasm is finely fibrous in appearance. X 159,500.

144

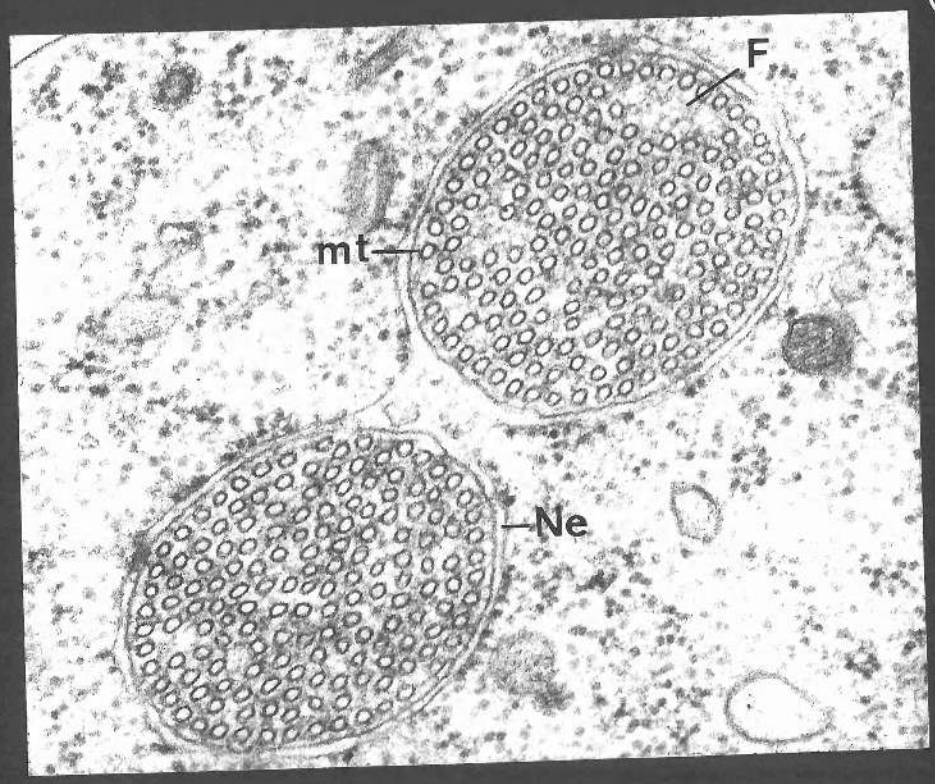

145

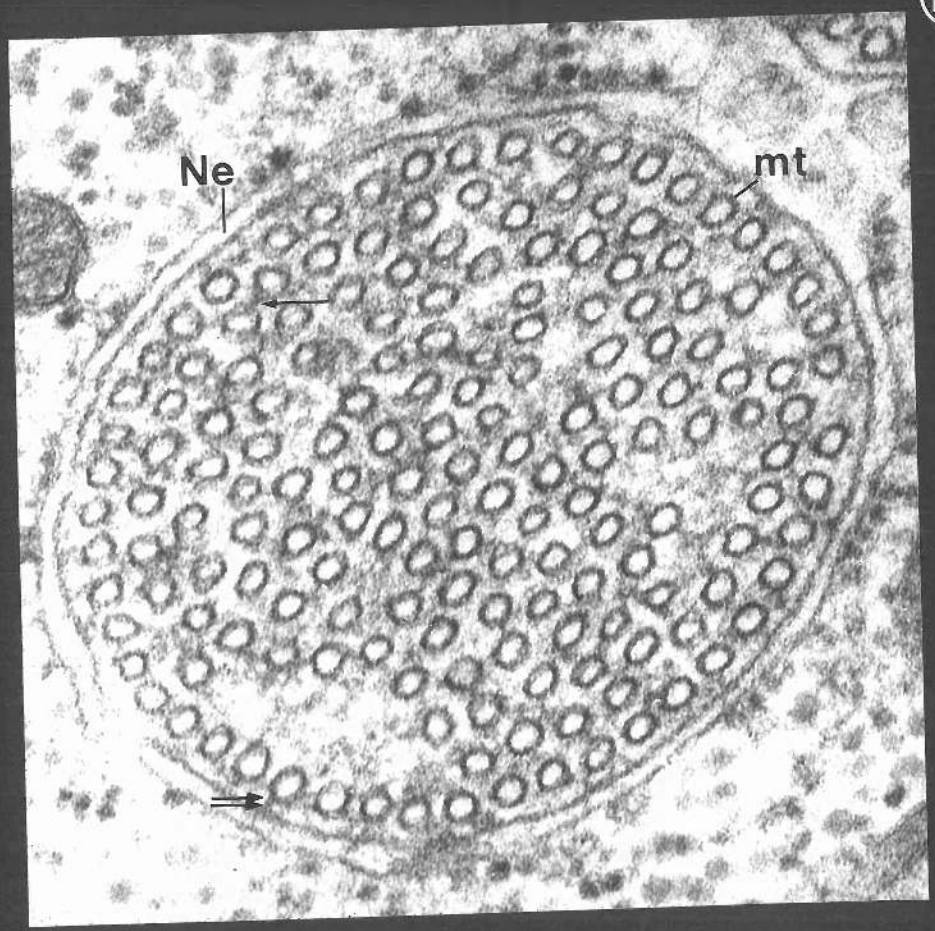

FIGURE 146

Cross-section through two P. tetraurelia late separation spindles nearer the terminal knobs than in Figure 144. Compare the smaller micronuclear diameters and the smaller numbers of microtubules. Most of the microtubules are about 31 nm in diameter. Note the size reduction or absence of fibrillar matrix patches. X 76,900.

FIGURE 147

Cross-section through a P. tetraurelia late separation spindle cut very close to (less than 5 µm) a terminal knob of the micronucleus. The micronuclear diameter is smallest in this region (compare with Figures 145 & 146). Microtubules are closely packed and are predominantly 24 nm in diameter. X 76,900.

FIGURE 148

Part of the chromatin-containing region of a P. tetraurelia separation spindle which shows the presence of a 24 nm microtubule and microfilamentous strands (arrows) amongst the chromatin. X 119,000.

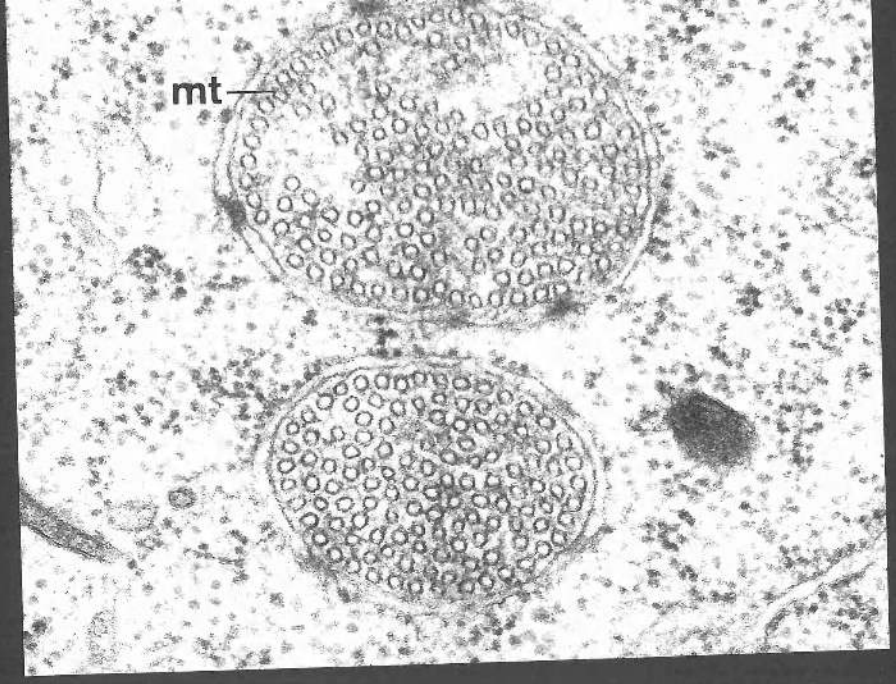

147

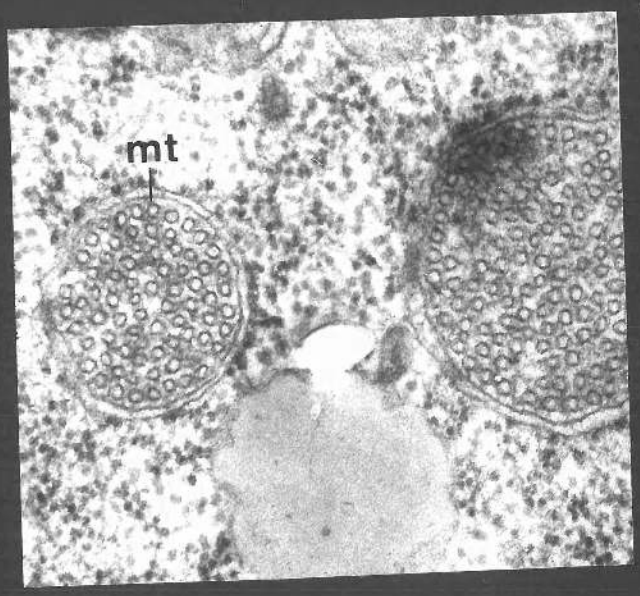

148

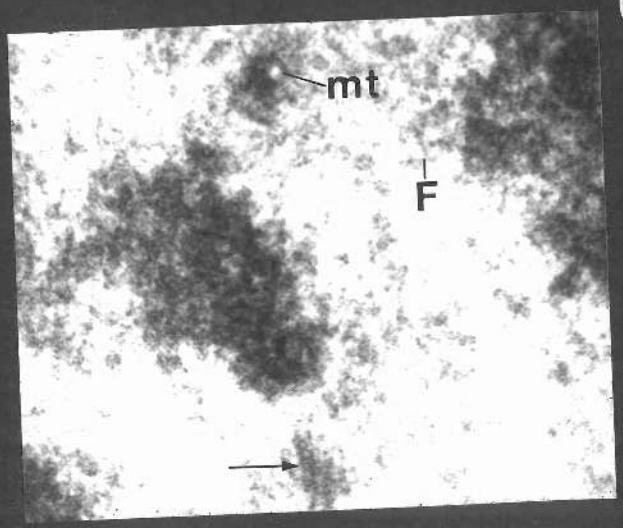

FIGURE 149

Cross-section through the mid-region of a late P. primaurelia micronuclear separation spindle. Nearly all of the microtubules have diameters of about 31 nm. Some microtubules appear to form a complete row directly beneath the nuclear envelope. Short bridges link adjacent microtubules (arrow) and bridges also link some microtubules to the nuclear envelope (double arrow). X 76,900.

FIGURE 150

Cross-section through a late P. primaurelia separation spindle cut less than 5 μm from the terminal knob region of the micronucleus. The micronuclear diameter is smaller than the mid-region micronuclear diameter and 24 nm microtubules predominate. Short bridges link adjacent tubules (arrow). X 76,900.

FIGURE 151

Section through part of the chromatin-containing terminal knob region of a P. primaurelia micronucleus showing the presence of 24 nm microtubules and microfibrils (arrows) within the nucleoplasm. X 119,000.

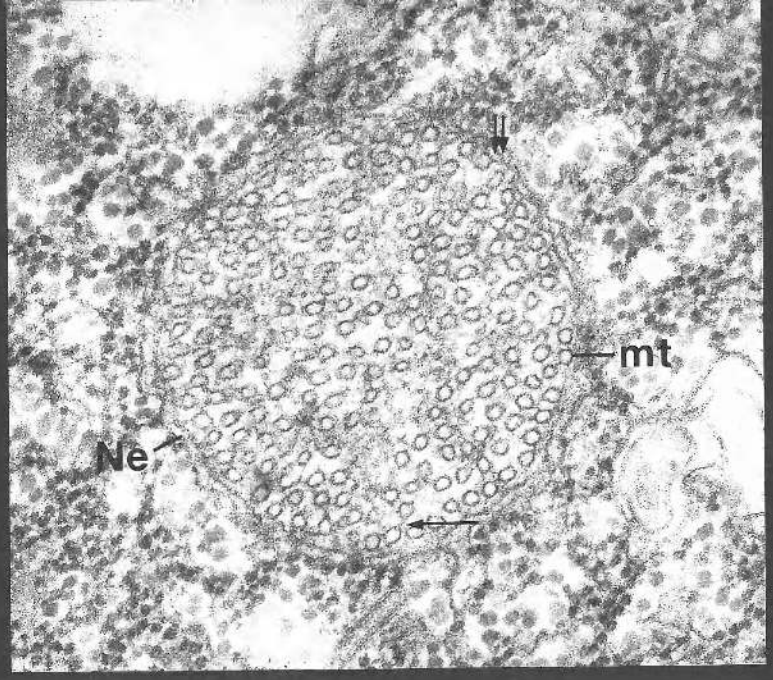

150

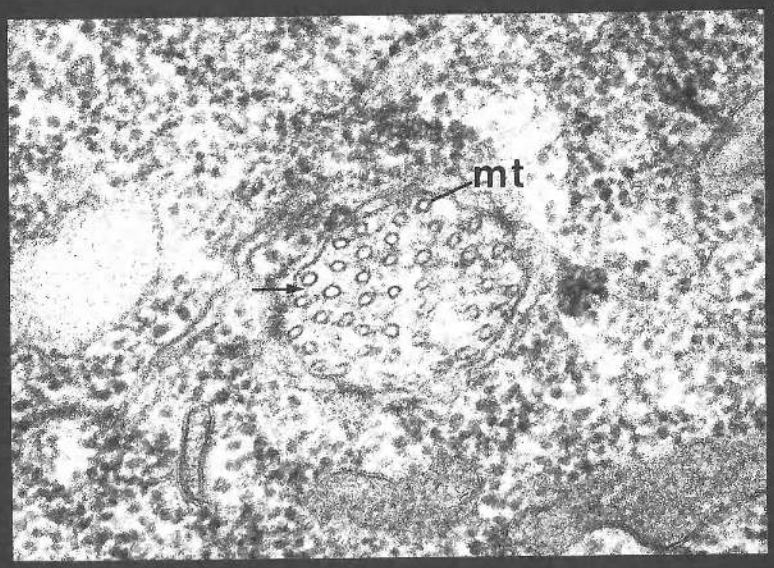

151

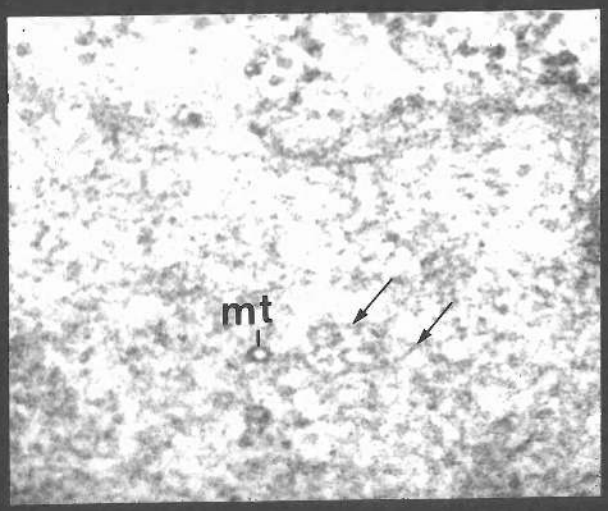

FIGURE 152

Cross-section through the mid-region of a cold-treated P. primaurelia late separation spindle. The intranuclear matrix is densely stained and is clustered around the spindle microtubules, except in certain areas where there are electron lucent 'spaces'. Microtubules are predominantly about 31 nm in diameter. The nuclear envelope is intact. X76,900.

FIGURE 153

Cross-section through a region of a cold-treated P. primaurelia separation spindle cut between the mid-region of the separation spindle and the terminal knob region of the micronucleus. Compared with Figure 152, the micronuclear diameter is smaller, the number of microtubules is smaller and the microtubules are predominantly about 24 nm in diameter. X 76,900.

(152)

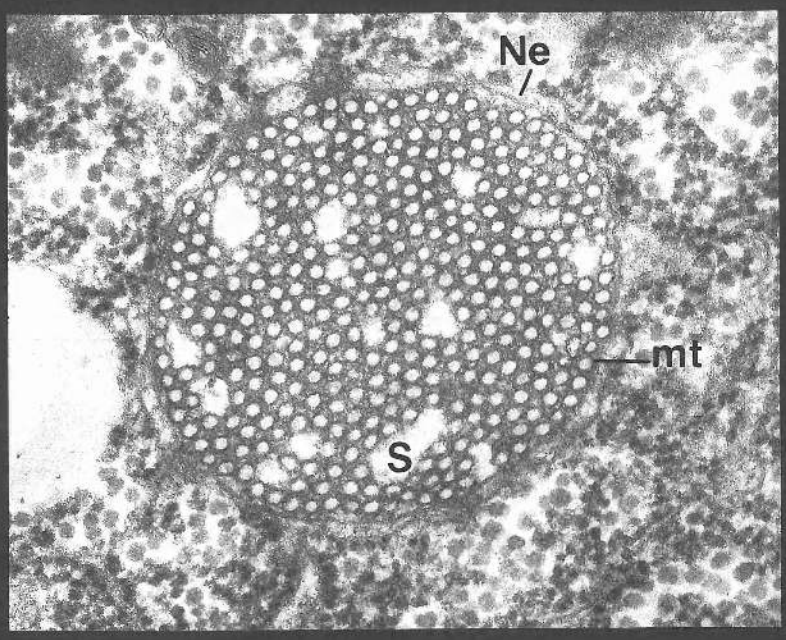

(153)

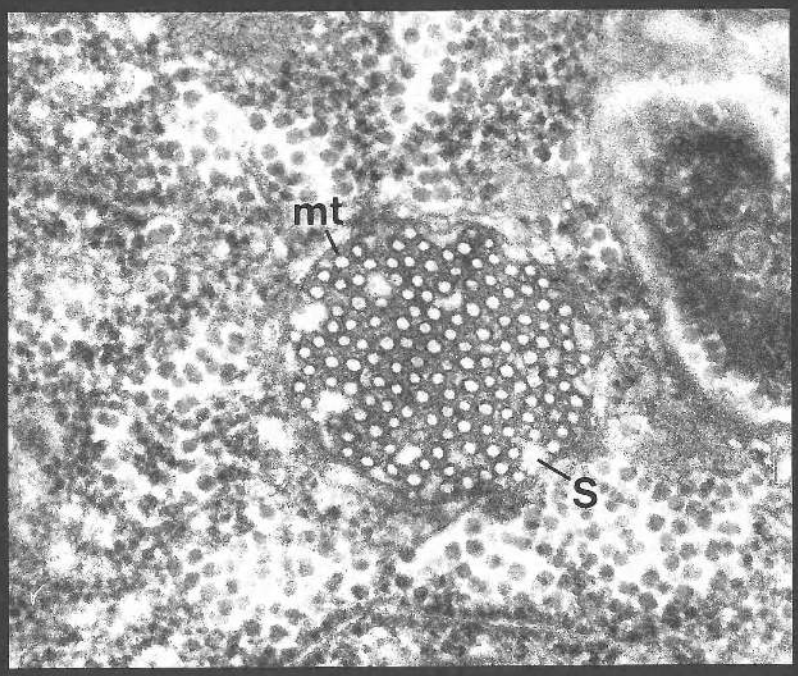

FIGURE 154

Section through the end of a late separation spindle and the chromatin-containing terminal knob region of a cold-treated P. primaurelia. Spindle microtubules are nearly all of the 24 nm variety (inset). Some tubules can be observed in association with the chromatin (arrow). X 76,900.

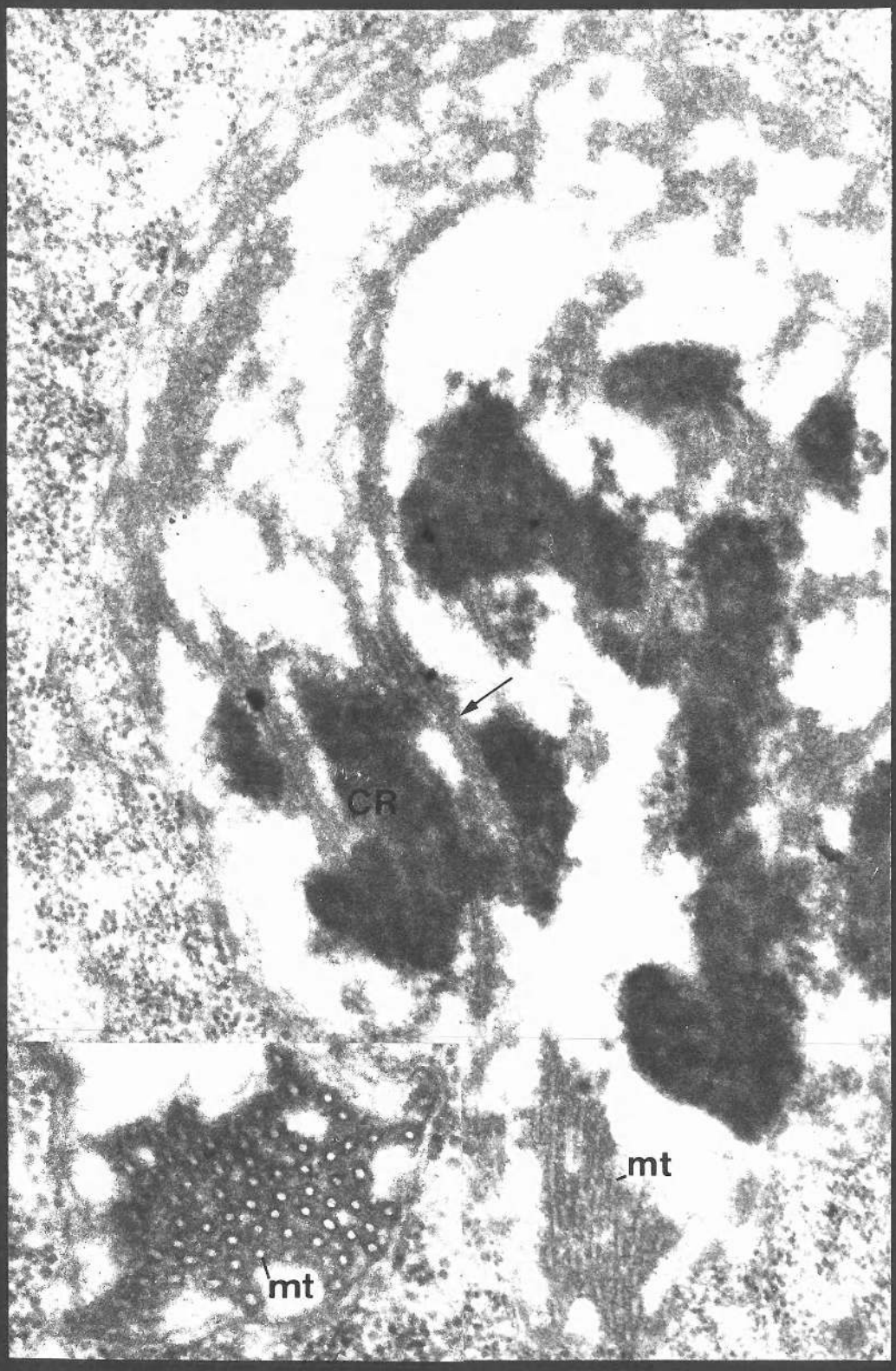
CR
mt
mt

FIGURE 155

Cross-section through part of the mid-region of a cold-treated P. primaurelia late separation spindle. The intranuclear matrix is densely stained which renders the cores of the microtubules particularly distinct, highlighting microtubule diameters. Compare with Figure 156, the control (untreated) spindle. X 159,500.

FIGURE 156

Cross-section of an untreated P. primaurelia separation spindle cut in the mid-region. Note the appearance of the intranuclear matrix, microtubule diameters and the presence of cross-bridges between tubules (arrows). X 159,500.

(155)

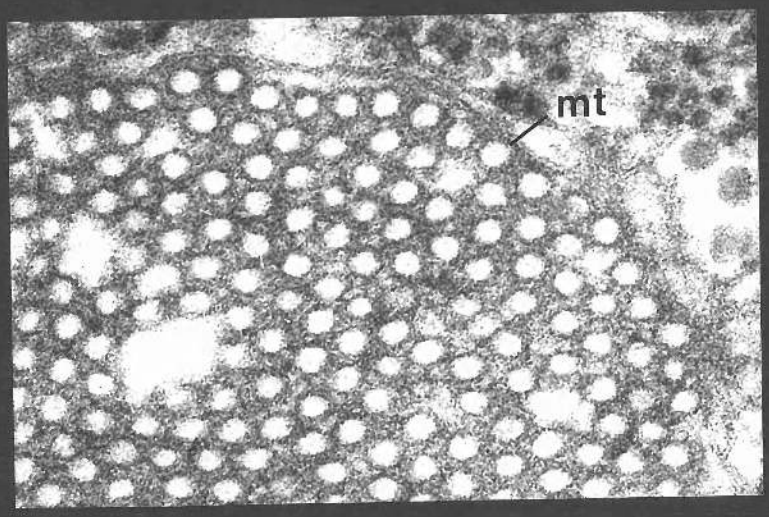

(156)

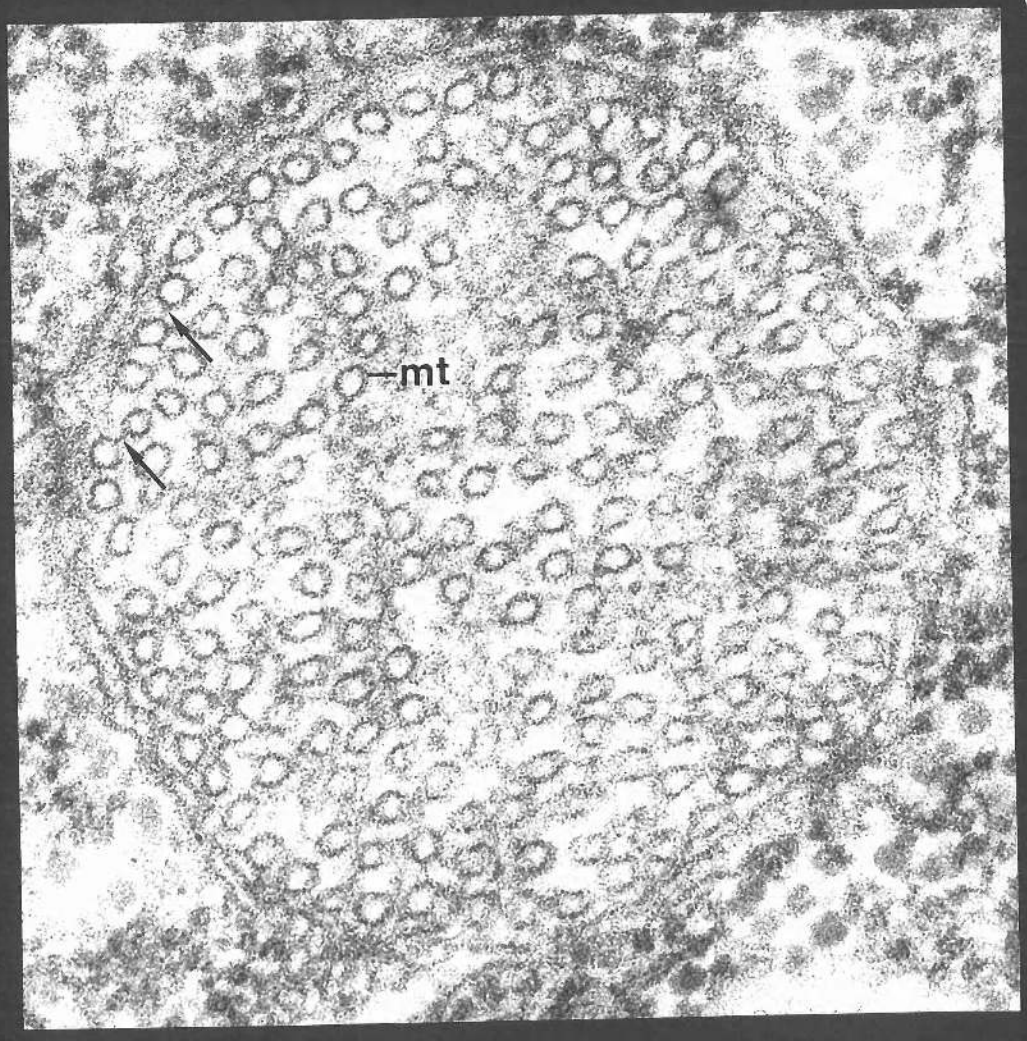

FIGURE 157

Cross-section through the mid-region of a P. primaurelia separation spindle during final stages of spindle elongation. Compare the micronuclear diameter with that of a less elongate (earlier) separation spindle (Fig. 149). There appears to be a complete row of tubules beneath the nuclear envelope. Microtubules are predominantly 31 nm in diameter and cross-bridges are apparent between tubules (arrow). X 76,900.

FIGURE 158

Cross-section through a P. primaurelia separation spindle during final stages of spindle elongation at a point nearer the terminal knob of the micronucleus than Fig. 157. The micronuclear diameter is smaller than the mid-region diameter and there are fewer microtubules. Microtubules are predominantly 31 nm in diameter. X 76,900.

FIGURE 159

Cross-section through a P. primaurelia separation spindle during final stages of spindle elongation at a point close to a terminal knob. Microtubules are predominantly about 31 nm in diameter and are often linked by short bridges (arrows). X 76,900.

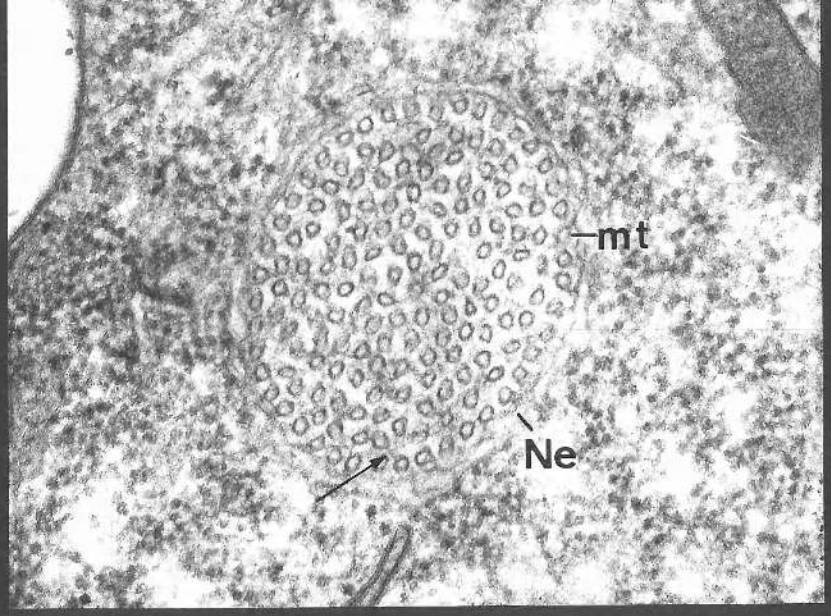

158

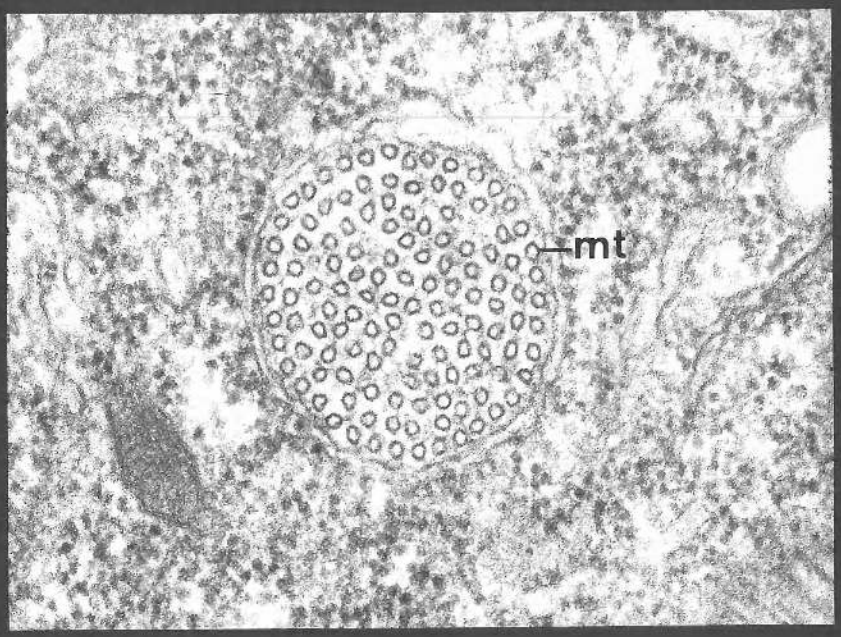

159

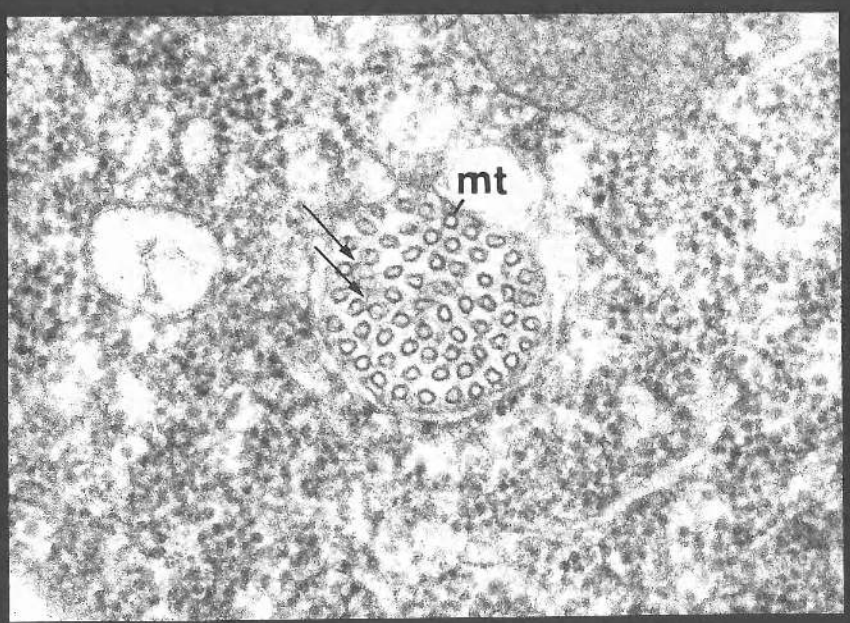

FIGURE 160

Part of an ammonium molybdate stained crystalline catalase crystal showing the lattice spacings. Only lattice spacings with a central electron lucent line may be counted and measured. Those without this line indicate obliqueness and would alter measurements considerably. X 195,800.

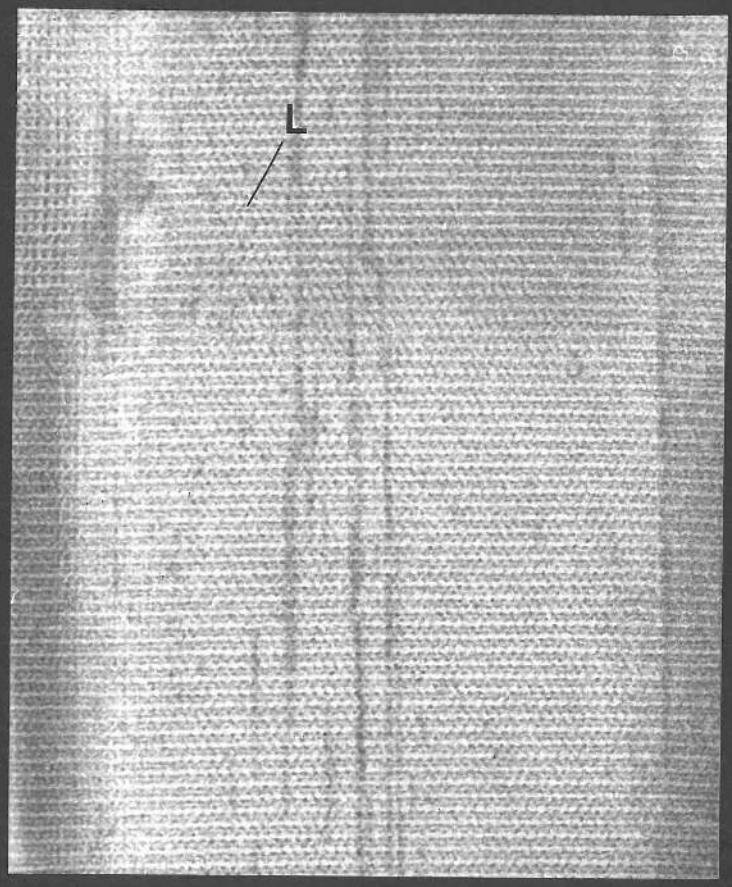
L